



HAL
open science

Role of oxidative and energy metabolism in skin aging and UV-B induced carcinogenesis

Seyed Mohsen Hosseini

► **To cite this version:**

Seyed Mohsen Hosseini. Role of oxidative and energy metabolism in skin aging and UV-B induced carcinogenesis. Dermatology. Université de Bordeaux, 2015. English. NNT : 2015BORD0117 . tel-01988753

HAL Id: tel-01988753

<https://theses.hal.science/tel-01988753>

Submitted on 22 Jan 2019

HAL is a multi-disciplinary open access archive for the deposit and dissemination of scientific research documents, whether they are published or not. The documents may come from teaching and research institutions in France or abroad, or from public or private research centers.

L'archive ouverte pluridisciplinaire **HAL**, est destinée au dépôt et à la diffusion de documents scientifiques de niveau recherche, publiés ou non, émanant des établissements d'enseignement et de recherche français ou étrangers, des laboratoires publics ou privés.

Université de Bordeaux

Année 2015

THÈSE

Pour le

DOCTORAT DE L'UNIVERSITÉ DE BORDEAUX

Mention : Science, Technologies, Santé

Option : Biologie Cellulaire et Physiopathologie

Présentée et soutenue publiquement

Le 9 Juillet 2015

Par **Mohsen HOSSEINI**

Role of Oxidative and Energy Metabolism in Skin Aging and UV-B induced Carcinogenesis

Membres du Jury

Pr. ROSENBAUM Jean.....	Président
Pr. EGLY Jean-Marc.....	Rapporteur
Dr. KLUZA Jérôme.....	Rapporteur
Dr. RACHIDI Walid.....	Examineur
Dr. ROSSIGNOL Rodrigue.....	Examineur
Pr. TAIEB Alain.....	Membre invité
Dr. REZVANI Hamid-Reza.....	Directeur

TABLE OF CONTENTS

	<u>Page</u>
List of Figures	iv
List of Tables	vi
Nomenclature	vii
Acknowledgements	xi
Abstract	xiii
I. Introduction	1
Chapter I. Solar Irradiation and Photoprotection	2
1. Skin structure and function	3
1.1. Skin Anatomy	4
1.2. Structure of Epidermis	4
1.2.1. Keratinocytes	4
1.2.2. Melanocytes	5
1.2.3. Langerhans Cells	5
1.2.4. Merkel Cells	5
1.3. Dermis Structure	5
1.4. Hypodermis	6
2. Solar Radiation	6
2.1. Effects of UV on Skin	9
2.1.1. Acute Skin Lesions	9
2.1.2. Chronic Skin Lesion under UV Effect	10
3. Key Players in the Response to UV	11
3.1. Growth Factors and their Receptors in the Cellular Response to UV	11
3.2. Immune System and Response to UV	11
3.3. DNA Damage and Response to UV	13
3.4. Reactive Oxygen Species (ROS)	15
3.4.1. NADPH Oxidase Enzyme Family	15
3.4.1.1. NADPH Oxidase 1 (NOX1)	18
3.4.1.2. NADPH oxidase 2 (NOX2)	18
3.4.1.3. NADPH Oxidase 3 (NOX3)	18
3.4.1.4. NADPH Oxidase 4 (NOX4)	19
3.4.1.5. NADPH Oxidase5 (NOX5)	19
3.4.1.6. DOUX1/DOUX2	19

3.4.2.	Role of ROS in Cellular Response to UV	19
3.4.3.	Oxidative Effects of ROS	19
3.4.4.	ROS as a Second Messenger	20
4.	Photoprotection	22
4.1.	Pigmentation	22
4.2.	DNA repair	23
4.2.1.	<i>in situ</i> Reversion of the Damage (Direct Reversal)	24
4.2.2.	Mismatches Repair	24
4.2.3.	Base Excision Repair System (BER)	25
4.2.4.	Nucleotide Excision Repair (NER)	25
4.2.5.	Repair by homologous recombination	27
4.2.6.	Repair by non-Homologous Religation (Non-Homologous End- Joining, NHEJ)	28
4.2.7.	DNA Damage Tolerance and Translational Synthesis	28
4.3.	Antioxidants Systems	30
4.3.1.	Antioxidant Enzyme Systems	30
4.3.2.	non-Enzymatic Antioxidant Systems	33
4.4.	Apoptosis	34
4.4.1.	General mechanisms of apoptosis	35
4.4.2.	UVB-induced Apoptosis	35
4.5.	Senescence or Aging	36
4.5.1.	Key players in Aging process	36
4.5.1.1.	Intrinsic Factors	36
4.5.1.2.	Extrinsic Factors	37
4.5.2.	Aging Biomarkers	38
4.5.3.	Aging in Organs	42
4.5.4.	Effects of Aging on the Skin	42
4.5.5.	Structural Changes in the Skin	43
4.5.5.1.	Epidermal Changes	43
4.5.5.2.	Dermal Changes	44
4.6.	Autophagy	44
4.6.1.	Macroautophagy	45
4.6.2.	Mitophagy	46
4.6.3.	Microautophagy	46
4.6.4.	Chaperone-mediated Autophagy	46
	Chapter II. Energy Metabolism	49
5.	Cellular Energy Metabolism	50

5.1. Glycolysis	52
5.2. Krebs Cycle, Electron Transport and Oxidative Phosphorylation	54
5.2.1. Overview of Krebs Cycle	55
5.2.2. Mitochondrial Composition	57
5.2.3. Electron Transport Chain (ETC)	58
5.2.3.1. Complex I/ NADH Ubiquinone Oxidoreductase	59
5.2.3.2. Complex II/ Succinate-Coenzyme Q Reductase	59
5.2.3.3. Complex III/ Coenzyme Q-Cytochrome c Reductase	60
5.2.3.4. Complex IV/ Cytochrome c oxidase	60
5.2.3.5. Complex V/ ATP synthase	61
5.2.4. Mitochondrial Turnover	62
5.3. Fatty Acid Metabolism	63
5.3.1. Fatty Acid Synthesis	63
5.3.2. Fatty Acid β -Oxidation	64
5.4. Nucleotide Synthesis	66
5.4.1. Purine Synthesis	66
5.4.2. Pyrimidine Synthesis	67
6. Energy Metabolism during Carcinogenesis	68
6.1. Cancer	68
6.2. Metabolic Flexibility	69
6.2.1. Determinant Factors of Metabolic Flexibility	70
6.2.2. Principal Factors involving in Regulation of metabolic flexibility	72
II. Articles	76
Articles 1 and 2	77
Skin aging	78
Articles 3 and 4	117
Skin Cancer	118
Article 5	149
Skin reconstruction	150
III. Conclusion and perspectives	178
IV. Appendix	193
Article 6	194
List of Publications	204
List of Presentations	205
V. References	207

« Le rôle du métabolisme oxydatif et énergétique dans le vieillissement cutané et la carcinogénèse UV-B induits »

Un nombre croissant de preuves suggère que l'équilibre de l'énergie cellulaire joue un rôle déterminant dans le processus de vieillissement et la carcinogénèse. Les mitochondries génèrent une grande quantité d'énergie par oxydation des glucides alimentaires (cycle de TCA) et des graisses (β -oxydation). Un dysfonctionnement dans ce processus peut entraîner l'apparition de maladies en particulier les troubles liés à l'âge et les cancers.

Une grande variété de facteurs; facteurs de stress intrinsèques et extrinsèques tels que les espèces réactive de l'oxygène (ROS), les oncogènes, des suppresseurs de tumeurs (intrinsèques), l'irradiation UV et le stress chimio-physique (extrinsèques) peuvent influencer le métabolisme mitochondrial.

De nombreux mécanismes de protection ont été mis au point pour éliminer les dommages supplémentaires et intracellulaires. Les enzymes antioxydants, les systèmes réparation de l'ADN, des points de contrôle du cycle cellulaire, l'apoptose, l'autophagie et le système immunitaire sont parmi les mécanismes qui tentent tous de minimiser les effets de ces dommages.

Toutes perturbations de ces systèmes de défense cellulaire peuvent être à l'origine de divers troubles tels que le vieillissement prématuré et le cancer. Dans ce projet de recherche, nous avons cherché à évaluer le rôle du métabolisme oxydatif et de l'énergie dans le vieillissement de la peau et le cancer induit par les UVB sur la peau.

Instabilité génomique, l'altération métabolique et le vieillissement précoce

Dans une première partie, nous avons cherché à établir un lien entre l'instabilité génétique, la production de ROS et l'altération métabolique dans le processus de vieillissement.

Afin de mieux comprendre la relation entre ces facteurs au cours de vieillissement, nous avons utilisé un modèle de souris transgéniques (le modèle de XPC knock-out). Le Xeroderma Pigmentosum de type C (XP-C) se caractérise principalement par une prédisposition aux cancers de la peau et le photovieillissement accéléré, mais il y a peu de données sur le vieillissement prématuré dans cette maladie.

Le rôle de XPC n'a jamais été montré au cours de vieillissement auparavant, c'est la raison pour laquelle nous avons essayé d'évaluer les marqueurs de vieillissement, la production des espèces réactives de l'oxygène (ROS) et le métabolisme énergétique en analysant deux groupes de souris, les souris jeunes et les souris vieilles en absence et en présence de XPC.

Après analyse de nos résultats, En conséquence, nous avons constaté que le niveau des marqueurs de vieillissement tels que la progérine, le p16INK4a, l'activité de la β -galactosidase et les espèces réactives de l'oxygène (ROS), qui augmentent normalement avec l'âge, et sont plus élevés chez les jeunes XPC^{-/-} que les souris jeunes XPC^{+/+}.

Nous avons également démontré une diminution significative de l'expression protéique et de l'activité des complexes mitochondriaux dans la peau des souris jeune XPC^{-/-} et les souris âgées XPC^{+/+} par rapport aux souris jeunes XPC^{+/+}. En outre, le profil métabolique chez les jeunes XPC^{-/-} ressemblait au profil trouvé chez les souris XPC^{+/+} âgées.

Les résultats obtenus sur le modèle de souris XPC KO ont démontré qu'un excès de stress oxydatif dû à une suractivation du NOX1, couplé à des altérations métaboliques, jouaient un rôle prépondérant dans le vieillissement prématuré. Notre équipe a déjà montré que la surexpression de NOX1 abouti à une surproduction de ROS dans les cellules déficientes XPC.

Afin de réduire la production de ROS induits par NOX1 et leurs dégâts respectifs dans des cellules déficientes XPC, notre équipe a décidé de développer un inhibiteur spécifique contre NOX1. Après avoir testé plusieurs séquences peptidiques différentes, nous avons identifié un peptide spécifique qui empêche l'assemblage de sous-unité NOX1A (Activator) à NOX1O (Organisateur). L'application topique de notre nouvel inhibiteur de NOX, induisant l'inhibition de la production de ROS et ainsi l'apparition d'altération métabolique, a permis d'empêcher le vieillissement cutané prématuré chez les souris XPC KO. Nos résultats suggèrent que l'InhNOX peut être considéré comme une cible prometteuse dans la prévention du vieillissement prématuré et les maladies liées à NOX.

UV, l'altération métabolique et la carcinogénèse cutanée

Les carcinomes cutanés sont les plus fréquents des cancers humains chez l'adulte. Leur incidence augmente régulièrement du fait de l'allongement de la durée de vie et des habitudes comportementales, en particulier l'exposition solaire répétée. En effet c'est sous la

dépendance des rayonnements UV que ceux-ci se développent et en particulier sous l'influence des UVB (60 à 70 % d'entre eux).

Le rôle des UV dans la genèse des carcinomes est soutenu par des arguments cliniques et épidémiologiques : l'incidence des carcinomes cutanés croît avec le niveau d'exposition solaire, ceux-ci surviennent préférentiellement sur les régions corporelles photo-exposées en association avec des lésions photo-induites bénignes (kératoses actiniques, lentigos solaires...) chez des sujets exposés au soleil. Une meilleure compréhension des mécanismes moléculaires de la réponse UVB-induite pourrait permettre l'identification de nouvelles cibles thérapeutiques et lutter contre la déviation du métabolisme énergétique des cellules cancéreuses ou précancéreuses.

Comprendre les mécanismes de la carcinogenèse épithéliale apparaît donc essentiel. En deuxième partie de ma thèse, notre intérêt s'est porté sur l'étude de la transformation métabolique dans le cancer cutané. En effet il existe une propriété particulière aux cellules cancéreuses, celle de modifier leurs caractéristiques énergétiques : on parle de remodelage bioénergétique. Une des propriétés des cellules cancéreuses consiste à métaboliser le glucose en acide lactique en grande quantité, même en présence d'oxygène : c'est l'effet Warburg. Pourtant la transformation métabolique des cellules cancéreuses reste peu connue, notamment la contribution de la reprogrammation du métabolisme dans l'initiation de la carcinogenèse.

Nous sommes donc intéressés particulièrement aux carcinomes épidermoïdes cutanés, également appelés carcinomes spinocellulaires. Ces carcinomes induits par l'exposition chronique aux UVB ont été étudiés en utilisant un modèle de souris de l'espèce SKH modifié génétiquement. Il a été démontré que les dommages induits par les UV dans la peau des souris SKH-1 reproduisaient de façon fidèle ceux observés dans la peau humaine.

Chez les souris SKH-1, l'exposition chronique aux rayonnements UV induit la survenue de carcinomes épidermoïdes cutanés, principalement bien différenciés et matures. Les tumeurs UVB-induites chez ces souris sont comparables à celles observées chez l'humain, et les données recueillies sont reconnues valides pour des analyses mécanistiques.

Nous avons donc cherché à étudier si la déficience du métabolisme mitochondrial prédisposait les kératinocytes soumis aux UVB à l'initiation de la transformation tumorale ou bien, au contraire, si en forçant les kératinocytes à utiliser la voie de la glycolyse pour leur production

d'ATP, nous arrivions à inhiber la formation de ces tumeurs UVB induites. Pour cela, nous avons créé un modèle murin original en croisant des souris *Tfam*^{flox/flox} avec des souris K14-Cre-ER^{T2} exprimant une CRE recombinase sous le contrôle du promoteur K14 spécifique des kératinocytes, avec des souris SKH-1 hairless.

L'objectif de cette partie a donc été d'étudier l'impact des altérations bioénergétiques dans l'initiation des cancers cutanés UVB induits :

-sur un modèle murin hairless dont le métabolisme mitochondrial est altéré grâce à la délétion du facteur de transcription mitochondrial *Tfam*.

-sur un modèle murin hairless non délété afin d'évaluer la voie principale énergétique mise en jeu.

Très peu d'informations sont disponibles sur la contribution de la reprogrammation du métabolisme énergétique dans l'initiation et la progression du cancer. Nous avons ensuite démontré que l'irradiation chronique aux UVB entraînait une diminution de l'activité de la glycolyse, du cycle TCA et de la β -oxydation des acides gras, tandis que la synthèse d'ATP mitochondrial et une partie de la chaîne de transport d'électrons (CTE) étaient up-régulés.

Nous avons montré que l'augmentation accrue de CTE était liée à la suractivation des dihydroorotate déshydrogénase (DHODH), alors que la diminution de l'activité DHODH ou ETC (chimiquement ou génétiquement) avait conduit à une hypersensibilité à l'irradiation UVB. Nos résultats indiquent que la voie DHODH, par l'induction de la synthèse d'ATP et de CTE, joue un rôle majeur dans l'efficacité de réparation d'ADN et la reprogrammation métabolique au cours de la carcinogenèse UVB-induits.

Nous espérons à terme mettre au point à partir des nouvelles cibles définies, une thérapie ciblant la déviation du métabolisme énergétique des cellules cancéreuses et/ou précancéreuses, à côté de celles déjà définies par notre équipe sur la production d'espèces réactives de l'oxygène (ROS) qui promeuvent l'effet Warburg.

LIST OF FIGURES

	<u>Page</u>
Fig.1. Cross-Section of the Skin	3
Fig.2. Solar Radiation and its Effects on Skin	8
Fig.3. Human Skin Phototypes	9
Fig.4. Major UV-induced DNA Damages	13
Fig.5. Subunit Composition of Mammalian NADPH oxidase isoforms	16
Fig.6. Melanin synthesis (A) and distribution of melanosomes in different skin types (B)	22
Fig.7. Nucleotide excision repair (NER) reactions	26
Fig.8. All types of DNA damages and repair mechanisms	29
Fig.9. Overview of antioxidants systems	31
Fig.10. Mechanism of enzymatic and non-enzymatic antioxidant activity	33
Fig.11. Multiple Pathways to Senescence	37
Fig.12. Skin Aging	40
Fig.13. A Model for the Role of Unresolved DNA Lesions in Aging	43
Fig.14. Different Types of Autophagy	44
Fig.15. Autophagy and its Inhibitors	47
Fig.16. Glycolysis Pathway	54
Fig.17. Mitochondria and oxidative phosphorylation chain	57
Fig.18. Organisation of Electron Transport Chain	59
Fig.19. <i>De novo</i> fatty acid biosynthesis	64
Fig.20. Overview of fatty acids β -oxidation	65

Fig.21. Purine <i>de novo</i> biosynthesis	66
Fig.22. Pyrimidine <i>de novo</i> biosynthesis	67
Fig.23. Therapeutic Targeting of the Hallmarks of Cancer	69
Fig.24. NOX enzymes as validated therapeutic targets	181
Fig.25. The role of NOX complexes and NOX-derived ROS in the progression of carcinogenesis	182
Fig.26. Integration of NOX oxidase-derived ROS with the hallmarks of cancer	183
Fig.27. Different Types of NOX Inhibitors and their Specific Site of Action	184
Fig.28. Overview of metabolic alterations in malignant cells	186
Fig.29. Nucleogenesis: Dihydroorotate dehydrogenase	188
Fig.30. Metabolic Targets for Cancer Therapy	189
Fig.31. The main pathways involved in carcinogenesis	191

LIST OF TABLES

	<u>Page</u>
Table 1. Layers of the Skin	3
Table 2. The solar spectrum wavelength ranges	7
Table 3. NADPH oxidase families	17
Table 4. Transcription Factors Sensitive to the Redox State	20
Table 5. Compartmentalization of Metabolic Pathways	50
Table 6. Overview of mitochondrial structure, inhibitors and disorders	61

NOMENCLATURE

Ⓐ

ACLY	ATP Citrate Lyase
ADP	Adenosine Diphosphate
AIF	Apoptosis Inducing Factor
AK	Actinic Keratoses
AKT	Serine/Threonine-Specific Protein Kinase
AMPK	5' AMP-Activated Protein Kinase
AP	Apuriniques Or Apyrimidinic Sites
AP1	Activator Protein1
Atg	Autophagy-Related Genes
ATP	Adenosine Triphosphate

Ⓑ

BCC	Basal Cell Carcinoma
Bcl-2	B-Cell Leukemia/Lymphoma-2
BER	Base Excision Repair System

Ⓒ

Ca²⁺	Calcium
CAD	Carbamoyl Phosphate Synthetase II
CAT	Catalase
CC	Cutaneous Carcinomas
CDK	Cyclin-Dependent Kinase
CGD	Chronic Granulomatous Disease
CH	Contact Hypersensitivity
CMA	Chaperone-Mediated Autophagy
CML	Chronic Myelogenous Leukemia
CNS	Central Nervous System
CO₂	Carbon Dioxide
COOH	Carboxylic Acid
CoQ	Ubiquinone
COX	Cytochrome C Oxidase
CPD	Cyclobutane Pyrimidine Dimer
CS	Cockayne Syndrome
CS	Citrate Synthase
CuZnSOD	Copper-Zinc Superoxide Dismutase

Ⓓ

DCA	Dichloroacetate
DHODH	Dihydroorotate Dehydrogenase
DNA	Deoxyribonucleic Acid
DOUX	Dual Oxidase
DPI	Diphenyleneiodonium
DSB	Double-Strand Breaks

Ⓔ

EC-SOD	Extracellular Superoxide Dismutase
EGF	Epidermal Growth Factor
END-1	Endothelin 1
ENDRB	Endothelin Receptor B
ER	Endoplasmic Reticulum
ERK	Extracellular Signal Regulated Kinase
ETC	Electron Transport Chain

Ⓕ

F6P	Fructose-6-Phosphate
FA	Fatty Acid
FAD	Flavin Adenine Dinucleotide
FAD	Flavin Adenine Dinucleotide
FASN	Fatty Acid Synthetase
FH	Fumarate Hydratase
FOX	Forkhead Box

Ⓖ

G3P	Glyceraldehyde 3-Phosphate
G6P	Glucose-6-Phosphat
G6PD	Glucose-6-Phosphate Dehydrogenase
GGR	Global Genome Repair
GLUT	Glucose Transporters
GPI	Glucose Phospho Isomerase
GSH	Glutathione Peroxidase
GTP	Guanosine-5'-Triphosphate

Ⓖ

H₂O₂	Hydrogen Peroxide
HGPS	Hutchinson–Gilford Progeria Syndrome
HIF1α	Hypoxia Inducible Factor 1 α
HITS	Multiple Genetic and Epigenetic Alterations
HLA	Human Leukocyte Antigen
Hmlh1	Human Mutl Homolog 1
Hnth	Human Endonuclease III
hOgg1	Human 8-Oxoguanine DNA N-Glycosylase 1
Hox-B5	Homeobox Protein
hTERT	Human Telomerase Reverse Transcriptase

I		NH₂	Amine Group
I/R	Ischemia-Reperfusion	NHEJ	Non-Homologous End-Joining,
IDH	Isocytate Dehydrogenase	Nix	Nip3-Like <i>Protein X</i>
IL	Interleukine	NO[•]	Nitric Oxide Radical
InhNOX	NOX Inhibitor	NOX	Nicotinamide Adenine Dinucleotide Phosphate Oxydase
J		NOXA	NADPH Oxydase Activator
JNK	Jun N-terminal Kinase	NOXO	NADPH Oxydase Organisator
K		NRF	Nuclear Respiratory Factor 1
Kcal	Kilo Calori	O	
KDa	Kilodalton	O₂	Molecular Oxygen
KL	KIT Ligand	¹O₂	Singlet Oxygen
L		O₂^{•-}	Superoxide Anion
LDH	Lactate Dehydrogenase	OH[•]	Free Radical Hydroxyl
LMDS	Locally Multiple Damages Sites	OMP	Orotidine-5'-Monophosphate
LMNA	Lamin A	ONOO[•]	Peroxynitrite
M		OXPHOS	Oxidative Phosphorylation Chain
Mapk	Mitogen-Activated Protein Kinase	P	
Mats	Molecular-Targeted Agents	PCNA	Proliferating Cell Nuclear Antigen
MC1R	Melanocortin 1 Receptor	PDH	Pyruvate Dehydrogenase
MCT	Monocarboxylate Transporters	PDK	Pyruvate Dehydrogenase Kinase
MM	Malignant Melanomas	PEO	Progressive External Ophthalmoplegia
MMP-1	Matrix Metalloproteinase-1	PEP	Phosphoenol Pyruvat
MnSOD	Manganese SOD	PFK	Phosphofructokinase
mRNA	Messenger RNA	PG	Phospho Glycerate
mtDNA	Mitochondrial DNA	PGC1α	Peroxisome Proliferator-Activated Receptor (PPAR)- Γ Coactivator-1 α
mTOR	Mechanistic Target Of Rapamycin	PHD	Prolyl Hydrylases
N		PI3K	Phosphatidylinositol-3- Kinase
Na⁺K⁺Atpase	Sodium-Potassium Adenosine Triphosphatase	PINK1	PTEN Induced Putative Kinase- Protein 1
NAD	Nicotinamide Adenine Dinucleotide	PIP₂	Phosphatidylinositol (3,4)- Bisphosphate
NADP	Nicotinamide Adenine Dinucleotide Phosphate	PIP₃	Phosphatidylinositol (3,4,5)- Trisphosphate
NADPH	Nicotinamide Adenine Dinucleotide Phosphate	PKC	Protein Kinase C
NARP	Neuropathy, Ataxia, And Retinitis Pigmentosa	PKM	Pyruvat Kinase
Nbs1	Nibrin	PMCA	Plasma Membrane Ca ²⁺ Atpase
nDNA	Nuclear DNA	PMLE	Polymorphous Light Eruption
NER	Nucleotide Excision Repair	PMS	Postmeiotic Segregation
NF-1	Nuclear Factor -1	Pol	Polymerase
NF-κb	Nuclear Factor Kappa-Light-Chain- Enhancer Of Activated B Cells	POMC	Pro-Opio-Melano-Cortin
		PRPP	5-Phospho-A-D-Ribosyl 1- Pyrophosphate
		pVHL	Von Hippel-Lindau

<u>R</u>		USF	Upstream Stimulatory Factor
Rac1	Ras-Related C3 Botulinum Toxin Substrate 1	USP7	Ubiquitin-Specific Protease 7
RAPTOR	Regulatory Associated Protein Of TOR	UV	Ultraviolet
Redox	Oxidation And Reduction	UVRAG	UV Radiation Resistance-Associated Gene Protein
RFC	Replication Factor C	UVSSA	UV-Stimulated Scaffold Protein A
RFC	Replication Factor C	<u>Y</u>	
RNA	Ribonucleic Acid	VDAC	Voltage Dependent Anion Carrier
ROS	Reactive Oxygen Species	VEGF	Vascular Endothelial Growth Factor
RPA	Replication Protein A	Vps34	Vacuolar Protein Sorting 34
rRNA	Ribosomal Ribonucleic Acid	<u>Z</u>	
RTK	Receptor Tyrosine Kinase	X-Gal	5-Bromo-4-Chloro-3-Indolyl-B-D-Galactopyranoside
<u>S</u>		XP	Pigmentosum Repair
SAPK	Stress-Activated Protein Kinase	XRCC	X-Ray Repair Complementing Defective Repair In Chinese Hamster Cells
SA-β-Galactosidase	Senescence-Associated β-Galactosidase	<u>Z</u>	
SCC	Spinocellular Carcinoma	Zn²⁺	Zinc Ion
SCF	Stem Cell Factor	<u>Others</u>	
SCID/ NOD	Severe Combined Immunodeficiency		
SCO2	Cytochrome Oxidase Deficient Homolog 2		
SDH	Succinate Dehydrogenase		
SLC	Solute Carrier		
SOD	Superoxide Dismutase		
SP1	Specificity Protein 1		
SSB	Single Strand Break	α-MSH	Alpha Melanocyte Stimulating Hormone
<u>T</u>		Δψ_m	Mitochondrial Transmembrane Potential
TCA	Tricarboxylic Acid Chain	4-OHT	4-Hydroxytamoxifen
TCR	Transcription-Coupled Repair	6-4 PP	Pyrimidine-Pyrimidone (6-4) Photoproduct
TF	Transcription Factor	8-oxo-dg	7,8-Hydro-8-Oxodeoxyguanosine
TFAM	Transcription Factor A, Mitochondrial		
TGF-β	Transforming Growth Factor-B		
TIM	Translocase Of Inner Membrane		
TNF-α	Tumor Necrosis Factor-A		
TOM	Translocase Of Outer Membrane		
TP53	Tumor Protein 53		
tRNA	Transfer Ribonucleic Acid		
Trx	Thioredoxin		
TTD	Trichothiodystrophy		
<u>U</u>			
UCA	Urocanic Acid		
UDP	Uridine-5'-Diphosphate		
UMP	Uridine-5'-Monophosphate		

DEDICATION

**Not necessarily the value of the work,
But Necessarily the Merit of All Great Effort & Enthusiasm Honestly went on it...**

Dedicated To:

My virtuous father, Ali HOSSEINI who could not sadly be here of course to witness all joy and happiness came to me for my graduation. He is always with me of course, I am sure and I would never forget all his generous encouragements during my studies and my thesis project which led me toward entering the realm of Cancer Therapy. His love and support are what carried me through difficult times, helped me believe in myself and led me to more than I ever hoped for...

There is not even a single day passing empty of thinking about you, Dad...

LOVE YOU FOREVER...

ACKNOWLEDGEMENTS

First and foremost, I would like to express my deepest gratitude to Hamid, my advisor, for his patience, motivation, enthusiasm, and immense knowledge. It has been an honor to be his first Ph.D. student. His guidance helped me in all the time of my life and my research work. I could not have imagined having a better advisor and mentor for my Ph.D study.

Besides my advisor, I would like to thank the members of jury who accept to be in the final committee; Pr. Egly, Pr. Taieb, Pr. Rosenbaum, Dr. Kluza, Dr. Rachidi and dear Rodrigue

I would like to thank Pr. De Verneuil to accept me in his laboratory and for his help on biochemical analysis.

I am also deeply thankful to Pr. Taieb, the head of Dermatology team, for his support, his kindness, his invitations to Arcachon and his delicious foods especially his fish soup.

My sincere thanks also goes to Rodrigue for his nice suggestions. He has encouraged me and helped me to develop my knowledge about metabolism. The discussion with him was a great opportunity for me to better understand metabolic changes in cancer.

Also I thank Walid who as a good friend was always willing to help and give his best suggestions, also I appreciate Martin for his kindness and his suggestions. I thank Vanessa for his patience and good/hard working. My research would not have been possible without their helps. Grateful thanks also to Mojgan for her suggestions, her kindness and her perfect antibodies.

Appreciation also goes out to Anne-Karin for her nice and hard work at NMR laboratory, she has taught me working hard and always be cool. Many thanks to Isabelle and Samir at Biochemistry service of Pellegrin hospital. They have offered me a good notion about team-working.

Thanks to Emilie, the Cellomet Chief Operating Officer, who was always full of energy such as a mitochondrion. Thank you for your kindness and encourages.

Many thanks to Zeinab for her work, her kindness and her helps. I wish you a nice PhD thesis.

I would also like to recognize the contributions and support of my colleagues. I thank Léa, Catherin, Dorian and Isabelle LG. Isabelle, I never forget your kindness.

I appreciate Marija and Véronique for their kindness and helps and also Pierre Costet to support my mice models during all these years.

In addition many thanks to Katia Obama and Isabelle Lammy for their kindness and helps. They are the nice people which I met during this time. I thank also my fellow labmates in Inserm U1035.

I would also like to thank my family, especially my mother, for the support they provided me through my entire life and in particular, I must acknowledge my love and best friend, Samira, without whose love, encouragement and editing assistance, I would not have finished this thesis.

ABSTRACT

Objective of the present research study was investigating the role of oxidative and energy metabolism in skin aging and UVB-induced skin cancer. In the first part, we aimed to find the link between genetic instability, ROS generation and metabolism alteration in the process of aging. The obtained results on XPC KO mice model demonstrated that excess of oxidative stress in addition to alterations in energy metabolism due to over activation of NOX1 play a causative role in premature skin aging. Topical application of novel NOX inhibitor prevented the premature aging in XPC KO mice through inhibition of ROS generation and alteration of energy metabolism. Our results suggest that the InhNOX can be considered as a promising target in prevention of premature aging and NOX-associated diseases.

Little information is available on the contribution of energy metabolism reprogramming in cancer initiation and promotion. To assess the role of metabolic reprogramming in different phases of carcinogenesis, in the second part of my thesis we employed a multistage model of ultraviolet B (UVB) radiation-induced skin cancer. We showed that chronic UVB irradiation results in decreased glycolysis, TCA cycle and fatty acid β -oxidation while at the same time mitochondrial ATP synthesis and a part of the electron transport chain (ETC) are up-regulated. Increased ETC was further found to be related to the over-activation of dihydroorotate dehydrogenase (DHODH). Decreased activity of DHODH or ETC (chemically or genetically) led to hypersensitivity to UVB irradiation. Our results indicated that DHODH pathway through induction of ETC and ATP synthesis represents the relation between DNA repair efficiency and metabolism reprogramming during UVB-induced carcinogenesis.

Key words: energy metabolism, ROS, NOX, aging, DHODH, cancer.

INTRODUCTION

Chapter I

Solar Irradiation and Photoprotection

1. Skin structure and function

Skin is the first physical barrier of the human body which accounts for 7% of its total weight with a surface area of 1.8 m².

Skin brings off several functional roles such as thermal, chemical and mechanical protection against the outer environment. Secretion of sweat and sebum and perception of external information are among these functional roles.

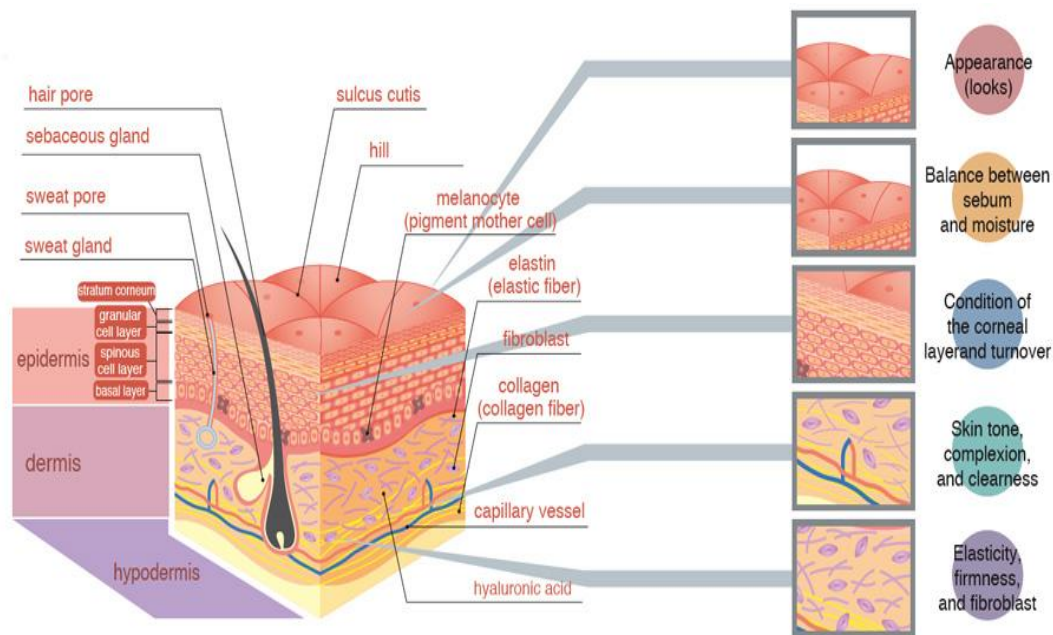


Fig.1. Cross-Section of the Skin (from <http://www.collagenetix.com>).

Table 1. Layers of the Skin.

Skin layers	Description
Epidermis	The upper or outer layer of the skin made up of keratinocytes, melanocytes, Langerhans and Merkel cells
Basement membrane	The connective tissue composed of a layer of basal lamina
Dermis	The inner layer of the skin containing blood and lymph vessels, hair follicles, glands, and a significant number of fibroblasts
Hypodermis	The deeper layer of the dermis mainly containing fat and connective tissue

1.1. Skin Anatomy

Skin is made up of three structural layers including epidermis, dermis and hypodermis (subcutis) which differ in function, thickness and strength. Epidermis is the outer layer which serves as the first and the most important barrier against the exterior environment. The second layer called dermis contains nerve endings, sweat glands, oil glands, and hair follicles giving a structural form to the skin. The layer found below the dermis called subcutis or hypodermis which is primarily used for fat storage.

1.2. Structure of Epidermis

Epidermis is mainly made up of keratinocytes (90-95%) and its thickness varies from 50µm on the eyelids to 0.8-1.5 mm on the feet soles and palms of the hand. Epidermis is rich in nerve endings and not irrigated by any blood vessels.

Epidermis is composed of five layers:

- Stratum Corneum (Horny Layer)
- Stratum Lucidum (Clear Layer)
- Stratum Granulosum (Granular Cell Layer)
- Stratum Spinosum (Spinous or Prickle Cell Layer)
- Stratum Basale (Basal or Germinativum Cell Layer)

Keratinocytes become regularly renewed from the cells originated from stratum basale the deepest layer of the skin. Then they migrate to the uppermost layer of epidermis known as stratum corneum. Consequently, epidermis becomes totally renewed by itself in every 25 to 50 days. Other cell types present in the epidermis in addition to keratinocytes include melanocytes, Langerhans and Merkel cells.

1.2.1. Keratinocytes

Keratinocytes are the main cells of the epidermis originating from the stratum basal layer. They synthesize a number of structural proteins (filaggrin, keratin), enzymes (proteases), lipids and antimicrobial peptides (defensins) which contribute to the maintenance of the barrier function of the skin. They serve a waterproof function in the skin as a barrier as well.

1.2.2. Melanocytes

Melanocytes are specialized melanin-producing cells, mainly present in the basal layer of the skin. They account for 5 to 10% of epidermal cells. Their product, melanin, a dark pigment serves as skin protector against solar radiation. The color of hair and skin is dependent on the synthesis of melanin where local accumulation of melanin and melanocytes give rise to freckles and nevi respectively. Melanocytes along with neighboring keratinocytes of basal and spinous layers constitute the epidermal melanization unit. Transfer of melanosomes (organelles containing melanin) from melanocytes to keratinocytes occurs within this unit.

1.2.3. Langerhans Cells

Located in the middle part of the epidermis (Stratum Spinosum), Langerhans cells (2-8% of epidermal cells) are pillars of innate immune defense of the skin. These dendritic cells are produced in the bone marrow. They migrate into the epidermis and contribute to the activation of the adaptive immune system cells. Indeed, they are able to ingest foreign particles and microorganisms and present their epitopes to T cells by the molecules of class II histocompatibility complex. Thus, they can migrate from the skin to the draining lymph nodes.

1.2.4. Merkel Cells

Present in small quantities in the basal layer (1% of cells), Merkel cells are cells of the neuroendocrine system which are closely related to sensory nerve endings. They form a Merkel disk and probably have a role in skin neurosensory/ neuroendocrine system which is still poorly understood.

1.3. Dermis Structure

Dermis is a flexible envelope which provides most of the biomechanical properties of the skin. Located beneath the epidermis, its thickness varies depending on the body part which is very thick in the palms and soles and very thin on the eyelids. Dermis is highly vascularized and is involved in the management of body temperature by the expansion or constriction of the vessels. It is also rich in collagen connective fibers and provides support and resistance for the skin. Elastin is another type of fiber present in dermis which is responsible for the

elasticity and flexibility of healthy skin. These two types of fibers are produced by fibroblasts, the main resident cells of the dermis and are gradually decreasing during aging.

Morphologically, dermis is made up of two parts of dense connective tissue:

- Papillary/ adventitial part: This layer is located under the basal layer of the epidermis and hosts epidermal appendages, receptors for pain (free nerve endings) and touch (lamellar Meissner corpuscles) as well. Some regions such as the ends of the fingers, palms and soles of the feet are dotted with small papillary projections.
- Reticular zone: This deep layer of the dermis contains blood vessels, sweat and sebaceous glands, pressure receptors (Pacinian corpuscles) and numerous phagocytic cells which prevent bacterial penetration.

1.4. Hypodermis

Hypodermis or subcutaneous tissue substantially consists of fat tissue and is divided in fat lobules by thin connective-tissue septa. The fat cells protect lower layers from cold and store energy. At this level, there are blood vessels of larger caliber, nerve fibers and hair roots as well as sebaceous and sweat glands. Hypodermis becomes thinner with aging.

2. Solar Radiation

Solar spectrum consists of continuous emission spectrums which among them are ultraviolet radiation with wavelengths less than 400 nm, visible light formed by the radiation wavelength between 400 and 700 nm and infrared radiation of high wavelengths above 700 nm (Table 1). UVs are arbitrarily divided into 3 wavelength ranges: UVA, UVB and UVC. Indeed, it is only UVA and a small fraction of UVB rays which reach the surface of the earth since UVC and the most of UVB are absorbed by the ozone layer and molecular oxygen in the stratosphere (Table 2 and Figure 2).

The amount of UVB radiation reaching the surface of the earth varies in different conditions such as time, season and altitude whereas the flow of UVA is more stable. Over 60% of the total UV irradiation is received between 11 am and 15 pm (solar time).

Sunlight before attenuation by the atmosphere contains 13 times more UVA than UVB with 6.3%, and 0.5% respectively. while after attenuation by the atmosphere, the solar light is composed of about 10^2 to 10^3 times more UVA than UVB.

The thinning of the ozone layer allows more UVB radiation to reach the earth's surface and consequently the skin. According to experts, every 1% reduction of the ozone layer is associated with an increase of 2% of UVB radiation flux at the surface of the earth. These UV radiations cause a range of acute and chronic skin lesions.

Table 2. The solar spectrum wavelength ranges.

Main Solar Waves	Spectrum Type	Wavelength (nm)	Wavelength Description
Short- Wave	UV-C	100-280 nm	Emitted from the sun, totally absorbed by earth's atmosphere before reaching the earth
	UV-B	280-320 nm	Emitted from the sun, 90% absorbed by earth's atmosphere but biologically very active
	UV-A	320-400 nm	Emitted from the sun, most reaches the ground
Long-Wave	Visible	400-780 nm	Visible light from violet to red (color of rainbow)
	NIR*	780-3 μ m	Heat radiation from the sun
	FIR**	3-50 μ m	Heat radiation from the atmosphere, clouds, earth and surrounding

* Near infrared (NIR)

**Far infrared (FIR)

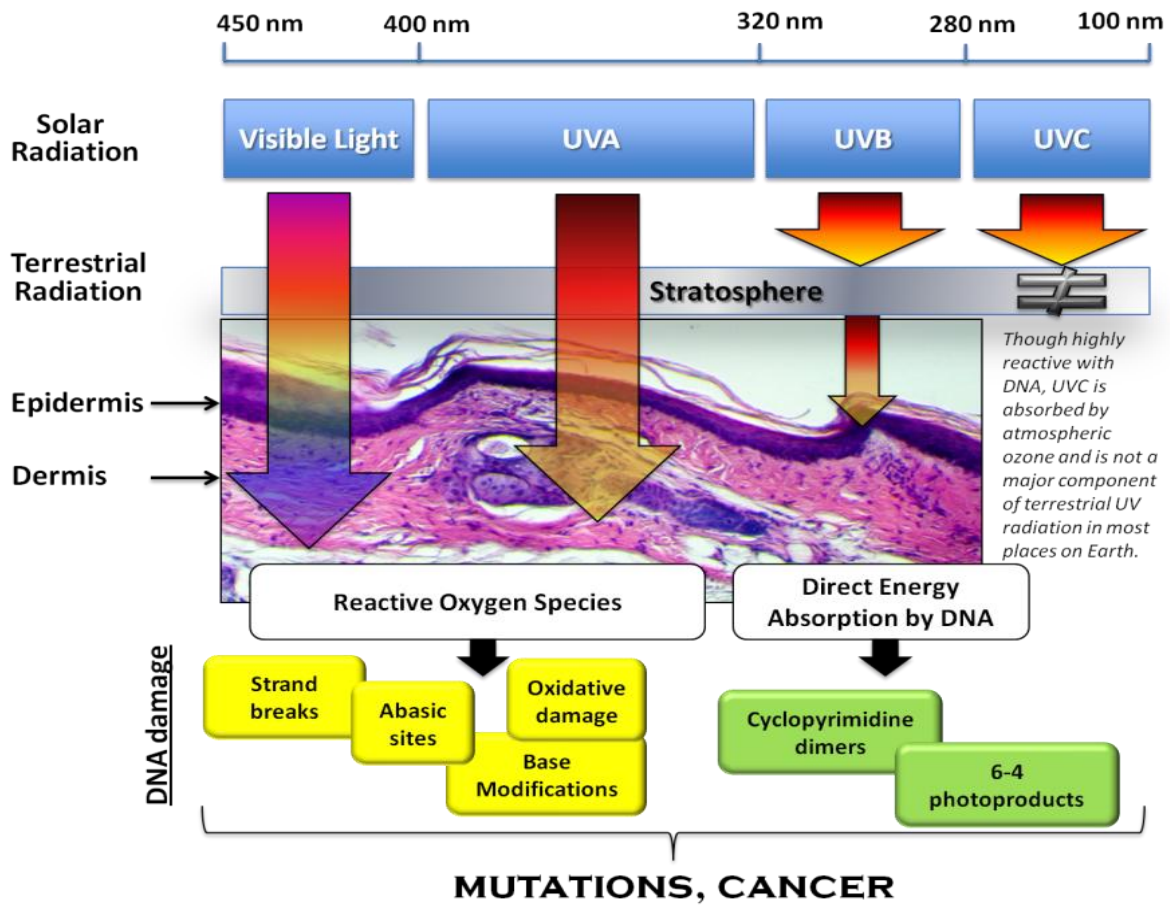


Fig.2. Solar Radiation and its Effects on Skin (D’Orazio et al. 2013).

Human skin is also exposed to other types of radiation called ionizing radiation (IR). These more energetic radiations transfer enough energy to electrons to tear them from their atom. Ionizing radiations include:

- Radiations of cosmic origin
- X- rays and γ rays
- α , β particles
- Neutrons

X-rays are the most energetic waves of the electromagnetic spectrum which are generated when electrons strike a metal target. γ rays are produced in the disintegration of radioactive atomic nuclei and in the decay of certain subatomic particles while α , β particles are emitted by radioactive atoms as they decay.

2.1. Effects of UV on Skin

Various factors such as the dose and wavelength of UV and skin characteristics play a role in the skin response to UV radiation. In the acute phase, response may be moderate leading to inflammation and sunburn while accelerated aging and skin cancer are chronic responses of the skin to UV radiation (Kullavanijaya and Lim 2005).

2.1.1. Acute Skin Lesions

A. Sunburn. Sunburn (Solar Dermatitis) is an acute inflammatory reaction triggered by keratinocytes which are damaged due to exposure to UVB. The release of inflammatory mediators results in local and systemic reactions such as fever. Sensitivity to UVB is individual-specific depending on the skin type. There are six types of skin categorized depending on the individual ability to react to the sun (Figure 3). Phototypes I and II tend to generate violent inflammatory reactions even after low exposure. These skin phototypes have a greater risk of developing skin cancer.

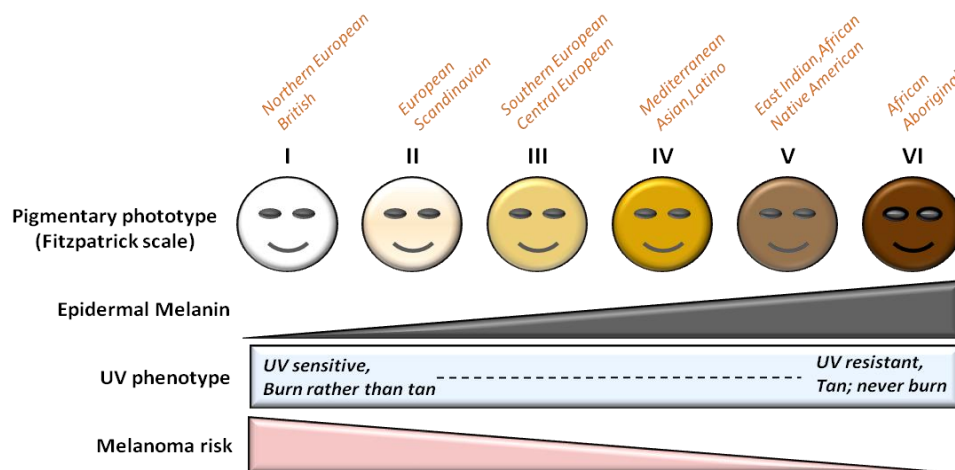


Fig.3. Human Skin Phototypes (D’Orazio et al. 2013).

B. Polymorphic Photoreaction ("Sun Allergy"). Polymorphous light eruption (PMLE) is the most common polymorphic photoreaction mainly affecting young women in the spring after severe exposure to UV especially UVA. It is manifested by pruritic papules in exposed areas, 2-48 hours after exposure. It is monomorphic and reappears in the same form after further exposure of unprotected skin to UV. Diagnosis is based on history and typical photo provocation. Photo tests allow confirmation of the diagnosis and possibly individual prevention by sun protection or preventive therapy.

C. Urticaria and Other Idiopathic Photodermatoses. Solar urticaria is a rare photodermatosis. Papules appear a few minutes after sun exposure (UVA, UVB or visible spectrum) in both covered and uncovered areas of the skin and persist from a few minutes to several hours.

Actinic prurigo is a chronic skin disease difficult to diagnose due to high similarity to other skin disorders. First described among Native Americans, it is related to immunogenetic predisposition (HLA, Human Leukocyte Antigen) (Hojyo-Tomoka et al. 2003). There are rare photodermatoses in children presenting with varioliform lesions called hydroa vaccini formis.

D. Phototoxic and Photoallergic Reactions. Numerous chemicals modify their structure under the effect of UV rays and can trigger allergic or toxic reactions. A typical example of phototoxic dermatitis reaction is caused by plants (photophytoprotophytodermatosis).

E. Dermatoses caused by UV. There is a whole list of diseases which are caused or aggravated by UV ranging from inflammatory autoimmune disorders such as systemic lupus erythematosus to metabolic diseases like porphyria (Murphy 2001).

2.1.2. Chronic Skin Lesion under UV Effect

- **Aging in the Skin** - UV lesions of the dermis and epidermis. Repetitive doses of UVA diminish the elasticity of the dermis and dry the skin by altering the stratum corneum and cause hyper and hypopigmentation. Dermal UVA effects are pathophysiologically due to the induction of lysozymes and secretion of metalloproteinases (Ohnishi et al. 2000; Fisher et al. 2001; Philips et al. 2011) at the level of collagen and elastic fibers, which are also considered as the initial phase of actinic elastosis. Senile keratosis, actinic keratoses and sebaceous gland hyperplasia are other effects of chronic sun exposure for the unprotected skin.

- **Immunosuppression.** UV irradiation can decrease the immune functionality of skin. More details on immunosuppressive effects of UV rays are discussed in section 3.2.

- **Skin Cancer.** Photocarcinogenesis is defined as the set of events leading to skin cancer after exposure to the sun. Ultraviolet irradiation is involved in the initiation and promotion of tumor leading to malignant transformation of keratinocytes or melanocytes. Based on their cellular origin, skin cancers are classified into two groups: melanomas and carcinomas. Melanomas come from melanocytes and carcinomas from keratinocytes. Cutaneous carcinomas are divided into basal cell carcinomas (BCC) and squamous cell carcinomas or

spinocellular carcinomas (SCC) (for more detail see my second review article on metabolism and skin cancer) (Matsumura and Ananthaswamy 2004; Young 2009).

3. Key Players in the Response to UV

The increased risk of skin cancer due to UV exposure and decrease in ozone layer has highlighted the urgent need to improve photoprotective measures. To this end, a vast knowledge on various cellular signaling pathways which modulate the skin responses to UV is essential. The four principal actors in induction of signal transduction against UV are activation of membrane receptors, immune system, direct DNA damages and oxidative stress.

3.1. Growth Factors and their Receptors in the Cellular Response to UV

Keratinocytes can respond to UV by releasing growth factors and induction of the activity of their receptors. It has been shown that UV-irradiated keratinocytes release a number of cytokines and growth factors such as EGF (Epidermal Growth Factor), TNF- α (Tumor Necrosis Factor- α) and TGF- β (Transforming Growth Factor- β) (Heck et al. 2004; Kawaguchi and Hearing 2011). Binding of these factors to the specific receptors leads to their activation through the phosphorylation of their tyrosine residues.

For example, activation of the membrane receptors triggers the initiation of kinase cascades among them a particular kinase family called MAPK_s (Mitogen-Activated Protein Kinases). MAPK_s is a family of kinases composed of three subgroups called ERK (Extracellular signal Regulated Kinase), p38 MAPK and JNK / SAPK (Jun N-terminal Kinase/ Stress-Activated Protein Kinase). Activation of these kinases leads to the phosphorylation of several substrates (Bender et al. 1997; Bode and Dong 2003).

Direct activation of growth factor receptors is the other mechanism by which UV can trigger signaling pathways. Indeed, several receptors like TNFR1, Fas and EGFR can be activated directly by irradiation without a need for their ligands (Rosette and Karin 1996; Aragane et al. 1998). In addition, it has been found that UV irradiation leads to down-regulation of EGF and TGF- β receptors as well as decreased receptor/ ligand binding (Heck et al., 2004).

3.2. Immune System and Response to UV

Many experimental studies have shown that UV radiation especially UVB has a suppressive effect on the immune system (Schwarz 2005; Rana et al. 2008). This effect was first

highlighted by a decrease in contact hypersensitivity (CH), a strong inflammatory reaction triggered by haptens applied to the skin, which is abolished in animals exposed to varying doses of UVB. This effect is also sometimes noted for subcutaneously injected antigens.

Photoimmunosuppression occurs in different ways:

- Direct effect of UV on Langerhans cells. This effect leads to a decrease of co-stimulatory functions of these cells on lymphocytes (Simon et al. 1992; Ullrich 1995; Seité et al. 2003).

- Production and release of cytokines (TNF- α , IL-1, IL-6, IL-8, IL-10, IL-12, IL-15) and prostaglandins by keratinocytes subsequently acting on the morphology and the capacity of migration or presentation of Langerhans cells (Kurimoto and Streilein 1992; Moodycliffe et al. 1994; Shreedhar et al. 1998; El-abaseri et al. 2013)

- The appearance of CD36⁺/ DR⁺/ CDI^{a-} cells in the epidermis after UV exposure (Cooper et al. 1986; D'Atri et al. 2011).

- The direct or indirect effects of UV on DNA have been shown to result in immunosuppression. Possible mechanisms involved in this event are: i) Induction of immunosuppressive cytokines production by damaged DNA, ii) the modulation of the activity of genes encoding for certain molecules involved in antigen presentation, and iii) activation of the intervening DNA repair enzymes in yet unknown steps (Simon et al. 1994; Nishigori et al. 1996; Vink et al. 1996; Halliday et al. 2012).

- Production of cis-urocanic acid by the isomerization of trans-urocanic acid (UCA), a photoreceptor located in the stratum corneum which has a role of water-sensing (Streilein et al. 1994; Norval et al. 1995; Gibbs et al. 2008). Indeed, a subcutaneous injection of cis-UCA has the same effect on inhibition of contact hypersensitivity as UVB (Kondo et al. 1995).

A role of the immune system in the tolerance of UV-induced skin cancers has been demonstrated by some studies (Domingo and Baron 2008; Yu et al. 2014). UV-induced tumors are highly antigenic and subject to rejection when transplanted into healthy and non-irradiated mouse skin. Instead, these tumors are not rejected when transplanted into the UVB irradiated syngeneic animals (Donawho and Kripke 1991). In addition, the elevated growth of tumor cells grafted into the UV-exposed mice compared to non-irradiated mice showed the importance of the immune system during photocarcinogenesis (Donawho et al. 1996).

In humans, 90% of subjects who have had at least one skin carcinoma failed to develop CH after irradiation while only 40% of healthy individuals correspond to this phenotype (Yoshikawa et al. 1990). This shows indirectly the importance of a predisposition to UV-induced immunosuppression in the occurrence of carcinomas. The evolution of certain viral and bacterial or parasitic infections after exposure to UVB shows a higher susceptibility to the infectious diseases in individuals frequently exposed to the sun (McLelland and Chu 1990; Langhoff et al. 1993; Vermeer and Hurks 1994; Fletcher 2004; Wang and Deubel 2011).

3.3. DNA Damage and Response to UV

UV-induced DNA damages have a great diversity due to the multiple interactions of radiations with the genome. Such damages may be the result of a direct absorption of photons by DNA bases or of an indirect effect related to the production of free radicals induced by UV irradiation. The main DNA damages are shown in figure 4.

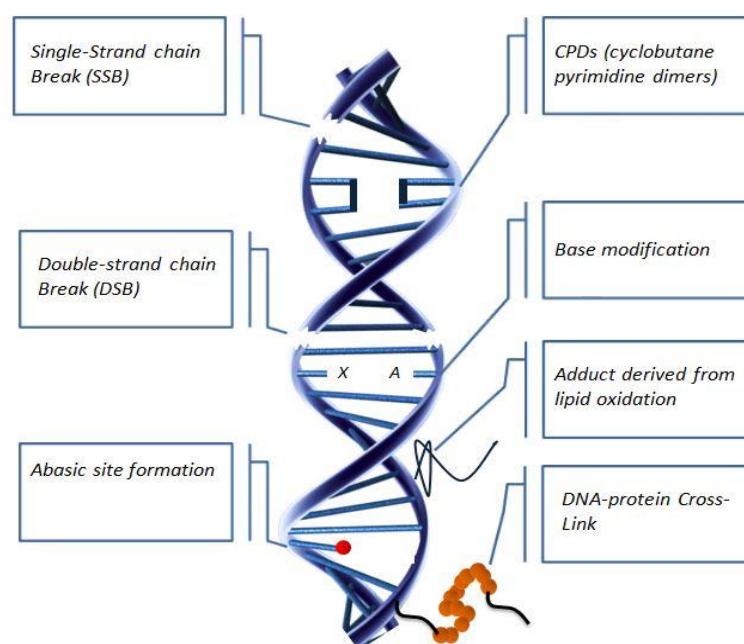


Fig.4. Major UV-induced DNA Damages.

A. Alterations of Nucleotide Bases. Damage to bases primarily are the result of the attack of free radicals to the DNA but they can be the direct effect of radiation as well (Ichihashi et al. 2003; Cadet et al. 2005; Rastogi et al. 2010). The most common direct damages include the formation of CPD_s (Cyclobutane Pyrimidine Dimers) and 6-4 PP_s (Pyrimidine-Pyrimidone (6-4) Photoproducts) (Figure 4). It has been shown that the 6-4 PP is 5 to 10 times less

prevalent than CPD although it is repaired more effectively (Tornaletti and Pfeifer 1996). One of the most abundant oxidative modifications of DNA bases is the C-8 hydroxylation of guanine which produce 7,8-hydro-8-oxodeoxyguanosine (8-oxo-dG). This modification is frequently considered as the marker of oxidative DNA damage. In addition, loss of bases can also occur by irradiation (Ravanat et al. 2001; Rastogi et al. 2010).

B. DNA Strand Breaks. The strand breaks are classified in two types:

- Single strand breaks (SSB_s): SSB is the fracturing of only one strand of DNA due to a break in phosphodiester bonds.
- Double-Strand Breaks (DSB_s): DSB_s consist of two breaks, located on different strands of DNA. These fractures are separated from each other by maximum 10 base pairs. DSB_s can result from ionizing events affecting both strands simultaneously or by two independent single-strand breaks. DSB_s are the most deleterious lesions and a large proportion of them can not be repaired by the cell after irradiation, thus exerting lethal effects. The number of SSB_s and DSB_s may be associated with the radiation dose and cell sensitivity as well (Rapp and Greulich 2004; Barnard et al. 2013).

C. DNA/Protein Bulky Adduct Formation. Radiations are capable of forming DNA bulky adducts by cross-linking the two strand breaks. This process has been shown that could be a start point of carcinogenesis. These DNA bridges result also in chromosomal aberrations. Radiations could also induce associations of proteins and DNA (Jenner et al. 1998; Hang 2010). Furthermore, certain chemical compounds such as malondialdehyde which originates from peroxidation of the cell membrane following irradiation (Morliere et al. 1995) can induce DNA/protein bulky adduct formation (Cheeseman 1993).

D. Locally Multiple Damages Sites (LMDS). LMDS_s consist of a large number of simple damages including damages to bases, SSB_s, DSB_s and associations of DNA/protein or DNA/DNA in a short sequence of DNA (Sutherland et al. 2001). These associations or "clusters" of damage are the result of an accumulation of several individual sublethal injuries.

E. Chromosomal Aberrations. Different types of chromosomal aberrations including translocations, deletions and inversions are induced by UV (dicentric, centric and acentric rings). They come from the connection of either two ends of chromosomes resulting mostly

from a DSB or from the association of a free end chromosome with other molecules which finally will inhibit DNA repair (Kemp and Jeggo, 1986).

3.4. Reactive Oxygen Species (ROS)

Molecular oxygen can easily acquire an extra electron and generate radical species. Among these species, there are restricted set called primary radicals which play specific role in physiology. Primary radicals derive either from oxygen or nitrogen through reductions. Superoxide anion $O_2^{\cdot-}$, free radical hydroxyl OH^{\cdot} and nitrogen monoxide NO^{\cdot} are the most known primarily radicals (Valko et al. 2007). Other free radicals namely secondary radicals are formed by the reaction of these primary radicals with the primary biochemical compounds. Other derivatives of oxygen such as singlet oxygen 1O_2 , hydrogen peroxide (H_2O_2) or of nitrogen like nitroperoxyde ($ONOO^{\cdot}$) though not free radicals, are reactive species which may act as radical precursors (Valko et al. 2007).

A large proportion of ROS production occurs in mitochondria as a by-product of energy metabolism (for more details see my review article on metabolism and skin cancer). Another site of ROS production is the endoplasmic reticulum (ER) where cytochrome p450 reductase generates ROS in the form of superoxide anion $O_2^{\cdot-}$. Hypoxanthine/Xanthine oxidase, lipoxygenase, cyclooxygenase and nicotinamide adenine dinucleotide phosphate (NADPH) oxidase are other participants in ROS generation. In the present thesis, I focused on inhibition of NADPH oxidase activity using a specific peptide to prevent accelerated aging.

Large groups of stimuli including physical or chemical factors, radiations, pH, temperature, and endogenous or exogenous factors can trigger the production of ROS. Cells utilize anti-oxidants in order to maintain the homeostasis of the redox system (described later). Increased level of ROS and imbalance of redox status can lead to many outcomes including cancer and aging.

3.4.1. NADPH Oxidase Enzyme Family

NADPH Oxidase (NOX) as a multi-isoform enzyme transfers an electron from NADPH to molecular oxygen (O_2) to generate superoxide anion ($O_2^{\cdot-}$). NOX was first identified in phagocytes with the potential of producing ROS as a protective mechanism against infections. Seven isoforms of NOX have been identified in human cells including NOX1 to NOX5, dual oxidase 1 (DOUX1) and DOUX2 (Drummond et al. 2011; Block and Gorin 2012a). These isoforms have six amino-terminal transmembrane segments with conserved histidine residues

which bind to the hemes and carboxy-terminal binding sites of FAD and NADPH (Figure 5) (Drummond et al. 2011; Block and Gorin 2012a). Despite of structural similarity, each of the seven isoforms has its own specific characteristics, distinct tissue expression and specific mechanism of activation (Table 3). For example, we could recently identify the expression of three isoforms including NOX1, NOX2 and NOX4 in the skin samples of human and mice (Hosseini et al. 2014b).

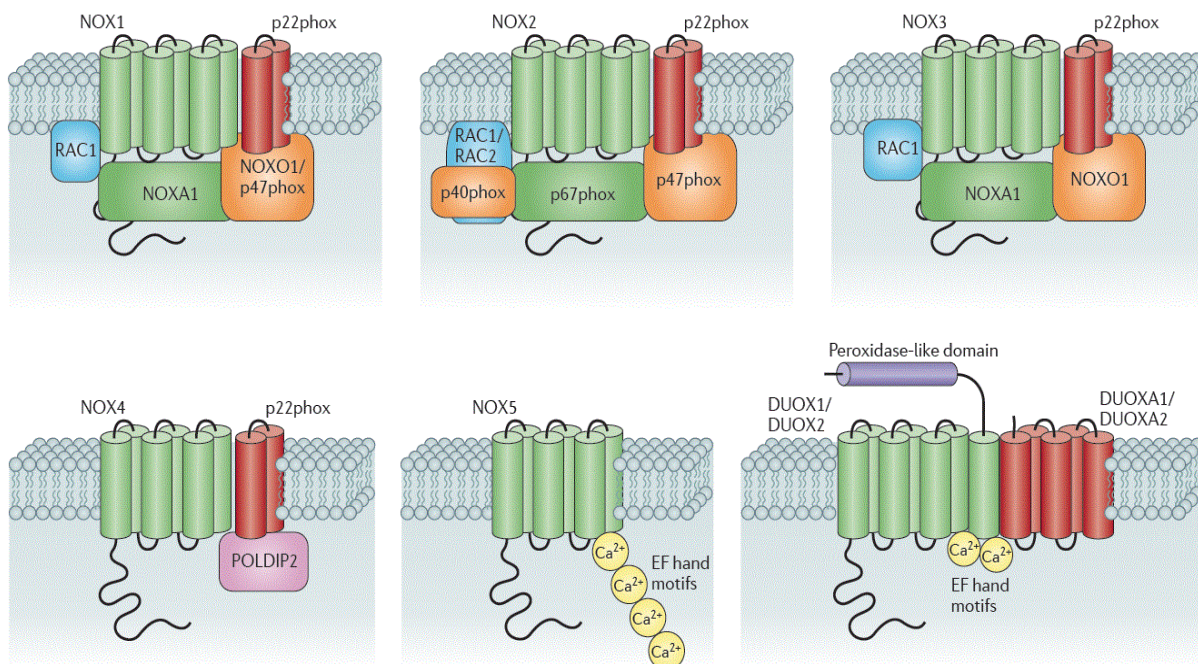


Fig.5. Subunit Composition of Mammalian NADPH oxidase isoforms (Altenhöfer et al. 2014). NOX1 is activated by binding of its organizer NOXO1 which along with a small GTPase, Rac, enable the binding of NOXA1 to activate the complex completely. NOX2 is activated in a similar manner by its organizer proteins, p47phox and Rac which enable the binding of the activator protein, p67phox. Activation of NOX2 can be promoted by the binding of p40phox to the complex. NOXA1 seems to be capable of activating NOX3 but its role still needs to be confirmed in vivo. NOX4 is the only NOX isoform which seems to be constitutively active in the absence of any cytosolic binding factors. NOX5, NOX6/ DUOX1, and NOX7/DUOX2 are mainly activated by calcium via their calcium binding sites. NOX isoforms (green), NOX stabilizing factor (red) and Complex organizing binding partners (blue)(Drummond et al. 2011; Altenhöfer et al. 2014).

Isoforms of NADPH oxidase catalyze the transfer of an electron from NADPH to molecular oxygen through biological membranes and convert oxygen into superoxide anion. Except for NOX4, DUOX1 and DUOX2, the other isoforms produce superoxide as a primary ROS molecule.

Generally, for the activation of each isoform, different subunits should be assembled together. For instance, NOX1 activation requires the assembly of five subunits (NOX1+RAC1+NOX1A+p22phox+NOX1O) which could generate $O_2^{\bullet-}$ from O_2 using NADPH as an electron donor (Hosseini et al. 2014b).

NOX catalytic and regulatory subunits have been implicated in a wide range of disorders including premature aging and cancer (Table 3). Over expression of NOX isomers with an increased level of ROS has also been detected in various cancer cell lines and human tumors (Block and Gorin 2012a). All these data therefore, point to an important role of NOX complex in premature aging and tumor initiation and progression as well.

Table 3. NADPH oxidase families.

	NOX1	NOX2	NOX3	NOX4	NOX5	DOUX1/2
PARTNERS	P22, NOXO1, NOXA1, Rac1	P22 ^{phox} , P47 ^{phox} , P67 ^{phox} , P40 ^{phox} , Rac2	P22 ^{phox} , P47 ^{phox} , P67 ^{phox} , NOXO1, NOXA1	P22 ^{phox} , Rac ±, Poldip2, NOXR1	- Ca ²⁺	DUOXA1/ DUOXA2 Ca ²⁺
TISSUES	Colon, stomach, uterus, Skin	Neutrophils, macrophages, monocytes, Skin	Inner ear, fetal Tissues	Kidney, CML, Skin, Heart, Pancreas	Lymphoid tissue, testes, ovaries	Thyroid, Lung, Intestine
FUNCTIONS	Host defense, regulation of blood pressure	Host defense, pH regulation	senescence	senescence, apoptosis, signaling of insulin	lymphocyte differentiation	Host defense, Thyroid hormone biosynthesis
DISEASES	Atherosclerosis, Cardiovascular Diseases, Prostatic adenocarcinoma	chronic granulomatous disease, Cardiovascular Diseases	Otoconia in the internal ear	atherosclerosis, colonic cancer, angiogenesis	male Infertility, prostatic adenocarcinoma	hypothyroidism

3.4.1.1. NADPH Oxidase 1 (NOX1)

NOX1 has a molecular mass of 55-60 kDa and an approximately 60% sequence identity to NOX2. It is composed of six transmembrane domains harboring two termini similar to NOX2. NOX1 has five subunits including NOX1, p22phox, RAC1, NOXO1 (NOX-organizer 1) and NOXA1 (NOX-activator1) whose assembly leads to its activation and results in production of reactive oxygen species (ROS) afterwards. While NOX1 alone can only produce a low level of ROS, the assembled complex is able to produce a large amount.

NOXO1 is involved in the phosphorylation-induced activation and further binding to the NOX1/p22 (called sometimes flavocytochrome b558). Then NOX1/p22/NOXO1 and NOXA1 join each other by activity of NOXO1. Finally binding of NOXA1 to RAC1 promotes electron flow through the flavocytochrome in a GTP-dependent manner and produces superoxide by transferring an electron from NADPH (Bedard and Krause 2007; Rezvani et al. 2011a; Altenhöfer et al. 2014).

Our study on the role of NOX1 in skin physiology has revealed the key role of this oxidase in skin aging and skin carcinogenesis (Hosseini et al. 2014b and unpublished data).

3.4.1.2. NADPH oxidase 2 (NOX2)

Current knowledge on the topography and structure of NOX isoforms has been obtained through diverse studies on the isoform NOX2. This complex is composed of six transmembrane domains with two termini (COOH and NH₂) which are facing the cytoplasm. Once transmembrane domains are assembled, the complex becomes activated and produces superoxide radicals. NOX2 has been identified in several organs such as colon, spleen, pancreas, prostate, testis, thymus, small intestine, ovary and placenta (Bedard and Krause 2007; Altenhöfer et al. 2014).

3.4.1.3. NADPH Oxidase 3 (NOX3)

The structure of NOX3 is highly similar to that of NOX1 and NOX2 in general. NOX3 has been detected in the inner ear, fetal spleen, fetal kidney, skull bone, and brain (Bedard and Krause 2007).

3.4.1.4. NADPH Oxidase 4 (NOX4)

NOX4 has a less similarity to NOX2 comparing NOX1 and NOX3 (~39%). Expression of this complex has been reported in kidney, keratinocytes, fibroblasts, melanoma cells, osteoclasts, endothelial cells, smooth muscle cells, hematopoietic stem cells and neurons (Bedard and Krause 2007).

3.4.1.5. NADPH Oxidase5 (NOX5)

This complex is different from other members of NOX family as it has a long intracellular NH₂ terminus containing a Ca²⁺ binding site. Expression of NOX5 has been demonstrated in testis, spleen, lymph nodes, vascular smooth muscle, bone marrow, pancreas, placenta, ovary, uterus, stomach, and various fetal tissues (Bedard and Krause 2007).

3.4.1.6. DOUX1/DOUX2

The so-called NOX6 and NOX7 isoforms or DOUX1 and DOUX2 have 50% similarity to NOX2 but they produce H₂O₂ instead of superoxide anion which is the main product of NOX2. DOUX1/2 are expressed in thyroid, airway epithelia and prostate (Bedard and Krause 2007).

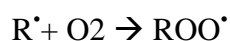
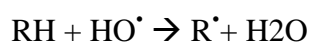
3.4.2. Role of ROS in Cellular Response to UV

Reactive oxygen species play a dual role in cellular response to UV. On the one hand, they act as toxic products by oxidizing biological macromolecules (proteins, lipids and nucleic acids) and on the other hand, they modulate the activity of certain transcription factors as second messengers.

3.4.3. Oxidative Effects of ROS

As free radicals are highly reactive, they quickly attack the first molecules they encounter especially lipids, nucleic acids and amino acids.

The first targets of these attacks are polyunsaturated fatty acids which are the main components of cell membranes (nuclear/ mitochondrial/ lysosomal). Briefly, HO[•] can trigger lipid peroxidation by extracting H from a methylene group for example according to the following reactions:





Peroxidized fatty acids corrupt membrane permeability and could lead to disintegration of the membrane. In the same way, the amino acids of a protein may undergo carbonylation (> C = O), which modifies proteins and make them sensitive to proteases. Finally the DNA bases can also be oxidized. This type of modification is a cause of mutations or replication arrest of DNA.

3.4.4. ROS as a Second Messenger

Numerous studies have shown that ROS can modulate the activity of certain transcription factors. Schreck and colleagues (Schreck et al. 1992) first showed that some transcription factors of the NFκB family can be activated by oxidizing agents and also by ionizing radiation.

Later, it was shown that several transcription factors and protein kinases possess redox sensitive elements, thus become activated by irradiation (Morel and Barouki 1998; Valko et al. 2007; Trachootham et al. 2008). Some of these factors are detailed in Table 4.

Table 4. Transcription Factors Sensitive to the Redox State

Factor	Function	Regulation	Ref
NFκB	This factor plays an important role in the rapid response to cellular stress.	This factor is controlled at two antagonistic levels (nuclear translocation and DNA binding) by the redox system.	(Anderson <i>et al.</i> 1994, Piette <i>et al.</i> 1997)
AP-1 (activator protein-1)	This factor composed of the Fos (c-fos) and Jun (c-Jun, JunB) family members, is involved in cell growth, differentiation and cellular stress.	Activation and DNA binding are two different stages sensitive to redox state of the cell. Activation is made by a kinase activated by ROS while the connection is controlled by oxidation of cysteine.	(Abate <i>et al.</i> 1990)
AP-2	This factor activates the gene transcription of intracellular adhesion protein ICAM-1, heme oxygenase and some metalloproteases.	This factor is activated by UVA via the production of singlet oxygen.	(Grether-Beck <i>et al.</i> 1996)

Hox B5	Its role in humans is not yet known.	Oxidizing conditions cause its dimerization by the formation of a disulfide bridge at the cysteine.	(Galang et Hauser 1993)
Sp1	This factor recognizes a specific sequence present in the promoters of many genes.	Its transcriptional activity and DNA binding are very disturbed by oxidative stress	(Wu et al. 1996)
NF-1 (nuclear factor -1)	This factor binds to the consensus sequence. One of the most interesting target gene is cytochrome p450 1A1 human (CYP1A1)	It has three critical cysteines in its binding domain to the DNA.	(Bandyopadhyay et Gronostajski 1994)
p53	This tumor suppressor is involved in regulating the cell cycle, DNA repair and apoptosis induction.	It has twelve cysteines in its protein sequence. Nine of them are in the DNA binding domain of which four are essential for binding. The presence of many cysteines allows considering several hypotheses explaining the role of oxidative stress.	(Parks <i>et al.</i> 1997)
USF (upstream stimulatory factor)	It regulates the expression of many genes involved in the immune response, stress, cell cycle and proliferation.	An intramolecular disulfide bridge prevents dimerization and inhibits its binding to DNA.	(Pognonec <i>et al.</i> 1992)

Majority of transcription factors (TFs) contain a series of functional cysteine residues in their protein sequences which make them sensitive to the redox changes via the thiol groups. These cysteine residues can be located in the DNA-binding domain of TF to ensure the recognition of a particular site by electrostatic interactions with the DNA. They may also form inter or intramolecular disulfide bridges essential for the three-dimensional conformation of the protein and finally, they involve in coordination of metal cations mainly Zn²⁺. Accordingly, oxidation of these cysteines changes the behavior of the transcription factor.

Besides the direct effects, there are various indirect effects of ROS in inflammation and cell injury. These include activation of phospholipases and subsequent generation of prostaglandins and leukotrienes, production of inflammatory cytokines (IL-1, TNF) and initiation of apoptotic machinery as well (Heck et al. 2004; Valko et al. 2006).

4. Photoprotection

Skin cells are the first body barriers against the physical, chemical and biological aggressions of the environment. A common type of these dangers is UV radiation. Natural photoprotection of skin against UV and photocarcinogenesis is ensured by pigmentation, DNA repair, antioxidants, senescence, apoptosis and autophagy.

4.1. Pigmentation

Melanin is produced in melanocytes by oxidation of tyrosine. It determines skin and hair pigmentation (color) and enables the tissue to resist against aggressions of UV. The two main types of melanin pigments with different photochemical characteristics are eumelanin and pheomelanin. The brown-black pigment, eumelanin, is a photoprotective factor while pheomelanin is yellow, cytotoxic with no photoprotective effects (Figure 6) (Ou-Yang et al. 2004). After synthesis, melanin is transferred to the neighboring keratinocytes giving pigmentation to the skin (Figure 6).

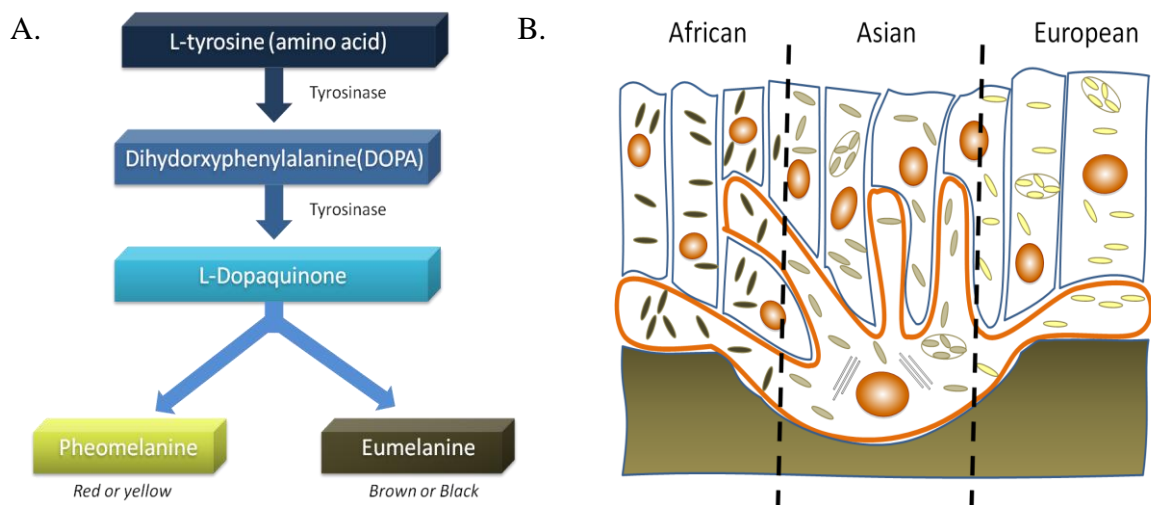


Fig.6. Melanin synthesis (A) and distribution of melanosomes in different skin types (B).

It is not the number of melanocytes that makes the difference between various phototypes. The difference is in fact related to a factor called melanin synthesis capacity which is the ratio of eumelanin to pheomelanin and also dependant on the rate and modalities of transferred melanosomes to the neighboring keratinocytes (Fitzpatrick 1986; Hunt et al. 1995; D’Orazio et al. 2010). Constitutive and UV-induced pigmentation are controlled by a complex signaling network containing four major pathways:

- **POMC/ MC1R:** POMC gene (Pro-Opio-Melano-Cortin) codes for a precursor polypeptide which produce alpha melanocyte stimulating hormone (α -MSH) after cleavage (Schauer et al. 1994; Wintzen and Gilchrest 1996). Binding of this ligand to its receptor, MC1R which is located on the melanocyte membranes, induces intracellular cascades leading to activation of several regulatory pathways involved in pigmentation and immune response (Corre et al. 2004; Millington 2006; Rouzaud et al. 2006).
- **END/ ENDRB:** Endothelin 1 (END-1) is synthesized by keratinocytes and binds to its receptor ENDRB on the melanocyte membrane. After activation, ENDRB receptor belonging to the G-protein coupled receptor family triggers various intracellular pathways and lead to pigmentation. The activated receptor is involved in pigmentation by stimulation of tyrosinase activity or by induction of the expression of POMC. The increased expression of endothelin after UVB irradiation is in fact a major stimulus in UV-induced pigmentation (Imokawa et al. 1997).
- **SCF/ KIT:** Secreted by keratinocytes, SCF (Stem Cell Factor) binds to its receptor KIT leading to activation of the MAPK pathway. The MAPK pathway is involved in constitutive pigmentation by activation of the transcription factor MITF (Imokawa 2004). Increased expression of KIT gene after exposure to UVB by an unknown mechanism also allows SCF/ KIT to intervene in the photo-induced pigmentation (Hachiya et al. 2001).
- **FGF2/ FGFR:** basic Fibroblast Growth Factor (β FGF or FGF2) which is synthesized by keratinocytes activates MAPK after binding to its receptor. Induction of MC1R gene expression by the increased expression of FGF2 following irradiation shows that this pathway may also contribute to photo-induced pigmentation (Scott et al. 2002).

4.2. DNA repair

During evolution, living organisms were forced to develop efficient repair systems for identifying and repairing DNA damage to ensure the survival of the species.

Different strategies have been evolved for the repair or tolerance of radiation-induced DNA injuries (Bernstein et al. 2002) :

- *In situ* reversion of the damage
- DNA mismatch repair
- Base excision repair- nucleotide excision repair
- Repair by homologous recombination
- Repair by non-homologous religation

4.2.1. *In situ* Reversion of the Damage (Direct Reversal)

This is the easiest, most effective and most correct repair system which deals with only three types of injuries including methylated bases, thymidine dimers and single strand breaks. The last two damages are UV-induced lesions. Although the enzyme photolyase is present in human cells to repair the light-induced reactivity dimers *in vivo*, it has other functions (van der Spek et al. 1996; Todo et al. 1997; Thoma 1999). Therefore, only one specific class of UV-induced lesions, fractures with single stranded 3'-OH, are repaired by the system in one step by the activity of polynucleotide ligase (DNA ligase I) (Tomkinson and Mackey 1998).

4.2.2. Mismatches Repair

Normal DNA replication provides an extremely high fidelity of genetic material with an error rate of 10^{-9} to 10^{-10} by an enzymatic correction system along with DNA polymerase.

The elimination of mismatches take place in four steps (Modrich 1997; Kolodner and Marsischky 1999; Stojic et al. 2004) :

- Recognition of mismatched base and assembly of repair complex
- Identification of the parental strand that carries the genetic information for eliminating the mismatched base and a small part of the sequence that encompasses it
- Repair synthesis by DNA polymerase activity
- DNA ligation by a DNA ligase to restore the normal integrity of DNA structure

Recognition of the mismatch is primarily performed by a heterodimer protein called hMutSa. Conformational changes in hMutSa will trigger an intervention of a repairsome complex containing hMLH1, polypeptides of postmeiotic segregation (PMS), DNA polymerase δ , a replication factor which is either PCNA (proliferative Cell Nuclear Antigen), RPA (Replication Protein A) or RFC (Replication Factor C), as well as 5'→3' exo-endonucleases, 3'→5' exonucleases, a DNA helicase and ligase. Base mismatch repair is often associated with other repair mechanisms which induce the integration of mismatch bases (e.g. base excision, recombination and translational repair) (Jiricny 2000). In addition, human cell lines deficient

in hMLH1 are also deficient in the transcription-coupled repair of oxidative damage induced by ultraviolet (Leadon and Avrutskaya 1997).

4.2.3. Base Excision Repair System (BER)

Base excision is a multi-enzymatic repair process that recognizes the base modifications such as methylation, oxidation, reduction or fragmentation of bases induced by ionizing radiation or normal oxidative metabolism (Fan and Wilson 2005).

Depending on the initial damage and glycosylation, two enzymatic pathways are involved in base excision repair mechanism including short patch and long patch (Thompson and West 2000; Bernstein et al. 2002).

Generally, initial recognition and subsequent excision of the modified bases by specialized DNA glycosylases such as hNth or hOGG1 leaves apurinic or apyrimidinic sites (AP). These sites are substrates of AP endonucleases. DNA polymerases β or δ associated with replication factor PCNA fill the gap with one to two or five to six nucleotides respectively using the undamaged complementary strand as a template. Finally, DNA ligase I or complex DNA ligase III/ XRCC1 perform the joining of DNA strands. Eight DNA glycosylases have been characterized in humans having various activities and specificities (Lindahl and Wood 1999). 8-oxoguanine DNA glycosylase (hOGG1) excises, among others, 7,8-dihydro-8-oxoguanine (8-oxoG) DNA, very mutagenic lesion causing G to T transversions (Van der kemp et al. 1996).

4.2.4. Nucleotide Excision Repair (NER)

DNA repair by nucleotides excision is probably the most important repair process as it is the most effective in removing bulky lesions which cause structural DNA distortions. These lesions are induced by ultraviolet light, ionizing radiation, mutagens, chemical carcinogens and certain therapeutic substances (Sarasin 1997; Ichihashi et al. 2003; Feuerhahn and Egly 2008; D'Orazio et al. 2013).

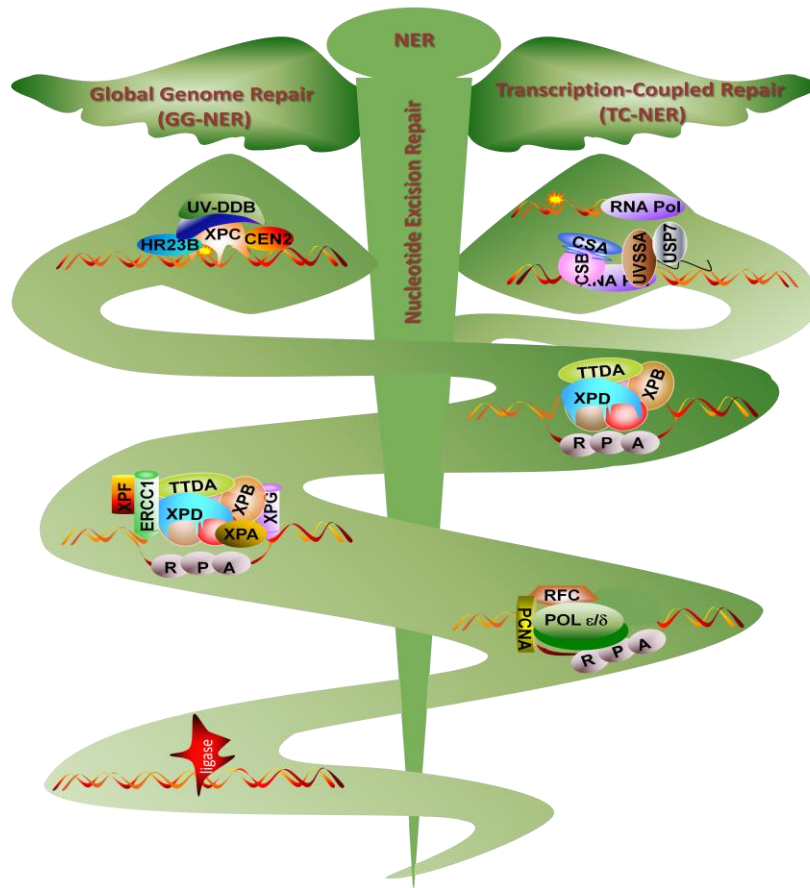


Fig.7. Nucleotide excision repair (NER) reactions (Hosseini et al. 2014a).

This process applies to various adducts such as cyclobutane pyrimidine dimers, 6-4 photoproducts, thymine glycols and other certain base modifications, adducts psoralen-thymine, cisplatin-guanine, mitomycin-guanine and interstrand cross-links. There are twenty different proteins involved in the process (Eisen and Hanawalt 1999). The main genes were discovered following the identification of genes related to hereditary diseases such as xeroderma pigmentosum (XP), trichothiodystrophy (TTD) and Cockayne syndrome in humans (Hoeijmakers 1993; Frit et al. 2002).

There are two different sub-pathways for NER: global genome repair (GGR) which is independent of transcription and transcription-coupled repair (TCR) (Figure 7) (de Boer and Hoeijmakers 2000; Feuerhahn and Egly 2008).

However, the repair process is done in the five following steps: recognition of the lesion, separation of double helix at the lesion site, incision at both sides of the lesion, excision of the lesion, reparative DNA synthesis (resynthesis) for filling the gap and ligation. In GGR, poly-

ubiquitination of XPC by XPE (UV-DDB) seems to stimulate the binding of XPC-RAD23B complexes to the damaged DNA and initiate GG-NER (Singh et al. 2015).

In TCR, damage is recognized by a stalled RNA polymerase II at a DNA lesion in transcriptionally active regions upon its interaction with CSB (ERCC6) and CSA (ERCC8) proteins (Singh et al. 2015). The UV-stimulated scaffold protein A (UVSSA) forms a complex with ubiquitin-specific protease 7 (USP7) which removes ubiquitin and stabilizes the ERCC6–RNA Pol II complex. RNA Pol II which is stalled on the DNA template is then displaced to provide access to NER factors in order to remove the transcription-stalling damage.

Damage recognition for both GGR and TCR pathways is followed by recruitment of TFIIH (including XPB, XPD, p8/TTDA and several other subunits) via interaction with either XPC or the arrested transcription apparatus. Unwinding the DNA helix is then triggered by TFIIH complex, XPG, XPA and replication protein A (RPA). The DNA around the damage is then incised by XPF-ERCC1 and XPG leading to the release of the oligonucleotide segment containing the damaged base(s). The resulted gap is then filled by a DNA polymerase (ϵ or δ) in presence of PCNA (Proliferating Cell Nuclear Antigen) and Replication Factor C (RFC). The 3' nick is finally closed by DNA ligase (Hosseini et al. 2014a).

Hereditary diseases related to NER deficiency, their clinical symptoms and the potential role of oxidative and energy metabolism in the clinical heterogeneity spectrum observed among different patients with NER defects are discussed in my fist review article (Vermeulen et al. 1994; de Boer and Hoeijmakers 2000; Hosseini et al. 2014a).

4.2.5. Repair by homologous recombination

Severe damages involving both DNA strands such as radiation-induced double-strand breaks or inter-strand cross-links induced by therapeutic agents (cisplatin, mitomycin C, and psoralen plus UVA) can be repaired by a genetic recombination between two homologous DNA molecules (Game 1993; Shinohara and Ogawa 1995).

Repair of double-strand breaks by homologous recombination contains several steps (Dasika et al. 1999; Van Dyck et al. 1999; Karran 2000). First, double-strand breaks are recognized by a protein complex called hRad50/ Mre11/Xrs2 (Nbs1) which attaches to the both ends of broken strands to excise a few nucleotides (Resection). Then hRad52 binds to the two opposite strands to protect them from digestion by cellular endonucleases (Dasika et al. 1999;

Van Dyck et al. 1999). Subsequently, in presence of hRad51 and other proteins, both strands bearing hRad52 start searching for DNA sequences similar to the 3' overhang. After finding such a sequence, the single-stranded nucleoprotein moves into the similar or identical recipient DNA duplex in a process called strand invasion. Then intact template strand will be used for a restorative DNA synthesis by a DNA polymerase resulting in formation of a cross-shaped structure known as Holliday junction.

Finally, separation of the product (resolution of Holliday junctions) and ligation of the gaps are carried out by nicking endonucleases and DNA ligase I, respectively, resulting in a damage repair without loss of any genetic information (Featherstone and Jackson 1999).

Another way for the repair of double-strand breaks is a pathway involving tandem or repeated sequences (synthesis-dependent strand annealing) (Figure 8). Not always faithful, this process is also a part of the repair by homologous recombination (Karran 2000).

4.2.6. Repair by non-Homologous Religation (Non-Homologous End-Joining, NHEJ)

This mechanism is preferentially used by mammalian cells to repair double-strand breaks and probably multiple localized damages. It also plays a key role in V (D) J recombination which ensures the diversity of immunoglobulins (Jeggo et al. 1995; Jeggo 1998; Featherstone and Jackson 1999). In contrast to homologous recombination, in non-homologous repair by religation of double strand breaks, there is no need for homology to another duplex DNA or even homologous base pairs at the ends of the broken DNA.

The non-homologous repair process is done in the following steps. First, radiation-induced double strand breaks are recognized by the complex Rad50/ Mre11/ Xrs2 (Nbs1) as in homologous recombination. Nbs1 protein indicates the presence of damage in the DNA to cell cycle control system (checkpoint) and regulates the activity of Mre11-Rad50 complex. Then, the heterodimeric protein Ku (Ku70 and Ku80) binds to the ends of broken DNA strands and assemble the catalytic subunits of the DNA-dependent protein kinase (DNA-PKcs) (465 kDa) (Featherstone and Jackson 1999). Finally, the gaps are probably filled by a DNA polymerase (not yet specified) and after alignment of the strands, DNA ligase IV links them together at the presence of XRCC4 protein.

4.2.7. DNA Damage Tolerance and Translational Synthesis

Most of radiations block the progression of DNA replication enzymes. In each cell, there are several mechanisms in order to control of the cell cycle (checkpoints) allowing cells to repair their DNA before replication or division (Favaudon 2000).

However, single-stranded DNA containing some damages can be replicated without repair by translational synthesis (Wood 1999). The confirmation of the existence of such a synthesis in humans comes from results obtained on the cells derived from patients with xeroderma pigmentosum variant (XPV) (Masutani et al. 1999a, 1999b).

XPV cells are relatively insensitive to UV radiation but patients have a high risk for cancer after sun exposure. They are deficient in post-replication repair resulting in a high frequency of mutations after UV irradiation (Lehmann et al. 1975). It was shown that XPV cell extracts have a very low capacity in replicating the DNA with a thymine dimer *in vitro* (Masutani et al. 1999b) while normal cell extracts were capable of replicating (cross-link) the lesion. Masutani and colleagues found a DNA polymerase called DNA polymerase η which is capable of translesional DNA synthesis by passing the cyclobutane pyrimidine dimers and 6-4 photoproducts quite faithfully. Another polymerase (ζ) present in normal cells allows translesional synthesis in the presence of thymine dimers but with introducing mutations.

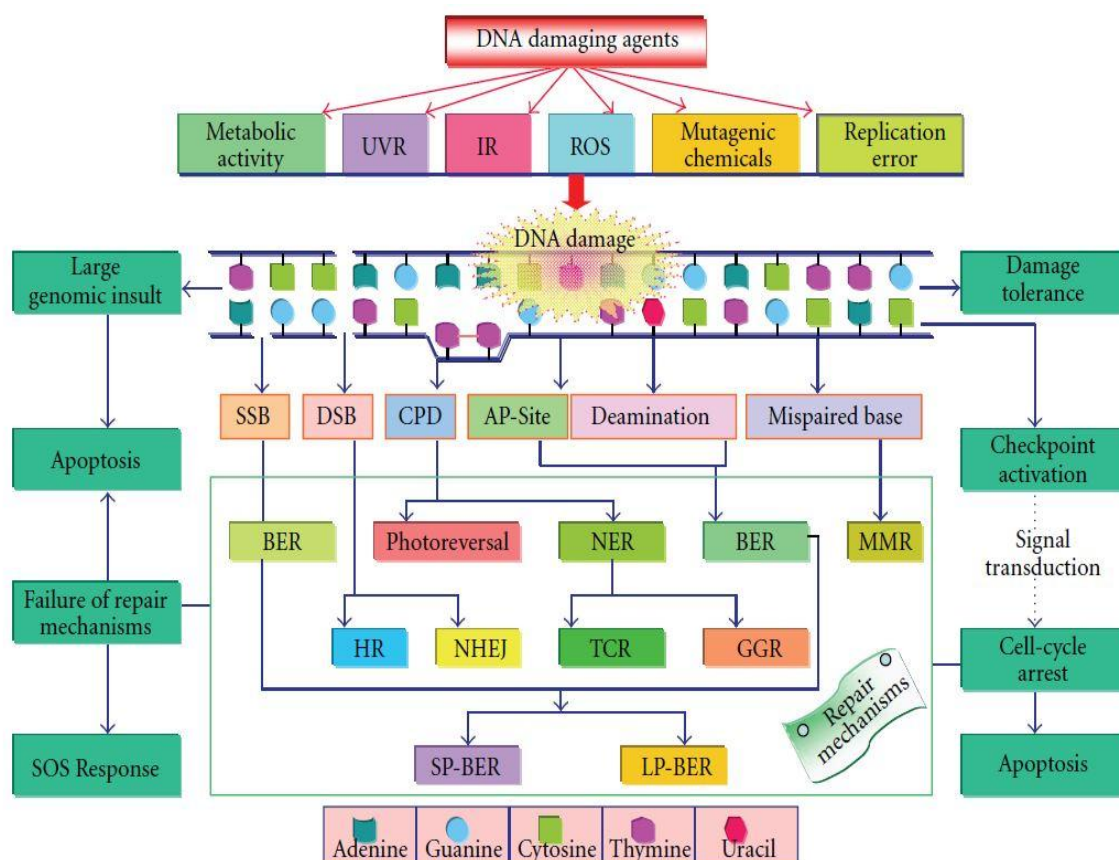


Fig.8. All types of DNA damages and repair mechanisms (Rastogi et al. 2010). Genomic damages induced by DNA damaging agents trigger several specific repair machineries to conserve the genomic integrity. Escape from severe damage and/or failure of repair mechanisms lead to apoptosis or induce a complex series of phenotypic changes such as SOS response (Rastogi et al. 2010).

4.3. Antioxidants Systems

ROS are responsible for many damages to cellular components due to their reactivity. In order to confront the oxidative action of free radicals, the body is guarded with protective mechanisms called “antioxidant defense systems”. Production of ROS is balanced by their consumption at equal speed through this system. An imbalance in the oxidant/ antioxidant system leads to oxidative stress. Currently, it is accepted that oxidative stress is involved in the pathophysiology of ischemia-reperfusion syndromes, aging and photocarcinogenesis and also in the etiology of many neurodegenerative disorders such as Alzheimer's, Parkinson's and Huntington's (Valko et al. 2006).

Control of oxidative stress is accomplished by three main complexes:

- Specific antioxidant enzyme systems
- Enzymes implicated in sequestration of free transition metals
- Diet antioxidants

4.3.1. Antioxidant Enzyme Systems

The antioxidant enzyme system comprises three different enzymes including superoxide dismutase (SOD), catalase (CAT), and glutathione peroxidase (GSH-peroxidase) plus other associated enzymes (Figure 9) (Matés 2000; Valko et al. 2006; Fernández-mejía 2013).

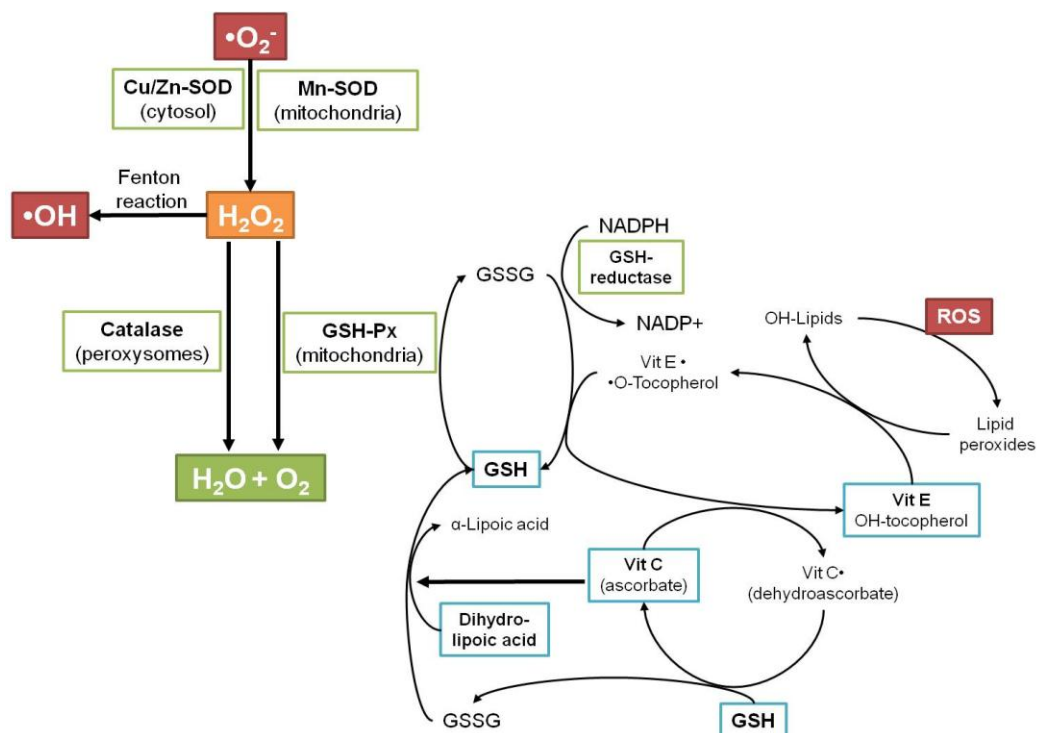


Fig.9. Overview of antioxidants systems (Fernández-mejía 2013).

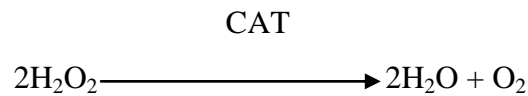
Superoxide dismutase or SOD catalyzes the dismutation of two $O_2^{\cdot-}$ ions to hydrogen peroxide at neutral pH:



The conversion of superoxide radical to H_2O_2 can be accomplished spontaneously but in fact, it would be accelerated about 10,000 times in presence of SOD. Three different forms of SOD have been identified in human cells. The copper-zinc superoxide dismutase (CuZnSOD) is found in the cytosol while manganese SOD (MnSOD) is located in the mitochondria and the extracellular superoxide dismutase (EC-SOD) in extracellular matrix of tissue. It has been shown that MnSOD is a life essential while CuZnSOD is important for the response to various types of stress including oxidative stress as well as response to xenobiotics, herbicides, dioxin and cytokines (Matés 2000).

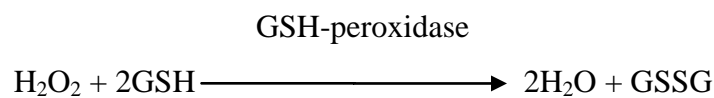
Extracellular superoxide dismutase (EC-SOD) is the only enzyme known for deactivating extracellular superoxide anion. Cytokines such as interferon γ and IL-1 regulate the activity of EC-SOD which on the contrary it is not induced by oxidants (Matés 2000; Ha et al. 2006).

Catalase which is located in cytosol and peroxisomes accelerates the spontaneous reaction of converting hydrogen peroxide into water and oxygen, thus prevents the formation of OH[•]:

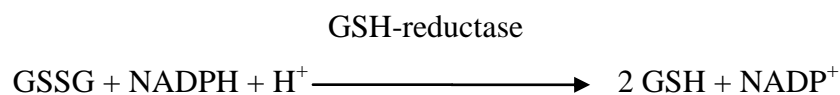


Catalase is very sensitive to its oxidation. However, oxidation of many sites is essential to induce a decrease in its enzymatic activity (Escobar et al. 1996). While catalase acts on H₂O₂ at concentrations ≤100 mmol/L, GSH-peroxidase detoxifies H₂O₂ at concentrations more than 100 mmol/L (Masaki et al. 1998).

GSH peroxidase and GSH reductase which are present in both cytosol and mitochondria forms an efficient antioxidant system for the cells. GSH peroxidase is responsible for conversion of hydrogen peroxide as well as lipid peroxides. In fact, hydrogen peroxide and lipoperoxide are reduced in the presence of glutathione.



Maintenance the activity of GSH-peroxidase requires regeneration of reduced glutathione GSH which is provided by GSH reductase. As part of this reaction, NADPH is used as a cofactor for GSH.

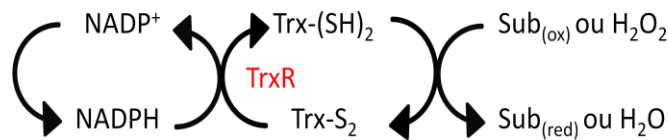


This reaction produces NADP⁺ which is converted to NADPH by G6PD (Glucose-6-phosphate dehydrogenase), an enzyme from the pentose pathway:



Consumption of reduced glutathione by GSH peroxidase causes a deficiency in levels of cellular glutathione and R-SH group (Matés 2000; Valko et al. 2006).

In addition to the three main enzymes, other enzymes including thioredoxin (Trx) peroxidase/reductase and heme oxygenase are also involved in this system. Trx peroxidase may reduce hydrogen peroxide and alkylperoxides by oxidizing Trx. The latter is regenerated by selenium thioredoxin reductase (Cha et al. 1995).



4.3.2. non-Enzymatic Antioxidant Systems

Antioxidant enzymes are not the only systems protecting the body against free radicals. Extension of free radical reactions in the presence of metals (by Fenton reaction as an example) is limited by trapping metals. Metals are seldom free in the body and usually are bound to various organic molecules such as transferrin, ferritin and metallothioneins. Following attachment to organic molecules, metals lose their stimulating activity of free-radical relatively or completely. For example, transcription of metallothioneins which are nuclear proteins constitutively expressed in the cells are activated following exposure to UVB and also in the presence of Fe (Parat et al. 1999). They can protect DNA from hydroxyl radical attacks probably by their thiol groups (Min et al. 1999). They can sequester metals and accordingly limit the formation of hydroxyl radicals through Fenton reaction (Hanada et al. 1993; Meneghini 1997).

The third line of defense in reducing free radicals is dietary antioxidants such as vitamin E (tocopherol), vitamin C (ascorbate), carotenes and flavonoids. These exogenous antioxidants have been shown to restrict damages induced by free radicals as well (Matés 2000; Valko et al. 2006).

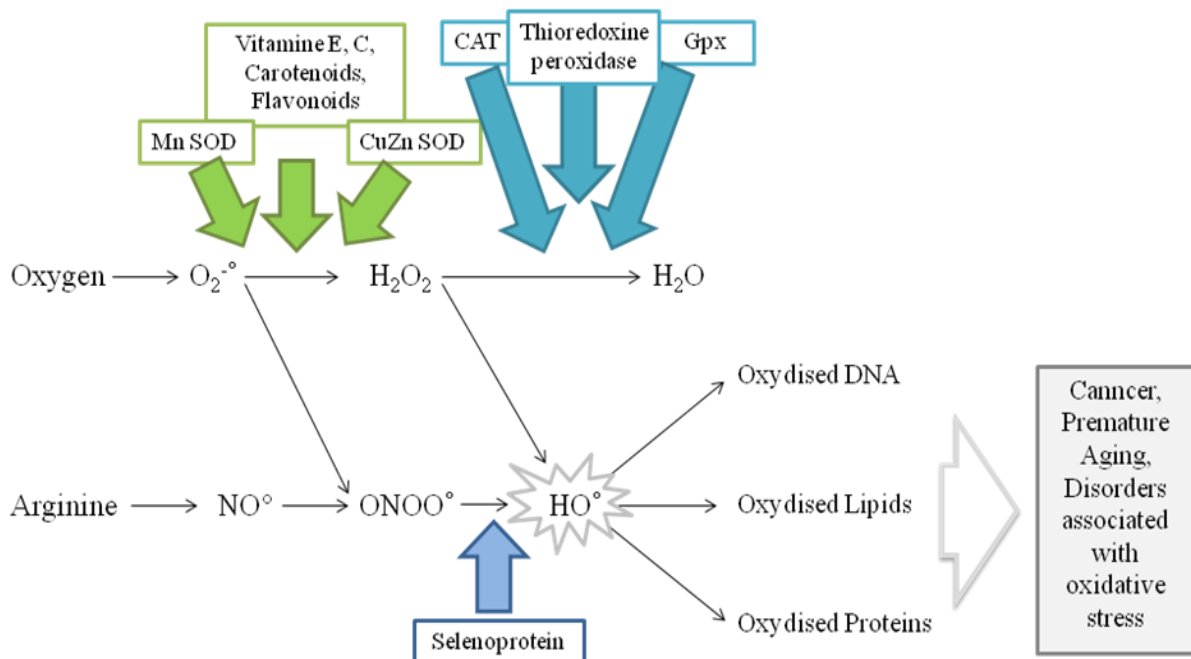


Fig.10. Mechanism of enzymatic and non-enzymatic antioxidant activity. ROS production in physiological condition or after a stress balance by antioxidants systems. The rupture of balance between oxidant and antioxidant systems leads to oxidative stress which causes the outbreak of apoptosis, cancer or the many other oxidative diseases.

4.4. Apoptosis

Cells have adopted several systems to reduce UV-induced damages. Programmed cell death or apoptosis is an active form of self-destruction in eukaryotic cells involving the reaction of organisms to physiological or pathological stimuli. It comes from the execution of a highly regulated program which induces the destruction of a cell while preserving the integrity of surrounding tissues with a sequence of well-defined events. The programmed cell death is quite different from the non-programmed death known as necrotic death. Necrosis is a destruction caused by various exogenous factors. Necrotic cell death is defined by an increase in the cell volume, swelling of the organelle, complete rupture and disappearance of the cell membrane and leakage of intracellular components into the cell environment. While necrosis is generally considered as an accidental form of cell death, new emerged evidence reveals that necrosis can also be a programmed process with a distinctive biochemical cascade (Kitanaka and Kuchino 1999; Bizik et al. 2004; Hitomi et al. 2009).

After receiving an apoptotic signal, cell will first undergo a loss of contact with surrounding cells. This is immediately followed by a significant reduction in cell volume and after that lipid organization of the plasma membrane will be impaired. For example, phosphatidylserine which is normally located in the inner leaflet of the plasma membrane is translocated to the outer layer by a phenomenon called "flip-flap". In addition, mitochondria undergo critical physiological changes. Among these changes, there is a decrease in mitochondrial transmembrane potential ($\Delta\psi_m$) resulting in the formation of a high conductance channel called permeability transition pore (Marchetti et al. 1996; Zamzami et al. 1996). Once open, these pores allow the penetration of water and solutes and in particular cytochrome c into the cytoplasm (Kluck et al. 1997). Besides, nuclear compartment goes through significant changes. Chromatin undergoes a strong condensation and fragmentation to oligonucleosomes following activation of endonucleases (Montague and Cidlowski 1996). The oligonucleosomal fragments of 180 bp are the ladder pattern observed in electrophoresis. Finally, cell will undergo a general compaction which results in its fragmentation into apoptotic bodies containing nuclear material as well as intact organelles without loss of

membrane integrity. These apoptotic bodies will be ingested by phagocytic cells (macrophages in particular) leading to the elimination of the cell. Apoptosis does not induce inflammation while it occurs during necrosis.

4.4.1. General mechanisms of apoptosis

Apoptosis comes in two major signaling pathways called intrinsic and extrinsic pathways. While intrinsic pathways involve mitochondria as a central component in apoptosis, extrinsic pathways are initiated by death receptors on the cell surface. The mitochondrial pathway is divided into two sub-pathways. One of the pathways leads to the activation of caspase family of proteases while the other is caspase-independent involving a mitochondrial protein called AIF (Apoptosis Inducing Factor). The cysteine proteases or caspases (cysteiny aspartate-specific proteinases and cysteine proteases aspartate) cleave their protein substrate at an aspartic residue of the carboxy-terminal part of their substrate. The catalytic site of the caspase comprises a cysteine residue (C) located in the center of the QACXG motif (where X = R, Q or G). There are 14 caspases numbered 1 to 14 which are different in molecular weight (32-55 kDa). Except for caspases -11, -12 and -13, they all exist in human cells (Koenig et al. 2001; Lamkanfi et al. 2002).

4.4.2. UVB-induced Apoptosis

UV irradiation leads to the increased expression of Fas receptor and its ligand, FasL (Hill et al. 1999). It can also induce the aggregation and activation of Fas receptor independent of binding to FasL (Schwarz et al. 1995; Rosette and Karin 1996; Rehemtulla et al. 1997; Aragane et al. 1998). These data illustrate the important role of death receptors in UV-induced apoptosis. In addition, release of cytochrome c into the cytoplasm and participation of Bcl-2 family proteins in apoptotic process after irradiation demonstrated the activation of mitochondrial pathway (Goldstein et al. 2000; Nijhawan et al. 2003). Therefore, both signaling pathways of apoptosis are activated in response to UV irradiation.

Numerous studies have shown that DNA damage is not the only effect of UV-induced apoptosis. Indeed, ROS production and direct activation of death receptors also appear to contribute to this response (Murphy 2001; Kulms et al. 2002; Haupt et al. 2003; Rezvani et al. 2006, 2007).

4.5. Senescence or Aging

Aging is a common biological phenomenon in the animal and plant kingdom. It is considered as an irreversible process which starts or accelerates at maturity and results in increasing rate of deviations from ideal state. Aging is characterized by a progressive failure in maintaining homeostasis under physiological stress conditions. These conditions increase the individual vulnerability and limit the viability (Mangoni and Jackson 2004). Aging comes into two categories as intrinsic and extrinsic. Genetic factors give rise to intrinsic aging while extrinsic aging occurs as a result of environmental factors. The anatomical and physiological changes associated with aging start many years before the appearance of external signs. These changes in addition to functional alterations in different organs modify the physical appearance of the body.

Senescence refers to a reduction in potential of cell division in normal human cells in culture. There are two theories at present which explain cellular senescence. The first theory argues that senescence results from an accumulation of random lesions caused by mutations, errors or free radicals. The other explains that senescence is an active process which involves changes in gene expression.

4.5.1. Key players in Aging process

4.5.1.1. Intrinsic Factors

Like all other organs, skin is also subjected to intrinsic aging. Biological mechanisms are linked to an imbalance between cellular degradation phenomena (eg. ROS and the end products of glycation) and repair systems (eg. antioxidants, DNA enzymes repair, proteases, proteinases, phospholipases and acyltransferase) (Sanches Silveira and Pedroso 2014).

DNA repair mechanisms play a major role in struggling against skin aging and skin cancer. Premature skin aging due to DNA repair deficiency in xeroderma pigmentosum, Hutchinson-Gilford, Cockayne, trichothiodystrophy and Werner, Bloom or Rothmund-Thomson syndromes supports this notion (de Boer et al. 2002; Hosseini et al. 2014b). Among other cellular repair systems, proteasomes are non-lysosomal proteolytic systems involved in several cellular functions particularly proteolysis of oxidized proteins. Aging brings a decline in proteasomal functioning in response to the action of reactive oxygen species and genetic alterations which is probably implicated in the phenomena of aging.

Progressive loss of telomeres is another major factor involved in aging mechanisms. Telomerase, an enzyme expressed in tumor, fetal and regenerative tissues (haematopoietic tissue and epidermis) is able to repair these chromosomal losses. However, the baseline activity of telomerase in epidermal and hematopoietic tissues is much lower than in tumor tissues.

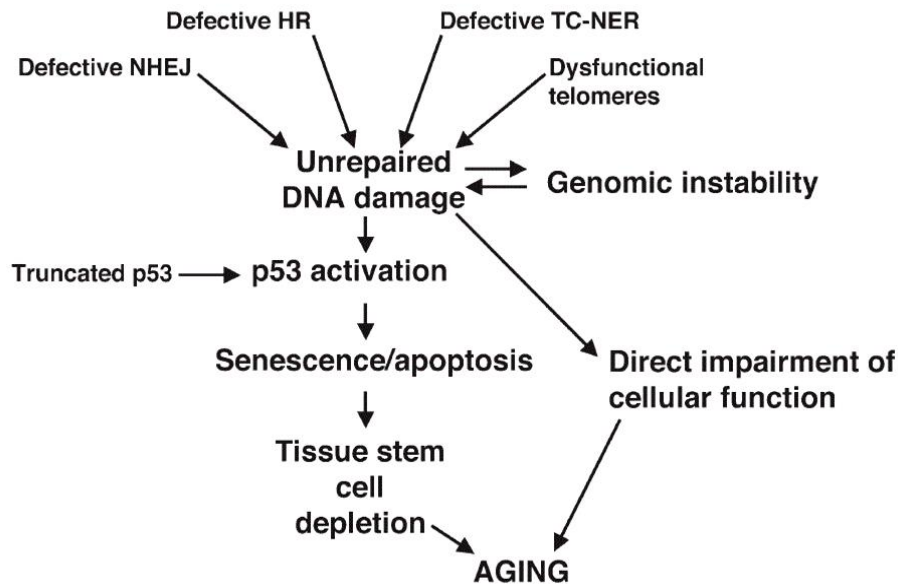


Fig.11. A Model for the Role of Unresolved DNA Lesions in Aging (Lombard et al. 2005). Unrepaired DNA lesions can trigger the cell cycle checkpoint machinery leading to senescence or apoptosis and subsequent cellular attrition and tissue dysfunction. Several types of unrepaired DNA damage—like DNA DSBs—can trigger genomic instability, which can in turn lead to further DNA damage. Unrepaired DNA damage can also directly compromise cellular processes like transcription, an effect that could also impair tissue function (Lombard et al. 2005).

4.5.1.2. Extrinsic Factors

UV radiation is accounted as the main factor driving extrinsic aging. The mechanism of action is either through direct interaction with cellular DNA (main mode of action of UVB) or indirect through the action of reactive oxygen species (main mode of action of UVA) (Sanches Silveira and Pedroso 2014). By direct interaction with DNA, UV induces the formation of photo-products which can lead to mutations, cell death or even initiation of carcinogenesis. At high doses of UV, activation of p53 protein triggers keratinocyte death through apoptosis. If a mutation occurs in a tumor suppressor or oncogene, keratinocytes lose their ability to die which can be a starting point for senescence or tumorigenesis.

In keratinocytes, UVA induces the expression of particular genes responsible for photoaging and photocarcinogenesis (Grether-Beck et al. 2000). UVA acts to induce the formation of ceramides through reactive oxygen species. UVA-induced ceramide formation leads in turn to the expression of ICAM-1 adhesion proteins which activate the transcription factor AP-2. AP-2 plays a central role in the process of photoaging (Grether-Beck et al. 2000). Mechanisms of action of other extrinsic factors are still poorly understood. For instance, tobacco aggravates the effects of UV radiation by induction of MMP-1, leading to a reduction in collagen content of dermal extracellular matrix (Qin et al. 2014; Quan and Fisher 2015).

4.5.2. Aging Biomarkers

There are a wide range of senescence biomarkers. These include cell cycle alterations, morphological transformations, over production of ROS, DNA damage accumulation, energy metabolism alterations, telomerase modifications, activation of tumor suppressor networks and also induction of SA- β -Galactosidase activity.

Animal cells in culture (*in vitro*) usually have a limited proliferative potential. After a number of multiplications, they acquire a senescent phenotype and eventually are dragged to death. Senescent cells can survive several weeks in a near state of quiescence (G_0) while of course unable to answer proliferative signals. Number of possible cell doublings in a culture before entering senescence depends on the donor age and the maximum lifespan of the studied species. For example, cells from patients with premature aging syndrome can only perform a few limited doublings. These data led to the hypothesis that aging of organisms can be due to the aging of individual cells.

The most known genes involved in senescence are p53, p63, p73, pRB, p16INK4a, p21CIP1/WAF1, p15INK4b, p57KIP2, RAF-1, oncogenic ras and hTERT (Fridman and Tainsky 2008). Separate studies have also revealed a set of genes with great potential in aging apart from the mentioned ones. These include p14ARF, E2F-1, IGFBP3, IGFBPrP1, PAI-1, MKK3, MKK6, Smurf2 and HIC-5 (Fridman and Tainsky 2008). Chromosomes 1q25, 1q41–42 and 6q13–6q21 are also the susceptible genomic regions involved in human senescence (Fridman and Tainsky 2008).

Measurement of high levels of p16Ink4a, proerin, p21, macroH2A, IL-6, phosphorylated p38 mitogen-activated protein kinase (p38 MAPK), DSBs and β -galactosidase activity is considered as the main *in situ* methods available for monitoring senescence (Van Deursen

2014). The four major aging markers which are classically measured to confirm senescence state include senescence-associated β -galactosidase (SA- β -gal) activity, progerin and p16Ink4a levels and telomere size.

- **Senescence-associated β -galactosidase (SA- β -gal) activity**

Senescence-associated β -galactosidase or SA- β -gal performs an enzymatic reaction which is specific to senescent cells. SA- β -gal is indeed a hypothetical hydrolase enzyme which catalyzes the hydrolysis of β -galactosidase into monosaccharides. Measurement of SA- β -gal activity in general, is done in a semi-quantitative manner by X-Gal staining procedure (Yang and Hu 2005).

- **Progerin Level**

Progerin is a truncated version of lamin A protein involved in Hutchinson–Gilford progeria syndrome (HGPS) in which patients suffer from premature aging in many organs. Lamin A (an intermediate filament) is a major structural component of the lamina, a scaffold of proteins in the nuclear membrane. More than 400 mutations associated to numerous disorders called laminopathies have been identified in this protein (Yang et al. 2013). The most prevalent HGPS mutation makes a splicing defect leading to the formation of a truncated version of lamin A named progerin (Gabriel et al. 2015). Accumulation of progerin in nuclear membrane results in a variety of defects in the nuclear structure and function including altered histone modification patterns, abnormal chromatin remodeling, impaired transport through nuclear pores, reduced DNA repair capacity and also increased telomere shortening (Dechat et al. 2008; Motegi et al. 2014). In fact, progerin has been demonstrated to be expressed in cells from aged individuals via sporadic use of the same cryptic splice site in lamin A whose constitutive activation causes HGPS (Dechat et al. 2008). Consistently, it has been demonstrated that progerin is more abundant in late-passage cells as in the dermis of aged individuals (Cao et al. 2011) in which exogenous expression of progerin leads to reduced cellular proliferation and premature senescence. It has been demonstrated that progerin expression was responsible for the modifications observed in nuclear functions of cells taken from old individuals (Cao et al. 2011), altogether suggesting progerin as a biomarker of physiological aging at least in skin.

- **P16Ink4a and Aging**

P16Ink4a known as a tumor suppressor is involved also in the cell cycle regulation. This protein specifically binds and inhibits the cyclin-dependent kinases 4 and 6. Excessive expression of p16ink4a promotes the cell cycle arrest in G phase and consequently leads to cellular senescent (figure 12) (Medema et al. 1995).

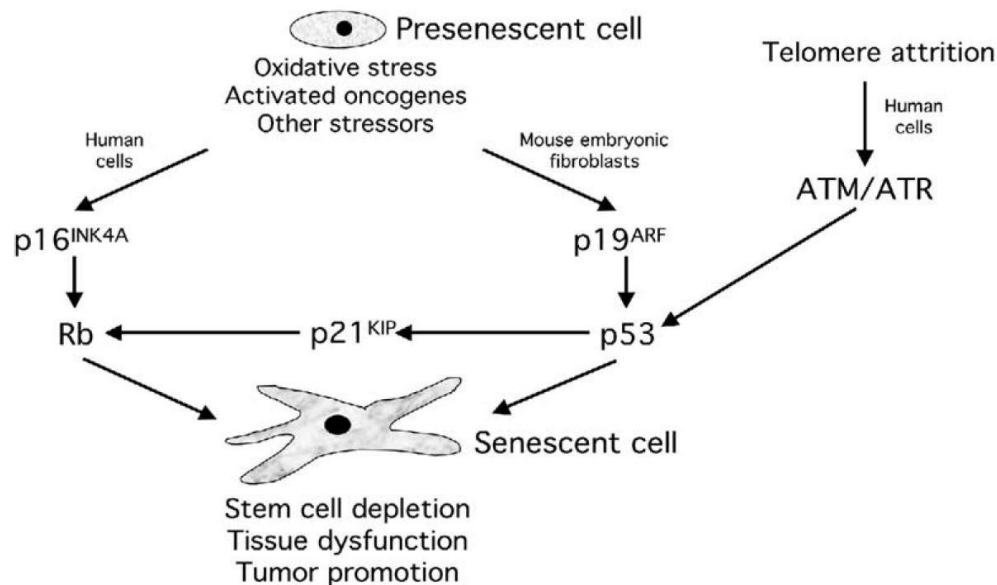


Fig.12. Multiple Pathways to Senescence (Lombard et al. 2005). These pathways are employed in a cell- and organism-specific fashion. In MEFs, activation of p19ARF leads to stabilization of p53. In certain human cell types (e.g., fibroblasts and keratinocytes), telomere attrition can activate p53 via the ATM and (potentially) ATR kinases. Senescence can also be triggered in human cells via p16 expression (Lombard et al. 2005). Senescence-inducing signals, including those that trigger a DNA-damage response (DDR), usually engage either the p53 or the p16–retinoblastoma protein (pRB) tumor suppressor pathways. Activation of these factors following stress can lead to premature senescence process (Campisi and d’Adda di Fagagna 2007).

- **Cell Cycle Alteration in Aging**

Senescence as a highly dynamic and multi-step process is closely associated with inactivation of cyclin-dependent kinases (CDKs), the key regulators of the cell cycle.

P53–p21 and p16Ink4a–RB pathways can trigger the growth arrest depending on the type of cellular stress. Moreover, these mediators regulate the activation or inactivation of CDKs which orchestrate the smooth running of DNA replication and mitosis. In presence of DNA damage or in response to oncogenic hyper-activation, cells activate the response to genotoxic

stress which leads to inactivation of CDKs and finally results in the blockade of cell cycle (Van Deursen 2014).

- **Role of Telomeres in Senescence**

Telomeres are the capping structures located at the end of double-stranded DNA of the chromosomes which protect the genome from loss of information. The size of a telomere is shortened with each cell division. Accordingly, when telomeres reach a critical size, cell would enter into senescence. They act as a biological clock regulating the life span of cells. Telomerase is an enzyme which adds bases to telomere ends. Telomeres are also involved in proliferation, protection against apoptosis, differentiation and DNA repair.

Reversing premature aging in mice by reactivation of telomerase reveals the importance of telomeres in the aging process in mice (Jaskelioff et al. 2011). Jaskliff and colleagues engineered a knock-in allele encoding a 4-hydroxytamoxifen (4-OHT)-inducible telomerase reverse transcriptase-oestrogen receptor (TERT-ER) under transcriptional control of the endogenous TERT promoter (Jaskelioff et al. 2011). As a result of telomerase deficiency, telomeres become progressively shorter in a few generations. These animals age much faster than normal mice. Activation of telomerase has been shown that could inhibit premature senescence only after 1 month treatment with 4-hydroxytamoxifen (4-OHT) (Jaskelioff et al. 2011). Interestingly, in cancer cases, telomerase expression is significantly increased.

- **Mitochondrial alterations and ROS level in Aging**

The role of mitochondria in cellular senescence has long been accepted. As described before, mitochondria are involved in production of cellular energy by oxidative phosphorylation. Moreover, this organelle generate ROS as byproduct of OXPHOS which are able to induce damage to macromolecules such as mtDNA resulting ultimately in senescence (Barzilai et al. 2012). Mitochondrial membrane dynamics is also involved in this process by modulation of mitophagy. It has been shown that inhibition of mitochondrial fission or/and fusion is associated with morphological changes in the cell and accumulation of giant mitochondria in the cells which can lead to cellular senescence. Furthermore, inhibition of mitochondriogenesis appears as part of the senescence program. Indeed, dysfunctional telomeres were shown to activate p53-dependent DNA damage responses finally resulting in reduced expression of mitochondrion components and DNA replication. This will reduce mitochondrial mass and respiratory activity afterwards (Moslehi et al. 2012).

Frequency of mutations in mtDNA is higher than nuclear DNA (Trifunovic et al. 2014). Trifunovic and colleagues demonstrated a link between increased mtDNA mutations and accelerated aging (Trifunovic et al. 2014). Moreover, a large number of studies have clearly shown a strong association between high rates of mtDNA mutations and skin photoaging in regular users of tanning beds (Reimann et al. 2008; Kaneko et al. 2012).

There is a mitochondrial aging theory which introduces mitochondrial dysfunction as the fundamental cause of cellular aging and senescence. Using a mouse model expressing a proofreading-deficient version of the mitochondrial DNA polymerase δ , Hiona and colleagues revealed that an increase in spontaneous mtDNA mutation rates results in accelerated aging in skeletal muscles (Hiona et al., 2010). Additionally, the skin aging part of my studies on XPC deficient mice well indicates the importance of mitochondrial function and activity in skin aging (Hosseini et al., 2014a).

4.5.3. Aging in Organs

Aging is associated with a reduction in functional capacity of the body. In general, this alteration is more evident in situations involving functional reserves. Decrease in functional reserves would induce a reduction in body's ability to adapt to aggression situations. This functional reduction is highly variable from one organ or individual to another.

4.5.4. Effects of Aging on the Skin

Skin like other organs will experience aging with most visible signs of aging. Aging processes in skin are characterized by alteration of elastic tissue, flattening of the dermal-epidermal junction, decline in the number of melanocytes and a fibrous thickening of the dermis leading ultimately to an appearance of the wrinkle and sagging skin (Figure 13). In addition to intrinsic factors, skin is subjected to extrinsic aggressions or external environmental factors which amplify the effect of intrinsic aging. Subject to this issue, ultraviolet (UV) radiation has a major role and as before described, UVA rays are certainly as harmful as UVB and responsible for photoaging. Skin is considered as the first revealer of aging process. Hence, detailed knowledge of the pathophysiological mechanisms of skin aging would enable us to prevent premature aging and reduce the effects of aging on skin.

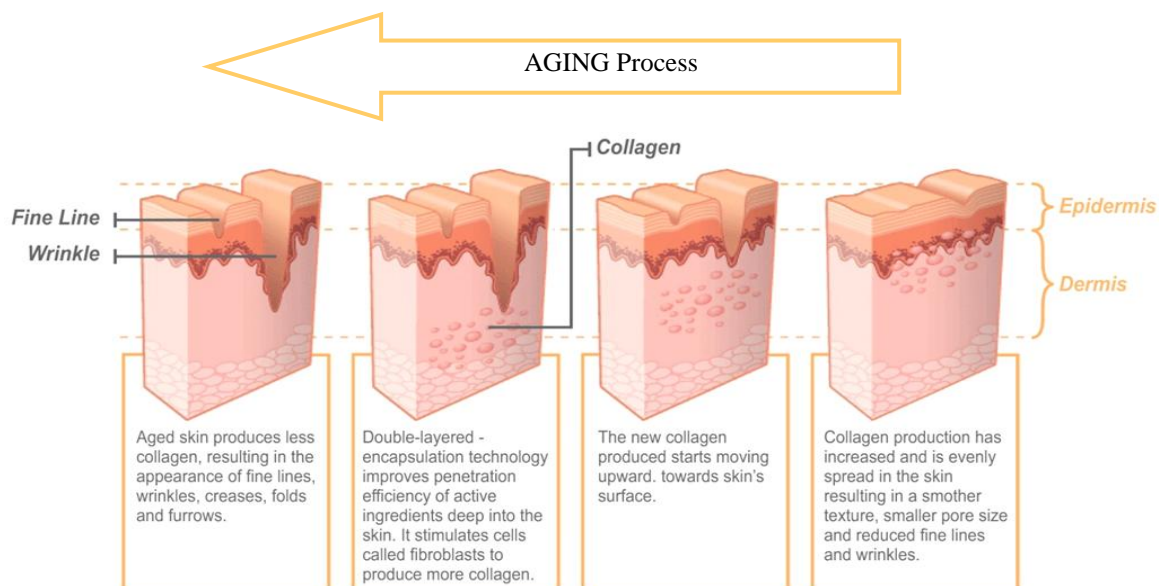


Fig.13. Skin Aging (from rg-cell.com).

4.5.5. Structural Changes in the Skin

Different types of skins are differently modified during skin aging. Intrinsic and extrinsic factors add deleterious effects on all skin structures during time. With aging, dead cells of the stratum corneum are first slowly removed and then in a slow process will be renewed as well. This process would explain the slow healing mechanisms of aging. By production of less pigment, skin becomes a little pale leading to a decrease in its protective role against UV radiation. Furthermore, dermis would produce less collagen and elastin causing a decrease in elasticity and a reduced resistance. Finally, alterations made by intrinsic and extrinsic factors cover a wide variety of changes in the skin including loss of moisture and dryness, disappearance of flexibility and elasticity, decrease in collagen production, loss of strong dermal-epidermal junction, reduction in resistance and development of wrinkles and brown spots (aging spots, solar-actinic lentigos).

The major cause of extrinsic aging is UV radiation which induces metalloproteinases activity and cause nuclear and mitochondrial DNA lesions.

4.5.5.1. Epidermal Changes

Epidermis as the surface layer of the skin is constantly renewed by the regulated proliferation of basal layer cells. With aging, the potential of differentiation in epidermal cells appears to be changed leading to a reduction in epidermal thickness (Kwon et al. 2008). Moreover, aging

is accompanied by a decrease in the water barrier function of the skin which in particular is linked to a decreased ability of cholesterol synthesis in this layer. Furthermore, it appears that recovery ability of the lipid barrier is also reduced during aging as there is a decrease in lamellar granule formation in the stratum granulosum. It has been demonstrated a reduction in the amount of Langerhans cells which are responsible for innate immune response in the skin. Mechanical protection is also modified by thinning of the subcutaneous fat and alteration of the dermal-epidermal junction.

4.5.5.2. Dermal Changes

Number of fibroblasts as the main cellular population of dermis is dramatically reduced in aging. Moreover, the amount of collagen and elastic fibers are depleted leading to the loss of thickness, flexibility and elasticity of the skin. Vascularisation is also depleted which results in skin to get pale and go through a drop in temperature of the surface and a disturbance in thermoregulation.

4.6. Autophagy

Autophagy is a catabolic process targeting and capturing cellular proteins and organelles to proteolytic degradation in lysosomes. This mechanism was first identified in 1963 by Christian de Duve who received a Nobel Prize for his work on lysosomes in 1974.

Autophagy is classified to three types including macroautophagy, microautophagy and chaperone-mediated autophagy (Figure 14). Being ATP-dependent, this process can be affected by all of the factors regulating intracellular ATP level particularly metabolic and nutrient statements (Maiuri et al. 2007; Wong et al. 2011; Boya et al. 2013).

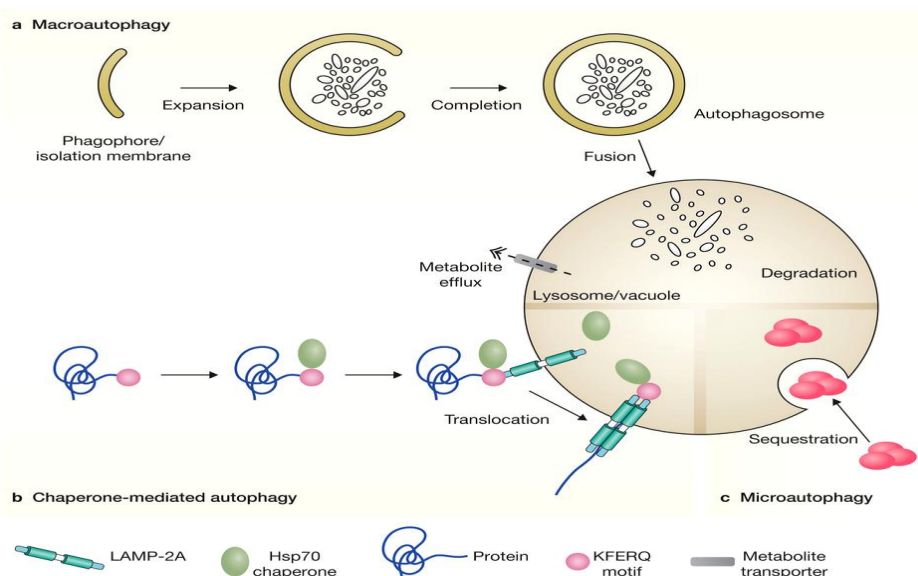


Fig.14. Different Types of Autophagy (Boya et al. 2013).

4.6.1. Macroautophagy

Macroautophagy which is commonly known as autophagy, fall into three stages. In the initiation step, an isolated known phagophore membrane is formed in the cell cytoplasm. Thereafter, during elongation, each end of the phagophore extends until the fusion of the two ends forms a double membrane vesicle called autophagosome. Portions of the cytoplasm are sequestered within the autophagosomes,. The last step is the fusion of autophagosomes and lysosomes. The formed structure which is called autolysosome allows degradation of the content with lysosomal enzymes (Ding and Yin 2012).

It was long believed that autophagy is a non-selective degradation process but indeed, two types including non-selective and selective autophagy are now accepted for macroautophagy (Ding and Yin 2012). Non-selective autophagy is induced in response to starvation or nutrient deprivation which enables amino acid recycling for survival. Selective macroautophagy in general occurs to specifically eliminate damaged organelles or aggregated proteins even in nutrient-rich statements. Selective autophagy comprises different processes including mitophagy, ribophagy, pexophagy, reticulophagy, lipophagy, agrephag and xenophagy (Mizumura et al. 2014). Among these selective forms, mitophagy plays a significant role in carcinogenesis and aging processes.

Mechanism of Macroautophagy

Macroautophagy is known as the major mechanism for degradation of damaged organelles and unused proteins. The mechanism starts by the assembly of ULK protein complex at the isolation membranes. ULK protein complex consists of four subunits including ULK1, Atg13, FIP200 and Atg101. Assembly of the complex could be dependent or independent of the regulator mTOR complex 1 (mTORC1). mTOR is involved in regulation of protein synthesis and is present in two different complexes including mTORC1 and mTORC2. Apparently, only mTORC1 complex is involved in the regulation of autophagy. To facilitate the formation of autophagosomes, initiation stage of macroautophagy also requires a Ras-like small GTPase B (RalB).

Other autophagy-related genes (atg) required for the first stage include Atg5 and Atg12 which are located on isolation membranes or autophagosomes (Maiuri et al. 2007; Wong et al.

2011). Following the first stage, nucleation and elongation are involved in the formation of a complete autophagosome. Beclin 1/ phosphatidylinositol-3- kinase (PI3K) complex along with UV radiation resistance-associated gene protein (UVRAG), Atg14, B-cell leukemia/lymphoma-2 (Bcl-2), p150, ambra1, endophilin B1, PI3K and Vacuolar protein sorting 34 (Vps34) proceed the membrane curvature of nucleation. Following this stage, other atg proteins participate in completing the elongation and expansion mechanism. These include Atg4, Atg7 and the Atg5–Atg12–Atg16L1 proteins. When the formation of autophagosome structure is completed, it fuses to the lysosomes and releases its contents into lysosomes. In general, all proteins involved in macroautophagy are liberated and return into the cytoplasm (Maiuri et al. 2007; Wong et al. 2011).

4.6.2. Mitophagy

Selective degradation of mitochondria by autophagy is known as mitophagy. Elimination of damaged mitochondria is an essential process for proper functioning of the cell (Ding and Yin 2012). In particular, mitophagy can reduce the production of ROS by mitochondria. Therefore, removal or disruption of mitophagy would result in accumulation of ROS and accordingly increase in indirect damages to the DNA (Ikeda et al. 2014). Mitophagy plays a key role in various cellular mechanisms such as energy homeostasis, cell growth, cell development and cell death. Thus, deregulation of its function can lead to the development of pathologies such as cancer, aging or neurodegenerative disorders (Ding and Yin 2012). In mammalian cells, NIX protein (also called BNIP3L) and PINK1 protein (PTEN induced putative kinase-protein 1) are involved in targeting of the mitochondria for macroautophagy.

4.6.3. Microautophagy

Microautophagy is the direct sequestration of cytoplasmic cargo in a boundary membrane by autophagic tubes which mediate both invagination and vesicle scission into the lumen (Li et al. 2012). Microautophagy is a degradation process proposed to be non-selective particularly in eukaryotic organisms. However, like macroautophagy, there are several forms of selective microautophagies commonly observed in yeast cells which specifically degrade certain organelles. These included micropexophagy, piecemeal microautophagy and micromitophagy.

4.6.4. Chaperone-mediated Autophagy

Chaperone-mediated Autophagy (CMA) is a highly selective mode of autophagy (Maiuri et al. 2007; Wong et al. 2011; Boya et al. 2013). Proteins degraded by CMA are specifically

recognized by cytosolic chaperone proteins and will be transported to the lysosome surface. CMA occurs in three steps: i) Recognition of the proteins supposed to be degraded by chaperone proteins, ii) Protein transport to the lysosomal membrane and its unfolding and iii) Translocation of the protein in the lysosomal lumen.

CMA is involved in the maintenance of protein homeostasis and provides a critical role in protein quality control through degradation of damaged or altered proteins. In fact, Chaperone-mediated Autophagy (CMA) is increased in response to the stress-induced damages to proteins and also by the formation of misfolded proteins in order to prevent their aggregation.

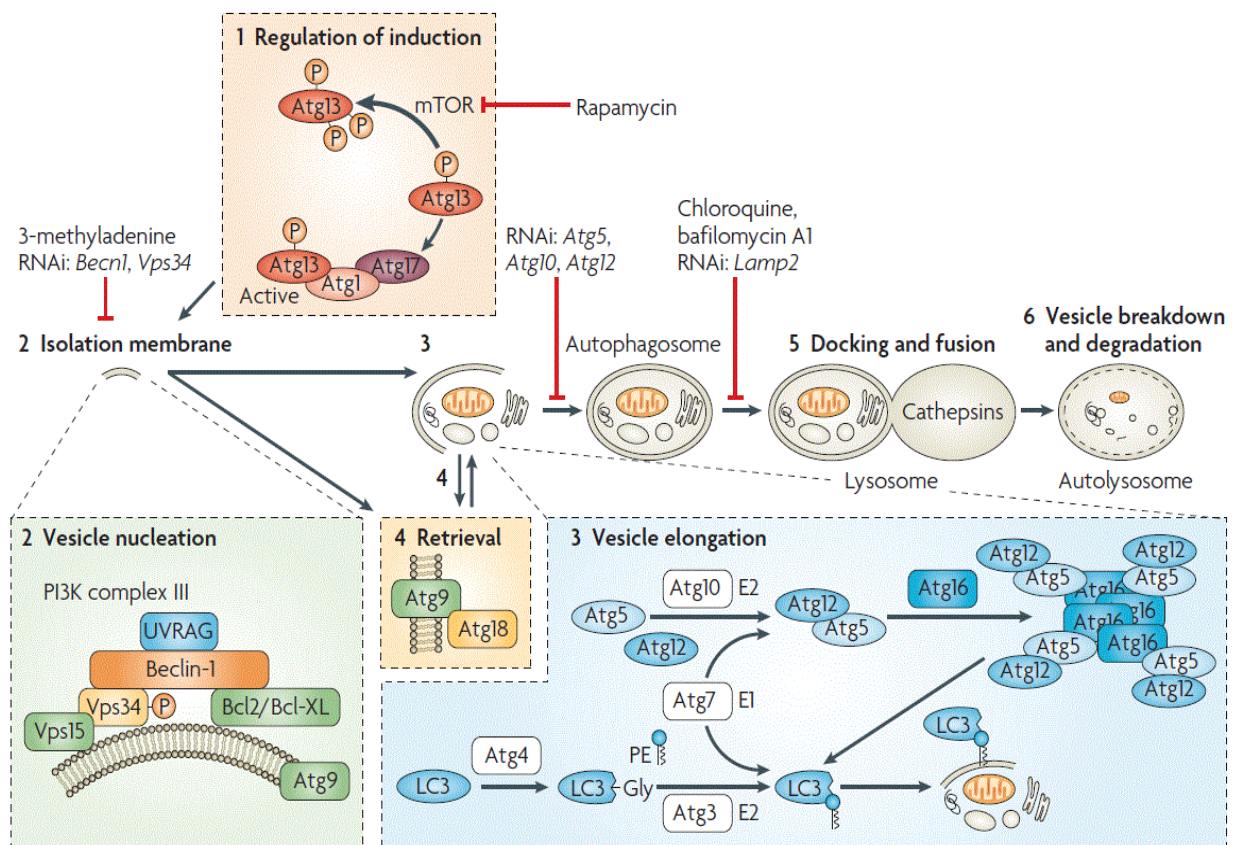


Fig.15. Autophagy and its Inhibitors (Maiuri et al. 2007).

Autophagy and Aging

The ability of cells to maintain homeostasis declines with age. Indeed, a number of cellular functions and activities including autophagy decline with aging. The link between aging and alteration or dysfunction of autophagy has been illustrated in many studies (Cuervo 2009;

Rubinsztein et al. 2011). One of the most known theories about this relationship is oxidative stress theory or mitochondrial theory of aging (Miquel et al. 1980; Donati 2006). This theory explains how ROS-induced damages are increased by dysfunction in mitochondrial respiratory chain. This event will ultimately reduce the autophagy rate leading to the biological manifestations of aging. The major targets of oxidative damages are mtDNA, ETC components and proteins. The increase in ETC components, proteins and mtDNA may cause the malfunction of all biological processes and eventually lead to aging (Donati 2006). Numerous studies on this issue consider the increase in autophagy as an important factor in retardation of aging process which improves the health span.

Autophagy and Cancer

Autophagy is primarily a pro-survival and adaptive response enabling cells to tolerate unfavorable conditions including those which surround cancer cells. Depending on the stage and context of cancer, autophagy plays a dual role by either suppressing or supporting tumorigenesis. In fact, autophagy is up regulated in tumor cells in response to various stressful conditions (e.g. chemotherapy agents) to ensure growth and survival of the tumor. On the other hand, autophagy may act as a tumor suppressor resulting in impaired inflammatory response and increased genomic instability. This happens in part due to the accumulation of damaged organelles and macromolecules and leads the initiation and progression of cancer.

Though growing evidence indicates that autophagy has an important role in tumorigenesis, its contribution to initiation and progression of skin cancer needs to be clarified using a model which shows different phases of carcinogenesis. In a study by Qiang et al., it was shown that UVB radiation induces autophagy through the activation of AMP kinase (Qiang et al. 2013). They showed that autophagy promotes cell survival by suppressing the activation of p62-mediated p38 which suggests that autophagy possibly facilitate UVB-induced tumor development. Wu et al. reported also that AMPK pathway among the main regulators of autophagy which is down regulated in human and mouse squamous cell carcinomas (Qiang et al. 2013).

Chapter II

Energy Metabolism

5. Cellular Energy Metabolism

Energy enters the body by food consumption but production of energy from nutrients entails a series of specific chemical reactions to make them accessible to the cells. Metabolism is a set of life-sustaining chemical reactions which convert food into energy. Biological molecules (nutrients) first become degraded and then re-synthesized during these processes.

Metabolism is divided into two categories: catabolism and anabolism. Catabolism consists of all enzymatic reactions which break down macromolecules and harvest energy by cell respiration. Anabolism is composed of processes in which cells consume energy in order to produce macromolecules including carbohydrates, proteins, lipids and nucleic acids. Macromolecules are the main sources of energy for the body which of course do not produce the same amount of energy in the form of ATP. Catabolism of 1 gram of carbohydrates, proteins and lipids releases 4.1, 5.3 and 9.3 Kcal, respectively.

Alteration in catabolism and anabolism pathways is reported in different types of cancer (Locasale and Cantley 2010; Cantor and Sabatini 2012; Galluzzi et al. 2013).

Compartmentalization of Metabolic Pathways

A metabolic pathway is composed of a series of chemical reactions catalyzed by different enzymes. These reactions require energy for synthesis of the molecules. Different metabolic pathways in the cells have common features and undergo general principles of regulation. In eukaryotic cells, metabolic pathways are compartmentalized, thus synthetic pathways are separated from degradative ones. Compartmentalization plays an important role in sustenance of eukaryotic cell. Metabolic roles of different cell organelles are described in Table 5.

In order to produce energy, eukaryotic cells use two major metabolic pathways including glycolysis (in cytosol) and Krebs cycle/ TCA (in mitochondria). The balance between these two pathways is crucial for eukaryotic cell life. The imbalance between these pathways have been reported in a wide range of cancers (Galluzzi et al. 2013).

Thereafter, many factors including nutrients, environmental and oxidative stress, calorie restriction and toxic agents could influence compartmentalization and energy metabolism.

Table 5. Compartmentalization of Metabolic Pathways.

Compartment	Metabolic pathway
Cell membrane	Transport
Nucleus	DNA replication, Transcription
Ribosome	Protein synthesis
Rough Endoplasmic Reticulum	Protein synthesis, Protein Processing, Glycosylation, Phospholipid Synthesis
Smooth Endoplasmic Reticulum	Synthesis of Fatty Acids, Lipids, Phospholipids, Steroids
Golgi	Protein Synthesis, Protein Processing, Polysaccharide Synthesis
Cytosol	Glycolysis, Gluconeogenesis, Pentose Phosphate Pathway, Fatty Acid Synthesis, Amino Acid Metabolism, Tetrapyrrole and Steroid Synthesis, Glycogen Synthesis
Peroxisomes	oxidative reactions, β -oxidation,
Mitochondria	TCA Cycle, Oxidative Phosphorylation, β -oxidation, Initiation of Gluconeogenesis, Amino Acid Metabolism,

	Tetrapyrrole and Steroid Synthesis, Urea cycle
Lysosome	Degradation of Macromolecules, Storage of Nutrients

5.1. Glycolysis

Glycolysis is the most important cytosolic pathway in term of energy production beside the many others involved in this issue. According to Warburg effect, alteration in glycolysis would increase the risk of carcinogenesis. German biochemist, Otto Warburg describes that cancer cells exhibit glucose fermentation with an increase in acidity even in normoxia conditions. He was awarded the Nobel Prize for his hypothesis in 1931 (Warburg et al. 1927; Warburg 1956).

Glycolysis relies on two steps known as energy-investment and energy-pay off respectively. Meanwhile, glucose is considered as the main substrate for producing energy in this process. Subsequent to the entry of glucose into the cell via specific glucose transporters (GLUT), glucose converts into glucose-6-phosphat (G6P) by hexokinase with a phosphorylation activity. Depending on cell demands, two different metabolic fates could occur to the cell either by passing on glycolysis or entering pentose phosphate pathway which produces essential monosaccharides for the synthesis of nucleotides.

In glycolysis, glucose-6-phosphate (G6P) converts to fructose-6-phosphate (F6P) by an isomerase (GPI) activity. Then, fructose-1, 6 bisphosphate is produced via phosphorylation of F6P by phosphofructokinase (PFK). Thereafter, fructose 1, 6-bis phosphate would convert into two three-carbon units called glyceraldehyde 3-phosphate (G3P) by lyase activity of fructose biphosphate aldolase. Subsequently, G3P is oxidized to 1,3bisphosphoglycerate (1,3PG) by activity of an oxidoreductase enzyme. This reaction reduces two molecules of NAD^+ using hydrogen in order to produce one $\text{NADH} + \text{H}^+$ for each trios. In the next step, through a transferase enzyme, phosphate group of 1,3PG is transferred to ADP to form ATP and phosphoglycerate (3-PG). Then a mutase enzyme converts 3-PG to 2-PG and a lyase enzyme forms a phosphoenolpyruvate from 2-PG afterwards. In the final step, PEP becomes dephosphorylated by the activity of pyruvate kinase in order to produce a molecule of

pyruvate. This happens at the presence of one ADP which gives rise to the formation of an ATP molecule (Figure16).

All of these reactions occur in cell cytoplasm and finally produces two molecules of ATP as well as 2 NADH from NAD^+ cofactor. In presence of oxygen, NAD^+ is renewed during the transfer of electrons to the respiratory chain while in hypoxia, NAD^+ can be quickly regenerated by reduction of pyruvate to lactate. This way of ATP production which occurs in the absence of oxygen is called anaerobic glycolysis. Pyruvate is considered as a key intersection in cell metabolic pathways due to the great potential in producing necessary cell macromolecules including carbohydrates (glyconeogenesis), fatty acids, amino acids and ethanol. In normoxia conditions, pyruvate is transported into mitochondria through mitochondrial pyruvate carrier and monocarboxylate transporters (MCTs). Thereafter, pyruvate undergoes oxidative decarboxylation by an enzymatic complex called pyruvate dehydrogenase (PDH) in order to form acetyl CoA. Acetyl-CoA then enters into citric acid cycle and generates NADH and FADH_2 which will be ultimately give up their hydrogen to the respiratory chain and renewed oxidized equivalents (NAD^+ and FAD).

Another way of producing acetyl-coA is β -oxidation of fatty acids. Acyl-CoA is synthesized from fatty acids by acyl-CoA synthetase at the outer mitochondrial membrane. A shuttle system allows the entry of acyl-CoA to the mitochondria and the formation of acetyl-CoA. Decarboxylation of acetyl-CoA in Krebs cycle is done through eight successive reactions which produce 3 NADH, 1 FADH_2 , 1 GTP (which converts into ATP) and two molecules of CO_2 . Final oxidation of NADH and FADH_2 in oxidative phosphorylation chain (OXPHOS) results in the formation of 3 and 2 molecules of ATP, respectively.

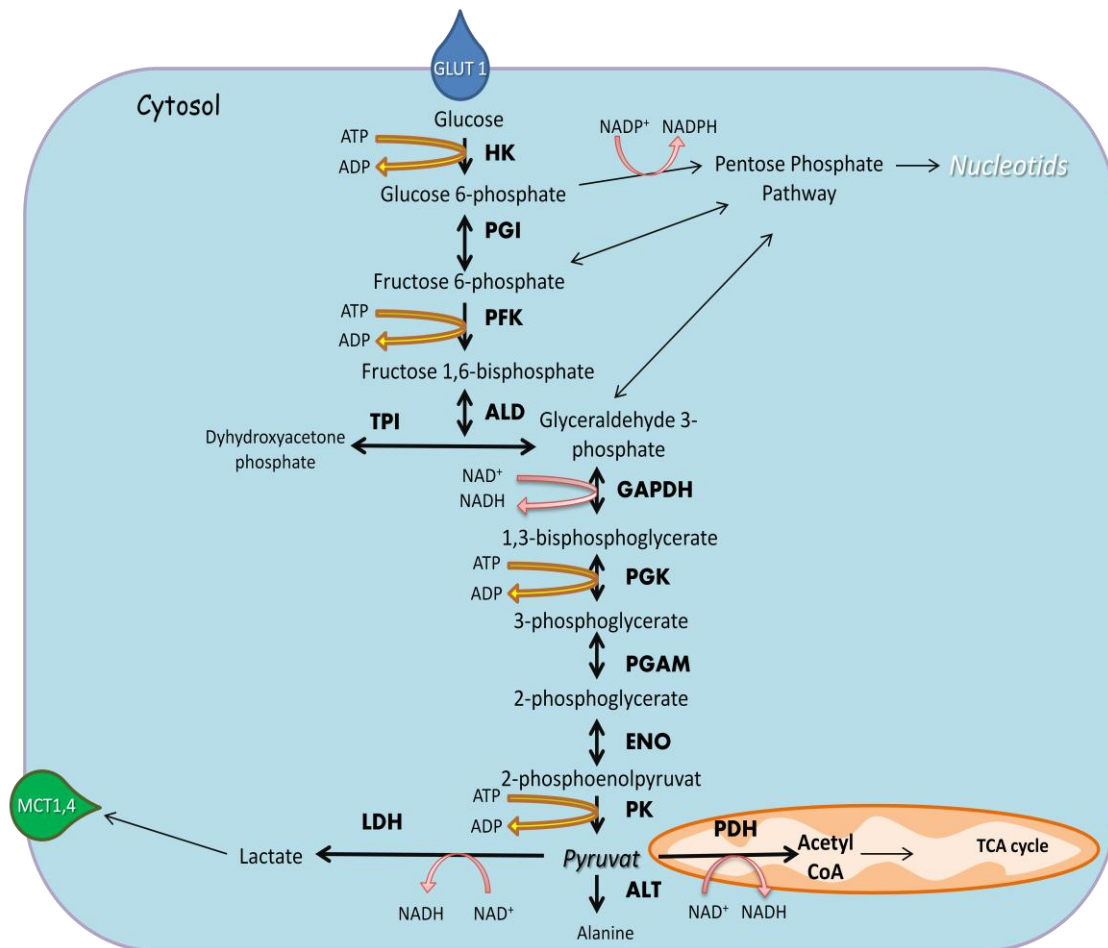


Fig.16. Glycolysis Pathway.

5.2. Krebs Cycle, Electron Transport and Oxidative Phosphorylation

Beside glycolysis and its role in production of a part of energy from glucose or glucagon, tremendous amount of energy is produced by mitochondria. Due to the critical role of this dynamic organelle in energy production, it is the so-called powerhouse of the cell.

Mitochondria is involved in several cellular processes including signaling, cell differentiation, cell death, cell cycle and cell growth as well as synthesis of amino acids, lipids, iron sulfur clusters and also ion homeostasis and thermogenesis. Homeostasis and thermogenesis are the central players in regulation of apoptosis (Frank et al. 2012).

Oxygen consumption by mitochondria accounts for 90% of cellular oxygen consumption, of which 80% is involved in ATP synthesis (Barrett et al. 2010). The produced ATP is then used in different processes including protein synthesis (27%), $\text{Na}^+\text{-K}^+\text{-ATPase}$ function (24%), gluconeogenesis (9%), $\text{Ca}^+\text{-ATPase(PMSA)}$ activity (6%), myosin ATPase function (5%) and ureagenesis (3%)(Barrett et al. 2010).

A growing body of evidence shows that mitochondrial morphology plays an important role in its function. In fact, under normal conditions, mitochondria appear as a single large interconnected membrane-bound tubular network within a cell. Alterations or defects in mitochondrial ultrastructure could affect its morphology and performance afterwards. Frequencies of fusion and fission events could control the length, size, shape and number of mitochondria. Fusion divides the organelle while fission links two separate mitochondria. Following an unbalanced fusion/ fission event, the length, size, shape and number of mitochondria would change.

Altered rate of fusion/ fission events has been demonstrated in disease-related processes such as apoptosis and mitophagy (Boland et al. 2013; Bernhardt et al. 2015). Moreover, it has been shown that UV irradiation results in a mitochondrial fusion (Bess et al. 2013).

Mitochondrial dysfunction or disorders are primarily caused by mutations in nuclear or mitochondrial DNA. Disorders such as Autism, Parkinson's, Alzheimer, Lou Gehring's, muscular dystrophy and chronic fatigue are cited as the result of a mitochondrial dysfunction (Chin-Chan et al. 2015; Milane et al. 2015; Ryan et al. 2015).

5.2.1. Overview of Krebs Cycle

Hans Krebs, pioneer German biochemist recognized two major biochemical pathways of the cell, urea cycle and the tricarboxylic acid cycle (TCA). TCA is also called Krebs cycle in honor of the scientist.

Pyruvate is the origin of most produced acetyl-CoA within Krebs cycle. Oxidative decarboxylation of pyruvate converts it into acetyl-CoA by the activity of pyruvate dehydrogenase (PDH). This enzyme can be inhibited following its phosphorylation by pyruvate dehydrogenase kinase (PDK). Dichloroacetate (DCA) is used as the inhibitor of pyruvate dehydrogenase kinase activity. This inhibition induces more PDH activity leading to an increase in mitochondrial metabolism.

The first specific reaction of the cycle is catalyzed by citrate synthase (CS) combining acetyl-CoA with oxaloacetate to produce citrate. This reaction is accompanied by reduction of NAD^+ and production of a molecule of CO_2 . This enzyme is highly regulated by NADH. Citrate is also exported out of the mitochondria via its specific transporter (SLC25A1) for the synthesis of fatty acids and amino acids.

In the following step, aconitase catalyzes the synthesis of isocitrate from citrate. Isocitrate then undergoes oxidative decarboxylation by isocitrate dehydrogenase allowing the formation of α -ketoglutarate. At the same time, NADH is synthesized by reduction of NAD^+ and is transferred to the electron transport chain. Thus isocitrate dehydrogenase (IDH) is the first enzyme which connects the cycle to the oxidative respiratory chain (OXPHOS).

There are three isoforms of isocitrate dehydrogenase (IDH). IDH1 is the cytosolic isoform and the two others, IDH2 and IDH3 are mitochondrial isoforms of the enzyme. While IDH2 uses NADPH for functioning, IDH3 operates with NADH. This enzyme makes the connection between Krebs and metabolism of amino acids.

α -ketoglutarate plays an important role in reactions catalyzed by amino-transferases. Indeed, α -ketoglutarate may also be synthesized from glutamine which then converts to glutamate. Deamination of this glutamate will form α -ketoglutarate. α -ketoglutarate dehydrogenase converts α -ketoglutarate to succinyl-CoA with reduction of NAD^+ to NADH. Then, succinyl-CoA synthetase by transforming succinyl-CoA to succinate allows the production of a molecule of GTP. Succinate dehydrogenase would oxidize succinate to fumarate thereafter by synthesizing a molecule of FADH_2 . This enzyme provides the necessary FADH_2 for the respiratory chain at complex II. Succinate dehydrogenase is bound to the inner membrane of the mitochondria and is the only enzyme of TCA cycle involved in respiratory chain. Thereafter, fumarate hydratase (FH) enables the synthesis of malate from fumarate and the last step is conversion of malate to oxaloacetate which is catalyzed by malate dehydrogenase. This reaction is accompanied by reduction of NAD^+ (Figure17).

Mutations in SDH gene have been found in paragangliomas of the head and neck (Baysal et al. 2000; Boedeker et al. 2007). Moreover, mutations of FH have also been identified in the uterus, breast and kidney cancers (Tomlinson et al. 2002; Lehtonen et al. 2006).

Evidently, these mutations lead to stabilization and subsequent up-regulation of a transcription factor called HIF1 α . In fact, accumulation of succinate or fumarate inhibits the activity of prolyl hydroxylases which in turn exert effects on transcription of HIF1 α (Dhup 2012).

TOM (Translocase of Outer Membrane) and TIM (Translocase of Inner Membrane). The inner membrane consists of 80% proteins and only 20% phospholipids which is quite different from the other biological membranes. Due to its particular lipid composition, this membrane is impermeable to ions, therefore transport of molecules requires the presence of TOM and TIM carriers.

Mitochondria have their own DNA which is transmitted to the daughter cells separately from nuclear DNA. As this DNA is not protected by histone proteins, rate of mutations is approximately 10 to 20 times more than nDNA (Neckelmann et al. 1987; Wang et al. 2003). Unlike nuclear DNA which is inherited from both parents, mtDNA inheritance is just maternal.

Mitochondrial DNA is typically organized as a double strand circular structure with an approximate length of 16,806 bp containing 37 genes. These genes code for two rRNAs, 22 tRNAs and 13 polypeptides. In addition, there are approximately 1500 nuclear-encoded mitochondrial proteins which are all essential for mitochondrial normal function. In each human cell, there are approximately 10-1000 mitochondria each containing 10^3 - 10^4 copies of mtDNA.

Based on the nucleotide content, the two strands of mtDNA are named differently. The strand rich in purines (G) is called heavy chain and carries 28 genes while the light strand which is rich in pyrimidines (C) carries only 9 genes (Strachan and Read 2004). Mitochondrial DNA has its own replication, transcription and translation system and is independent of the nuclear DNA for all of these processes. The two strands of mtDNA have different origins of replication with heavy chain being synthesized at first and the light strand replicated afterwards. mtDNA replicates in a D-loop fashion.

5.2.3. Electron Transport Chain (ETC)

Operation of the electron transport system and OXPHOS was first proposed as the chemiosmotic theory by Peter Mitchell (Mitchell 1961). Electrons released during oxidative reactions are transferred to the electron transport chains (ETC) which include a series of electron donors and acceptors. NADH and FADH₂ are the electron donors and molecular oxygen is the final electron acceptor. Electrons enter into ETC through complex I and II and are transferred to ubiquinone during the oxidation of NADH or FADH₂. Glycerol 3-phosphate

dehydrogenase and electron transfer flavoprotein can also transfer electrons to ubiquinone and participate in ETC.

This electron transfer is coupled with the extrusion of protons to the inter-membrane space using active pumps to produce a proton gradient (chemical gradient) and a transmembrane charge (electrical gradient) as well. Then protons go back to the mitochondrial matrix via ATP synthase complex where it results in generating ATP from ADP (Figure 18). The proton gradient is however essential not only for production of ATP but also indispensable to import proteins into the inner membrane and mitochondrial matrix.

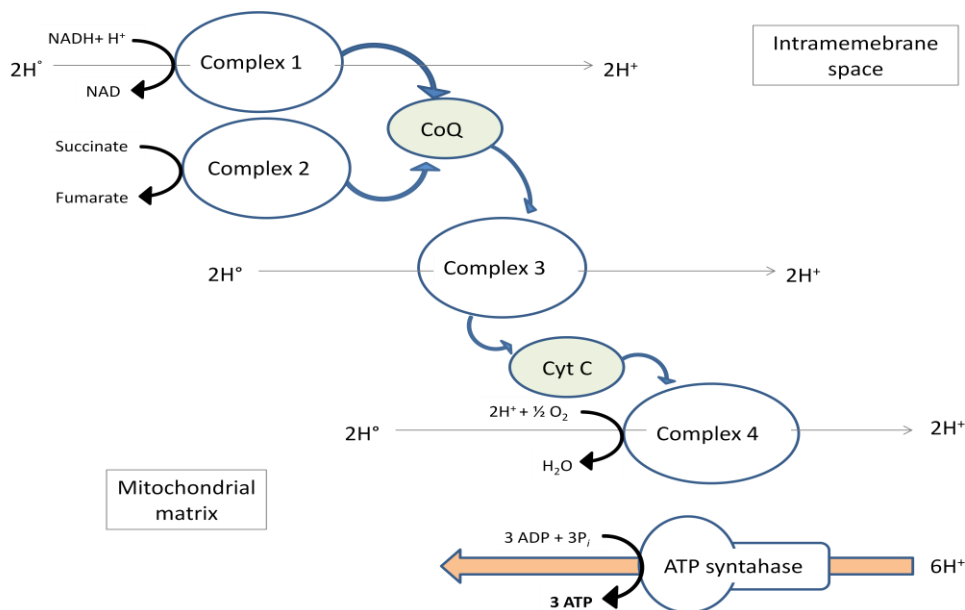


Fig.18.Organisation of Electron Transport Chain.

5.2.3.1. Complex I/ NADH Ubiquinone Oxidoreductase

Complex I or NADH-coenzyme Q reductase is a protein complex responsible for transferring electrons from NADH to ubiquinone. Complex I is the largest complex of the electron transport system with 45 subunits and a total size of ≈ 1000 kDa (Remacle et al. 2008). In mammals, 14 of the subunits are considered essential for the catalytic activity of the complex (Hirst et al. 2003; Remacle et al. 2008) while others may play a role in its regulation and assembly (Friedrich et al. 1994).

5.2.3.2. Complex II/ Succinate-Coenzyme Q Reductase

Succinate-coenzyme Q reductase transfers electrons from FADH₂ to ubiquinone. This enzyme complex is part of the Krebs cycle and is linked to the mitochondrial inner membrane. It consists of four subunits which are encoded by the nuclear DNA. Complex II is only involved in the transfer of electrons into the inter-membrane space and is not accompanied with proton translocation.

Complex I and II are the main entry points of electrons to ETC. However, there are other ways for electrons to enter. These include the transfer flavoprotein oxidoreductase ubiquinone-electrons and glycerol-3-phosphate dehydrogenase (Wattmough and Frerman 2010). Therefore, these enzymes reduce ubiquinone (CoQ) which acts as an electron-carrier between complexes II and III. It picks up reducing equivalents from Complexes I and II and transfers them to complex III.

Defect in human complex II has been correlated with neurodegenerative disorders such as Friedreich ataxia (Rötig et al. 1997) and Huntington's disease (Butterworth et al. 1985). Dysfunction in this complex due to a few mutations can be the cause of many cancers such as paragangliomas (Hoekstra and Bayley 2013). Decrease in activity of complex II has been shown to be associated with an increase in cell proliferation which lead to tumorigenesis through activation of HIF1 α and subsequent increase in glycolysis and angiogenesis (Gimenez-Roqueplo et al. 2001).

5.2.3.3. Complex III/ Coenzyme Q-Cytochrome c Reductase

Complex III also known as cytochrome bc₁ complex participates in both electron transfer from CoQ to cytochrome c and also development of proton gradient. Indeed, two protons are transferred into the intermembrane space for each oxidized ubiquinol. This complex is a dimer made up of two monomers, each consisting of 11 subunits of which only one subunit (cyt b) is encoded by mtDNA.

5.2.3.4. Complex IV/ Cytochrome c oxidase

Cytochrome c oxidase is the last enzyme in ETC which transfers electrons to the oxygen as the final electron acceptor. In mammals, cytochrome c oxidase (COX) consists of 13 subunits of which three are encoded by mtDNA. The reduction of O₂ to H₂O in Complex IV requires four electrons. Complex IV is also interesting for its possible capacity to work in a second respiratory control mechanism with the proton-motive force. This mechanism is based on the allosteric inhibition (independent of mitochondrial membrane potential) of COX by

attachment of ATP. Indeed, when ATP/ ADP ratio is high, ATP can bind to the subunit IV leading to inhibition of complex IV and adjustment of the energy production to its physiological demand.

5.2.3.5. Complex V/ ATP synthase

Complex V uses the proton-motive force in order to generate ATP from ADP. This step is known as the final step in oxidative phosphorylation (OXPHOS). Complex V can be divided into two main parts; F₁ and F₀. F₁ carries the catabolic center of ATPase complex and involved in charge of transporting hydrogen ions. The catalytic mechanism involves conformational changes in F₁ which carries the nucleotide binding sites, producing ATP from ADP and inorganic orthophosphate (Pi). Protons previously transferred by complexes I, III and IV are present in greater amounts in the intermembrane space and therefore tend to go back into the mitochondrial matrix. As the inner membrane is impermeable to protons, they can cross the lipid bilayer at level of F₀ rotors of ATP synthase. (Stock et al. 2000; Nakamoto et al. 2009).

Table 6. Overview of mitochondrial structure, inhibitors and disorders.

Complex	I	II	III	IV	V
Nuclear DNA subunits	39	4	10	10	14
Mitochondrial DNA subunits	ND1 ND2 ND3 ND4 ND5 ND6 ND4L	-	Cytochrome b	Cytochrome oxidase I, Cytochrome oxidase II, Cytochrome oxidase III	ATPase6, ATPase8

Enzyme	NADH-CoQ reductase	succinate-CoQ reductase	CoQ-cytochrome C reductase	cytochrome C oxidase	ATP synthase
Inhibitor	Rotenon, Amytal	TTFA malonate	Antimycin A	Cyanide, carbon monoxide, Azide	Oligomycin
Disorders	Alpers Alzheimer's/ Parkinsonism Cardiomyopathy Deficiency Barth Lethal Infantile Encephalopathy Infantile CNS Leber's Leigh Longevity MELAS MERRF Myopathy ± CNS PEO Spinal cord	Kearns-Sayre Leigh's Myopathy Infantile ± CNS Paraganglioma Pheochromocytoma	Cardiomyopathy Fatal infantile GRACILE Leber's Myopathy ± CNS PEO	Alper's Ataxia Deafness Leber's Leigh's Myopathy Infantile Fatal Benign Adult Rhabdomyolysis PEO, KSS, MNGIE MERRF, MELAS	Cardiomyopathy Encephalopathy Leber's Leigh Multisystem NARP

5.2.4. Mitochondrial Turnover

About 54 years ago, Fletcher and Sanadi (Fletcher and Sanadi 1961) obtained the basic information about proteins involved in mitochondrial turnover using radiolabeled mitochondrial proteins. More recent studies on mitochondrial biogenesis, autophagy, mitophagy and fusion/ fission confirmed the importance of mitochondrial turnover in the maintenance of mitochondrial quality control. In fact, the balance between biogenesis and autophagic destruction maintains the mitochondrial quality control.

Environmental and oxidative stress, cell differentiation, cell division, low temperature and caloric restrictions are the main factors possibly stimulating mitochondrial biogenesis, a process which is accompanied by variations in mitochondrial size, number and mass. Comparison of muscles involved in ordinary and sustained physical activity has demonstrated that energy demand regulates mitochondrial biogenesis and activity (Jornayvaz and Shulman 2010). PGC-1 α (peroxisome proliferator-activated receptor (PPAR)- γ coactivator)-1 family is a master regulator, a transcriptional co-activator and a central inducer of mitochondrial biogenesis. It has been shown that it also involves in a variety of other biological responses such as adaptive thermogenesis, gluconeogenesis and glucose-fatty acid metabolism. PGC-1 α regulates mitochondrial biogenesis by modulation of a few transcription factors. NRF1 (nuclear respiratory factor 1), NRF2 and mitochondrial transcription factor A (mtTFA) also known as TFAM are the main PGC-1 α downstream transcription factors. NRF1 and NRF2 can also increase the expression of TFAM by binding to the upstream region of TFAM gene.

TFAM is a key activator of mitochondrial transcription which binds to the promoter of mtDNA. It also involves in mtDNA replication. Therefore, TFAM modulates energy metabolism by affecting mtDNA transcription, and copy number and consequently mitochondrial activity and biogenesis. During my thesis, I examined the effect of knocking out of TFAM (TFAM KO) on UVB-induced tumorigenesis.

5.3. Fatty Acid Metabolism

5.3.1. Fatty Acid Synthesis

Fatty acid synthesis generally occurs in the cytosol of liver cells and adipose tissues. Acetyl CoA which is known as the major substrate of fatty acid biosynthesis is produced from pyruvate, acetate, amino acid catabolism and citrate degradation. Excess of citrate level triggers fatty acid synthesis whereas palmitoyl CoA represses this process.

The first reaction begins with a biotin-dependent enzyme which catalyzes the irreversible carboxylation of acetyl-CoA to malonyl-CoA. This enzyme called acetyl-CoA carboxylase requires one molecule of ATP for its activity. Reactions of fatty acid synthesis apart from acetyl-CoA carboxylase are carried out by a multienzyme complex called Fatty acid synthetase (FASN), a multifunctional protein with 7 catalytic activities. Synthesis of palmitate

from acetyl-CoA, malonyl-CoA and NADPH is considered as the main task of FASN (Figure19).

Production of each molecule of palmitate requires 14 NADPHs and 7ATPs. Eukaryotic cells stock the excessive amount of carbohydrates in the cell in the form of palmitic acid. The process of fatty acid elongation adds acetyl groups to the growing chain of palmitate. Elongation of fatty acids occurs in three cellular compartments: cytosol, mitochondria, and endoplasmic reticulum. Over expression of FASN in malignant cells has been also reported in many types of cancers such as cancers of breast, lung and prostate.

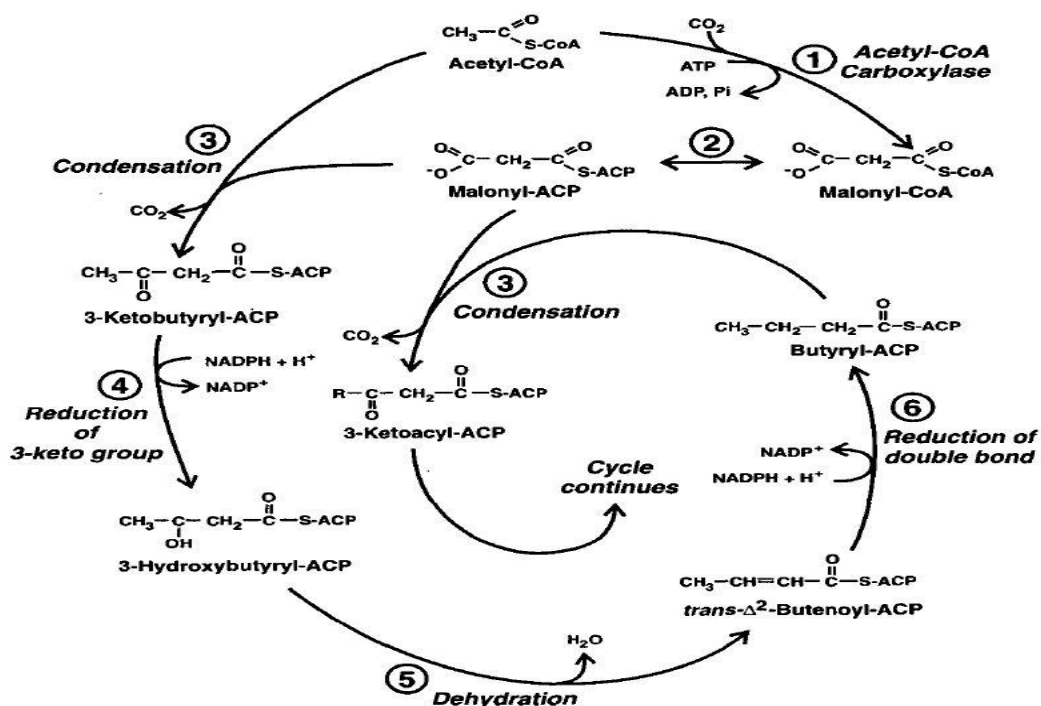


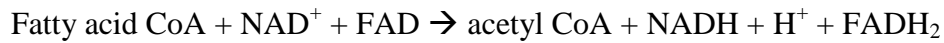
Fig.19. De novo fatty acid biosynthesis (Ohlogge and Browse 1995).

5.3.2. Fatty Acid β-Oxidation

In addition to glucose, β-oxidation of fatty acids is also a source of energy production. Adipose tissue is considered as the richest source of energy in the body. Free fatty acids are the main sources of energy in heart and muscles in the resting phase.

Fatty acid β-Oxidation is a multistep process which breaks down fatty acids for energy production. This process occurs in mitochondria with a close link to ETC. β-Oxidation of fatty acids can also occur in peroxisomes. However, fatty acids with a very long chain are handled by the mitochondria (Figure 20).

Lipoprotein lipase is the enzyme which catalyzes the hydrolytic cleavage of fatty acids from triglycerides and is circulating in the blood. Fatty acids enter the cells by leaving glycerol behind and this is the only way they can do the process. Fatty acid β -Oxidation occurs in three steps: 1. Transport of acyl-CoA into mitochondria, 2. Degradation of acyl-CoA to acetyl-CoA, and 3. Oxidation of acetyl-CoA through TCA cycle. The overall reaction is:



In each cycle of acyl-CoA oxidation, one molecule of acetyl-CoA, one of FADH_2 and one NADH are produced. The last step in this process is oxidation of acetyl-CoA to CO_2 via Krebs cycle.

Oxidation of fatty acids is a highly energetic process. As an example, oxidation of one molecule of palmitate (a fatty acid with 16 carbons) leads to the production of 7 FADH_2 , 7 NADH, and 8 molecules of acetyl-CoA, thus ultimately leading to 131 molecules of ATP. Since activation of palmitate by acyl-CoA synthetase requires two molecules of ATP, the net formation of ATP from a palmitate molecule is equal to 129 ATP (Carracedo et al. 2013).

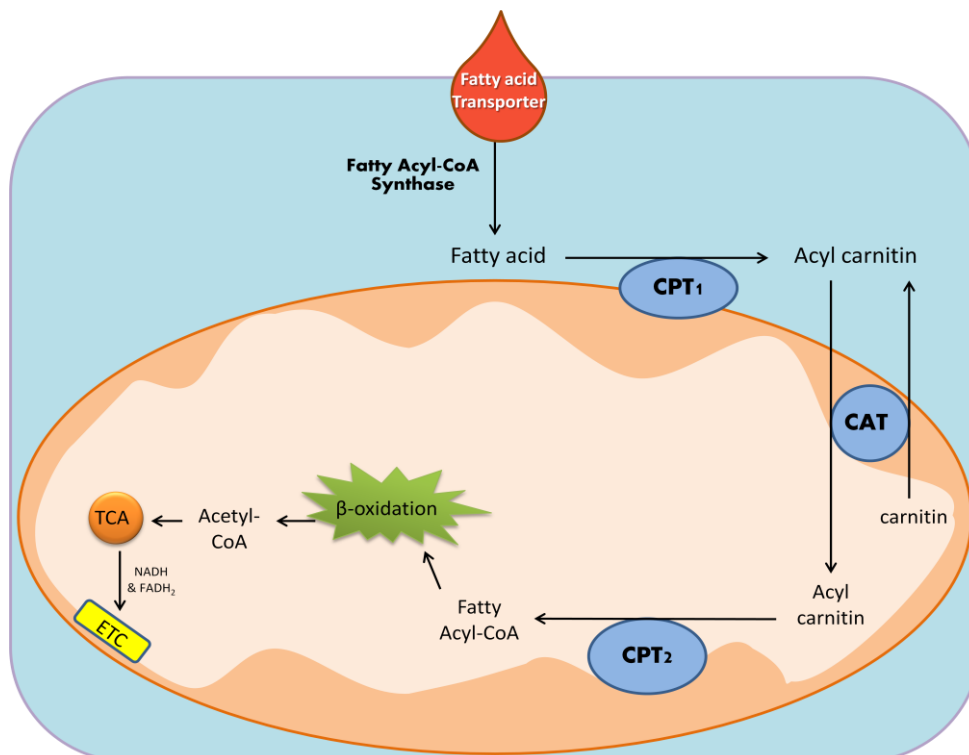


Fig.20. Overview of fatty acids β -oxidation.

5.4. Nucleotide Synthesis

Synthesis of nucleotides is conducted in several steps requiring a large amount of energy. A nucleotide is composed of a nitrogenous base, a ribose sugar (as the central metabolite of the pentose phosphate pathway) and a phosphate group. Formation of 5-phospho-a-D-ribose 1-pyrophosphate (PRPP) is an essential step in purine and pyrimidine synthesis. ATP by giving two molecules of phosphate to ribose 5-phosphate transforms it to PRPP which is an intermediate in biosynthesis of purines, pyrimidines, NAD, histidine and tryptophan.

5.4.1. Purine Synthesis

Purine synthesis begins with adding glutamine-derived ammonia to PRPP. The first reaction is catalyzed by pyrophosphate amidotransferase which is activated by PRPP. This enzyme catalyzes the reaction of PRPP with glutamine and water to produce 5'-phosphoribosylamine, glutamate and pyrophosphate. Finally, phosphoribosylamine converts into Inosine-5'-monophosphate or IMP (Figure 21). IMP is the precursor of guanine and adenine. Other notable purines include hypoxanthine, xanthine, theobromine, caffeine, uric acid and isoguanine. The entire process of purine synthesis requires 5 molecules of ATP.

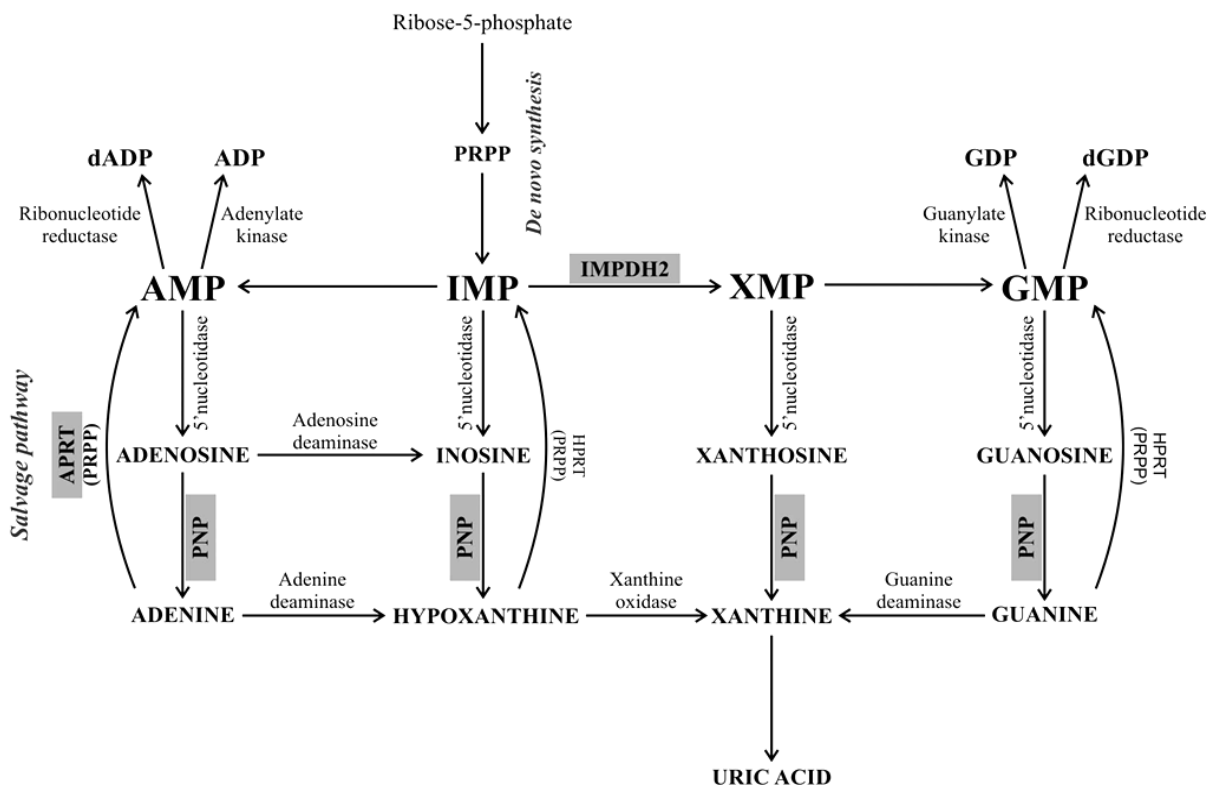


Fig.21. Purine *de novo* biosynthesis (Pospisilova 2013).

5.4.2. Pyrimidine Synthesis

The first step of this process is the formation of carbamoyl phosphate by carbamoyl phosphate synthetase II activity. Then carbamoyl phosphate is converted to carbamoyl aspartic acid by the activity of aspartic transcarbamoylase. In the next step, carbamoyl aspartic is dehydrated to dihydroorotate by dihydroorotase. Carbamoyl phosphate synthetase II, aspartic transcarbamoylase and dihydroorotase are coded by the same enzyme called CAD.

Then dihydroorotate converts to orotate within the mitochondria by dihydroorotate dehydrogenase (DHODH). At this step, ribose-5-phosphate is joined to N-1 of orotate giving orotidine-5'-monophosphate (OMP). In this reaction, the donor of ribose phosphate is PRPP and enzyme is orotate phosphoribosyl transferase. Decarboxylation of OMP by OMP decarboxylase gives UMP. Phosphorylation of UMP consequently generates UDP which is the precursor of thymidine and cytosine (Figure 22).

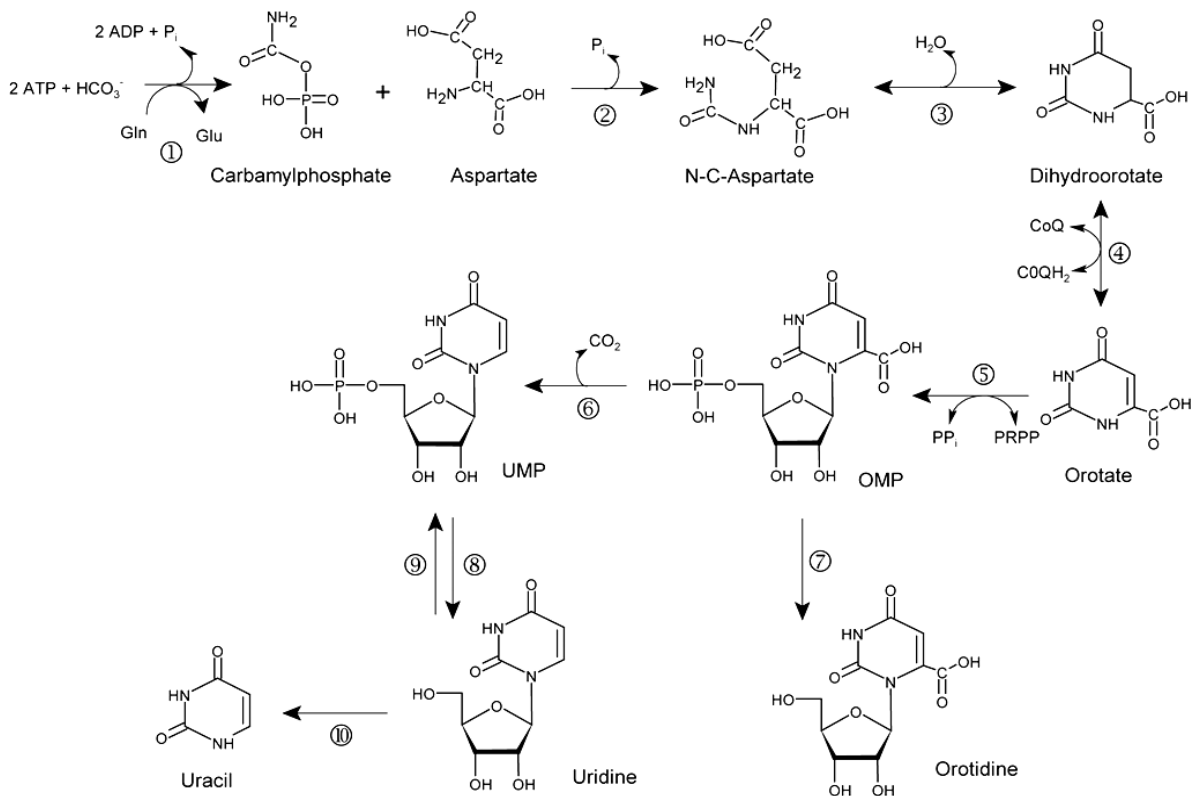


Fig.22. Pyrimidine *de novo* biosynthesis. 1) carbamylphosphate synthetase; 2) aspartate transcarbamoylase; 3) dihydroorotase; 1+2+3) CAD; 4) dihydroorotate dehydrogenase; 5) orotate phosphoribosyltransferase; 6) orotidine 5'-monophosphate decarboxylase; 5+6) UMP synthase; 7) orotidine 5'-monophosphate phosphohydrolase; 8) pyrimidine 5'-nucleotidase; 9) uridine kinase; 10) uridine phosphorylase(Van Kuilenburg et al. 2004).

6. Energy Metabolism during Carcinogenesis

6.1. Cancer

Cancer is a disease characterized by an abnormal cellular proliferation in normal tissues of the body. Benign tumors are well demarcated by regular cells that often grow slowly. In contrast, malignant cells are defined as the cells that grow rapidly with a possible invasion to surrounding tissues. Tumors are found in solid, liquid or metastatic form. Solid tumors are formed by cancer cells surrounded by a tissue or stroma (consisting of support cells, modified fibroblast) which are infiltrated with blood vessels bringing necessary sugars, amino acids and oxygen for tumor growth.

Solid tumors which represent 90% of human cancers can develop from any tissue within the body such as skin, mucosa, bones and organs. There are two tumor types:

- 1) Carcinomas which are derived from epithelial cells including skin, breast, lung, prostate, intestine, liver etc.
- 2) Sarcomas which arise from connective tissue such as bone cancer and cartilage.

Liquid cancers are dividing into two known types: i) leukemias which are blood and bone marrow cancers, ii) Lymphomas as the cancers of the lymphatic system including nodes and also spleen and liver.

While just 10% of cancer cases are hereditary, the majority occurs as a sporadic event.

Carcinogenesis is triggered by acquiring certain characteristics which enable a cell to divide indefinitely. A cell should acquire ten biological capabilities (summarized in figure 22) to be considered as a cancer cell (Hanahan and Weinberg 2011). One of these hallmarks is cells exhibiting differential aspects of cellular metabolism relative to normal cells.

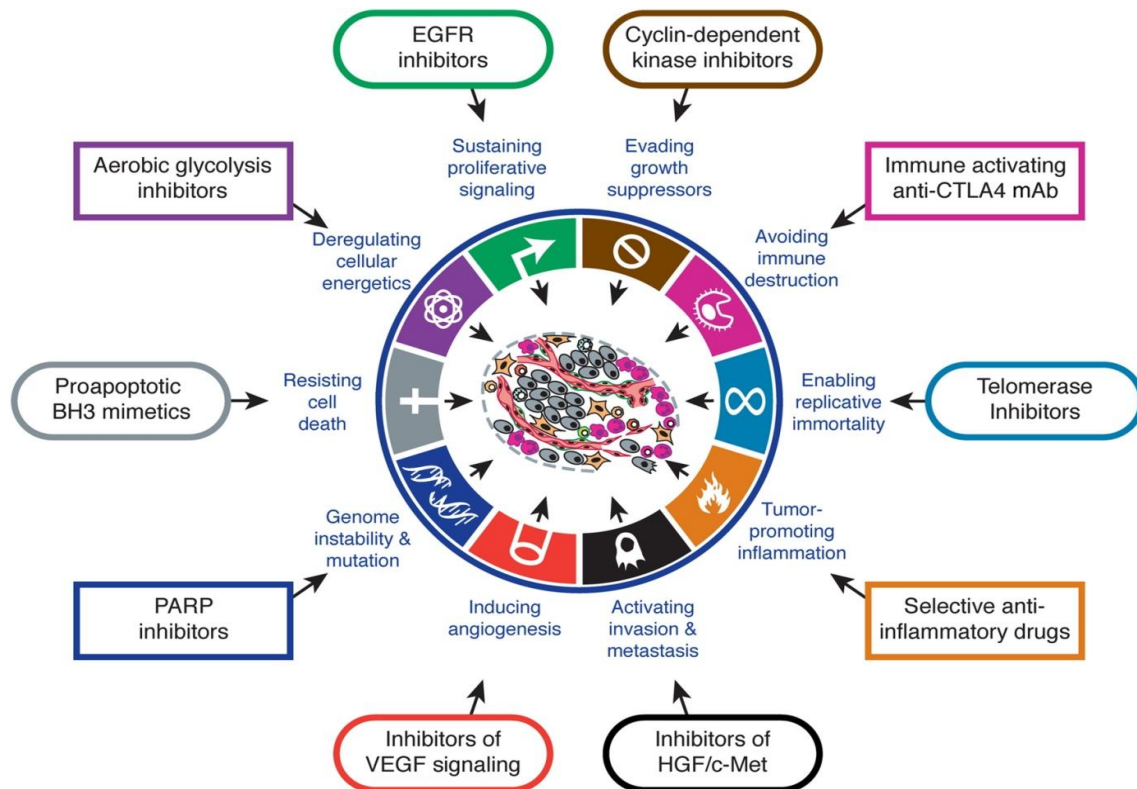


Fig.23. Therapeutic Targeting of the Hallmarks of Cancer (Hanahan and Weinberg 2011)

6.2. Metabolic Flexibility

Metabolic flexibility is the ability of cells to modify their metabolic circuits by activating compensatory or alternative pathways (non-canonical) to maintain their energy homeostasis and other needs. Any disruption in this process leads to a variety of disorders such as cancer or metabolic diseases. For the first time, metabolism alteration in malignant cells was shown by Otto Warburg in the 1920s. He reported that malignant cells have an increased utilization of glucose via glycolysis to produce ATP despite the presence of oxygen. Warburg described an increased rate of lactate production as well assuming that cancer occurs when the mitochondrial oxidative metabolism is altered. His theory was abandoned after the discovery of genes until 1996 when Horton and colleges identified a mitochondrial mutation in renal carcinoma (Horton et al. 1996). Consequent investigations have revealed the significant role of metabolism alteration in carcinogenesis.

6.2.1. Determinant Factors of Metabolic Flexibility

Dysregulation of mitochondrial metabolism may lead not only to a decline in energy production but also to increased production of ROS and accumulation of DNA damage. In addition to mitochondrial diseases in result of defects in OXPHOS (caused by mutations in nuclear or mitochondrial genes) (Table 6), many other disorders such as cancer and premature aging are associated with alteration in the mitochondrial energy homeostasis (Schapira et al. 1998; Wallace 2001; Hosseini et al. 2014b).

For years, it was believed that increased glycolysis in cancer cells is due to a mitochondrial dysfunction. However, in recent years, we have gained a better understanding of the mechanisms leading to the metabolic shift observed in highly proliferative malignant cells. Indeed, these changes are observed not only in cancer cells but also in most of the cells with significant proliferation rates (DeBerardinis et al. 2008). Some of the governing mechanisms for metabolism reprogramming are as follows:

- Post-translational modifications and rapid degradation or stabilization of nodal enzymes could trigger the rapid metabolism alteration. For example, in hypoxia conditions, stabilization of HIF1a and phosphorylation of PDH leads to down-regulation of OXPHOS and up-regulation of glycolysis.
- In each cell there is a system of sensors that control many cellular parameters such as energy metabolism. These sentinels activate signaling pathways leading to a reorganization of metabolic circuits. For example, decreased ATP/ ADP ratio leads to AMPK activation which stimulates catabolism and blocks anabolism.
- Mutations in a few genes such as SDH, FH and IDH in some cancers allow the stabilization of HIF1a, thus switching metabolism toward glycolytic pathway.
- According to thermodynamics and kinetics rules and particularly the mass-action law, over-activation of an enzyme could block the activation of another enzyme or another pathway. For example, high rates of NADH blocks IDH and reduces the activity of Krebs cycle.
- Second messengers like calcium or ROS also provide rapid means of metabolism remodeling. For example, cleavage of aconitase by ROS leads to extrusion of citrate into cytosol, thereby inducing synthesis of lipids. In this case, glucose converts to fat as in diabetic hyperglycemia.

- Expression of certain isoforms can also change the biochemical pathways of energy transduction. For example, hypoxia-inducible factor 1 (HIF-1) reciprocally regulates the expression of COX4 subunit by activating transcription of the genes encoding COX4-2 and LON, a mitochondrial protease which is required for COX4-1 degradation. Thus, mammalian cells respond to hypoxia by altering COX subunit composition. Another example is PKM which is a rate-limiting enzyme converting PEP to pyruvate in the glycolytic pathway. PKM2 acts more slowly than PKM1 allowing the accumulation of glycolytic intermediates which will be used by anabolic pathways. PKM2 is shown to be upregulated in cancer. PKM2 can translocate to the nucleus where it will interact with HIF-1 α and regulate the expression of numerous glycolytic enzymes. These events ultimately lead to an increased rate of cell proliferation (Ward and Thompson 2012).
- Another mechanism implicated in metabolism reprogramming is mitochondrial dysfunction in cancer owing to: i) Reduction of pyruvate entry into the mitochondria, ii) Reduction in mitochondrial biogenesis due to the interaction of p53 or iii) inhibition of the respiratory chain activity triggered by mutated p53 via SCO2 or HIF1 α through an isoform switch in COX4A-1/2.
- Activation of PI3K/ Akt pathway promotes glycolysis by induction of glucose entry into the cell. Akt promotes glycolysis by stimulating certain enzymes such as hexokinase (HK) and phosphofructokinases 1(PFK1). Moreover, AKT can boost lipid synthesis from glucose(Porstmann et al. 2005).
- The presence of hexokinase II also seems to be very essential in establishing Warburg effect. This enzyme catalyzes the phosphorylation of glucose and hexoses to produce glucose-6-phosphate as the first step of glycolysis. Apparently, hexokinase can bind to the to the mitochondrial outer membrane via the porin-like protein voltage-dependent anion channel (VDAC) and provide access to the ATP produced by ATP synthase (Bustamante and Pedersen 1977; Mathupala et al. 2009) . This phenomenon would increase its activity and induce a much higher glycolytic flux thereafter(Bustamante and Pedersen 1980). This association is observed in several cell types but it appears to be much higher in cancer cells.
- It appears that there is a truncated Krebs cycle in some cancer cells. For example, ATP citrate lyase (ACLY) enzymes and fatty acid synthases which convert acetyl-CoA to fat are over expressed in proliferating cells and tumors (Currie et al. 2013; Corominas-faja et al. 2014). To upregulate the lipid synthesis, pyruvate which enters the mitochondria is

converted into acetyl-CoA. Following interaction with oxaloacetate, citrate is produced. This citrate is then exported into the cytosol, where it is converted back to acetyl CoA and oxaloacetate. The latter is used as an important precursor in lipid synthesis in these cells (Kuhajda et al. 1994; Bauer et al. 2004). This citrate and oxaloacetate efflux into the cytosol, however, could cause a loss of these intermediates in the mitochondria which possibly could lead to a reduction of lipid synthesis. Glutaminolysis can counteract this loss of intermediates in the Krebs cycle. Glutamine is converted to glutamate in the mitochondria which then enters the TCA cycle in the form of α -ketoglutarate, ultimately leading to the formation of oxaloacetate (Reitzer et al. 1979). Glutamine consumption rate in cancer cells is higher than "normal" cells (Wise and Thompson 2010).

In brief, the role of mitochondria seems to be changed in cancer cells. While they are primarily responsible for energy production in normal cells, they become important components of anabolic reactions in cancer cells to support the high demands of biosynthesis in proliferating cells (DeBerardinis et al. 2008).

Mitochondria actually produce several essential precursors for biosynthesis of lipids, proteins and nucleic acids via the intermediates in Krebs cycle. A large portion of cancer cells produce most of their energy through aerobic glycolysis. Several studies have shown that some types of cancer cells could use OXPHOS more than glycolysis to produce ATP (Herst and Berridge 2007; Zheng 2012). In addition, several types of cancer cells can survive and proliferate in culture media deprived of glucose. For example, when glucose is replaced by galactose, cells derive their energy from glutaminolysis. Given that galactose can be oxidized by glycolysis, cells use glutamine as a substrate of the Krebs cycle, thereby providing electrons for ETC and producing ATP afterwards (Rossignol et al. 2004). All these data show that mitochondria in cancer cells are not necessarily dysfunctional.

6.2.2. Principal Factors involving e in Regulation of metabolic flexibility

Several proteins and pathways such as HIF1a, AMPK, mTOR, PI3K/AKT, P53, FOXO, HNF, RAS and SIRT are involved in the regulation of energy metabolism flexibility. Here I focus on some key factors having an important role in carcinogenesis and premature aging.

➤ HIF1a

Oxygen concentration as well as PH distribution and nutrient supply play a crucial role in maintenance of the normal metabolism. In most of the cancer cases, a dramatic decrease in oxygen levels has been reported. In general, limitation in oxygen diffusion in the tissue is approximately 150-200 μm but a distance over 70 μm from a blood vessel can cause a lack of oxygen in the cells and create a hypoxia condition (Vaupel 2004). Hypoxia leads to activation of hypoxia inducible factor (HIF), a heterodimeric transcription factor and trans-activator which consists of an α and a β subunit. mRNAs encoding the two subunits of HIF1 are constitutively and stably expressed in most of the cells (Gradin et al. 1996).

HIF1a mediates cellular responses to oxygen availability. It has a short stability in normoxia conditions and is targeted to degradation by Von hippel-Lindau (pVHL) in proteasomes. In the first step of destruction, HIF1a is hydroxylated by prolyl hydroxylases PHD1, PHD2 or PHD3 (Myllyharju 2013). pVHL complex, which has an E3-ubiquitin ligase activity, then mediates ubiquitination of HIF1a. This reaction leads to the degradation of HIF1a by proteasomes. In hypoxia conditions, HIF1a is stabilized owing to the inactivation of PHD in absence of oxygen. Stabilized HIF-1a will then translocate into the nucleus and activate the hypoxia inducible target genes (Kang et al. 2010).

The stabilization of HIF1a stimulates the expression of glucose transporters (Glut1 and GLUT3) and several glycolytic enzymes such as hexokinase II, phosphofructokinase, pyruvate kinase, lactate dehydrogenase and pyruvate dehydrogenase kinase (Kim et al. 2006). These changes induce a huge glucose uptake into the cell as well as an increased production of lactate and production of ATP by glycolysis. Moreover, phosphorylation of pyruvate dehydrogenase by pyruvate dehydrogenase kinase inhibits the entry of pyruvate in Krebs cycle, thereby decreasing the mitochondrial ATP production (Papandreou et al. 2006). HIF1 α may be regulated by some mitochondrial intermediates such as succinate and fumarate which inhibit PHD enzymes. In 2008, Hervouet and colleges showed that HIF1 α is able to induce a decrease in mitochondrial biogenesis (Hervouet et al. 2008).

Skin -our experimental model- contains a mild hypoxic microenvironment (Bedogni et al. 2005) suggesting a high expression of HIF-1a. Indeed, it has been demonstrated that HIF-1a has important roles in skin physiology and pathophysiology including wound healing, premature aging and epidermal carcinogenesis (Rezvani et al. 2011b).

➤ **AMPK**

In mammals, cells must maintain a stable energy balance characterized by a ratio of 10:1 for ATP/ADP. Indeed, this ratio may be decreased in hypoxia conditions or in deprivation of glucose.

AMPK is composed of two regulatory subunits (β and γ) and one catalytic (α) subunit. Each of the three subunits is encoded by several genes in mammals. This enzyme is activated by phosphorylation of threonine 172 which is located in the activation loop of α subunit. In activated form, AMPK is considered as a metabolic or energy sensor (Hardie et al. 2012). On one hand, it activates metabolic pathways which produce ATP including glycolysis, β -oxidation of fatty acids, mitochondrial metabolism and synthesis of ketone bodies (catabolism). On the other hand, it inhibits ATP-consuming metabolic pathways such as synthesis of cholesterol and triglycerides in adipocytes (anabolism). AMPK could also modulate the secretion of insulin by pancreas.

AMP-activated protein kinase (AMPK) is a sensor of energy status and is considered as gatekeeper for activity of the master regulator of mitochondria, PGC-1 α . Indeed, AMPK activation would exert “anti-Warburg” or “anti-aerobic glycolysis” effects. Once activated by falling energy status, it promotes ATP production by increasing the activity or expression of proteins involved in OXPHOS metabolism. Faubert et al. showed that inhibition of AMPK in lymphoma cells drives a switch to glycolysis by an increase in glucose uptake and lactate production (Hardie et al. 2012; Faubert et al. 2013).

➤ **PI3K / AKT / mTOR**

PI3K / AKT / mTOR pathway is an intracellular signaling pathway which plays an important role in regulation of apoptosis, autophagy, proliferation, angiogenesis and cell cycle. Most components of this pathway are oncogenes or tumor suppressors which explain the frequent deregulation of this pathway in different cancers. Activation of this pathway usually begins by the membrane receptor tyrosine kinases (RTKs) and the GTPase switch protein (RAS). The signal for activation of the pathway is propagated through class 1A PI3Ks and is strongly controlled by a multistep process. Activation of PI3K converts the domain of phosphatidylinositol (3,4)-bisphosphate (PIP₂) lipids to phosphatidylinositol (3,4,5)-trisphosphate (PIP₃). Then AKT and PDK1 link to PIP₃ at the cytosolic membrane where PDK1 phosphorylates AKT at T308 (Hemmings and Restuccia 2012). Phosphorylation and

subsequent activation of AKT results in the phosphorylation and activation of numerous substrates which control the key cellular processes like apoptosis, cell cycle progression, transcription and translation.

mTOR is the best-studied downstream substrate of AKT. mTOR exists in two distinct complexes:

- TORC1 complex which is associated with a protein called RAPTOR (Regulatory Associated Protein of TOR) and two other proteins. This complex is sensitive to rapamycin.

- TORC2 complex which is linked to a protein called RICTOR (Rapamycin Insensitive Companion of TOR) and other proteins. This type of mTOR is insensitive to rapamycin and AKT is its only known substrate.

Activation of mTOR ultimately leads to inhibition of autophagy and apoptosis and will induce protein synthesis.

ARTICLES

Articles 1 and 2

Skin Aging

The first part deals with a review article summarizing the works done on the role of oxidative and energy metabolism in nucleotide excision repair disorders. Based on growing *in vitro* and *in vivo* evidence, we proposed that the effects of NER factors in oxidative and energy metabolism may be the mechanism underlying clinical heterogeneity.

The original article entitled “Premature Skin Aging Features Rescued by Inhibition of NADPH Oxidase Activity in XPC-Deficient Mice” is then presented. In this work we showed that continuous oxidative stress due to overactivation of NOX1 has a causative role in the underlying pathophysiology of XPC.

Oxidative and Energy Metabolism as Potential Clues for Clinical Heterogeneity in Nucleotide Excision Repair Disorders

Mohsen Hosseini^{1,2}, Khaled Ezzedine^{1,2,3,4}, Alain Taieb^{1,2,3,4} and Hamid R. Rezvani^{1,2,3}

This review is an update to one published previously in the *Journal of Egyptian Women's Dermatologic Society*: Rezvani HR (2013) Nucleotide excision repair diseases: molecular biology underlying the clinical heterogeneity. *Journal of Egyptian Women's Dermatologic Society* 10: 49–57.

Nucleotide excision repair (NER) is an important DNA repair pathway involved in the removal of a wide array of DNA lesions. The absence or dysfunction of NER results in the following distinct disorders: xeroderma pigmentosum (XP), Cockayne syndrome (CS), cerebro-oculo-facio-skeletal (COFS) syndrome, UV-sensitive syndrome (UV^SS), trichothiodystrophy (TTD), or combined syndromes including XP/CS, XP/TTD, CS/TTD, and COFS/TTD. In addition to their well-characterized role in the NER signaling pathway, NER factors also seem to be important in biological processes that are not directly associated with DNA damage responses, including mitochondrial function and redox homeostasis. The potential causative role of these factors in the large clinical spectrum seen in NER diseases is discussed in this review.

Journal of Investigative Dermatology advance online publication, 9 October 2014; doi:10.1038/jid.2014.365

INTRODUCTION

Nucleotide excision repair (NER) is one of the most important pathways for repairing numerous types of DNA damage produced by UV radiation, ionizing irradiation, carcinogenic chemicals, and chemically active endogenous metabolites, including reactive oxygen and nitrogen species (Gillet and Scharer, 2006). The coordinated action of ~30 proteins in NER results finally in the release of a 24- to 32-mer oligonucleotide comprising the damaged base(s) and its replacement by a newly synthesized reparative DNA. NER

consists of two distinct subpathways: global genome NER (GG-NER), which removes lesions in the whole genome DNA, and transcription-coupled NER (TC-NER), which repairs DNA lesions in the transcribed strand of active genes. The main difference between these two subpathways is in the DNA damage recognition step. In fact, although DNA damage recognition on the untranscribed part of the genome by xeroderma pigmentosum group C complementing protein (XPC) triggers GG-NER, the stopped RNA polymerase II (RNAPolII) at a lesion on the transcribed strand activates TC-NER. Following DNA damage recognition by a specific subpathway, the subsequent repair procedure is conducted by a common mechanism. A schematic NER process is presented in Figure 1a. Impaired NER activity results in one of the following distinct diseases: xeroderma pigmentosum (XP), Cockayne's syndrome (CS), trichothiodystrophy (TTD), UV-sensitive syndrome (UV^SS), cerebro-oculo-facio-skeletal (COFS) syndrome, or combined syndromes including XP/CS, XP/TTD, CS/TTD, and COFS/TTD (Moriwaki and Kraemer, 2001; Cleaver, 2005, 2012) (Table 1 and Figure 1b). The various clinical features observed in diseases belonging to the same spectrum, the NER diseases, are most striking and may indicate that various genes implicated in these diseases affect the skin differently through their partially identified and/or unidentified additional functions. In this review, we discuss the effects of different NER factors in oxidative and energy metabolism as a new paradigm for explaining clinical heterogeneity in NER genetic disorders.

CLINICAL AND MOLECULAR HETEROGENEITY IN NER DISORDERS

Xeroderma pigmentosum

XP, a rare autosomal recessive disorder of DNA repair, was first described in 1874 by von Hebra and Kaposi (1874). The term XP refers to the phenotype that includes xerosis and hyperpigmentation. Other main clinical symptoms of XP patients include photosensitivity, actinic damage to the skin, and cancer on UV-exposed areas of the skin and mucous membranes of the eyes and mouth. A recent study on 97 XP patients revealed that non-melanoma and melanoma skin cancer is increased, respectively, 10,000- and 2,000-fold in XP patients under the age of 20 years compared with the expected number from the Kaiser Permanente skin cancer database. Interestingly, although the median age at diagnosis of the first non-melanoma skin

¹Inserm U1035, Bordeaux, France; ²Université de Bordeaux, Bordeaux, France; ³Centre de Référence pour les Maladies Rares de la Peau, CHU de Bordeaux, Bordeaux, France and ⁴Département de Dermatologie & Dermatologie Pédiatrique, CHU de Bordeaux, Bordeaux, France

Correspondence: Hamid Reza Rezvani, Inserm U1035, Bordeaux F-33000 France. E-mail: hamid-reza.rezvani@u-bordeaux.fr

Abbreviations: BER, base-excision repair; COFS, cerebro-oculo-facio-skeletal; CSA and CSB, Cockayne syndrome A and B; GG-NER, global genome nucleotide excision repair; NER, nuclear excision repair; OXPHOS, oxidative phosphorylation; ROS, reactive oxygen species; TC-NER, transcription-coupled nucleotide excision repair; TTD, trichothiodystrophy; UV^SS, UV-sensitive syndrome; XP, xeroderma pigmentosum

Received 22 October 2013; revised 1 August 2013; accepted 4 August 2014

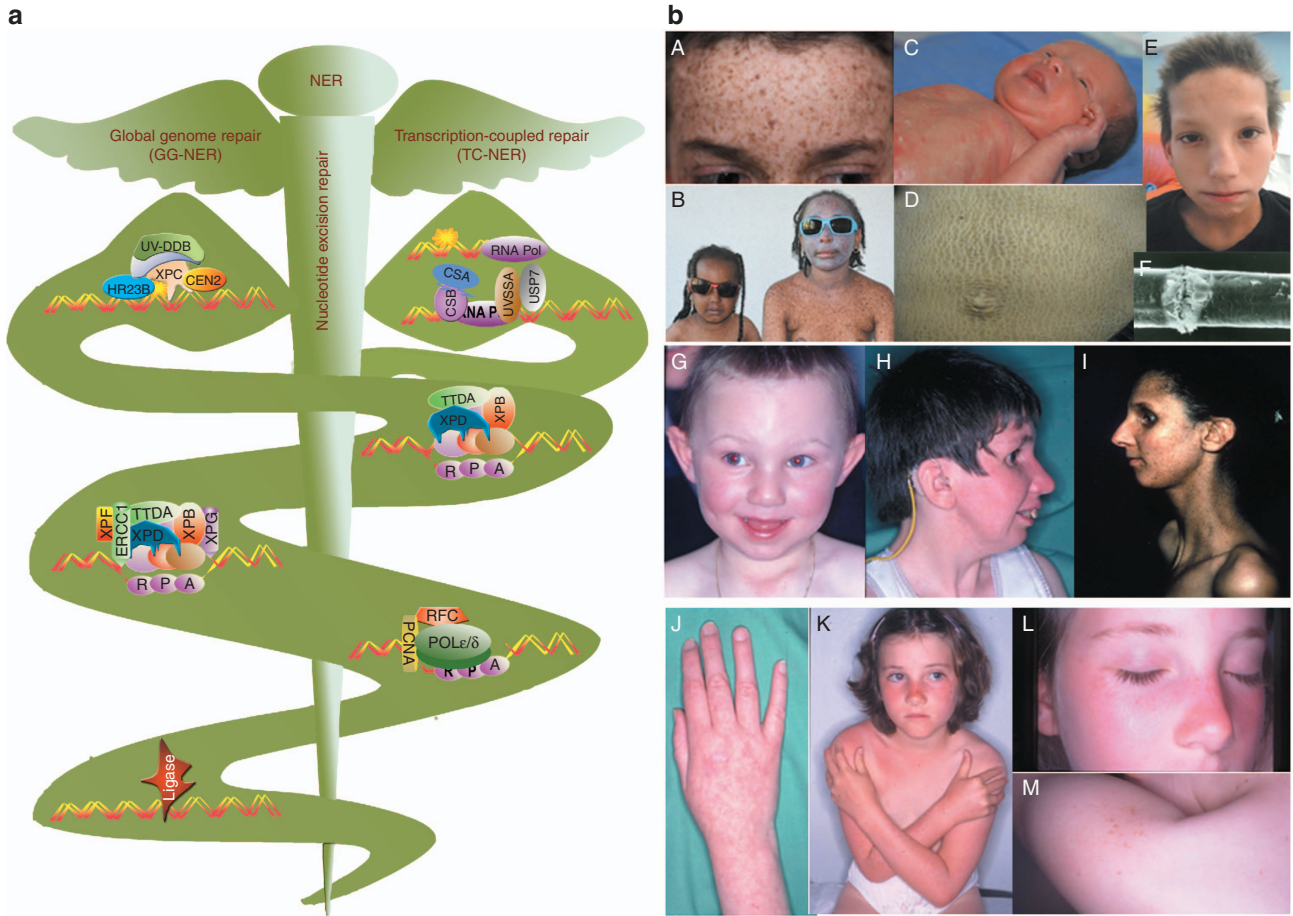


Figure 1. Molecular and clinical heterogeneity of nucleotide excision repair (NER). (a) NER consists of a series of reactions by which a wide variety of helix-distorting lesions from genomic DNA are recognized and repaired. Depending on whether the damage presents in a transcriptionally inactive or active region, global genome NER (GG-NER) or transcription-coupled NER (TC-NER) is activated, respectively. In GG-NER, poly-ubiquitylation of xeroderma pigmentosum (XP)C by XPE (UV-DDB) seems to stimulate the binding of xeroderma pigmentosum group C complementing protein (XPC)–HR23B complexes to damaged DNA and initiation of GG-NER. In TC-NER, damage is recognized by a stalled RNA polymerase II at a DNA lesion in a transcriptionally active region upon its interaction with the Cockayne syndrome (CS)B (ERCC6) and CSA (ERCC8) proteins. The UV-stimulated scaffold protein A (UVSSA) protein forms a complex with ubiquitin-specific protease 7 (USP7), which removes ubiquitin and stabilizes the ERCC6–RNA Pol II complex. RNA Pol II, which is stalled on the DNA template, is then displaced to provide access to NER factors to remove the transcription-stalling damage. Damage recognition is followed by recruitment of transcription factor II H (TFIIH) (including XPB, XPD, p8/TTDA, and several other subunits) via interaction with either XPC or the arrested transcription apparatus. Unwinding the DNA helix is then triggered by the TFIIH complex, XPG, XPA, and replication protein A (RPA). The DNA around the DNA damage is then incised by XPF-ERCC1 and XPG, leading to the release of the oligonucleotide containing the damaged base(s). The resulting gap DNA region is then filled by a DNA polymerase (δ or ϵ) in the presence of proliferating cell nuclear antigen (PCNA) and replication factor C (RFC). The 3' nick is finally closed by DNA ligase. (b) Clinical phenotype of XP-C, trichothiodystrophy (TTD), Cockayne, UV^s syndromes. XP-C is characterized by a marked photosensitivity, typical skin freckling of photoaging associated with poikiloderma, and early development of skin cancer (A, B). Photosensitive TTD is characterized by collodion baby syndrome in newborns (C), an ichthyosiform aspect of the skin (D), and hair brittleness (E) with trichoschisis (scanning electron microscopy) appearing early in childhood (F). XP/CS is characterized by a typical facial appearance including microcephaly, large ears, a thin nose (G), sensorineural hearing loss and dental anomalies (H), pigmentary abnormalities (I), and abnormally large hands (J). UV^s is characterized by slight erythema and dryness (K), slight telangiectasia only seen on the cheek and nose (L), and a number of freckles on sun-exposed areas (M). Written informed consent was obtained from the patients or parents of minor children for publication of their pictures.

cancer in XP patients is 9 years, the median age at diagnosis of first melanoma is 22 years (Bradford *et al.*, 2011). In addition to skin cancers, XP patients have a 10- to 20-fold increased risk of developing internal malignancies. Indeed, internal cancers such as glioma, leukemia, lung, uterus, breast cancer, and other solid tumors have been reported in XP patients (Kraemer *et al.*, 1987, 1994; DiGiovanna *et al.*, 1998; Giglia *et al.*, 1998; Bradford *et al.*, 2011). Besides skin cancers and internal tumors, 20–30% of XP patients suffer from progressive neurological degeneration (XP with neurological complications or De Sanctis–Cacchione

syndrome), resulting in sensorineural deafness, ataxia, areflexia, diminished deep-tendon reflexes, microcephaly, walking difficulties, intellectual deficiency, and progressive cognitive impairment. The time of onset of neurological abnormalities can vary from the age of 2 years to middle age. The most common causes of death are sequentially skin cancer, neurologic degeneration, and internal cancer (Kraemer *et al.*, 1987; Bradford *et al.*, 2011). Overall, the clinical spectrum of XP is heterogeneous and is dependent on the patterns of exposure to sunlight and on the mutated XP gene and very probably other

Table 1. Genes affected in NER diseases and their functions

Defective pathway	Gene	Gene MIM number	Cytogenetic location	No. of exons	Protein size (kDa/AA)	Interacting partners ¹	Main function in NER	Disease
GG-NER	<i>XPC</i>	613208	3p25.1	16	105.9/940	HR23B-Centrin2	Recognition of DNA damage	XP
	<i>XPE (DDB2)²</i>	600811	11p11.2	10	48/427	DDB1	Recognition of DNA damage/E3 ligase	XP XP/CS TTD
TC-NER	<i>CSA (ERCC8)</i>	609412	5q12.1	14	44/396	RNA Pol II, CSB	Ubiquitination of RNA polymerase II	CS UV ^s S
	<i>CSB (ERCC6)</i>	609413	10q11.23	24	168.4/1493	RNA Pol II, CSA	DNA-dependent ATPase	CS UV ^s S XP/CS COFS
	<i>UV^sS-A</i>	614632	4p16.3	14	80.5/709	RNA Pol II, USP7	Ubiquitination and dephosphorylation of RNA polymerase II	UV ^s S
GG-and TC-NER	<i>XPA</i>	611153	9q22.33	6	31.3/273		Structural function, binding to a damaged strand	XP-Neur
	<i>XPB (ERCC3)</i>	133510	2q14.3	15	89.3/782	TFIIH	Helicase 3'→5', ATPase	XP-Neur XP/CS TTD
	<i>XPB (ERCC3)</i>	126340	19q13.32	23	86.9/760	TFIIH	Helicase 5'→3'	XP, XP-Neur XP/CS,TTD XP/TTD, CS/TTD COFS, COFS/TTD
	<i>XPF (ERCC4)</i>	133520	16p13.12	11	103.3/916	ERCC1	5' Nuclease	XP XP-Neur
	<i>XPG (ERCC5)</i>	133530	13q33.1	15	133.3/1186		3' Nuclease	XP-Neur XP/CS COFS
	<i>TTD-A (GTF2H5)</i>	608780	6p25.3	3	8/71	TFIIH	Stabilize the TFIIH complex	TTD
	<i>COFS4 (ERCC1)</i>	126380	19q13.32	10	32.5/297	ERCC4	5' Nuclease	COFS
Postreplication repair	<i>XPV (POLH)</i>	603968	6p21.1	11	78.4/713		Polymerase eta (bypass polymerase)	XP
Unknown	<i>C7ORF11 (TTDN1)</i>	609188	7p14.1	2	19.1/179		Unknown	Nonphotosensitive TTD

Abbreviations: COFS, cerebro-oculo-facio-skeletal syndrome; CS, Cockayne syndrome; DDB, DNA damage-binding; ERCC, excision repair cross-complementing rodent repair deficiency; GG-NER, global genome nucleotide excision repair; NER, nucleotide excision repair; RNA Pol II, RNA polymerase II; TC-NER, transcription-coupled nucleotide excision repair; TFIIH, transcription factor II H; TTD, trichothiodystrophy; XP, xeroderma pigmentosum; XPC, xeroderma pigmentosum group C complementing protein; XP-Neur, xeroderma pigmentosum with neurological abnormalities.

¹Only major partners are shown.

²XPE protein is a heterodimer composed of two subunits, DDB1 and DDB2.

modifying genes defining the phototype such as melanocortin-1 receptor. Indeed, seven XP genes (named XP-A to XP-G), which are involved in the repair of UV-induced photoproducts by the process of NER, have so far been incriminated in XP. In addition, defects in DNA polymerase η results in a milder form of the XP disease, called XP variant, with a delayed onset of skin cancer around 40 years of age. Unlike other XP complementary groups, XP variant cells have proficient NER but are defective in their replication of UV-damaged DNA. DNA polymerase η, which belongs to the low-fidelity Y-family of DNA polymerase, is required for bypass replication of cyclobutane pyrimidine dimers and other lesions by inserting the appropriate nucleotides in the newly synthesized DNA (Moriwaki and Kraemer, 2001; Cleaver, 2005).

Cockayne syndrome

CS, a rare autosomal recessive genetic disorder characterized by progressive developmental defects, was first reported by

Edward Alfred Cockayne in 1936 (Cockayne, 1936). The disease is characterized by profound postnatal decline of somatic and brain growth resulting in dwarfing and limited cognition, although sociability is not affected. CS patients have a characteristic facies with deep-set eyes, prominent ears, and a wizened facial appearance. Clinical symptoms include premature aging, profound cachexia, photosensitivity, retinal pigmentary changes, immature sexual development, basal ganglia calcifications, progressive sensorineural deafness beginning with high-frequency hearing loss, short stature, and progressive neurological degeneration. However, CS is a progressive disorder, and most symptoms emerge and aggravate with time. On the basis of the severity of symptoms, CS patients are classified as CS type I (classical or moderate subtype), type II (early-onset or severe subtype), and type III (late-onset or mild subtype). Although most symptoms are present in all CS subtypes, the time of onset and the progression rate are different among the subtypes. Indeed,

although early-onset CSs present congenital signs of the disease, late-onset patients may only be affected in late childhood or adulthood. CS patients, contrarily of XP, do not have pigmentary changes and are not found to have an increase risk of skin cancer. Furthermore, unlike XP patients, who have cerebral atrophy and primary neuronal degeneration in the gray matter, CS patients have dysmyelination in the white matter, retinal and Purkinje cell loss, and growth retardation, but no loss of personality. The genetic basis of CS is dependent on mutations within two genes, i.e., CSA (ERCC8) and CSB (ERCC6). The proteins resulting from these two CS genes are not only involved in TC-NER but also function in base-excision repair (BER), transcription, and in mtDNA repair (Nance and Berry, 1992; Moriwaki and Kraemer, 2001; Cleaver, 2005; Laugel, 2013).

UV-sensitive syndrome

UV^SS is a human DNA repair-deficiency disorder with mild clinical manifestations. By comparing >100 photosensitive individuals in 1993, Cleaver and Thomas concluded that a subset (i.e., UV^SS) was distinct from XP and CS (Cleaver and Thomas, 1993). In fact, UV^SS individuals manifest only UV hypersensitivity without any neurological or developmental abnormalities and no known predisposition to cancer. UV^SS comprises three groups, UV^SS/CS-A, UV^SS/CS-B, and UV^SS-A, caused by mutations in ERCC8, ERCC6, and UV-stimulated scaffold protein A, respectively. Moreover, there is an additional group of UV^SS patients who have mutations in an as yet unidentified gene(s) (Cleaver, 2012). Although the cellular and biochemical responses of UV^SS and CS cells to UV light are indistinguishable (Spivak, 2005), UV^SS patients do not clinically express neurological or developmental symptoms, and thus the question arises as to how molecular defects within the same TC-NER pathway and even different mutations within the same genes lead to such diverse disorders.

Trichothiodystrophy

TTD is a rare autosomal recessive complex neuroectodermal disease first described by Pollitt *et al.* (1968) and named by Price *et al.* (1980). The patients usually present with dry sparse hair. Hair shafts break easily with trauma. The term 'TTD' was proposed to group several phenotypes on the basis of a common deficiency in sulfur proteins of the hair shaft. The early phenotype is dominated by abnormal terminal differentiation of the epidermis and hair, which causes ichthyosis (collodion baby is common) and hair brittleness (hair with tiger-tail banding when observed in polarized light). Moreover, several manifestations occur in this phenotype, including mental retardation, ichthyotic skin, reduced stature, osseous anomalies, and hypogonadism, but none is a constant trait (Itin *et al.*, 2001; Hoesijmakers, 2009). TTD patients are divided into two categories: a group with DNA repair deficiency, so-called 'photosensitive' TTD, and a group without DNA repair deficiency.

Although the causative mutations have yet not been identified in all photosensitive TTDs, three complementation groups have been described. The main one is due to mutations within the *XPD* (ERCC2) gene. Two other groups correspond

to mutations in the *XPB* (ERCC3) or *p8/TFB5*, also termed TTD (Hashimoto and Egly, 2009; Morice-Picard *et al.*, 2009). Mutation in these NER factors and subsequent NER deficiency results rather in premature aging features without cancer occurrence (Itin *et al.*, 2001; Moriwaki and Kraemer, 2001; Cleaver, 2005). In the group of patients without DNA repair anomalies, mutations in *C7orf11* encoding TTDN1 of unknown function have been found. However, mutations in this gene have been ruled out in some nonphotosensitive patients including those described by Howell *et al.* (1981) (Sabinas syndrome) and Pollitt *et al.* (1968), suggesting further genetic heterogeneity in the group without DNA repair anomalies.

Cerebro-oculo-facio-skeletal syndrome

COFS syndrome (MIM 214150) is a recessively inherited neurodegenerative disorder defined by craniofacial and skeletal abnormalities, severely reduced muscle tone, and impairment of reflexes. Symptoms may include large, low-set ears, small eyes, microcephaly (abnormal smallness of the head), micrognathia (abnormal smallness of the jaws), clenched fists, wide-set nipples, vision impairments, involuntary eye movements, and mental retardation, which can range from moderate to severe. Reported cases of COFS have a considerable clinical heterogeneity with possible confusing overlaps between COFS syndrome and other diseases such as MICRO syndrome (MIM 600118), Martsolf syndrome (MIM 212720), and CS. In this regard, Laugel *et al.* (2008) have proposed the following diagnosis criteria for COFS syndrome: congenital microcephaly, congenital cataracts and/or microphthalmia, arthrogryposis, severe developmental delay, severe postnatal growth failure, and facial dysmorphism with prominent nasal root and/or overhanging upper lip and a DNA repair defect in the TC-NER pathway. In addition to ERCC6 mutations (COFS1), which also cause CSB, several other mutations have been implicated in the COFS phenotype, namely *XPD* (COFS2), *XPG* (COFS3), or *ERCC1* (COFS4). Finally, in a few COFS patients, the causative mutations have not yet been identified (Laugel *et al.*, 2008).

Overlap syndromes (XP/CS complex, XP/TTD, CS/TTD, and COFS/TTD)

Careful and precise assessment of clinical features of each NER disorder has led to the identification of rare subsets of NER patients in whom combined features of XP/CS, XP/TTD, COFS/TTD, or CS/TTD coexist in the same patient (Table 1). In fact, depending on the mutation and possibly other components of the genetic background of patients, mutations in some NER factors lead to overlap disorders incorporating features of two distinct NER diseases. For instance, mutations in the *XPD* gene have been implicated in XP, TTD, or COFS syndrome, as well as in overlap syndromes including XP/CS, XP/TTD, CS/TTD, or COFS/TTD. Similarly, mutations in *XPB*, *XPG*, and *CSB* genes may result in combined features of XP and CS (XP/CS) (Ahmad and Hanaoka, 2008; DiGiovanna and Kraemer, 2012).

Overall, whereas XP patients are known to be at an increased risk for skin cancer, patients with TTD, CS, or COFS

syndrome present accelerated aging without the increased risk of skin cancer. UV^{SS} patients present neither neurological abnormalities nor predisposition to cancer. Considering this clinical heterogeneity, a major issue is how specific these varied signs and symptoms are to the defect in the NER pathway. We indeed propose below that the effects of NER factors in oxidative and energy metabolism may be the mechanism underlying clinical heterogeneity.

NER FACTORS AND OXIDATIVE METABOLISM

The major pathway for the repair of oxidative DNA lesions is the BER pathway (Seeberg *et al.*, 1995; Cadet *et al.*, 2000). However, recent studies have shown that XPC, XPA, XPD, XPG, CSA, and CSB are also involved in the response to oxidative DNA damage.

XPC and oxidative DNA damage

Numerous studies are in favor of a protective role of XPC against oxidative DNA damage. Indeed, it has been shown that XP-C cells are highly susceptible to the detrimental effects of DNA-oxidizing agents, X-ray, and agent-induced disturbance in redox signaling (D'Errico *et al.*, 2006; Kassam and Rainbow, 2007; Liu *et al.*, 2010) owing to the accumulation of oxidative DNA damage. Underlining the role of XPC on redox homeostasis, we have also reported that XPC silencing in normal human keratinocytes triggers metabolic alterations that drive mutation accumulation and tumorigenesis among others owing to a disturbed redox homeostasis (Rezvani *et al.*, 2011b,c). Finally, a very recent study demonstrated that Xpc^{-/-} mice harbor a slow accumulation of mutations upon pro-oxidant exposure (Melis *et al.*, 2013).

The protective function of XPC has been ascribed to its ability to affect the key BER enzymes (Miao *et al.*, 2000; Shimizu *et al.*, 2003; D'Errico *et al.*, 2006) and/or catalase activity (Vuillaume *et al.*, 1992; Quilliet *et al.*, 1997). Moreover, a recent study has proposed the direct recognition of some oxidative damage by XPC as a third protective mechanism. In the latter study, Menoni *et al.* (2012) have shown a rapid XPC recruitment to sites of oxidative DNA lesions in living cells without triggering the recruitment of other GG-NER factors.

The role of XPC in both the redox homeostasis and the repair of oxidative DNA damage may, at least partially, shed light on how XPC expression may predispose to internal cancer. Indeed, aged XPC-deficient mice accumulate an elevated level of mutations in their lung tissue and consequently exhibit an increased incidence of lung tumor compared with wild-type counterparts (Hollander *et al.*, 2005; Melis *et al.*, 2008). Human XPC is located at 3p25, and its allelic loss was interestingly found in the majority of lung cancers (Hollander *et al.*, 2005). In addition to lung tumors, the frequency of other internal cancers is also increased in Xpc^{-/-} mice (Hollander *et al.*, 2005; Miccoli *et al.*, 2007; Melis *et al.*, 2008). Similarly, primary internal tumors (e.g., glioma, adenocarcinoma neuroendocrine cancer of the thyroid, lung, and uterus cancers) have been reported in XP-C patients (Giglia *et al.*, 1998; Bradford *et al.*, 2011). Analysis of the p53 gene in internal tumors revealed that the mutations

do not correspond to UV signatures and could rather result from oxidative DNA lesions (Giglia *et al.*, 1998). Furthermore, some polymorphisms in the human Xpc gene, as well as the expression level of XPC, have been associated with a higher risk of lung, leukemia, prostate, bladder, colorectal, and breast cancers (Hu *et al.*, 2005; Lee *et al.*, 2005; Chen *et al.*, 2007; Francisco *et al.*, 2008; Qiu *et al.*, 2008; Vineis *et al.*, 2009; de Verdier *et al.*, 2010; Xu *et al.*, 2012; He *et al.*, 2013). XPC polymorphisms are linked not only to the risk of cancer but also to neurodegenerative diseases. Indeed, a very recent work associated the expression of XPC variants with the younger age at onset of Huntington disease (Berger *et al.*, 2013), a neurodegenerative disease that has been linked with oxidative DNA damage and stress responses (Stack *et al.*, 2008). However, neurological degeneration is very rare in XP-C patients, and only two patients with neurological abnormalities have been yet diagnosed (Bernardes de Jesus *et al.*, 2008; Khan *et al.*, 2009).

Contribution of XPA, XPD, and XPG in response to oxidative DNA damage

With regard to the role of XPA in cellular responses to oxidative stress, real-time quantification of superoxide and nitric oxide derivatives released by a living cell indicated that XP-A fibroblasts provide larger oxidative bursts than control cells (Arbault *et al.*, 2004). It has also been shown that fibroblasts lacking functional XPA present increased genotoxicity and reduced capacity for repairing oxidative damage when subjected to oxidative stress (Low *et al.*, 2008). Accordingly, analysis of the autopsied brains of XP-A patients revealed increased oxidative damage to DNA and RNA, enhanced lipid peroxidation, and a disturbed expression of Cu/ZnSOD and MnSOD, suggesting the existence of oxidative stress in XP-A cells (Hayashi *et al.*, 2005). Comparing proteome and transcriptome signatures of XPA-deficient and XPA-proficient *Caenorhabditis elegans* in a very recent study indicated that several proteins implicated in oxidative stress responses were activated in xpa mutants. In accordance, increased steady-state level of reactive oxygen species (ROS) was found in XPA-deficient nematodes (Arczewska *et al.*, 2013).

Although the critical role that XPD and XPG, as subunits of the transcription factor II H transcription/repair complex, have in basal transcription may be behind the heterogeneity of the phenotypes observed in patients bearing a mutation in one of these factors (Compe and Egly, 2012), their roles in oxidative and energy metabolism could also be considered. Indeed, XP-D fibroblasts with low catalase activity are known to exhibit significantly larger oxidative bursts than control cells (Arbault *et al.*, 2004). In fact, large amounts of hydrogen peroxide were released following an oxidative burst by XP-D fibroblasts owing to the sustained production of superoxide as compared with controls, suggesting the increased activity of superoxide-generating NADPH oxidases in XP-D cells (Arbault *et al.*, 2004). In addition to XPD, XPG also has additional activities in the repair of oxidative damage. XPG promotes the activity of the DNA glycosylase NTH1, an enzyme involved in the BER, independently of its nuclease

activity (Bessho, 1999; Klungland *et al.*, 1999). Studies on XP-G patients with and without CS symptoms suggest that the C-terminal region of XPG has an essential role in mediating functions of XPG within and outside NER. Genotypic/phenotypic analysis indicated that a localized defect in nuclease activity, which only affects the NER-specific functions, gives rise to an XP phenotype with sensitivity to UV light, abnormal pigmentation, increased risk of skin cancer, and no neurological abnormalities. The analysis revealed that the mutations preventing the expression of the full-length protein result in the XP/CS phenotype displaying severe developmental retardation, dwarfism, and neurological abnormalities in addition to the XP symptoms, suggesting that nuclease-independent stimulation of the repair of oxidative lesions might contribute to the XP/CS phenotype (Nospikel and Clarkson, 1994; Moriwaki *et al.*, 1996; Nospikel *et al.*, 1997; Lindenbaum *et al.*, 2001; Emmert *et al.*, 2002; Scharer, 2008). The consequences of XPG deficiency in mouse models are in agreement with the genotypic/phenotypic analysis of XP-G patients. In fact, consistent with observations in patients, while a mouse expressing XPG containing a mutation that abolishes nuclease activity displayed the classical XP phenotype (Tian *et al.*, 2004), mice in which the last 360 amino acids in the C terminus of XPG were deleted displayed the symptoms associated with the XP/CS complex (Shiomi *et al.*, 2004, 2005). Similarly, mice in which exon 3 had been deleted lacked any functional XPG protein and displayed a XP-G/CS phenotype (Harada *et al.*, 1999).

CSA and CSB in repair of oxidative DNA damage

Severe progeroid syndromes in patients with deficiency in transcription-coupled repair subpathway of NER suggest that transcriptional impediments might be particularly relevant to the aging process (Schumacher *et al.*, 2008; Capell *et al.*, 2009; Cleaver *et al.*, 2009). However, comparing premature aging features in NER diseases including XP, TTD, and CS suggest that inactivation of NER alone is not sufficient to cause progeroid features. Complete inactivation of NER owing to deficiency in XPA in *Xpa*^{-/-} mice, for e.g., does not cause CS- and TTD-like progeroid features but instead leads to a very mild aging phenotype (Andressoo *et al.*, 2006, 2009; Cleaver *et al.*, 2009). Therefore, it has been proposed that accelerated aging in CS and TTD could be related to the impaired repair of oxidative DNA damages (Andressoo *et al.*, 2006; Schumacher *et al.*, 2008; Andressoo *et al.*, 2009; Cleaver *et al.*, 2009). In support of this notion that CS phenotype is related to increased oxidative stress, CS-A and CS-B fibroblasts have been reported to have an altered redox balance with increased steady-state levels of intracellular ROS and basal and induced DNA oxidative damage. These cells also show defective repair of oxidative damage (D'Errico *et al.*, 2007; Pascucci *et al.*, 2012). Studies of these two proteins in mouse models indicated that, although mouse CSB-deficient cells are hypersensitive to ionizing radiation and other oxidative stressors (de Waard *et al.*, 2003, 2004; Gorgels *et al.*, 2007) mouse CSA-deficient cells fail to show this sensitivity (de Waard *et al.*, 2004), suggesting a functional difference between human and mouse CSA, at least in responses to oxidative DNA damage. The

dependence of the CS phenotype on the repair deficiency of oxidative damage has received further support by comparing the sensitivity of UV^SS and CS cells to ROS. Results indicated that CS-A and CS-B cells are more sensitive to treatment with hydrogen peroxide than normal or UV^SS cells (Spivak and Hanawalt, 2006).

The defect in the repair of oxidative DNA damage in CS-B cells is attributed to a decrease in *OGG1* (8-oxoguanine DNA glycosylase) gene expression and protein level (Dianov *et al.*, 1999; Tuo *et al.*, 2002), reduced catalytic activity of endonuclease VIII-like 1 (NEIL1) (Muftuoglu *et al.*, 2009), and/or diminished APE1 incision activity (Wong *et al.*, 2007), which are the key enzymes in modulating BER processes. Another mechanism by which the CSB protein influences cellular responses to oxidative stress is via interaction with poly-ADP ribose-polymerase 1, a nuclear enzyme that is involved in the repair of DNA single-strand breaks (Thorslund *et al.*, 2005). In addition to affecting nuclear DNA lesions, CSA and CSB have been recently reported to contribute to BER of oxidative mtDNA damage via direct interaction with mtOGG1 (Kamenisch *et al.*, 2010) and/or mitochondrial transcription factor A (TFAM) (Berquist *et al.*, 2012), which has been reported to have a strong affinity to oxidative mtDNA lesions in addition to its role in mtDNA replication and transcription (Canugovi *et al.*, 2010). Accordingly, higher levels of oxidative DNA damage have been found in mtDNA of CSB-deficient mice associated with changes in the respiratory chain complexes (Osenbroch *et al.*, 2009).

Overall, it now seems clear that NER factors have an important role in the repair mechanisms of oxidative DNA damage in both nuclear and mtDNA.

NER PROTEINS AND ENERGY METABOLISM

There is now overwhelming evidence that cellular redox status affects mitochondrial energy metabolism (Rezvani *et al.*, 2011b,c; Furda *et al.*, 2012; Lu *et al.*, 2012). Indeed, increased oxidative stress may lead to the oxidation of lipids, proteins, and nucleic acids, which may finally affect mitochondrial functions. The activities of several key enzymes involved in mitochondrial oxidative phosphorylation (OXPHOS) have been found to be reduced under various oxidative conditions (Tretter and Adam-Vizi, 2000; Rezvani *et al.*, 2011b,c; Furda *et al.*, 2012; Lu *et al.*, 2012). As the key factors of energy metabolism, mitochondria are involved in both tumorigenesis and the aging process. Indeed, functional studies of mitochondria in aged humans and animals suggest that the bioenergetic function of mitochondria declines with age (Muller-Hocker, 1989; Yen *et al.*, 1989; Cooper *et al.*, 1992; Muller-Hocker *et al.*, 1993; Sugiyama *et al.*, 1993; Hsieh *et al.*, 1994; Lesnefsky and Hoppel, 2006). The precise analysis of the metabolism of tumor cells has finally led to identify the reprogramming of energy metabolism as an emerging hallmark of cancer cells (Hanahan and Weinberg, 2011). Metabolism alterations may, therefore, represent an attractive explanation to elucidate the clinical heterogeneity of NER patients.

With regard to the effect of XPC on energy metabolism, knockdown of XPC in cultured human keratinocytes has been

found to result in increased ROS-mediated reduced OXPHOS and increased glycolysis. The crucial event related to the alteration of the metabolism following knockdown of XPC is the resulting activation of protein kinase B (PKB) and NADPH oxidase-1 with an associated overproduction of ROS that leads to specific deletions in mtDNA. XPC-deficient cells containing mtDNA deletions were found to be capable of forming squamous cell carcinoma when xenografted into immunodeficient mice. On the contrary, the impairment of protein kinase B (PKB) or NOX activation in these XPC-deficient cells leads to the blockade of increased ROS production, mtDNA deletions, and subsequent neoplastic transformation (Rezvani *et al.*, 2011b,c), strongly suggesting that the defect in GG-NER is not the only driver of tumorigenesis in XPC-deficient cells. In fact, the increased intracellular ROS level and altered metabolism associated with GG-NER deficiency in XPC-deficient cells may function synergistically to promote tumorigenesis. In agreement, a very recent study, in which the interactome of XPC using a yeast two-hybrid screening has been characterized, uncovered 15 XPC-interacting proteins with function in metabolism (Lubin *et al.*, 2014).

Mitochondrial dysfunction has been very recently reported in XPA-deficient cells. The mitochondrial abnormalities in these cells have been found to be caused by SIRT1 attenuation. Indeed, hyperactivation of the DNA damage sensor poly-ADP ribose-polymerase 1 in XPA-deficient cells leads to decreased activation of the SIRT1, which in turn triggers depression of PGC-1 α (Fang *et al.*, 2014), a central transcriptional coactivator involved in the regulation of the steady-state level of mitochondrial ROS and mitochondrial biogenesis (Austin and St-Pierre, 2012). Interestingly, impairment of poly-ADP ribose-polymerase activation using pharmacological inhibitors of poly-ADP ribose-polymerase has been found to rescue XPA deficiency-induced mitochondrial alterations (Fang *et al.*, 2014).

In addition to XPC and XPA, XPD, CSA, and CSB can also alter metabolism. Indeed, XPD^{TTD} mice have been found to have a marked shift in lipid metabolism and cholesterol homeostasis as compared with wild-type controls. In addition, a downregulation in the tricarboxylic acid cycle and the OXPHOS genes has also been observed in these mice (Park *et al.*, 2008). Similarly, it has been reported that glycolysis is increased in CS cells. In particular, Pascucci *et al.* (2012) reported that primary fibroblasts derived from CS-A and CS-B patients present a loss of the mitochondrial membrane potential and a significant decrease in the rate of basal OXPHOS. Accordingly, Scheibye-Knudsen *et al.* (2012) reported that all CS-B cells compared with control cells showed increased extracellular acidification rates, which could be due to an increased glycolysis-mediated production of lactate. This hypothesis was supported by elevated lactate levels found by ¹H nuclear magnetic resonance spectroscopic analysis in the brain of CS patients (Koob *et al.*, 2010). CSB has been also reported to act as an mtDNA quality control, inducing mitochondrial autophagy in response to stress. Impairment of autophagy in CSB-deficient cells, indeed, results in an abnormal bioenergetic profile (Scheibye-Knudsen *et al.*,

2012). A modified metabolism has also been demonstrated in Csb^{m/m}/Xpa^{-/-} mice, which harbor the complete inactivation of NER and present a phenotype mimicking the human progeroid CS syndrome. Indeed, mouse liver transcriptome analysis revealed a significant downregulation of key genes involved in glycolysis, tricarboxylic acid, and OXPHOS pathways and a significant upregulation of genes associated with glycogen synthesis (van der Pluijm *et al.*, 2007).

On the basis of this set of data, the alteration of oxidative and energy metabolisms are likely to offer clues for explaining the diversity of the clinical presentation of NER patients and could help to set up adequate tools for the diagnosis and treatment of NER diseases (Figure 2).

FROM CLINICAL OBSERVATIONS TO ANTIOXIDANT PHOTOPROTECTIVE THERAPY IN NER DISEASES

The defect in repair of UV-induced damage has been shown to be overcome in cell culture by the intracellular delivery of the bacterial DNA incision repair enzyme T4 endonuclease V (T4N5) (Tanaka *et al.*, 1975). Topical application of this enzyme encapsulated in a liposome (commercially called Dimericine) has been shown to be of interest for XP patients. Indeed, Dimericine reduces the incidence of premalignant actinic keratosis and basal cell carcinomas in XP patients (Yarosh *et al.*, 2001). Correction of NER deficiency through gene transfer has been successfully tested *in vitro* and *ex vivo*

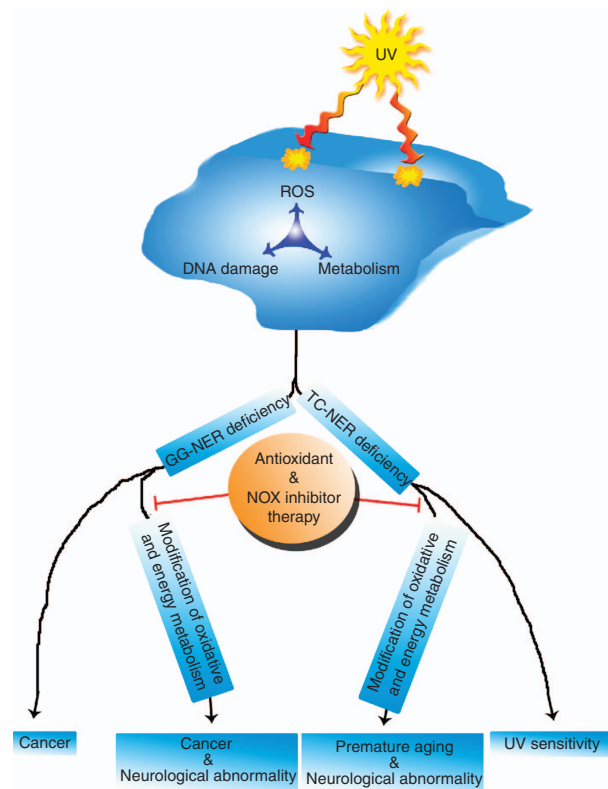


Figure 2. Modification of oxidative and energy metabolism could provide valuable tools for both diagnosis and therapy. GG-NER, global genome nucleotide excision; NOX, NADPH oxidase-1; ROS, reactive oxygen species; TC-NER, transcription-coupled nucleotide excision repair.

(Zeng *et al.*, 1997; Zhou *et al.*, 2003; Bernerd *et al.*, 2005; Marchetto *et al.*, 2006; Warrick *et al.*, 2012). Further improvement of gene therapy approaches may pave the way for the generation of “safe” transgenic epidermis, which can be useful especially in NER patients who need reconstructive surgery. In these cases, a possible immune reaction should also be feared, in particular, when patients present with a total absence of NER proteins. With regard to all these limitations, alternative therapies helping to halt or reduce NER disease symptoms should be considered. There is now growing evidence, some of which presented in this review, that the increased intracellular ROS level and altered metabolism in NER-deficient cells may function synergistically with altered DNA damage response signaling to promote tumorigenesis and/or premature aging features. Photoprotective therapy using antioxidant enzymes and/or NADPH oxidase inhibitors may, therefore, be of help in limiting photosensitivity and tumorigenesis, as well as in slowing accelerated aging in some XP patients (Figure 2).

We have recently demonstrated that the tumorigenic transformation of XPC knockdown keratinocytes is associated with bioenergetics remodeling. This metabolic alteration is in turn dependent on the overactivation of NADPH oxidase-mediated ROS generation. Silencing of NADPH oxidase-1 expression has been found to abrogate the tumoral transformation of XPC-deficient keratinocytes (Rezvani *et al.*, 2011b,c), suggesting that metabolism and oxidative stress could account for the skin photosensitivity and carcinogenesis in NER diseases. In support of this notion, growing evidence show that UV-induced ROS generation contributes to photosensitivity and carcinogenesis by affecting genomic stability, apoptosis, the immune system, and pigmentation (Kulms *et al.*, 2002; Katiyar, 2003; Bickers and Athar, 2006; Rezvani *et al.*, 2006; Maresca *et al.*, 2008; Grivennikov *et al.*, 2010; Afaq, 2011). The reduction of the deleterious effects of UV-induced ROS through an increase in antioxidant defense systems supports this concept (Maalouf *et al.*, 2002; Katiyar, 2003; Morley *et al.*, 2003; Pelle *et al.*, 2003; Afaq, 2011; Panich *et al.*, 2011). We have tested the therapeutic concept of the possible reinforcement of natural antioxidant photoprotective defenses against UV-induced apoptosis and possibly skin cancer. We have found that both normal and XPC-deficient human keratinocytes sustainably overexpressing catalase are more protected against UVB-induced damage mediated by an increased ROS level (Rezvani *et al.*, 2006, 2007a, b, 2008, 2011a). Antioxidant therapy has also been tested in *Xpa*^{-/-} mice. Increased UVB-induced photosensitivity in *Xpa*^{-/-} mice was rescued with a systemic antioxidant treatment (Yao *et al.*, 2012).

Increased oxidative stress may also have a key role in neurodegenerative diseases and premature aging. Fang *et al.* (2014) very recently reported that XPA deficiency triggers autophagy upregulation through increased ROS level-mediated 5' AMP-activated protein kinase activation. They found that treatment of cells with an ROS scavenger blocks, at least partially, XPA deficiency-induced increased autophagy. The alterations in intracellular ROS content, oxidative DNA damage, and metabolic profile found in the primary fibroblasts

of CS-A and CS-B patients were partially rescued by the cell culture medium supplementation with an antioxidant (Pascucci *et al.*, 2012). Furthermore, UV^S cells are less sensitive to oxidative stress than CS cells (Spivak and Hanawalt, 2006). These results suggest that continuous oxidative stress in CS cells has a causative role in the underlying pathophysiology and support the concept of the potential beneficial effects of photoprotective therapy using antioxidant enzymes and/or NADPH oxidase inhibitors to limit the accelerated aging of CS patients.

CONCLUSION AND PERSPECTIVES

There is no concrete evidence that oxidative and energy metabolism is the exact mechanism underlying clinical heterogeneity of NER disease. However, the aim of this review is to highlight for dermatologists, other clinicians, and scientists, as indicated in the title, a “potential” role of metabolism in this process. On the basis of growing evidence provided by *in vitro* and *in vivo* experiments, we propose the theory that the effects of NER factors in oxidative and energy metabolism may be the mechanism underlying clinical heterogeneity (Figure 2). By devising this theory, we hope to provide a theoretical framework for new clinical experiments that will lead to a more comprehensive understanding of the molecular mechanism(s) underlying the puzzling complexity of the phenotypes. We hope that dermatologists will add to classical clinical tests a metabolic workup that is easily achievable in order to provide conclusive evidence for or against this theory. This may ultimately lead to the implementation of new strategies for the therapy of NER diseases.

CONFLICT OF INTEREST

The authors state no conflict of interest.

ACKNOWLEDGMENTS

We acknowledge the patients' support group Les Enfants de La Lune. HRR gratefully acknowledges support from the ARC “Association pour la Recherche sur le Cancer” and the Fondation Maladies Rares. We are also grateful to Professor P Thomas for giving permission for the use of photographs.

REFERENCES

- Afaq F (2011) Natural agents: cellular and molecular mechanisms of photoprotection. *Arch Biochem Biophys* 508:144–51
- Ahmad SI, Hanaoka F (2008) Molecular mechanisms of xeroderma pigmentosum. Preface. *Adv Exp Med Biol* 637:vii–xiv
- Andressoo JO, Hoeijmakers JH, Mitchell JR (2006) Nucleotide excision repair disorders and the balance between cancer and aging. *Cell Cycle* 5:2886–8
- Andressoo JO, Weeda G, de Wit J *et al.* (2009) An Xpb mouse model for combined xeroderma pigmentosum and cockayne syndrome reveals progeroid features upon further attenuation of DNA repair. *Mol Cell Biol* 29:1276–90
- Arbault S, Sojic N, Bruce D *et al.* (2004) Oxidative stress in cancer prone xeroderma pigmentosum fibroblasts. Real-time and single cell monitoring of superoxide and nitric oxide production with microelectrodes. *Carcinogenesis* 25:509–15
- Arczewska KD, Tomazella GG, Lindvall JM *et al.* (2013) Active transcriptomic and proteomic reprogramming in the *C. elegans* nucleotide excision repair mutant *xpa-1*. *Nucleic Acids Res* 41:5368–81
- Austin S, St-Pierre J (2012) PGC1alpha and mitochondrial metabolism-emerging concepts and relevance in ageing and neurodegenerative disorders. *J Cell Sci* 125:4963–71

- Berger F, Vaslin L, Belin L *et al.* (2013) The impact of single-nucleotide polymorphisms (SNPs) in OGG1 and XPC on the age at onset of Huntington disease. *Mutat Res* 755:115–9
- Bernardes de Jesus BM, Bjoras M, Coin F *et al.* (2008) Dissection of the molecular defects caused by pathogenic mutations in the DNA repair factor XPC. *Mol Cell Biol* 28:225–35
- Bernerd F, Asselineau D, Frechet M *et al.* (2005) Reconstruction of DNA repair-deficient xeroderma pigmentosum skin in vitro: a model to study hypersensitivity to UV light. *Photochem Photobiol* 81:19–24
- Berquist BR, Canugovi C, Sykora P *et al.* (2012) Human Cockayne syndrome B protein reciprocally communicates with mitochondrial proteins and promotes transcriptional elongation. *Nucleic Acids Res* 40:8392–405
- Bessho T (1999) Nucleotide excision repair 3' endonuclease XPG stimulates the activity of base excision repair enzyme thymine glycol DNA glycosylase. *Nucleic Acids Res* 27:979–83
- Bickers DR, Athar M (2006) Oxidative stress in the pathogenesis of skin disease. *J Invest Dermatol* 126:2565–75
- Bradford PT, Goldstein AM, Tamura D *et al.* (2011) Cancer and neurologic degeneration in xeroderma pigmentosum: long term follow-up characterizes the role of DNA repair. *J Med Genet* 48:168–76
- Cadet J, Bourdat AG, D'Ham C *et al.* (2000) Oxidative base damage to DNA: specificity of base excision repair enzymes. *Mutat Res* 462:121–8
- Canugovi C, Maynard S, Bayne AC *et al.* (2010) The mitochondrial transcription factor A functions in mitochondrial base excision repair. *DNA Repair* 9:1080–9
- Capell BC, Tloutan BE, Orlow SJ (2009) From the rarest to the most common: insights from progeroid syndromes into skin cancer and aging. *J Invest Dermatol* 129:2340–50
- Chen Z, Yang J, Wang G *et al.* (2007) Attenuated expression of xeroderma pigmentosum group C is associated with critical events in human bladder cancer carcinogenesis and progression. *Cancer Res* 67:4578–85
- Cleaver JE (2005) Cancer in xeroderma pigmentosum and related disorders of DNA repair. *Nat Rev Cancer* 5:564–73
- Cleaver JE (2012) Photosensitivity syndrome brings to light a new transcription-coupled DNA repair cofactor. *Nat Genet* 44:477–8
- Cleaver JE, Lam ET, Revet I (2009) Disorders of nucleotide excision repair: the genetic and molecular basis of heterogeneity. *Nat Rev Genet* 10:756–68
- Cleaver JE, Thomas GH (1993) Clinical syndromes associated with DNA repair deficiency and enhanced sun sensitivity. *Arch Dermatol* 129:348–50
- Cockayne EA (1936) Dwarfism with retinal atrophy and deafness. *Arch Dis Child* 11:1–8
- Compe E, Egly JM (2012) TFIIH: when transcription met DNA repair. *Nat Rev Mol Cell Biol* 13:343–54
- Cooper JM, Mann VM, Schapira AH (1992) Analyses of mitochondrial respiratory chain function and mitochondrial DNA deletion in human skeletal muscle: effect of ageing. *J Neurol Sci* 113:91–8
- D'Errico M, Parlanti E, Teson M *et al.* (2006) New functions of XPC in the protection of human skin cells from oxidative damage. *EMBO J* 25:4305–15
- D'Errico M, Parlanti E, Teson M *et al.* (2007) The role of CSA in the response to oxidative DNA damage in human cells. *Oncogene* 26:4336–43
- de Verdier PJ, Sanyal S, Bermejo JL *et al.* (2010) Genotypes, haplotypes and diplotypes of three XPC polymorphisms in urinary-bladder cancer patients. *Mutat Res* 694:39–44
- de Waard H, de Wit J, Andressoo JO *et al.* (2004) Different effects of CSA and CSB deficiency on sensitivity to oxidative DNA damage. *Mol Cell Biol* 24:7941–8
- de Waard H, de Wit J, Gorgels TG *et al.* (2003) Cell type-specific hypersensitivity to oxidative damage in CSB and XPA mice. *DNA Repair (Amst)* 2:13–25
- Dianov G, Bischoff C, Sunesen M *et al.* (1999) Repair of 8-oxoguanine in DNA is deficient in Cockayne syndrome group B cells. *Nucleic Acids Res* 27:1365–8
- DiGiovanna JJ, Kraemer KH (2012) Shining a light on xeroderma pigmentosum. *J Invest Dermatol* 132:785–96
- DiGiovanna JJ, Patronas N, Katz D *et al.* (1998) Xeroderma pigmentosum: spinal cord astrocytoma with 9-year survival after radiation and isotretinoin therapy. *J Cutan Med Surg* 2:153–8
- Emmert S, Slor H, Busch DB *et al.* (2002) Relationship of neurologic degeneration to genotype in three xeroderma pigmentosum group G patients. *J Invest Dermatol* 118:972–82
- Fang EF, Scheibye-Knudsen M, Brace LE *et al.* (2014) Defective Mitophagy in XPA via PARP-1 Hyperactivation and NAD(+)/SIRT1 Reduction. *Cell* 157:882–96
- Francisco G, Menezes PR, Eluf-Neto J *et al.* (2008) XPC polymorphisms play a role in tissue-specific carcinogenesis: a meta-analysis. *Eur J Hum Genet* 16:724–34
- Furda AM, Marrangoni AM, Lokshin A *et al.* (2012) Oxidants and not alkylating agents induce rapid mtDNA loss and mitochondrial dysfunction. *DNA Repair* 11:684–92
- Giglia G, Dumaz N, Drougard C *et al.* (1998) p53 mutations in skin and internal tumors of xeroderma pigmentosum patients belonging to the complementation group C. *Cancer Res* 58:4402–9
- Gillet LC, Schärer OD (2006) Molecular mechanisms of mammalian global genome nucleotide excision repair. *Chem Rev* 106:253–76
- Gorgels TG, van der Pluijm I, Brandt RM *et al.* (2007) Retinal degeneration and ionizing radiation hypersensitivity in a mouse model for Cockayne syndrome. *Mol Cell Biol* 27:1433–41
- Grivennikov SI, Greten FR, Karin M (2010) Immunity, inflammation, and cancer. *Cell* 140:883–99
- Hanahan D, Weinberg RA (2011) Hallmarks of cancer: the next generation. *Cell* 144:646–74
- Harada YN, Shiomi N, Koike M *et al.* (1999) Postnatal growth failure, short life span, and early onset of cellular senescence and subsequent immortalization in mice lacking the xeroderma pigmentosum group G gene. *Mol Cell Biol* 19:2366–72
- Hashimoto S, Egly JM (2009) Trichothiodystrophy view from the molecular basis of DNA repair/transcription factor TFIIH. *Hum Mol Genet* 18:R224–30
- Hayashi M, Araki S, Kohyama J *et al.* (2005) Oxidative nucleotide damage and superoxide dismutase expression in the brains of xeroderma pigmentosum group A and Cockayne syndrome. *Brain Dev* 27:34–8
- He J, Shi TY, Zhu ML *et al.* (2013) Associations of Lys939Gln and Ala499Val polymorphisms of the XPC gene with cancer susceptibility: a meta-analysis. *Int J Cancer J Int Cancer* 133:1765–75
- Hoeijmakers JH (2009) DNA damage, aging, and cancer. *N Engl J Med* 361:1475–85
- Hollander MC, Philburn RT, Patterson AD *et al.* (2005) Deletion of XPC leads to lung tumors in mice and is associated with early events in human lung carcinogenesis. *Proc Natl Acad Sci USA* 102:13200–5
- Howell RR, Arbisser AI, Parsons DS *et al.* (1981) The Sabinas syndrome. *Am J Hum Genet* 33:957–67
- Hsieh RH, Hou JH, Hsu HS *et al.* (1994) Age-dependent respiratory function decline and DNA deletions in human muscle mitochondria. *Biochem Mol Biol Int* 32:1009–22
- Hu Z, Wang Y, Wang X *et al.* (2005) DNA repair gene XPC genotypes/haplotypes and risk of lung cancer in a Chinese population. *Int J Cancer* 115:478–83
- Itin PH, Sarasin A, Pittelkow MR (2001) Trichothiodystrophy: update on the sulfur-deficient brittle hair syndromes. *J Am Acad Dermatol* 44:891–920
- Kamenisch Y, Fousteri M, Knoch J *et al.* (2010) Proteins of nucleotide and base excision repair pathways interact in mitochondria to protect from loss of subcutaneous fat, a hallmark of aging. *J Exp Med* 207:379–90
- Kassam SN, Rainbow AJ (2007) Deficient base excision repair of oxidative DNA damage induced by methylene blue plus visible light in xeroderma pigmentosum group C fibroblasts. *Biochem Biophys Res Commun* 359:1004–9
- Katiyar SK (2003) Skin photoprotection by green tea: antioxidant and immunomodulatory effects. *Curr Drug Targets Immune Endocr Metabol Disord* 3:234–42

- Khan SG, Oh KS, Emmert S *et al.* (2009) XPC initiation codon mutation in xeroderma pigmentosum patients with and without neurological symptoms. *DNA Repair* 8:114–25
- Klungland A, Hoss M, Gunz D *et al.* (1999) Base excision repair of oxidative DNA damage activated by XPG protein. *Mol Cell* 3:33–42
- Koob M, Laugel V, Durand M *et al.* (2010) Neuroimaging in Cockayne syndrome. *AJNR Am J Neuroradiol* 31:1623–30
- Kraemer KH, Lee MM, Andrews AD *et al.* (1994) The role of sunlight and DNA repair in melanoma and nonmelanoma skin cancer. The xeroderma pigmentosum paradigm. *Arch Dermatol* 130:1018–21
- Kraemer KH, Lee MM, Scotto J (1987) Xeroderma pigmentosum. Cutaneous, ocular, and neurologic abnormalities in 830 published cases. *Arch Dermatol* 123:241–50
- Kulms D, Zeise E, Poppelmann B *et al.* (2002) DNA damage, death receptor activation and reactive oxygen species contribute to ultraviolet radiation-induced apoptosis in an essential and independent way. *Oncogene* 21:5844–51
- Laugel V (2013) Cockayne syndrome: the expanding clinical and mutational spectrum. *Mech Ageing Dev* 134:161–70
- Laugel V, Dalloz C, Tobias ES *et al.* (2008) Cerebro-oculo-facio-skeletal syndrome: three additional cases with CSB mutations, new diagnostic criteria and an approach to investigation. *J Med Genet* 45:564–71
- Lee GY, Jang JS, Lee SY *et al.* (2005) XPC polymorphisms and lung cancer risk. *Int J Cancer* 115:807–13
- Lesnfsky EJ, Hoppel CL (2006) Oxidative phosphorylation and aging. *Ageing Res Rev* 5:402–33
- Lindenbaum Y, Dickson D, Rosenbaum P *et al.* (2001) Xeroderma pigmentosum/cockayne syndrome complex: first neuropathological study and review of eight other cases. *Eur J Paediatr Neurol* 5:225–42
- Liu SY, Wen CY, Lee YJ *et al.* (2010) XPC silencing sensitizes glioma cells to arsenic trioxide via increased oxidative damage. *Toxicol Sci* 116:183–93
- Low GK, Fok ED, Ting AP *et al.* (2008) Oxidative damage induced genotoxic effects in human fibroblasts from Xeroderma Pigmentosum group A patients. *Int J Biochem Cell Biol* 40:2583–95
- Lu W, Hu Y, Chen G *et al.* (2012) Novel role of NOX in supporting aerobic glycolysis in cancer cells with mitochondrial dysfunction and as a potential target for cancer therapy. *PLoS Biol* 10:e1001326
- Lubin A, Zhang L, Chen H *et al.* (2014) A human XPC protein interactome—a resource. *Int J Mol Sci* 15:141–58
- Maalouf S, El-Sabban M, Darwiche N *et al.* (2002) Protective effect of vitamin E on ultraviolet B light-induced damage in keratinocytes. *Mol Carcinog* 34:121–30
- Marchetto MC, Correa RG, Menck CF *et al.* (2006) Functional lentiviral vectors for xeroderma pigmentosum gene therapy. *J Biotechnol* 126:424–30
- Maresca V, Flori E, Briganti S *et al.* (2008) Correlation between melanogenic and catalase activity in *in vitro* human melanocytes: a synergic strategy against oxidative stress. *Pigment Cell Melanoma Res* 21:200–5
- Melis JP, Kuiper RV, Zwart E *et al.* (2013) Slow accumulation of mutations in Xpc^{-/-} mice upon induction of oxidative stress. *DNA Repair* 12:1081–6
- Melis JP, Wijnhoven SW, Beems RB *et al.* (2008) Mouse models for xeroderma pigmentosum group A and group C show divergent cancer phenotypes. *Cancer Res* 68:1347–53
- Menoni H, Hoeijmakers JH, Vermeulen W (2012) Nucleotide excision repair-initiating proteins bind to oxidative DNA lesions *in vivo*. *J Cell Biol* 199:1037–46
- Miao F, Bouziane M, Dammann R *et al.* (2000) 3-Methyladenine-DNA glycosylase (MPG protein) interacts with human RAD23 proteins. *J Biol Chem* 275:28433–8
- Miccoli L, Burr KL, Hickenbotham P *et al.* (2007) The combined effects of xeroderma pigmentosum C deficiency and mutagens on mutation rates in the mouse germ line. *Cancer Res* 67:4695–9
- Morice-Picard F, Cario-Andre M, Rezvani H *et al.* (2009) New clinico-genetic classification of trichothiodystrophy. *Am J Med Genet A* 149A:2020–30
- Moriwaki S, Kraemer KH (2001) Xeroderma pigmentosum—bridging a gap between clinic and laboratory. *Photodermatol Photoimmunol Photomed* 17:47–54
- Moriwaki S, Stefanini M, Lehmann AR *et al.* (1996) DNA repair and ultraviolet mutagenesis in cells from a new patient with xeroderma pigmentosum group G and cockayne syndrome resemble xeroderma pigmentosum cells. *J Invest Dermatol* 107:647–53
- Morley N, Curnow A, Salter L *et al.* (2003) N-acetyl-L-cysteine prevents DNA damage induced by UVA, UVB and visible radiation in human fibroblasts. *J Photochem Photobiol B* 72:55–60
- Muftuoglu M, de Souza-Pinto NC, Dogan A *et al.* (2009) Cockayne syndrome group B protein stimulates repair of formamidopyrimidines by NEIL1 DNA glycosylase. *J Biol Chem* 284:9270–9
- Muller-Hocker J (1989) Cytochrome-c-oxidase deficient cardiomyocytes in the human heart—an age-related phenomenon. A histochemical ultracytochemical study. *Am J Pathol* 134:1167–73
- Muller-Hocker J, Seibel P, Schneiderbanger K *et al.* (1993) Different *in situ* hybridization patterns of mitochondrial DNA in cytochrome c oxidase-deficient extraocular muscle fibres in the elderly. *Virchows Arch A Pathol Anat Histopathol* 422:7–15
- Nance MA, Berry SA (1992) Cockayne syndrome: review of 140 cases. *Am J Med Genet* 42:68–84
- Nouspikel T, Clarkson SG (1994) Mutations that disable the DNA repair gene XPG in a xeroderma pigmentosum group G patient. *Hum Mol Genet* 3:963–7
- Nouspikel T, Lalle P, Leadon SA *et al.* (1997) A common mutational pattern in Cockayne syndrome patients from xeroderma pigmentosum group G: implications for a second XPG function. *Proc Natl Acad Sci USA* 94:3116–21
- Osenbroch PO, Auk-Emblem P, Halsne R *et al.* (2009) Accumulation of mitochondrial DNA damage and bioenergetic dysfunction in CSB defective cells. *FEBS J* 276:2811–21
- Panich U, Tangsupa-a-nan V, Onkoksoong T *et al.* (2011) Inhibition of UVA-mediated melanogenesis by ascorbic acid through modulation of antioxidant defense and nitric oxide system. *Arch Pharm Res* 34:811–20
- Park JY, Cho MO, Leonard S *et al.* (2008) Homeostatic imbalance between apoptosis and cell renewal in the liver of premature aging Xpd mice. *PLoS ONE* 3:e2346
- Pascucci B, Lemma T, Iorio E *et al.* (2012) An altered redox balance mediates the hypersensitivity of Cockayne syndrome primary fibroblasts to oxidative stress. *Ageing Cell* 11:520–9
- Pelle E, Huang X, Mammone T *et al.* (2003) Ultraviolet-B-induced oxidative DNA base damage in primary normal human epidermal keratinocytes and inhibition by a hydroxyl radical scavenger. *J Invest Dermatol* 121:177–83
- Pollitt RJ, Jenner FA, Davies M (1968) Sibs with mental and physical retardation and trichorrhexis nodosa with abnormal amino acid composition of the hair. *Arch Dis Child* 43:211–6
- Price PA, Parthemore JG, Deftos LJ (1980) New biochemical marker for bone metabolism. Measurement by radioimmunoassay of bone GLA protein in the plasma of normal subjects and patients with bone disease. *J Clin Invest* 66:878–83
- Qiu L, Wang Z, Shi X (2008) Associations between XPC polymorphisms and risk of cancers: A meta-analysis. *Eur J Cancer* 44:2241–53
- Quilliet X, Chevallier-Lagente O, Zeng L *et al.* (1997) Retroviral-mediated correction of DNA repair defect in xeroderma pigmentosum cells is associated with recovery of catalase activity. *Mutat Res* 385:235–42
- Rezvani HR, Ali N, Nissen LJ *et al.* (2011a) HIF-1 α in epidermis: oxygen sensing, cutaneous angiogenesis, cancer, and non-cancer disorders. *J Invest Dermatol* 131:1793–805
- Rezvani HR, Cario-Andre M, Pain C *et al.* (2007a) Protection of normal human reconstructed epidermis from UV by catalase overexpression. *Cancer Gene Ther* 14:174–86
- Rezvani HR, Dedieu S, North S *et al.* (2007b) Hypoxia-inducible factor-1 α , a key factor in the keratinocyte response to UVB exposure. *J Biol Chem* 282:16413–22
- Rezvani HR, Ged C, Bouadjar B *et al.* (2008) Catalase overexpression reduces UVB-induced apoptosis in a human xeroderma pigmentosum reconstructed epidermis. *Cancer Gene Ther* 15:241–51

- Rezvani HR, Kim AL, Rossignol R *et al.* (2011b) XPC silencing in normal human keratinocytes triggers metabolic alterations that drive the formation of squamous cell carcinomas. *J Clin Invest* 121:195–211
- Rezvani HR, Mazurier F, Cario-Andre M *et al.* (2006) Protective effects of catalase overexpression on UVB-induced apoptosis in normal human keratinocytes. *J Biol Chem* 281:17999–8007
- Rezvani HR, Rossignol R, Ali N *et al.* (2011c) XPC silencing in normal human keratinocytes triggers metabolic alterations through NOX-1 activation-mediated reactive oxygen species. *Biochim Biophys Acta* 1807:609–19
- Scharer OD (2008) XPG: its products and biological roles. *Adv Exp Med Biol* 637:83–92
- Scheibye-Knudsen M, Ramamoorthy M, Sykora P *et al.* (2012) Cockayne syndrome group B protein prevents the accumulation of damaged mitochondria by promoting mitochondrial autophagy. *J Exp Med* 209:855–69
- Schumacher B, Garinis GA, Hoeijmakers JH (2008) Age to survive: DNA damage and aging. *Trends Genet* 24:77–85
- Seeborg E, Eide L, Bjoras M (1995) The base excision repair pathway. *Trends Biochem Sci* 20:391–7
- Shimizu Y, Iwai S, Hanaoka F *et al.* (2003) Xeroderma pigmentosum group C protein interacts physically and functionally with thymine DNA glycosylase. *EMBO J* 22:164–73
- Shiomi N, Kito S, Oyama M *et al.* (2004) Identification of the XPG region that causes the onset of Cockayne syndrome by using Xpg mutant mice generated by the cDNA-mediated knock-in method. *Mol Cell Biol* 24:3712–9
- Shiomi N, Mori M, Kito S *et al.* (2005) Severe growth retardation and short life span of double-mutant mice lacking Xpa and exon 15 of Xpg. *DNA Repair* 4:351–7
- Spivak G (2005) UV-sensitive syndrome. *Mutat Res* 577:162–9
- Spivak G, Hanawalt PC (2006) Host cell reactivation of plasmids containing oxidative DNA lesions is defective in Cockayne syndrome but normal in UV-sensitive syndrome fibroblasts. *DNA Repair* 5:13–22
- Stack EC, Matson WR, Ferrante RJ (2008) Evidence of oxidant damage in Huntington's disease: translational strategies using antioxidants. *Ann N Y Acad Sci* 1147:79–92
- Sugiyama S, Takasawa M, Hayakawa M *et al.* (1993) Changes in skeletal muscle, heart and liver mitochondrial electron transport activities in rats and dogs of various ages. *Biochem Mol Biol Int* 30:937–44
- Tanaka K, Sekiguchi M, Okada Y (1975) Restoration of ultraviolet-induced unscheduled DNA synthesis of xeroderma pigmentosum cells by the concomitant treatment with bacteriophage T4 endonuclease V and HV (Sendai virus). *Proc Natl Acad Sci USA* 72:4071–5
- Thorslund T, von Kobbe C, Harrigan JA *et al.* (2005) Cooperation of the Cockayne syndrome group B protein and poly(ADP-ribose) polymerase 1 in the response to oxidative stress. *Mol Cell Biol* 25:7625–36
- Tian M, Jones DA, Smith M *et al.* (2004) Deficiency in the nuclease activity of xeroderma pigmentosum G in mice leads to hypersensitivity to UV irradiation. *Mol Cell Biol* 24:2237–42
- Tretter L, Adam-Vizi V (2000) Inhibition of Krebs cycle enzymes by hydrogen peroxide: A key role of [alpha]-ketoglutarate dehydrogenase in limiting NADH production under oxidative stress. *J Neurosci* 20:8972–9
- Tuo J, Jaruga P, Rodriguez H *et al.* (2002) The cockayne syndrome group B gene product is involved in cellular repair of 8-hydroxyadenine in DNA. *J Biol Chem* 277:30832–7
- van der Pluijm I, Garinis GA, Brandt RM *et al.* (2007) Impaired genome maintenance suppresses the growth hormone–insulin-like growth factor 1 axis in mice with Cockayne syndrome. *PLoS Biol* 5:e2
- Vineis P, Manuguerra M, Kavvoura FK *et al.* (2009) A field synopsis on low-penetrance variants in DNA repair genes and cancer susceptibility. *J Natl Cancer Inst* 101:24–36
- von Hebra F, Kaposi M (1874) *On Diseases of Skin Including the Exanthemata (Translated by W tay)*, Vol. 3. The New Sydenham Society: London
- Vuillaume M, Daya-Grosjean L, Vincens P *et al.* (1992) Striking differences in cellular catalase activity between two DNA repair-deficient diseases: xeroderma pigmentosum and trichothiodystrophy. *Carcinogenesis* 13:321–8
- Warrick E, Garcia M, Chagnoleau C *et al.* (2012) Preclinical corrective gene transfer in xeroderma pigmentosum human skin stem cells. *Mol Ther* 20:798–807
- Wong HK, Muftuoglu M, Beck G *et al.* (2007) Cockayne syndrome B protein stimulates apurinic endonuclease 1 activity and protects against agents that introduce base excision repair intermediates. *Nucleic Acids Res* 35:4103–13
- Xu P, Chen B, Feng J *et al.* (2012) Polymorphisms in XPC provide prognostic information in acute myeloid leukemia. *Int J Hematol* 96:450–60
- Yao Y, Harrison KA, Al-Hassani M *et al.* (2012) Platelet-activating factor receptor agonists mediate xeroderma pigmentosum A photosensitivity. *J Biol Chem* 287:9311–21
- Yarosh D, Klein J, O'Connor A *et al.* (2001) Effect of topically applied T4 endonuclease V in liposomes on skin cancer in xeroderma pigmentosum: a randomised study. Xeroderma Pigmentosum Study Group. *Lancet* 357:926–9
- Yen TC, Chen YS, King KL *et al.* (1989) Liver mitochondrial respiratory functions decline with age. *Biochem Biophys Res Commun* 165:944–1003
- Zeng L, Quilliet X, Chevallier-Lagente O *et al.* (1997) Retrovirus-mediated gene transfer corrects DNA repair defect of xeroderma pigmentosum cells of complementation groups A, B and C. *Gene Ther* 4:1077–84
- Zhou NY, Bates SE, Bouziane M *et al.* (2003) Efficient repair of cyclobutane pyrimidine dimers at mutational hot spots is restored in complemented Xeroderma pigmentosum group C and trichothiodystrophy/xeroderma pigmentosum group D cells. *J Mol Biol* 332:337–51

Premature Skin Aging Features Rescued by Inhibition of NADPH Oxidase Activity in XPC-Deficient Mice

Mohsen Hosseini^{1,2}, Walid Mahfouf^{1,2}, Martin Serrano-Sanchez^{1,2}, Houssam Raad^{1,2}, Ghida Harfouche^{1,2}, Marc Bonneu³, Stephane Claverol³, Frederic Mazurier^{1,2,4}, Rodrigue Rossignol^{1,5}, Alain Taieb^{1,2,4,6} and Hamid Reza Rezvani^{1,2,4}

Xeroderma pigmentosum type C (XP-C) is characterized mostly by a predisposition to skin cancers and accelerated photoaging, but little is known about premature skin aging in this disease. By comparing young and old mice, we found that the level of progerin and p16^{INK4a} expression, β -galactosidase activity, and reactive oxygen species, which increase with age, were higher in young $Xpc^{-/-}$ mice than in young $Xpc^{+/+}$ ones. The expression level of mitochondrial complexes and mitochondrial functions in the skin of young $Xpc^{-/-}$ was as low as in control aged $Xpc^{+/+}$ animals. Furthermore, the metabolic profile in young $Xpc^{-/-}$ mice resembled that found in aged $Xpc^{+/+}$ mice. Furthermore, premature skin aging features in young $Xpc^{-/-}$ mice were mostly rescued by inhibition of nicotinamide adenine dinucleotide phosphate oxidase 1 (NOX1) activity by using a NOX1 peptide inhibitor, suggesting that the continuous oxidative stress due to overactivation of NOX1 has a causative role in the underlying pathophysiology.

Journal of Investigative Dermatology advance online publication, 15 January 2015; doi:10.1038/jid.2014.511

INTRODUCTION

Progeroid syndromes are a group of diseases characterized by signs of premature aging. They comprise diseases such as the Hutchinson–Gilford progeria syndrome, xeroderma pigmentosum (XP), trichothiodystrophy (TTD), and the Cockayne syndrome (CS). Most of them usually show only a limited number of features of premature aging and include defects in various DNA repair systems such as nucleotide excision repair (NER), leading to the accumulation of DNA damage, which is thought to be an important mediator of aging (Schumacher *et al.*, 2008; Capell *et al.*, 2009; Kamenisch and Berneburg, 2009). NER is one of the most versatile DNA repair systems and is responsible for removing a wide variety of helix-distorting DNA lesions, including UV-induced photoproducts and several forms of oxidative lesions. The absence or dysfunction of NER proteins results in one of the following

distinct diseases: XP, TTD, and CS (Kraemer *et al.*, 2007; Cleaver *et al.*, 2009).

The defects in XP patients fall into seven NER complementation groups: XP-A to XP-G and a separate group XP variant (XP-V). XP patients may be homozygous or compound heterozygous for the genetic changes in the genes involved in NER. About 60% of XP patients have an early and severe sun sensitivity that damages the skin and eyes (Lehmann *et al.*, 2011). XP-C, one of the more common forms in Europe, United States of America, and Japan, is due to inactivation of the xeroderma pigmentosum, complementation group C (XPC) protein, which is involved in global genome repair but not in transcription-coupled repair. Probably as a consequence of this, XP-C patients do not usually present extreme sunburn reactions (Lehmann *et al.*, 2011). In addition to its role in NER of UV-induced damage, XPC has been shown in several recent studies to have a protective role against oxidative DNA damage (D'Errico *et al.*, 2006; Melis *et al.*, 2013; Hosseini *et al.*, 2014). We have reported that XPC silencing in normal human keratinocytes leads to the activation of NADPH oxidase (NOX), which, in turn, triggers a disturbed redox homeostasis and mitochondrial dysfunction in the context of cancer induction (Rezvani *et al.*, 2011a, b). In addition to tumoral transformation, both oxidative stress and energy metabolism are also considered as crucial in the aging process. Although still controversial, studies have shown good correlations between aging and increased mitochondrial production of reactive oxygen species (ROS) in humans and animals (Cui *et al.*, 2012). Functional studies of mitochondria in aged humans and animals suggest that the bioenergetic function of

¹Inserm U1035, Bordeaux, France; ²Université de Bordeaux, Bordeaux, France; ³Centre Génomique Fonctionnelle de Bordeaux, Université de Bordeaux, Bordeaux, France; ⁴Centre de Référence pour les Maladies Rares de la Peau, CHU de Bordeaux, France; ⁵Université de Bordeaux, Maladies Rares: Génétique et Métabolisme (MRGM), Bordeaux, France and ⁶Département de Dermatologie and Dermatologie Pédiatrique, CHU de Bordeaux, France

Correspondence: Hamid Reza Rezvani, Bordeaux University, INSERM U1035, Bordeaux F-33000, France. E-mail: hamid-reza.rezvani@u-bordeaux.fr

Abbreviations: CS, Cockayne syndrome; NER, nucleotide excision repair; NOX, NADPH oxidase 1; ROS, reactive oxygen species; SA- β -gal, senescence-associated beta-galactosidase; TTD, trichothiodystrophy; XP, xeroderma pigmentosum; XP-C, xeroderma pigmentosum type C

Received 4 August 2014; revised 18 September 2014; accepted 7 October 2014; accepted article preview online 1 December 2014

mitochondria declines with age (Muller-Hocker, 1989; Muller-Hocker *et al.*, 1993; Lesnefsky and Hoppel, 2006).

In this study, we sought whether XPC deficiency results in clear premature skin aging features in mouse skin and what the role of NOX might be in this process.

RESULTS

Xpc knockout results in increased expression of aging biomarkers, elevation of steady-state ROS levels, and altered metabolism

To test whether knockout of *Xpc* is associated with accelerated aging, we first evaluated the expression of progerin in the skin of young and old proficient and deficient XPC mice (*Xpc*^{+/+}

and *Xpc*^{-/-}, respectively; Figure 1a and b). Progerin is a truncated version of lamin A protein, which is involved in Hutchinson–Gilford progeria syndrome, a syndrome in which patients suffer from premature aging of many organs (De Sandre-Giovannoli *et al.*, 2003; Eriksson *et al.*, 2003). It has been reported that the same molecular mechanism responsible for Hutchinson–Gilford progeria syndrome is activated in healthy cells during aging (Scaffidi and Misteli, 2006) and that progerin is more abundant in late-passage cells and in the dermis of aged individuals (McClintock *et al.*, 2007), suggesting that progerin is a biomarker of physiological aging, at least in the skin. Results showed that the progerin level increased with age and that its expression was higher in

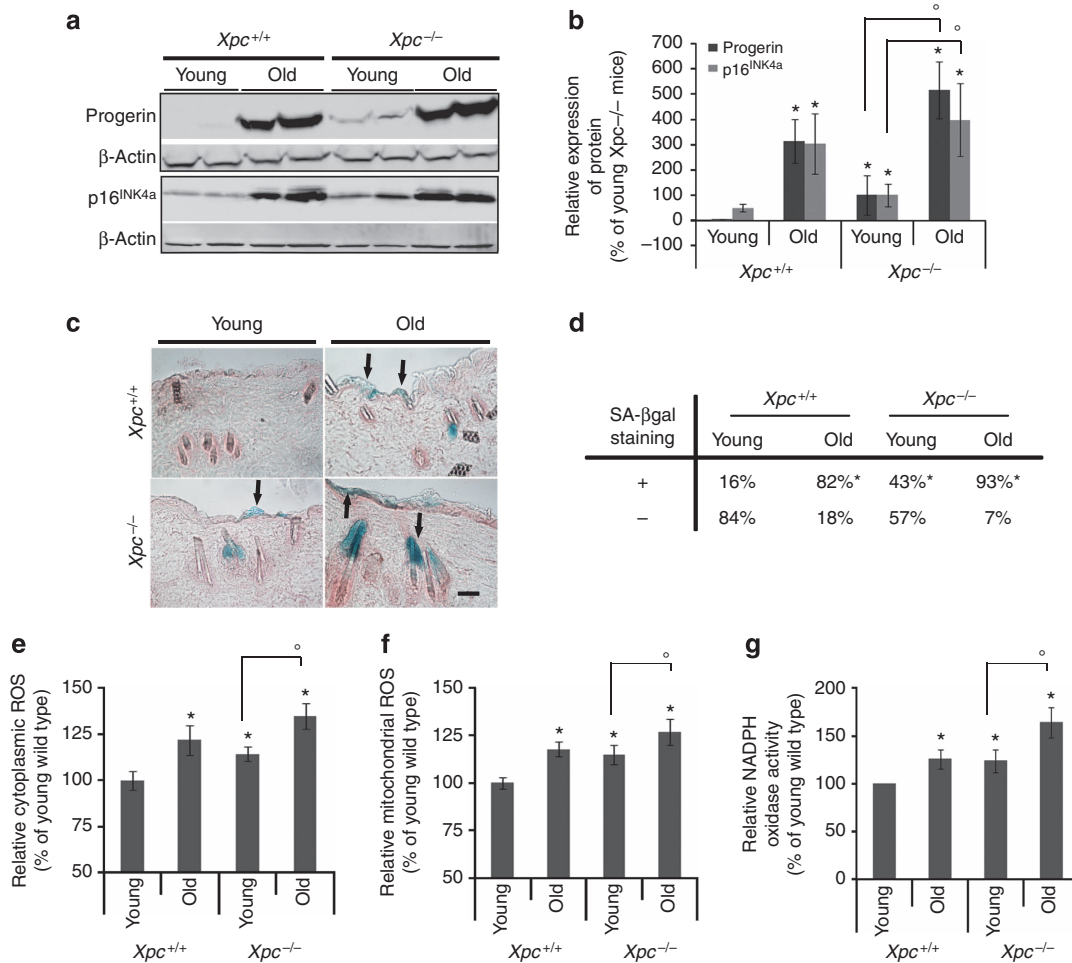


Figure 1. Both aging and xeroderma pigmentosum, complementation group C deficiency lead to an increase in progerin and p16^{INK4a} expression, senescence-associated beta-galactosidase (SA-β-gal) activity, the reactive oxygen species (ROS) level, and NADPH oxidase NOX activity in the skin. Skin biopsies were taken from 4-month-old (young) and 1.5-year-old (old) XPC-proficient (*Xpc*^{+/+}) and -deficient (*Xpc*^{-/-}) mice (N=12 mice in each group). (a) Total protein extracts of skin biopsies were assessed by western blot for the expression of progerin and p16^{INK4a}. β-Actin was used as a loading control. (b) The protein bands corresponding to progerin and p16^{INK4a} were quantified and normalized with β-actin. The average density ± SD is presented as the relative value to the density in young *Xpc*^{-/-} mice. *P<0.05 for mice in each group versus young wild-type mice, °P<0.05 for old versus young *Xpc*^{-/-} mice. (c) Representative photomicrographs of dorsal skin sections of mice stained for SA-β-gal activity (blue) and counterstained with nuclear fast red (red). Arrows indicate SA-β-gal-positive cells. (d) Percentage of skin sections with SA-β-gal-positive (+) or -negative (-) activity. (e, f) Intracellular ROS levels were measured in keratinocytes isolated from skin biopsies of young and old *Xpc*^{+/+} and *Xpc*^{-/-} mice using the cytoplasmic probe, CM-H₂DCF-DA (e), or the mitochondrial probe, MitoSOX (f). The average ROS level in young wild-type mice was set at 100%. The results were then compared with it and are expressed as the average percentage of young wild-type mice ± SD. (g) NOX activity was measured (relative light unit per μg protein) in skin biopsies of young and old *Xpc*^{+/+} and *Xpc*^{-/-} mice. Results were normalized to young wild-type mice. *P<0.05 for each group versus young *Xpc*^{+/+} and °P<0.05 for old versus young *Xpc*^{-/-} mice. Bar = 100 μm.

Xpc^{-/-} mice than in wild-type mice (Figure 1a and b). We next evaluated two classical biomarkers of aging, i.e., p16^{INK4a} expression (Krishnamurthy *et al.*, 2004) and senescence-associated beta-galactosidase (SA-β-gal) activity (Dimri *et al.*, 1995; Velarde *et al.*, 2012). The p16^{INK4a} level was increased with age and was higher in young *Xpc*^{-/-} than in young wild-type mice (Figure 1a and b). SA-β-gal activity increased significantly focally in several areas of the stratum corneum, hair follicles, sebaceous glands, and very rarely in the basal layers as a function of age and/or XP-C deficiency (Figure 1c and d).

As oxidative stress has been shown to be important in aging, we then verified whether ROS levels correlate with increased expression of aging biomarkers. To this end, we measured both cytoplasmic and mitochondrial steady-state levels of ROS in keratinocytes isolated from young and old XP-C-proficient and -deficient mice (Figure 1e and f). A significant increase in both cytoplasmic and mitochondrial steady-state ROS levels occurred in the old mice compared with the young ones. Furthermore, the level of ROS was higher in *Xpc*^{-/-} cells than in *Xpc*^{+/+} keratinocytes (Figure 1e and f). As we have already demonstrated that NOX overactivation is the mechanism underlying XPC downregulation-induced enhancement of ROS generation in human keratinocytes (Rezvani *et al.*, 2011a, b), we investigated whether NOX activity was modified during aging. NOX activity increased significantly with age and was higher in the skin of *Xpc*^{-/-} mice than in wild-type counterparts (Figure 1g).

As both cellular redox status and aging have been described to affect mitochondrial energy metabolism (Rezvani *et al.*, 2011a; Furda *et al.*, 2012), mitochondrial function was then compared between young and old *Xpc*^{-/-} and *Xpc*^{+/+} mice (Figure 2). Results indicated a marked decrease in the relative expression level of the complexes I subunit NDUFB8, II subunit SDHB, and III subunit UQCRC2 in the skin of old wild-type mice compared with the young counterparts. Interestingly, the relative expression level of these complexes in the skin of young *Xpc*^{-/-} was as low as that measured in the old wild-type mice (Figure 2a–d). Complex IV (Figure 2e–g) and II (Figure 2f and g) activities were also lower in the skin of aged wild-type mice than in that of young wild-type mice. Activities of these complexes in young *Xpc*^{-/-} were significantly lower than in the young wild-type mice (Figure 2e–g). Our results further indicated that aging was associated with less oxygen consumption and lower ATP content (Figure 2h and i). The oxygen consumption rate and the ATP level in young *Xpc*^{-/-} mice were significantly lower than those in young wild-type mice (Figure 2h and i).

To screen the effects of aging and the *Xpc* knockout on metabolism profile, a quantitative proteomic approach was used. Results showed a significant reduction in the expression of several proteins involved in the pentose phosphate pathway, the tricarboxylic acid cycle, mitochondrial oxidative phosphorylation, and fatty acid β-oxidation during aging, as well as in the skin of young *Xpc*^{-/-} compared with young *Xpc*^{+/+} mice (Supplementary Table S1 and Supplementary Figure S1 online).

Taken together, our results suggest a premature onset of the skin aging process in the youth of *Xpc*^{-/-} mice.

Inhibition of NOX1/4 activity blocks premature skin aging features in *Xpc* knockout mice

As there is now overwhelming evidence that cellular redox status has an important role in aging (Kamenisch and Berneburg, 2009; Cui *et al.*, 2012), we speculated that NOX overactivation-mediated increased ROS levels in XPC-deficient mice could be the mechanism underlying the premature skin aging profile. To elucidate this hypothesis, NOX inhibition in XPC-deficient mice could be helpful. To find an inhibitor, we first investigated which NOXs among seven members (NOX1 to NOX5, Duox1, and Duox2) of the NOX family are expressed in mouse skin. Western blotting revealed that NOX1, NOX2, and NOX4 (Figure 3a) but not the others (data not shown) are expressed in it. Therefore, we first used the pharmacological NOX inhibitor GKT137831, a specific NOX inhibitor developed recently by GenKyoTex, which has been shown to inhibit NOX1 and NOX4 with high affinity and NOX2 with lower potency and almost without any affinity for xanthine oxidase and other ROS-producing and redox-sensitive enzymes (Gaggini *et al.*, 2011; Aoyama *et al.*, 2012). Although not affecting protein expression levels of NOX1 and NOX4 (Supplementary Figure S2a online), GKT137831 blocked their activity efficiently in both *Xpc*^{+/+} and *Xpc*^{-/-} keratinocytes (Supplementary Figure S2b online). We then examined whether oral administration of the NOX inhibitor GKT137831 could block NOX activity in mouse skin. To this end, we examined the effect of GKT137831 on UVB-induced NOX activation and consequent ROS generation, because we have already shown that UVB irradiation results in an immediately increased ROS level mediated by NOX activation (Rezvani *et al.*, 2006, 2007). Wild-type mice were treated with GKT137831 at 20 mg kg⁻¹ per day by oral administration and then irradiated with UVB. Measurement of NOX activity in mouse skin immediately after irradiation showed that this dose can efficiently block UVB-induced NOX activation (Figure 3b), as well as NOX-dependent ROS production following UVB irradiation (Figure 3c).

To investigate the role of NOX activity on premature skin aging in XP-C-deficient mice, 1-month-old *Xpc*^{+/+} and *Xpc*^{-/-} mice were treated daily by oral administration of placebo or GKT137831 for 3 months. As shown in Figure 3d, treatment of *Xpc*^{-/-} mice with GKT137831 restored NOX activity to the level observed in treated *Xpc*^{+/+} mice. In fact, following treatment with GKT137831, a reduction in NOX activity was seen even in wild-type mice, which could be attributed to the residual activity of NOX family members. However, the level of NOX activity was approximately the same in GKT137831-treated XPC-deficient and proficient mice. That treatment also blocked *Xpc* knockout-induced increased cytoplasmic and mitochondrial ROS levels (Figure 3e and f). Evaluation of aging biomarkers in mice treated with placebo or GKT137831 revealed that NOX inhibition completely blocked XPC downregulation-induced increased progerin and p16^{INK4a} expression, as well as enhanced SA-β-gal activity (Figure 3g–j).

Treatment of *Xpc*^{-/-} mice with GKT137831 abrogated the decreased expression of oxidative phosphorylation complexes

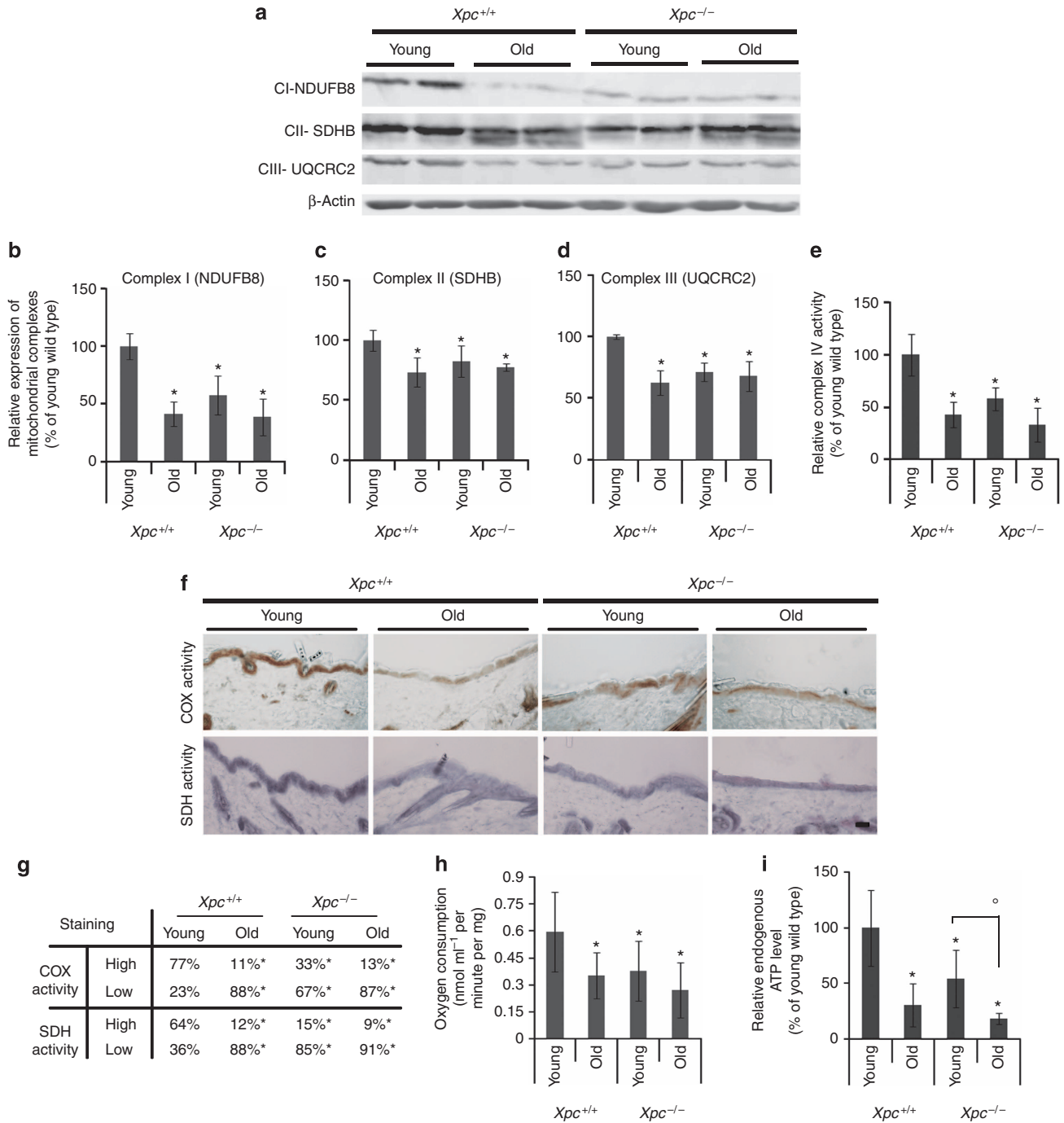


Figure 2. Xeroderma pigmentosum, complementation group C (XPC) deficiency results in mitochondrial function deficiency. (a) Expression of oxidative phosphorylation (OXPHOS) complexes was assessed by western blot analysis in young and old proficient and deficient XP-C mice. (b–d) The bands corresponding to different OXPHOS complexes were quantified and normalized with β-actin. The average density ± SD is presented as the relative value to the density in young wild-type mice. (e) Complex IV activity was measured in young and old mice. The average level of complex IV activity in young wild-type mice was set at 100%. The results were then normalized to the young wild-type mice. (f) Representative photomicrographs of dorsal skin sections stained for cytochrome c oxidase (COX) activity (brown color) and succinate dehydrogenase (SDH) activity (blue color). (g) Percentage of skin sections with high and low COX and SDH activity. Oxygen consumption (h) and total endogenous ATP levels (i) were measured in young and old mice. The average level of each factor in young wild-type mice was set at 100%. The results were then normalized to the young wild-type mice. N = 12 mice in each group. *P < 0.05 for each group versus young *Xpc*^{+/+} and °P < 0.05 for old versus young *Xpc*^{-/-} mice. Bar = 100 μm.

I, II, and III in *Xpc*^{-/-} mice (Figure 4a–d) and restored the activity of complex IV (Figure 4e–g) and II (Figure 4f and g) to the level found in *Xpc*^{+/+} mice. Similarly, the oxygen

consumption rate and the ATP level in the skin of *Xpc*^{-/-} mice treated with GKT137831 resembled that of the placebo-treated *Xpc*^{+/+} (Figure 4h and i).

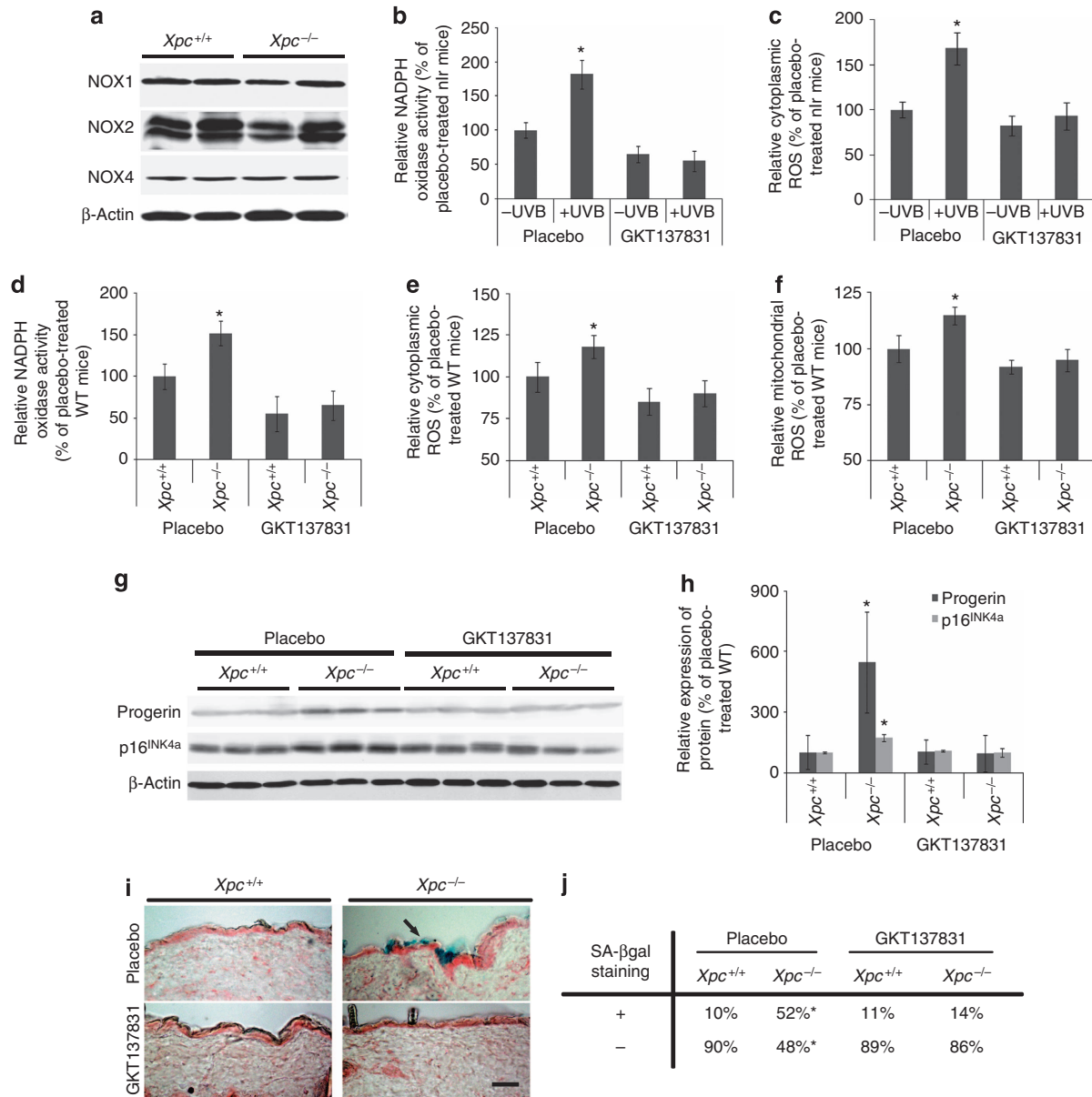


Figure 3. Oral administration of the pharmacological NADPH oxidase (NOX) inhibitor GKT137831 restores xeroderma pigmentosum, complementation group C (XPC) deficiency–induced increased NOX activation, the reactive oxygen species (ROS) level, and aging biomarkers in mouse skin. (a) Total protein extracts of skin biopsies were assessed for expression of different NOX family members by western blot. β-Actin was used as a loading control. (b, c) XPC-proficient mice were treated with GKT137831 at 20 mg kg⁻¹ per day for 5 days. Mice were irradiated with UVB (150 mJ cm⁻²) after last treatment. NOX activity (relative light unit per μg protein) (b) and intracellular ROS levels (c) were measured in mouse skin. Results were normalized to the non-irradiated mice and expressed as average percentage of non-irradiated mice ± SD. *P < 0.05 for irradiated mice versus non-irradiated mice. (d–j) One-month-old *Xpc*^{+/+} and *Xpc*^{-/-} mice were treated daily by oral administration of placebo or GKT137831 for 3 months. NOX activity (d), cytoplasmic (e), and mitochondrial (f) ROS were measured in placebo- and inhibitor-treated mice. The results were then compared with the wild-type (WT) mice treated with placebo and are expressed as the average percentage of these mice ± SD. (g) Total protein extracts of skin biopsies were assessed for expression of progerin and p16^{INK4a} by western blot. (h) The protein bands corresponding to progerin and p16^{INK4a} were quantified and normalized with β-actin. The average density ± SD is presented as the relative value to the density in placebo-treated WT mice. (i) Representative photomicrographs of dorsal skin sections of mice stained for senescence-associated beta-galactosidase (SA-βgal) activity (blue) and counterstained with nuclear fast red (red). Arrows indicate SA-βgal-positive cells. (j) Percentage of skin sections with SA-βgal-positive (+) or -negative (-) activity. N = 12 for each group and *P < 0.05 for mice in each group versus placebo-treated WT mice. Bar = 100 μm.

A peptide targeting NOXO1 and NOXA1 interaction blocks NOX1 activity specifically

Although NOX1 and NOX4 are very similar, their functions appear to be non-redundant (Bedard and Krause, 2007).

Therefore, we sought to identify which NOX could block premature skin aging features in XPC-deficient mice. The greatest challenge, however, was developing a specific NOX1 or NOX4 inhibitor, which does not yet exist. Despite their

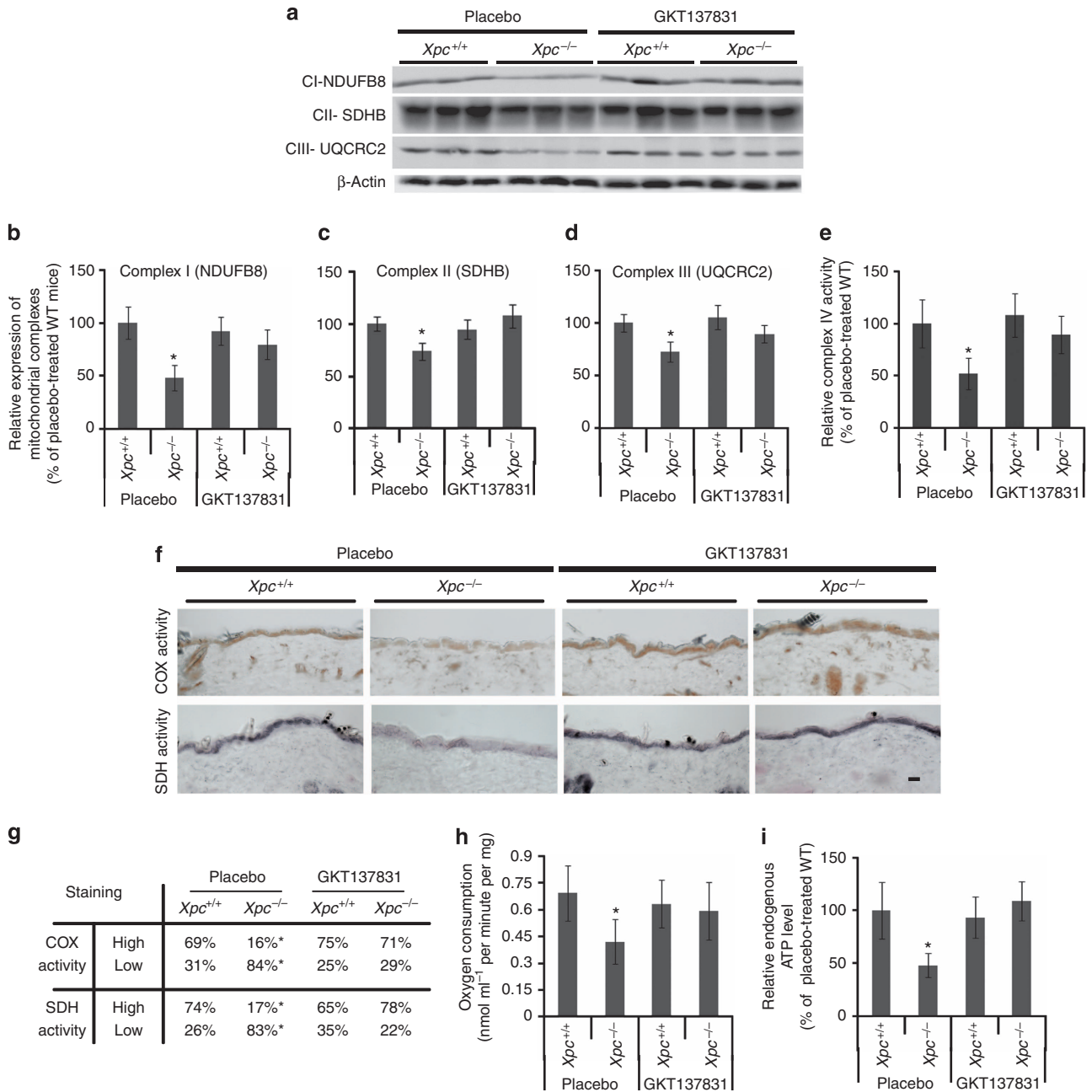


Figure 4. NADPH oxidase 1 (NOX) inhibition restores xeroderma pigmentosum, complementation group C (XPC) deficiency-induced mitochondrial function deficiency. One-month-old *Xpc*^{+/+} and *Xpc*^{-/-} mice were treated daily by oral administration of placebo or GKT137831 for 3 months. (a) Expression of oxidative phosphorylation (OXPHOS) complexes was assessed by western blot analysis in placebo- and GKT137831-treated *Xpc*^{+/+} and *Xpc*^{-/-}. (b–d) The bands corresponding to different OXPHOS complexes were quantified and normalized with β-actin. The average density ±SD from six mice in each group is presented as the relative value to the density in young wild-type (WT) mice. (e) Complex IV activity was measured in different groups of mice. (f) Representative photomicrographs of dorsal skin sections stained for cytochrome c oxidase (COX) activity (brown color) and succinate dehydrogenase (SDH) activity (blue color). (g) Percentage of skin sections with high and low COX and SDH activity. Oxygen consumption (h) and total endogenous ATP levels (i) were measured in different groups of mice. The average level of each factor in WT mice treated with placebo was set at 100% and the results were then normalized to these mice. N = 12 mice in each group and *P < 0.05 for each group versus placebo-treated *Xpc*^{+/+}. Bar = 100 μm.

similar structure, NOX1 and NOX4 differ in their mechanism of activation. Although NOX4 requires p22phox and perhaps Rac as its subunits, NOX1 consists of five heterosubunits (NOX1, p22phox, NOXA1, NOXO1, and the small GTPase

Rac), which, when activated, associate to form an active enzyme complex generating O₂⁻ from oxygen using NADPH as an electron donor (Bedard and Krause, 2007). We speculated that a selective NOX1 inhibition could be achieved by

blocking the assembly of the NOX1 complex. To examine this hypothesis, we tested various peptide inhibitors targeting the proline-rich region of human NOXO1 or the SH3 domain of human NOXA1 (data not shown). We found one peptide, hereafter called InhNOX, that blocks NOX1 activity in human and mice (Supplementary Figures S3, S4 and S5 online). The InhNOX peptide comprises a tat sequence (R-K-K-R-R-Q-R-R-R), which is N-terminal to the sequence P-P-T-V-P-T-R-P-S. A scramble peptide (tat-V-T-P-P-T-S-R-P-P) was used as control. Initially, the trypan blue exclusion assay and the MTT assay were used to evaluate the cytotoxic effects of each peptide. No significant cytotoxicity was observed after treatment with less than 50 μM of peptides (Supplementary Figure S3a and b online). To examine the efficiency and the specificity of this peptide, NOX activity and ROS levels were first assessed in HT29 cells in which NOX1 is the only active member of the NOX family (Gianni *et al.*, 2008). Results showed that treatment with InhNOX resulted in a significant reduction in NOX activity and ROS levels (Supplementary Figure S4a and b online). To examine further the specificity of InhNOX peptide, keratinocytes in which the expression of endogenous NOX1, NOX2, and NOX4 protein was inhibited by using shRNA technology were treated with InhNOX. Equally decreased NOX activity and ROS levels were found in shNOX1-transduced cells, InhNOX-treated cells, and shNOX1-transduced cells treated with InhNOX, demonstrating that InhNOX blocked NOX1-dependent ROS generation with very high (near 100%) efficiency and specificity (Supplementary Figure S5a and b online).

To evaluate whether this peptide had an inhibitory effect on NOX1 activity in mouse skin, we first compared the effect of InhNOX on NOX activity in human and mouse keratinocytes. Results revealed 40% and 37% reduction in NOX activity, respectively, in human and mouse keratinocytes treated with InhNOX (Supplementary Figure S5c online), suggesting a similar preventive effect of InhNOX on NOX activity in human and mouse cells. To determine the efficient dose of InhNOX *in vivo*, mice were then treated topically with different doses of InhNOX and skin biopsies were harvested at different times post treatment. Results showed that InhNOX inhibited NOX activity efficiently for up to 48 hours when administered at 3 and 12 mg kg^{-1} (Supplementary Figure S5d online). The effect of InhNOX on UVB-irradiated mice was then tested to find the optimal topical dose of the peptide inhibitor upon stimulation. Results showed that topical application of InhNOX at 3 and 12 mg kg^{-1} efficiently blocked UVB-induced NOX activation in mouse skin (Supplementary Figure S5e and f online).

Taken together, our results demonstrate that InhNOX, as a novel NOX1 inhibitor, is able to inhibit NOX1 activation efficiently in human and mouse cells *in vitro* and *in vivo*.

Inhibition of NOX1 activity blocks premature skin aging features in *Xpc* knockout mice

To investigate whether NOX1 activity affects premature skin aging in XPC-deficient mice, 1-month-old mice were treated with scrambled peptide or InhNOX for 3 months. Results

showed that InhNOX treatment blocked XPC knockout-induced NOX activation (Figure 5a), elevation of ROS levels (Figure 5b and c), increased progerin and p16^{INK4a} expression (Figure 5d and e), and enhanced SA- β -gal activity (Figure 5f and g). This treatment also restored the expression of oxidative phosphorylation complexes I, II, and III (Figure 5h–k), the activities of complexes IV and II (Figure 5l–n), the oxygen consumption rate (Figure 5o), and ATP levels (Figure 5p) to those found in the skin of *Xpc*^{+/+} mice.

A quantitative proteomic approach was finally used to assess the effects of NOX1 inhibition on modifications to the XP-C deficiency-induced metabolic profile. Results showed that treatment of mice with InhNOX restored the majority of the observed modifications in young *Xpc*^{-/-} mice to the level found in the skin of young wild-type mice (Supplementary Table S1 and Supplementary Figure S1 online).

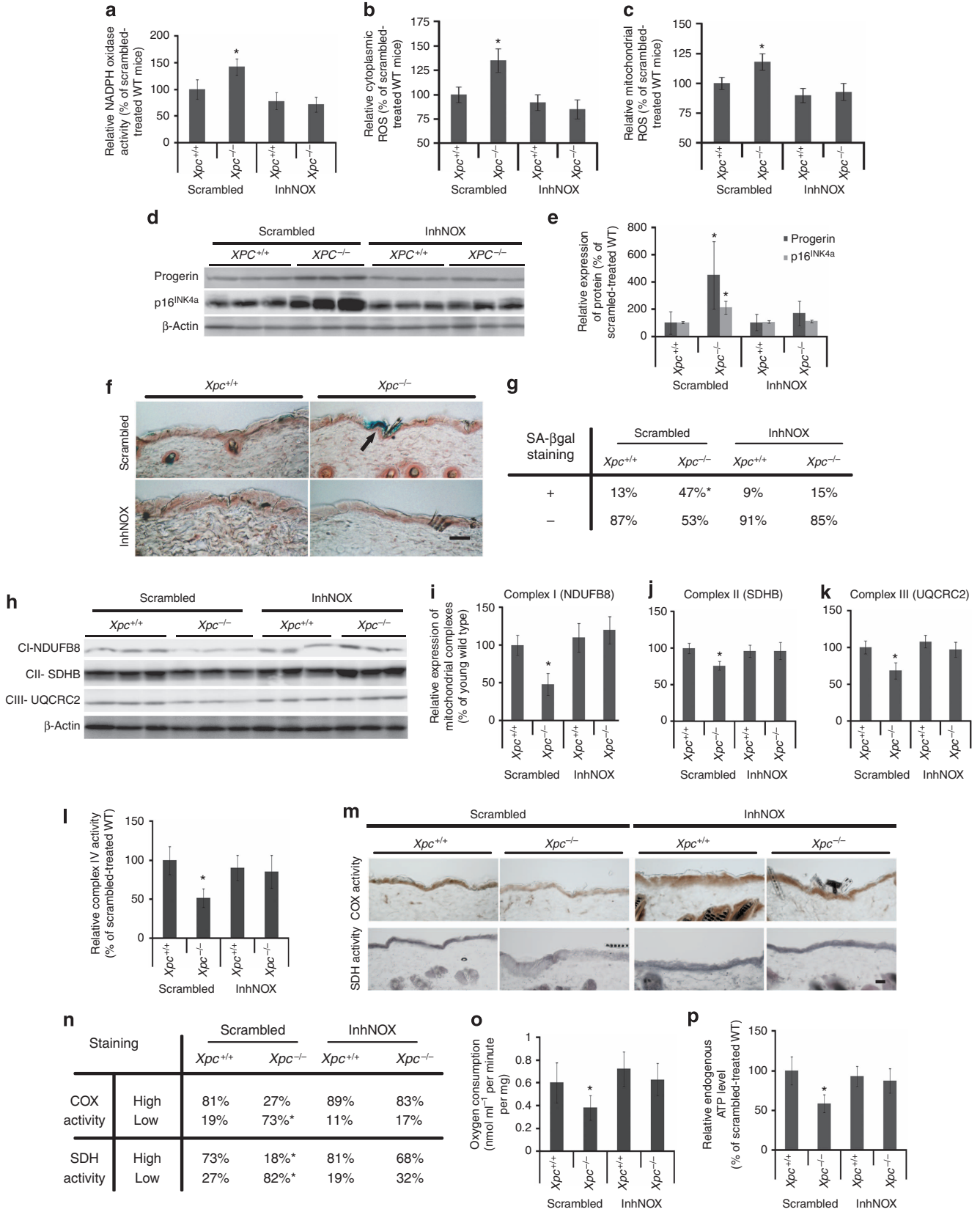
Altogether, these results indicate that inhibition of NOX1 activity blocks XPC deficiency-induced premature skin aging.

DISCUSSION

Our results clearly demonstrate the premature onset of the skin aging process in the youth of *Xpc*^{-/-} mice. The increased risk of developing internal cancers in XP-C patients (Kraemer *et al.*, 1987), the age-dependent accumulation of oxidative stress-mediated spontaneous lesions in the *Hprt* gene (Wijnhoven *et al.*, 2000), the increased incidence of spontaneous lung and liver tumors in old *Xpc*^{-/-} mice (Hollander *et al.*, 2005; Wijnhoven *et al.*, 2007; Melis *et al.*, 2008), and the significant shorter life span of *Xpc*^{-/-} mice compared with wild-type counterparts (Wijnhoven *et al.*, 2007; Melis *et al.*, 2008) all suggest that XPC deficiency induces a mild premature aging phenotype, which is in agreement with our results.

ROS in NER deficiency-induced premature aging

Sever progeroid syndromes in patients with a deficiency in the transcription-coupled repair sub-pathway of NER suggest that *transcriptional* impediments might be particularly relevant to the aging process (Capell *et al.*, 2009; Cleaver *et al.*, 2009). However, comparing premature aging features in NER diseases, including XP, TTD, and CS, suggests that inactivation of NER alone is not sufficient to cause progeroid features. Complete inactivation of NER due to deficiency in XP-A in *Xpa*^{-/-} mice, e.g., does not cause CS- and TTD-like progeroid features but instead leads to a very mild aging phenotype. Therefore, it has been proposed that accelerated aging in CS and TTD could be related to the impaired repair of oxidative DNA damage (Andressoo *et al.*, 2006, 2009; Cleaver *et al.*, 2009). Premature skin aging features in *Xpc*^{-/-} mice could be also related to XPC deficiency-induced oxidative DNA damage because several studies have already highlighted the protective role of XP-C against oxidative DNA damage. This protective function of XPC has been ascribed to its ability to affect the key base-excision repair enzymes (Shimizu *et al.*, 2003; D'Errico *et al.*, 2006), catalase activity (Vuillaume *et al.*, 1992), and/or NOX activity (Rezvani *et al.*, 2011a; Hosseini *et al.*, 2014). In agreement with our data suggesting the existence of oxidative stress in *Xpc*^{-/-} mice, it has been reported that spontaneous mutation frequencies in the *Hprt*



gene are 30-fold higher in the spleen of *Xpc*^{-/-} mice as compared with normal mice and that the majority of these mutations result from oxidative damage (Wijnhoven *et al.*, 2000). Moreover, *Xpc*^{-/-} mice harbor a slow accumulation of mutations upon pro-oxidant exposure (Melis *et al.*, 2013).

The effects of NOX1 activation in XP-C deficiency-induced premature skin aging features

To identify the molecular events associated with aging, the age-related modifications of the gene expression profile have been studied in various mouse tissues (Cao *et al.*, 2001; Lee *et al.*, 2002). Results revealed that aging is particularly associated with modifications in the expression of genes involved in stress responses, as well as a clear decline in the expression of metabolic and biosynthetic genes. Consistently, our results indicate an aging-associated decrease in mitochondrial respiratory proteins and function, as well as a marked decline in several proteins involved in the tricarboxylic acid cycle, the pentose phosphate pathway, and fatty acid β -oxidation, leading ultimately to lower ATP production. Decreased ATP levels could, in turn, reduce the efficiency of the turnover of damaged molecules, leading to the features of aging. In fact, one of the mechanisms explaining aging could be oxidative stress-mediated alterations in mitochondrial functions (Cui *et al.*, 2012). The effect of oxidative stress on mitochondrial function has been related to a deficiency in mitochondrial respiration during cell growth due to somatic mutations in mtDNA (Cui *et al.*, 2012). It is becoming increasingly clear that mtDNA mutations can induce mild aging phenotypes in mice with a wild-type nuclear genome (Ross *et al.*, 2013). Our present results indicate that the activation of NOX1 in *Xpc*^{-/-} mice results in a decline in mitochondrial metabolism because of increased ROS levels. It is likely that NOX1 activation-induced increased ROS leads to enhanced oxidation of nuclear and mtDNA followed by the induction of mtDNA deletions and alterations in mitochondrial bioenergetics. Importantly, all these modifications (i.e., increased aging biomarkers and ROS levels, as well as metabolic profile alteration) can be mitigated by a treatment with the small-molecule NOX inhibitor GKT137831 or NOX1 peptide inhibitor, indicating that NOX1 activation-induced ROS generation is the major cause of the premature skin aging phenotype in *Xpc*^{-/-} mice.

Conclusion and perspectives

Regarding the mechanism linking NOX1 activation and XPC expression, we have already shown that accumulation of unrepaired damaged DNA bases in XPC-deficient cells could result in activation of the non-homologous end joining repair pathway and subsequently the AKT pathway, which in turn mediates induction of NADPH oxidase (Rezvani *et al.*, 2011a). The activation of NOX1 in XPC-deficient cells triggers neoplastic transformation of keratinocytes (Rezvani *et al.*, 2011a), as well as premature skin aging. Further studies are needed to identify the effect of the NOX1 inhibitor on the life span of *XPC*^{-/-} mice, as well as on UVB-induced skin cancer.

MATERIALS AND METHODS

Transgenic mice

Xpc knockout mice originated from Cheo *et al.* (1997) and were a generous gift from E.C. Friedberg (University of Texas Southwestern Medical Center, Dallas, TX). Mice were bred and maintained in a pathogen-free mouse facility at the Bordeaux University. All mouse experiments were carried out with the approval of Bordeaux University Animal Care and Use Committee.

Isolation of skin samples and keratinocytes

One part of the dorsal skin was excised and snap-frozen in liquid nitrogen for western blotting and measurement of enzymatic activities. The other part was used for isolation of keratinocytes. To this end, the epidermis and dermis were separated by trypsinization at 37 °C for 1 hour. Keratinocyte suspensions were isolated from the epidermal sheet in Hank's balanced salt solution on ice.

Western blotting procedure

Western blotting was performed as previously described (Rezvani *et al.*, 2011a, b). Briefly, equal amounts of total protein were resolved by SDS-PAGE and electrophoretically transferred to polyvinylidene difluoride membranes. The membranes were then incubated overnight at 4 °C with a 1:1,000 dilution of the anti-progerin (Santa Cruz Biotechnology, TEBU, Le Perray en Yvelines, France), anti-NOX1, anti- β -actin (Sigma, Saint Quentin Fallavier, France), anti-NOX4 (Abcam, Paris, France), and anti-NOX2 (a generous gift of Dr Mark T. Quinn, Montana State University) antibodies or a total oxidative phosphorylation antibody cocktail (Abcam). After additional incuba-

←

Figure 5. Topical application of InhNOX restores xeroderma pigmentosum, complementation group C (XPC) deficiency-induced increased NADPH oxidase (NOX) activation, the reactive oxygen species (ROS) level, and aging biomarkers and metabolism profile modifications. One-month-old *Xpc*^{+/+} and *Xpc*^{-/-} mice were treated topically with 3 mg kg⁻¹ of scramble peptide or InhNOX three times per week for 3 months. NOX activity (a), cytoplasmic (b), and mitochondrial (c) ROS were measured in mouse skin biopsies. The results were then compared with the wild-type (WT) mice treated with scramble peptide and are expressed as the average percentage of these mice \pm SD. (d) The expression level of progerin and p16^{INK4a} were assessed by western blot in skin biopsies. (e) The protein bands corresponding to progerin and p16^{INK4a} were quantified and normalized with β -actin. (f) Representative photomicrographs of dorsal skin sections stained for senescence-associated beta-galactosidase (SA- β -gal) activity (blue) and counterstained with nuclear fast red (red). (g) Percentage of skin sections with SA- β -gal-positive or -negative activity. (h) Total protein extracts of skin biopsies were assessed for expression of oxidative phosphorylation (OXPHOS) complexes by western blot analysis. (i-k) The bands corresponding to different OXPHOS complexes were quantified and normalized with β -actin. (l) Complex IV activity was measured in different groups of mice. (m) Representative photomicrographs of dorsal skin sections stained for cytochrome c oxidase (COX) activity (brown color) and succinate dehydrogenase (SDH) activity (blue color). (n) Percentage of skin sections with high and low COX and SDH activity. Oxygen consumption (o) and total endogenous ATP levels (p) were measured in different groups of mice. The average level of each factor in WT mice treated with scramble peptide was set at 100% and the results were then normalized to these mice. *N* = 12 mice in each group and **P* < 0.05 for each group versus scramble peptide-treated *Xpc*^{+/+}. Bar = 100 μ m.

tion with a 1:10,000 dilution of an anti-Ig horseradish peroxidase-linked antibody (Vector Laboratories, Biovalley S.A, Marne la Vallée, France) for 1 hour, blots were developed using the chemiluminescence ECL reagent (Perkin Elmer, Courtaboeuf, France).

Mitochondrial enzyme histochemistry

Skin samples were embedded in frozen optimum cutting temperature medium, cut into 20 μm sections, and subjected to histochemical staining for the activities of COX and SDH. Briefly, sections were reacted for 45 minutes at 37 °C with COX staining solution (4 mM diaminobenzidine tetrahydrochloride, 100 μM cytochrome c and 20 $\mu\text{g ml}^{-1}$ catalase in 0.2 M phosphate buffer, pH 7.0) or 40 minutes at 37 °C with SDH media (1.5 mM nitroblue tetrazolium, 1 mM sodium azide, 200 μM phenazine methosulphate, 130 mM sodium succinate, in 0.2 M phosphate buffer, pH 7.0).

SA- β -gal activity staining

Frozen optimum cutting temperature-embedded samples were cut into 10 μm sections, processed for SA- β -gal staining using the Senescence Detection Kit (BioVision, Mountain View, CA), and counterstained with nuclear fast red. Four fields were taken at $\times 40$ magnification for each skin section and three sections per animal were analyzed. Skin sections with several SA- β -gal staining (blue staining in at least two out of four fields) were considered as a SA- β -gal-positive section.

Proteomic analysis

Sample preparation, nano-scale liquid chromatographic tandem mass spectrometry analysis, database search, processing of results, and label-free quantitative data analysis are detailed in the Supplementary Data section.

NOX inhibitor GKT137831

This inhibitor is a member of the pyrazolopyridine dione family, is a specific inhibitor of NADPH isoforms NOX1 and NOX4 (NOX1 $K_i = 110 \text{ nmol l}^{-1}$ and Nox4 $K_i = 140 \text{ nmol l}^{-1}$), and has been shown to inhibit NOX1- and NOX4-derived ROS *in vitro* and *in vivo* (Gaggini *et al.*, 2011; Aoyama *et al.*, 2012). For the purpose of oral administration, GKT137831 was solubilized in de-ionized water comprising 1.2% methyl cellulose (Sigma) and 0.1% polysorbate 80 (Sigma). This solution without GKT137831 was used as placebo treatment.

Statistics

Student's *t*-test was applied for statistical evaluation and a **P*-value of <0.05 was considered significant. Results are presented as means \pm SD.

CONFLICT OF INTEREST

The authors state no conflict of interest. A patent is pending on InhNOX with HR, FM, GH, and AT as inventor and Bordeaux University as owner of the patent.

ACKNOWLEDGMENTS

We acknowledge the patients' support group "Les Enfants de La Lune". HRR gratefully acknowledges support from the ARC "Association pour la Recherche sur le Cancer" and the Fondation Maladies Rares. We thank Pierre Cau for helpful discussions and are grateful to P. Costet (University of Bordeaux) for his valuable expertise. HR and GH were supported by grants from "La ligue contre le cancer".

SUPPLEMENTARY MATERIAL

Supplementary material is linked to the online version of the paper at <http://www.nature.com/jid>

REFERENCES

- Andressoo JO, Hoeijmakers JH, Mitchell JR (2006) Nucleotide excision repair disorders and the balance between cancer and aging. *Cell Cycle* 5: 2886–8
- Andressoo JO, Weeda G, de Wit J *et al.* (2009) An Xpb mouse model for combined xeroderma pigmentosum and cockayne syndrome reveals progeroid features upon further attenuation of DNA repair. *Mol Cell Biol* 29:1276–90
- Aoyama T, Paik YH, Watanabe S *et al.* (2012) Nicotinamide adenine dinucleotide phosphate oxidase in experimental liver fibrosis: GKT137831 as a novel potential therapeutic agent. *Hepatology* 56:2316–27
- Bedard K, Krause KH (2007) The NOX family of ROS-generating NADPH oxidases: physiology and pathophysiology. *Physiol Rev* 87:245–313
- Cao SX, Dhahbi JM, Mote PL *et al.* (2001) Genomic profiling of short- and long-term caloric restriction effects in the liver of aging mice. *Proc Natl Acad Sci USA* 98:10630–5
- Capell BC, Tloutan BE, Orlow SJ (2009) From the rarest to the most common: insights from progeroid syndromes into skin cancer and aging. *J Invest Dermatol* 129:2340–50
- Cheo DL, Ruven HJ, Meira LB *et al.* (1997) Characterization of defective nucleotide excision repair in XPC mutant mice. *Mutat Res* 374:1–9
- Cleaver JE, Lam ET, Revet I (2009) Disorders of nucleotide excision repair: the genetic and molecular basis of heterogeneity. *Nat Rev Genet* 10:756–68
- Cui H, Kong Y, Zhang H (2012) Oxidative stress, mitochondrial dysfunction, and aging. *J Signal Transduct* 2012:646354
- D'Errico M, Parlanti E, Teson M *et al.* (2006) New functions of XPC in the protection of human skin cells from oxidative damage. *EMBO J* 25:4305–15
- De Sandre-Giovannoli A, Bernard R, Cau P *et al.* (2003) Lamin a truncation in Hutchinson-Gilford progeria. *Science* 300:2055
- Dimri GP, Lee X, Basile G *et al.* (1995) A biomarker that identifies senescent human cells in culture and in aging skin *in vivo*. *Proc Natl Acad Sci USA* 92:9363–7
- Eriksson M, Brown WT, Gordon LB *et al.* (2003) Recurrent de novo point mutations in lamin A cause Hutchinson-Gilford progeria syndrome. *Nature* 423:293–8
- Furda AM, Marrangoni AM, Lokshin A *et al.* (2012) Oxidants and not alkylating agents induce rapid mtDNA loss and mitochondrial dysfunction. *DNA Repair* 11:684–92
- Gaggini F, Laleu B, Orchard M *et al.* (2011) Design, synthesis and biological activity of original pyrazolo-pyrido-diazepine, -pyrazine and -oxazine dione derivatives as novel dual Nox4/Nox1 inhibitors. *Bioorg Med Chem* 19:6989–99
- Gianni D, Bohl B, Courtneidge SA *et al.* (2008) The involvement of the tyrosine kinase c-Src in the regulation of reactive oxygen species generation mediated by NADPH oxidase-1. *Mol Biol Cell* 19:2984–94
- Hollander MC, Philburn RT, Patterson AD *et al.* (2005) Deletion of XPC leads to lung tumors in mice and is associated with early events in human lung carcinogenesis. *Proc Natl Acad Sci USA* 102:13200–5
- Hosseini M, Ezzedine K, Taieb A *et al.* (2014) Oxidative and energy metabolism as potential clues for clinical heterogeneity in nucleotide excision repair disorders. *J Invest Dermatol*; e-pub ahead of print 9 October 2014, doi:10.1038/jid.2014.365
- Kamenisch Y, Berneburg M (2009) Progeroid syndromes and UV-induced oxidative DNA damage. *J Invest Dermatol Symp Proc* 14:8–14
- Kraemer KH, Lee MM, Scotto J (1987) Xeroderma pigmentosum. Cutaneous, ocular, and neurologic abnormalities in 830 published cases. *Arch Dermatol* 123:241–50
- Kraemer KH, Patronas NJ, Schiffmann R *et al.* (2007) Xeroderma pigmentosum, trichothiodystrophy and Cockayne syndrome: a complex genotype-phenotype relationship. *Neuroscience* 145:1388–96
- Krishnamurthy J, Torrice C, Ramsey MR *et al.* (2004) Ink4a/Arf expression is a biomarker of aging. *J Clin Invest* 114:1299–307

- Lee CK, Allison DB, Brand J *et al.* (2002) Transcriptional profiles associated with aging and middle age-onset caloric restriction in mouse hearts. *Proc Natl Acad Sci USA* 99:14988–93
- Lehmann AR, McGibbon D, Stefanini M (2011) Xeroderma pigmentosum. *Orphanet J Rare Dis* 6:70
- Lesnefsky EJ, Hoppel CL (2006) Oxidative phosphorylation and aging. *Ageing Res Rev* 5:402–33
- McClintock D, Ratner D, Lokuge M *et al.* (2007) The mutant form of lamin A that causes Hutchinson-Gilford progeria is a biomarker of cellular aging in human skin. *PLoS One* 2:e1269
- Melis JP, Kuiper RV, Zwart E *et al.* (2013) Slow accumulation of mutations in Xpc mice upon induction of oxidative stress. *DNA Repair* 12:1081–6
- Melis JP, Wijnhoven SW, Beems RB *et al.* (2008) Mouse models for xeroderma pigmentosum group A and group C show divergent cancer phenotypes. *Cancer Res* 68:1347–53
- Muller-Hocker J (1989) Cytochrome-c-oxidase deficient cardiomyocytes in the human heart—an age-related phenomenon. A histochemical ultracytochemical study. *Am J Pathol* 134:1167–73
- Muller-Hocker J, Seibel P, Schneiderbanger K *et al.* (1993) Different in situ hybridization patterns of mitochondrial DNA in cytochrome c oxidase-deficient extraocular muscle fibres in the elderly. *Virchows Arch A Pathol Anat Histopathol* 422:7–15
- Rezvani HR, Dedieu S, North S *et al.* (2007) Hypoxia-inducible factor-1alpha, a key factor in the keratinocyte response to UVB exposure. *J Biol Chem* 282:16413–22
- Rezvani HR, Kim AL, Rossignol R *et al.* (2011a) XPC silencing in normal human keratinocytes triggers metabolic alterations that drive the formation of squamous cell carcinomas. *J Clin Invest* 121:195–211
- Rezvani HR, Mazurier F, Cario-Andre M *et al.* (2006) Protective effects of catalase overexpression on UVB-induced apoptosis in normal human keratinocytes. *J Biol Chem* 281:17999–8007
- Rezvani HR, Rossignol R, Ali N *et al.* (2011b) XPC silencing in normal human keratinocytes triggers metabolic alterations through NOX-1 activation-mediated reactive oxygen species. *Biochim Biophys Acta* 1807:609–19
- Ross JM, Stewart JB, Hagstrom E *et al.* (2013) Germline mitochondrial DNA mutations aggravate ageing and can impair brain development. *Nature* 501:412–5
- Scaffidi P, Misteli T (2006) Lamin A-dependent nuclear defects in human aging. *Science* 312:1059–63
- Schumacher B, Garinis GA, Hoeijmakers JH (2008) Age to survive: DNA damage and aging. *Trends Genet* 24:77–85
- Shimizu Y, Iwai S, Hanaoka F *et al.* (2003) Xeroderma pigmentosum group C protein interacts physically and functionally with thymine DNA glycosylase. *EMBO J* 22:164–73
- Velarde MC, Flynn JM, Day NU *et al.* (2012) Mitochondrial oxidative stress caused by Sod2 deficiency promotes cellular senescence and aging phenotypes in the skin. *Ageing* 4:3–12
- Vuillaume M, Daya-Grosjean L, Vincens P *et al.* (1992) Striking differences in cellular catalase activity between two DNA repair-deficient diseases: xeroderma pigmentosum and trichothiodystrophy. *Carcinogenesis* 13:321–8
- Wijnhoven SW, Hoogervorst EM, de Waard H *et al.* (2007) Tissue specific mutagenic and carcinogenic responses in NER defective mouse models. *Mutat Res* 614:77–94
- Wijnhoven SW, Kool HJ, Mullenders LH *et al.* (2000) Age-dependent spontaneous mutagenesis in Xpc mice defective in nucleotide excision repair. *Oncogene* 19:5034–7

Supplementary materials

Supplementary figure legends

Figure S1: Metabolic profile in young *Xpc* knockout mice resembles that of old wild-type mice and NOX1 inhibition restores XPC deficiency-induced modifications in metabolic profile. Proteomic analysis was used to investigate the effects of aging and XPC deficiency on profile expression of several proteins in skin biopsies of 4-month-old (young) and 1.5-year-old (old) XPC-proficient (*Xpc*^{+/+}) and -deficient (*Xpc*^{-/-}) mice. To test the effect of inhibition of NOX1 activity on the metabolic profile of mice, one-month-old *Xpc*^{+/+} and *Xpc*^{-/-} mice were treated topically with scramble peptide or InhNOX for three months. Skin biopsies were then subjected to proteomic analysis. The quantity of each protein was compared among the different groups and the results are expressed as mean fold change of expression of each protein as indicated at the top of each column of the heat map. As shown in the first column, comparison of old and young skin mice reveals a decreased expression of several proteins involved in metabolism during skin aging. The same comparison in *XPC*^{-/-} mice in the second column shows that the expression levels of these proteins were approximately the same. Comparison of protein expression levels between young *XPC*^{+/+} and *XPC*^{-/-} in the third column indicates that there was a marked reduction in the expression level of several proteins involved in the metabolism of XPC-deficient mice. Comparison of protein expression levels between old *XPC*^{+/+} and *XPC*^{-/-} in the fourth column shows that the expression level of these proteins are similar in aged mice. Finally, the protein expression level in young mice treated with scrambled peptide (column five) was resembled to non-treated young mice (column 3), indicating a decreased expression level of those proteins in XPC-deficient mice compared with wild-type mice. Interestingly, as shown in the sixth column, InhNOX treatment restored the expression level of the majority of these proteins to that found in wild-type mice.

ATP5B: ATP synthase subunit beta, ATP5h: ATP synthase subunit d, ATP5I: ATP synthase subunit e, ECHS1: Enoyl-CoA hydratase, G6PD: Glucose-6-phosphate 1-dehydrogenase, HCDH: Hydroxyacyl-coenzyme A dehydrogenase, IDH3B: Isocitrate dehydrogenase 3 (NAD⁺) beta, LCAD: Long-chain specific acyl-CoA dehydrogenase, NDUFS3: NADH dehydrogenase [ubiquinone] iron-sulfur protein 3, OGDC-E1: 2-oxoglutarate dehydrogenase, PDHE1B: Pyruvate dehydrogenase E1 component subunit beta, PGD: 6-phosphogluconate dehydrogenase, SDHA: Succinate dehydrogenase [ubiquinone] flavoprotein subunit, SDHB: Succinate dehydrogenase complex subunit B, TK: Transketolase.

Figure S2. GKT137831 blocks NOX1/4 activity efficiently in mouse keratinocytes

(a, b) *Xpc*^{+/+} and *Xpc*^{-/-} keratinocytes were transduced with lentiviral vectors expressing shCtrl, shNOX1, shNOX2 or shNOX4. Four days after transduction, cells were treated with 10 μM of GKT137831 for 24h. (a) Total protein extracts of keratinocytes were then assessed for expression of different NOX family members by Western blot. β-actin was used as a loading control. (b) NOX activity was measured in different cells. **P* < 0.05 versus placebo-treated shCtrl *Xpc*^{+/+} cells, † *P* < 0.05 versus placebo-treated shCtrl *Xpc*^{-/-} cells, and ° *P* < 0.05 versus GKT137831-treated shCtrl-transduced keratinocytes.

Figure S3. Cytotoxic effect of InhNOX treatment on human keratinocytes

Human keratinocytes were treated with indicated concentrations of scrambled peptide or InhNOX. The cytotoxic effect of each treatment was measured 24, 48 and 72 hours post-treatment using trypan blue exclusion assay (a) and MTT assay (b). The percentage of viability in treated keratinocytes was normalized to the non-treated cells (NTC).

Figure S4. InhNOX efficiently inhibits NOX1 activity in HT29

HT29 cells (human colon adenocarcinoma cell line) were treated with 10 or 50 μ M of InhNOX or scrambled peptide. NOX activity (**a**) and the relative ROS level (**b**) and the ROS level were measured 24 h post-treatment. Both NOX activity and ROS level were normalized to the non-treated cells (NTC). (* $P < 0.05$)

Figure S5. InhNOX blocks NOX1 activity specifically and efficiently in human and mouse cells. (**a, b**) Human keratinocytes were transduced with lentiviral vectors expressing shCtrl, shNOX1, shNOX2 or shNOX4. Four days after transduction, cells were treated with 10 μ M of scrambled peptide, InhNOX or GKT137831 for 24h. NOX activity (**a**) and relative ROS level (**b**) were then measured in different cells. ROS level was normalized to counterpart scramble-treated cells. * $P < 0.05$ versus scramble-treated shCtrl cells and ° $P < 0.05$ versus InhNOX-treated shNOX1-transduced keratinocytes. (**c**) NOX activity was measured in human and mouse keratinocytes 24h post-treatment with 10 μ M of scramble peptide or InhNOX. (**d**) Mice were treated topically with indicated doses of scramble peptide or InhNOX. Skin biopsies were harvested 2 h, 24 h, 48 h and 72 h post-treatment (five mice per dose and time). NOX activity was measured and normalized to the vehicle-treated mice. (**e**) Mice were treated topically with 3 and 12 mg/kg of scramble peptide or InhNOX. Twenty min after treatment, mice were exposed to UVB (150 mJ/cm²). Skin biopsies were harvested 0.5 h and 24 h post-treatment. At 47.5 h after first treatment, mice were treated again with the same concentration of scramble peptide and InhNOX and exposed to UVB 20 min later. Skin biopsies were then harvested at 48 and 72 h after first treatment. NOX activity was measured and then normalized to the vehicle-treated and non-irradiated mice. N= 5 mice per group and * $P < 0.05$. nIr, non-irradiated mice.

Supplementary Materials and Methods

Mouse genomic DNA isolation and genotyping

Mouse genomic DNA was obtained from tail clip samples following their overnight digestion at 45°C with 100 µl of 100 mM Tris, pH 8.0, 5 mM EDTA, 0.2% SDS, 200 mM NaCl, 100 µg/ml proteinase K. Samples were then diluted with 300 µl of water and boiled for 5 min before use for PCR. *Xpc* genotyping was carried out using the following primers: *Xpc*-wt: □ forward primer, ATTGCGTGCATACCTTGCAC; reverse primer, TATCTCCTCCTCAAACCCTGCTC; *Xpc*-del: forward primer, CGCATAGCCTTCTATCGCCT; reverse primer, TATCTCCTCCTCAAACCCTGCTC. Amplification products were detected on 2% agarose gel stained with ethidium bromide.

Detection of NADPH Oxidase activity in cell-free system

NADPH oxidase activity was measured in plasma membranes obtained from skin specimens as already explained (Rezvani *et al.*, 2011a; Rezvani *et al.*, 2011b). Briefly, skin specimens were incubated for 10 min at 4°C with 300 µl of hypotonic solution supplemented with protease inhibitor cocktail (Sigma, Saint Quentin Fallavier, France). Following sonication for five 20 s bursts, the homogenate was centrifuged at 1,000 x g for 15 min at 4°C. The supernatant was withdrawn and centrifuged at 12,000 x g for one hour at 4°C. The supernatant was referred to as the cytosol, and the pellet consisting of crude membranes was resuspended in the Hank's buffer supplemented with 0.9 mM CaCl₂ and 0.5 mM MgCl₂. 50 µg of plasma membrane were added to 200 µl of reaction mixture containing 2 mM luminol, 500 U/ml horseradish peroxidase and 0.8 M glucose (all from Sigma). After incubation for 1 min at 37°C, the NADPH oxidase activation

was initiated in the presence of 2µg/ml phorbol myristate acetate (PMA) and 200 µM NADPH. The relative light units (RLU) of chemiluminescence were recorded every 30 sec for a total of 90 min at 37 °C using a luminometer.

Measurement of endogenous and mitochondrial ATP production

The amount of intracellular ATP was measured by a luciferin/luciferase-based assay using an ATP bioluminescence assay kit HSII (Roche Applied Science, Meylan Cedex, France) in accordance with the manufacturer's instructions, as already explained (Rezvani *et al.*, 2011a). In brief, skin samples were lysed with 0.2 ml of cell lysis reagent. ATP concentrations in the lysates were quantified. A standard curve for ATP concentration was plotted using standard ATP solution. ATP levels were calculated and normalized to protein lysate concentrations.

Measurement of mitochondrial oxygen consumption rates

Skin respiration was measured with 10 mg section/ml using a Clark oxygen electrode (oxygraph Hansatech) in a 2 ml glass cell thermostatically controlled at 37°C.

Complex IV (cytochrome c-oxidase) activity

Cytochrome *c*-oxidase activity was determined spectrophotometrically with cytochrome *c* (II) as the substrate. The oxidation of cytochrome *c* was monitored at 550 nm at 30°C using a double-wavelength Xenius spectrophotometer from SAFAS (Monaco) and standardized reproducible methods as already described (Rezvani *et al.*, 2011a; Rezvani *et al.*, 2011b).

Measurement of intracellular ROS

The intracellular production of ROS was assessed using a CM-H₂DCF-DA cytoplasmic probe or the MitoSOXTM red mitochondrial superoxide indicator (both from Molecular Probes, Invitrogen) as already described (Rezvani *et al.*, 2007; Rezvani *et al.*, 2006). Briefly, CM-H₂DCF-DA (5 μM) or MitoSOX (5 μM) were added onto keratinocytes immediately after their isolation from mouse skin. Keratinocytes were then incubated for 15 min at 37°C in the dark. After two washes with PBS, the cells were immediately analyzed by flow cytometry. Ten thousand individual data points were collected for each sample.

Details of Proteomic analysis:

Sample preparation for proteomic analysis

Skin samples were lysed in RIPA buffer containing protease inhibitor cocktail (Sigma). Ten µg of each protein sample were solubilized in Laemlli buffer and were deposited onto SDS-PAGE gel for concentration and cleaning purposes. Separation was stopped after proteins had entered the resolving gel. After colloidal blue staining, bands were cut out of the SDS-PAGE gel and subsequently cut into 1 mm x 1 mm gel pieces. Gel pieces were destained in 25 mM ammonium bicarbonate 50% ACN, rinsed twice in ultrapure water and shrunk in ACN for 10 min. After ACN removal, gel pieces were dried at room temperature, covered with trypsin solution (10 ng/µl in 40 mM NH₄HCO₃ and 10% ACN), rehydrated at 4 °C for 10 min, and finally incubated overnight at 37 °C. Spots were then incubated for 15 min in 40 mM NH₄HCO₃ and 10% ACN at room temperature with rotary shaking. The supernatant was collected and an H₂O/ACN/HCOOH (47.5:47.5:5) extraction solution was added onto gel slices for 15 min. The extraction step was repeated twice. Supernatants were pooled and concentrated in a vacuum centrifuge to a final volume of 40 µL. Digests were finally acidified by addition of 2.4 µL of formic acid (5%, v/v) and stored at -20 °C.

nLC-MS/MS analysis

Peptide mixture was analyzed on an Ultimate 3000 nanoLC system (Dionex, Amsterdam, The Netherlands) coupled to a Q-Exactive quadrupole Orbitrap benchtop mass spectrometer (Thermo Fisher Scientific, San Jose, CA). Ten microliters of peptide digests were loaded onto a 300-µm-inner diameter x 5-mm C₁₈ PepMapTM trap column (LC Packings) at a flow rate of 30 µL/min. The peptides were eluted from the trap column onto an analytical 75-mm id x 15-cm C18 Pep-Map column (LC Packings) with a 4–40% linear

gradient of solvent B in 108 min (solvent A was 0.1% formic acid in 5% ACN, and solvent B was 0.1% formic acid in 80% ACN). The separation flow rate was set at 300 nL/min. The mass spectrometer operated in positive ion mode at a 1.8-kV needle voltage. Data were acquired in a data-dependent mode. MS scans (m/z 300-2000) were recorded at a resolution of $R = 70\,000$ (@ m/z 200) and an AGC target of 1×10^6 ions was collected within 100 ms. Dynamic exclusion was set to 30 s and the top 15 ions were selected from fragmentation in HCD mode. MS/MS scans with a target value of 1×10^5 ions were collected with a maximum fill time of 120 ms and a resolution of $R = 35\,000$. Additionally, only +2 and +3 charged ions were selected for fragmentation. Other settings were as follows: spray voltage, 1.8 kV, no sheath or auxiliary gas flow, heated capillary temperature, 200 °C; normalized HCD collision energy of 25% and an isolation width of 3 m/z .

Database search and processing of results

Data were searched by SEQUEST through Proteome Discoverer 1.4 (Thermo Fisher Scientific Inc.) against a subset of the 2013.08 version of UniProt database restricted to *Mus musculus* Reference Proteome Set (42,882 entries). Spectra from peptides higher than 5000 Da or lower than 350 Da were rejected. The search parameters were as follows: mass accuracy of the monoisotopic peptide precursor and peptide fragments was set to 10 ppm and 0.02 Da respectively. Only b- and y-ions were considered for mass calculation. Oxidation of methionines (+16 Da) was considered as variable modification and carbamidomethylation of cysteines (+57 Da) as fixed modification. Two missed trypsin cleavages were allowed. Peptide validation was performed using the Percolator algorithm (Kall et al., 2007) and only “high confidence” peptides were retained, corresponding to a 1% False Positive Rate at peptide level.

Label-Free Quantitative Data Analysis

Raw LC-MS/MS data were imported into Progenesis LC-MS 4.1 (Nonlinear Dynamics Ltd, Newcastle, U.K). Data processing included the following steps: (i) detection of features, (ii) alignment of features across the 12 samples, (iii) Volume integration for 2-6 charge-state ions, (iv) Normalization on total protein abundance, (v) Importation of sequence information, (vi) ANOVA test at peptide level and filtering for features $p < 0.05$, (vii) Calculation of protein abundance (sum of the volume of corresponding peptides), (viii) ANOVA test at protein level and filtering for features $p < 0.05$. Noticeably, only non-conflicting features and unique peptides were considered for calculation at protein level. Quantitative data were considered for proteins quantified by a minimum of 2 peptides.

Supplementary Reference

Kall, L., Canterbury, J.D., Weston, J., Noble, W.S., and MacCoss, M.J. (2007). Semi-supervised learning for peptide identification from shotgun proteomics datasets. *Nat. Methods* 4, 923-925.

Figure S1



Figure S2

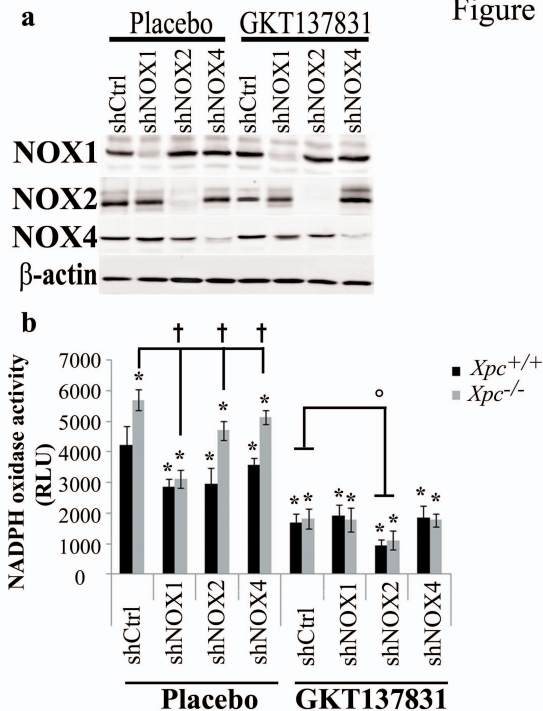
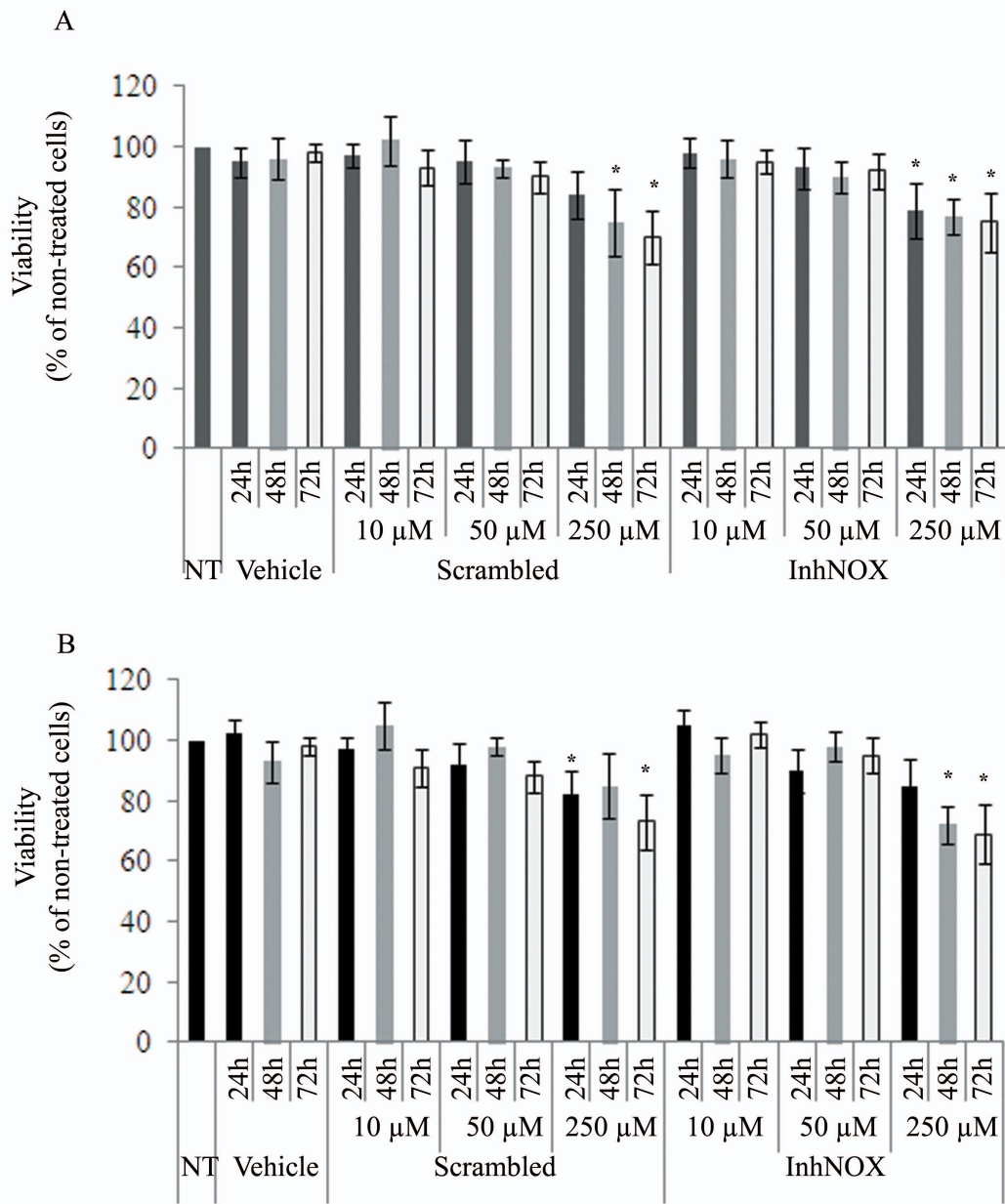
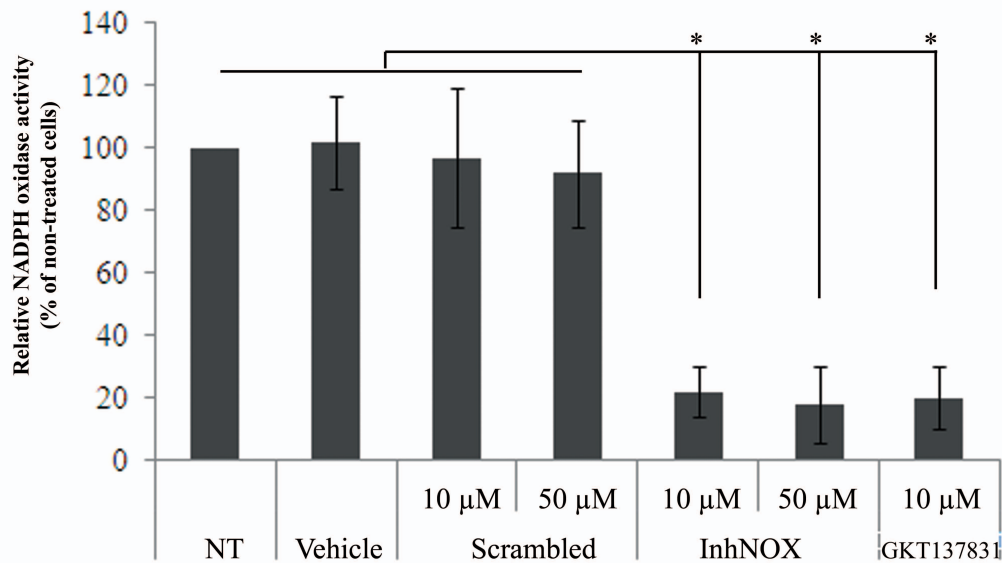


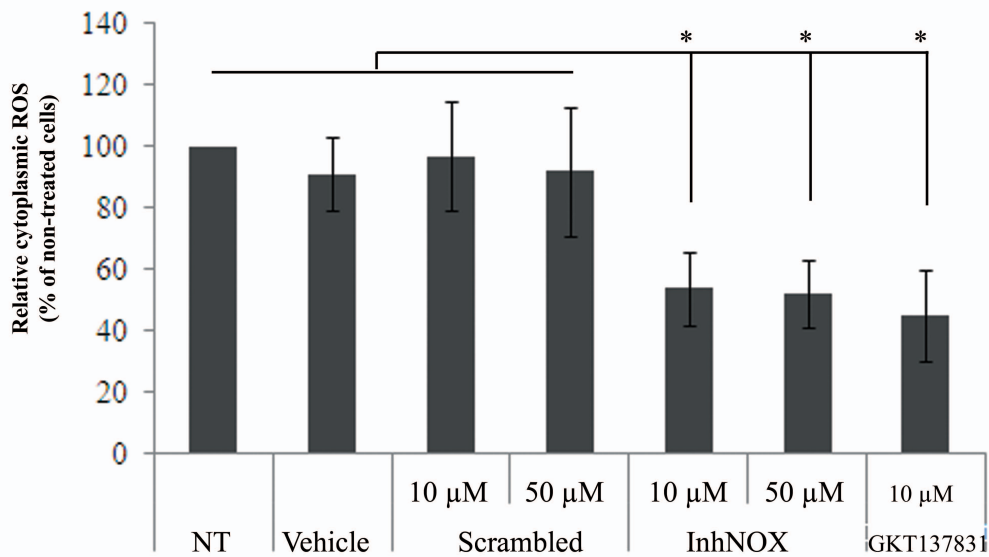
Figure S3



A



B



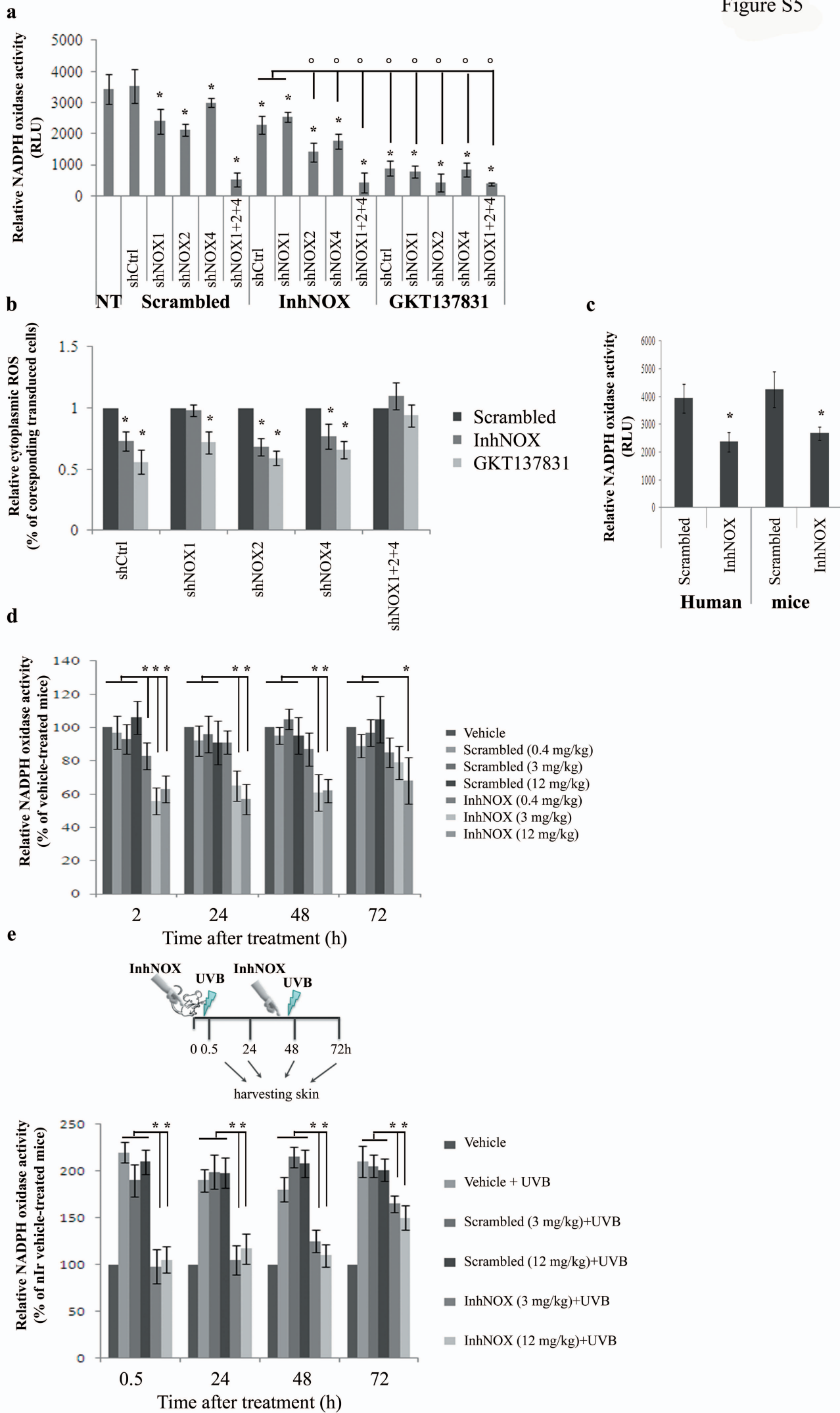


Table S1. The effects of aging, XPC deficiency and topical application of NOX1 inhibitor on metabolic profile of skin.

Process	Accession	Protein name	old vs young								<i>Xpc</i> ^{-/-} vs <i>Xpc</i> ^{+/+}								<i>Xpc</i> ^{-/-} vs <i>Xpc</i> ^{+/+}							
			<i>Xpc</i> ^{+/+}				<i>Xpc</i> ^{-/-}				young/young				old/old				Scrambled				InhNOX			
			Peptides used for quantitation	Confidence score	Fold Change	Anova (p)	Peptides used for quantitation	Confidence score	Fold Change	Anova (p)	Peptides used for quantitation	Confidence score	Fold Change	Anova (p)	Peptides used for quantitation	Confidence score	Fold Change	Anova (p)	Peptides used for quantitation	Confidence score	Fold Change	Anova (p)	Peptides used for quantitation	Confidence score	Fold Change	Anova (p)
Pentose phosphate pathways	Q00612	Glucose-6-phosphate 1-dehydrogenase X	3	7.26	-2.21	1.45E-05	6	19.24	-2.75	2.43E-04	5	16.61	-2.68	5.12E-04	3	6.97	-2.66	8.06E-03	8	27.13	-2.59	8.06E-03	6	17.35	-1.11	1.93E-01
	Q93092	Transaldolase	2	8.93	-3.25	3.69E-05	3	75.14	-2.86	2.46E-04	2	7.87	-3.18	2.23E-02	3	9.57	-1.79	8.83E-02	4	12.02	-2.94	1.99E-02	3	7.68	-1.33	1.15E-01
	Q9CPQ9	Fructose-bisphosphate aldolase	15	56.10	-6.29	5.26E-05	7	27.80	-1.71	3.45E-03	3	8.59	-2.61	5.74E-04	4	7.92	1.31	4.06E-02	3	10.23	-2.18	4.38E-02	13	53.53	-1.43	5.42E-02
	P40142	Transketolase	6	14.83	-2.95	1.13E-04	6	14.97	-1.40	7.54E-02	4	12.00	-2.52	2.34E-02	3	6.07	-1.62	7.74E-03	5	21.88	-2.18	1.64E-02	3	12.82	-1.13	8.73E-01
	Q9DCD0	6-phosphogluconate dehydrogenase, decarboxylating	8	32.25	-2.80	1.44E-04	2	6.61	-1.68	4.66E-02	6	24.00	-2.68	6.96E-04	11	26.18	-1.52	4.61E-03	10	38.29	-3.00	1.41E-02	7	23.27	-1.18	2.89E-01
TCA cycle	Q8BMF4	Dihydropyridyllysine-residue acetyltransferase component of pyruvate dehydrogenase complex, mitochondrial	2	4.02	-2.94	6.82E-03	5	21.02	-1.64	2.03E-03	4	11.49	-2.34	2.13E-03	3	9.00	-1.95	1.54E-02	2	6.92	-2.03	2.89E-02	3	12.49	-1.43	3.60E-02
	Q9D051	Pyruvate dehydrogenase E1 component subunit beta, mitochondrial	4	17.58	-4.13	1.87E-03	2	6.41	-2.29	1.44E-03	2	5.55	-5.96	2.13E-02	5	19.39	-3.48	3.93E-03	5	16.11	-3.29	1.68E-02	3	6.82	-1.09	5.27E-01
	Q9D6R2	Isocitrate dehydrogenase [NAD] subunit alpha, mitochondrial	6	20.36	-2.56	1.90E-03	2	4.36	-2.06	3.45E-03	3	9.41	-1.70	4.16E-02	2	6.95	-1.45	2.83E-02	4	14.53	-1.91	4.33E-03	4	13.2	-1.21	1.87E-02
	O08749	Dihydropyridyl dehydrogenase, mitochondrial	2	6.35	-2.17	1.97E-03	6	20.20	-2.36	3.18E-03	3	10.13	-1.95	1.61E-03	3	12.34	-2.96	1.91E-02	3	13.43	-1.58	1.67E-02	2	8.52	-1.32	1.02E-02
	P35486	Pyruvate dehydrogenase E1 component subunit alpha, somatic form, mitochondrial	4	14.08	-5.78	1.99E-03	3	8.79	-1.45	7.66E-02	2	5.55	-4.96	2.13E-02	2	3.35	-3.44	3.42E-03	3	15.33	-3.30	1.32E-02	3	3.26	-1.25	9.75E-02
	Q91VA7	Isocitrate dehydrogenase 3 (NAD+) beta	2	5.08	-2.67	4.40E-03	2	3.83	-1.48	3.35E-02	3	7.24	-4.39	2.11E-02	4	15.65	-2.81	3.54E-03	3	14.63	-4.67	2.29E-02	4	9.02	-1.30	3.33E-01
	Q8K2B3	Succinate dehydrogenase [ubiquinone] flavoprotein subunit, mitochondrial	5	18.09	-2.36	4.49E-03	4	13.26	-2.82	4.54E-03	3	6.39	-2.11	4.62E-03	4	12.27	-2.25	1.65E-03	5	19.94	-2.57	3.26E-03	4	9.02	-1.11	4.51E-01
	Q99K10	Aconitate hydratase, mitochondrial	6	15.96	-1.70	4.81E-03	4	14.54	-1.57	8.45E-02	6	22.43	-2.21	1.92E-02	7	24.94	-2.26	1.34E-02	15	57.96	-1.35	2.20E-02	7	26.04	-1.55	3.35E-03
	P08249	Malate dehydrogenase, mitochondrial	2	9.52	-10.39	2.40E-02	2	6.81	-1.57	2.04E-03	2	4.06	-4.10	5.72E-03	4	25.02	1.54	4.18E-02	5	19.71	-3.39	1.30E-03	4	15.91	-1.21	1.09E-02
	Q60597	2-oxoglutarate dehydrogenase, mitochondrial	2	5.30	-6.18	5.26E-03	3	6.24	-1.66	3.02E-03	2	3.80	-5.23	5.73E-03	9	25.42	-3.32	6.18E-03	4	15.10	-4.87	2.60E-02	3	8.08	-1.82	3.28E-05
	Q9CQA3	Succinate dehydrogenase [ubiquinone] iron-sulfur subunit, mitochondrial	3	7.23	-2.25	5.41E-03	2	7.55	-1.14	9.37E-02	2	4.68	-1.72	2.46E-02	2	4.02	1.24	6.82E-02	2	5.85	-1.91	2.97E-02	3	8.12	-1.08	6.91E-01
	Q9Z219	Succinyl-CoA ligase [ADP-forming] subunit beta, mitochondrial	3	7.34	-2.58	6.73E-03	2	3.99	-3.62	7.17E-03	2	4.02	-1.49	6.82E-03	2	8.93	-1.89	6.98E-03	2	13.83	-1.26	2.52E-02	2	5.26	-1.36	3.51E-03
Oxidative phosphorylation	Q91VR2	ATP synthase subunit gamma, mitochondrial	8	33.99	-2.95	7.17E-03	3	13.04	-1.90	8.21E-03	3	11.69	-1.78	8.88E-03	5	7.72	-4.20	1.04E-02	6	21.89	-1.54	2.67E-02	3	13.41	-1.43	1.46E-02
	P56480	ATP synthase subunit beta, mitochondrial	4	18.12	-2.80	3.37E-03	3	12.31	-1.16	8.48E-02	7	32.55	-1.83	1.07E-02	6	22.09	-1.41	6.35E-03	8	36.26	-1.92	2.04E-02	9	43.76	-1.25	1.11E-01
	Q9CQQ7	ATP synthase subunit b, mitochondrial	2	4.61	-2.94	4.02E-03	4	14.10	-1.69	1.14E-02	2	3.40	-1.94	1.37E-03	4	19.50	-1.27	5.13E-02	5	15.85	-1.75	5.13E-03	5	7.72	1.09	1.29E-01
	Q91YT0	NADH dehydrogenase [ubiquinone] flavoprotein 1, mitochondrial	2	3.98	-2.26	7.41E-03	2	8.89	-2.32	1.05E-02	2	4.39	-1.63	1.17E-02	2	8.07	-1.26	1.22E-02	3	7.04	-1.50	4.78E-03	3	6.90	-1.41	2.64E-03
	Q03265	ATP synthase subunit alpha, mitochondrial	6	19.21	-1.72	5.24E-03	13	48.10	-1.39	3.08E-02	9	28.09	-1.37	8.47E-03	8	38.07	1.32	6.48E-02	21	81.78	-1.23	4.05E-02	7	29.57	-1.27	1.04E-02
	Q9CPQ8	ATP synthase subunit g, mitochondrial	2	3.42	-8.83	7.67E-04	2	3.56	-1.83	1.32E-02	2	5.10	-6.62	1.22E-02	3	6.90	-1.72	1.31E-02	2	5.59	-7.41	1.63E-03	3	8.66	-1.26	6.76E-02
	Q9DCT2	NADH dehydrogenase [ubiquinone] iron-sulfur protein 3, mitochondrial	4	12.25	-5.93	7.77E-03	2	4.51	-2.05	1.34E-02	2	4.46	-4.76	6.72E-03	3	7.49	-1.17	1.43E-01	2	7.40	-3.26	2.93E-02	2	5.83	-1.11	3.72E-01
	Q9D819	Inorganic pyrophosphatase	6	19.21	-2.75	8.00E-03	3	7.49	-1.62	1.43E-02	3	7.44	-1.78	1.41E-02	5	24.80	1.19	7.50E-02	2	10.64	-1.81	2.54E-02	3	7.49	1.00	9.83E-01
	Q8K2B3	Succinate dehydrogenase [ubiquinone] flavoprotein subunit, mitochondrial	5	18.09	-2.36	4.49E-03	4	13.26	-2.82	4.54E-03	3	6.39	-2.11	4.62E-03	4	12.27	-2.25	1.65E-03	5	19.94	-2.57	3.26E-03	4	9.02	-1.11	4.51E-01
	Q9DB20	ATP synthase subunit O,	3	10.63	-1.75	1.53E-02	3	4.91	1.30	5.83E-02	3	7.60	-2.53	1.75E-02	2	7.55	-1.36	1.94E-02	3	10.25	-2.37	4.71E-03	3	10.15	-1.43	1.19E-02

		mitochondrial																								
	Q9CZ13	Cytochrome b-c1 complex subunit 1, mitochondrial	8	24.12	-4.19	5.35E-03	6	15.13	-1.89	1.97E-02	3	7.00	-1.70	2.45E-02	2	5.42	-1.57	2.43E-02	5	17.62	-1.75	2.11E-03	3	9.65	-1.46	1.23E-02
	Q9D0M3	Cytochrome c1, heme protein, mitochondrial	6	24.88	-2.61	3.61E-03	2	4.35	-1.71	2.00E-02	2	6.10	-3.18	1.71E-02	2	4.94	-1.21	9.54E-02	4	14.36	-2.42	2.26E-02	3	9.25	-1.49	1.13E-02
	Q9DB77	Cytochrome b-c1 complex subunit 2, mitochondrial	2	5.98	-1.99	1.55E-02	3	7.96	-1.19	7.20E-02	3	9.77	-1.84	1.42E-02	2	8.71	1.06	6.25E-02	7	33.83	-2.08	5.12E-03	4	15.97	-1.80	2.33E-02
	Q9CQA3	Succinate dehydrogenase [ubiquinone] iron-sulfur subunit, mitochondrial	2	7.39	-2.65	8.95E-03	2	6.10	-1.38	5.20E-02	3	6.68	-1.72	2.46E-02	3	13.53	1.15	7.57E-02	2	5.85	-1.91	2.97E-02	3	7.96	-1.08	6.91E-01
	Q91VD9	NADH-ubiquinone oxidoreductase 75 kDa subunit, mitochondrial	3	9.21	-4.25	6.51E-03	4	10.20	-1.80	7.17E-03	2	10.16	-2.79	1.82E-02	2	4.05	1.27	9.72E-02	2	8.02	-1.87	1.38E-02	3	13.53	-2.33	2.19E-02
	Q9DCX2	ATP synthase subunit d, mitochondrial	2	8.89	-3.02	1.70E-02	3	6.65	-1.49	2.72E-02	5	16.93	-2.60	2.90E-02	6	23.19	-1.04	8.85E-02	5	19.90	-2.17	2.69E-02	4	15.45	-1.10	1.29E-01
Fatty acid β oxidation	P51660	Peroxisomal multifunctional enzyme type 2	8	23.36	-3.00	3.25E-02	2	6.37	-1.42	3.66E-02	7	29.57	-2.37	6.65E-04	5	15.67	-1.23	2.43E-02	6	19.82	-2.18	1.72E-02	8	31.11	-1.05	2.66E-01
	Q8C178	Acyl-coenzyme A oxidase	6	20.20	-2.42	2.34E-02	3	11.17	-1.84	1.40E-04	2	5.83	-4.32	4.18E-03	5	18.33	-1.80	4.76E-03	2	8.70	-5.11	9.11E-03	3	8.08	-1.25	3.81E-02
	Q61425	Hydroxyacyl-coenzyme A dehydrogenase, mitochondrial	7	22.76	-3.24	4.13E-02	8	35.79	-1.46	1.49E-03	9	43.76	-2.37	3.56E-03	4	13.40	-1.34	3.49E-02	5	16.37	-2.05	6.93E-03	2	6.64	1.03	7.14E-01
	Q8BH95	Enoyl-CoA hydratase, mitochondrial	2	5.38	-4.22	1.36E-03	5	18.66	-1.46	2.86E-03	2	5.18	-2.38	2.93E-03	3	10.15	1.41	7.81E-02	4	12.07	-2.64	1.45E-02	3	22.88	-1.07	5.68E-01
	P51174	Long-chain specific acyl-CoA dehydrogenase, mitochondrial	2	9.91	-4.97	1.83E-03	3	8.30	-2.47	3.10E-03	7	26.04	-4.51	3.35E-03	2	7.01	-2.14	3.56E-02	3	11.37	-4.16	8.13E-03	7	34.75	-1.28	6.94E-01
	P50544	Very long-chain specific acyl-CoA dehydrogenase, mitochondrial	2	5.05	-3.90	2.16E-03	7	28.24	-1.37	3.48E-02	3	8.19	-3.25	3.35E-03	2	10.66	-1.30	5.40E-02	5	16.01	-2.30	4.41E-03	3	13.41	-1.43	4.87E-02
	P45952	Medium-chain specific acyl-CoA dehydrogenase, mitochondrial	2	4.64	-1.91	4.61E-02	2	5.52	-1.43	6.52E-03	2	8.00	-1.68	1.20E-02	5	18.98	-1.11	6.40E-02	2	9.01	-1.59	4.37E-03	4	11.47	-1.23	1.89E-01

Articles 3 and 4

Skin Cancer

The second part the thesis project starts with a review article in which the link between identified mutations in skin cancers and energy metabolism is discussed. In the light of data presented in this review, it appears that metabolism reprogramming should be studied in more detail in skin cancers.

The original article entitles “UVB irradiation rewires cellular metabolism through over-activation of dihydroorotate dehydrogenase to coordinate DNA repair and ATP synthesis” is presented afterwards. In this work, we will see that UVB irradiation affects energy metabolism which in turn regulates the cell fate.

ARTICLE IN PREPARATION

UV, Mutations and Metabolism in Skin Cancers: A Therapeutic Perspective

Mohsen Hosseini^{1,2}, Zeinab Kasraian^{1,2}, Hamid Reza Rezvani^{1,2,3*}

1. Inserm U 1035, 33076 Bordeaux, France
2. Université de Bordeaux, 146 rue Léo Saigant, 33076 Bordeaux, France
3. Centre de Référence pour les Maladies Rares de la Peau, CHU de Bordeaux, France
4. Département de Dermatologie & Dermatologie Pédiatrique, CHU de Bordeaux, France

*** Correspondence**

INSERM U1035, Bordeaux, F-33000 France

Email address: hamidreza.rezvani@u-bordeaux2.fr

Phone: +33-557-575-683

Fax: +33-557-571-374

Abstract

Skin responds to UV radiation through various adaptive mechanisms such as cell death, modifications in proliferation and differentiation. However, photoadaptation is not optimal and the accumulations of mutations in nuclear and mitochondrial DNA as well as increased ROS level contribute to photo-aging and carcinogenesis. Mitochondrial alterations with subsequent metabolic reprogramming influences other cell signaling pathways. A comprehensive study of UV-induced metabolic reprogramming and its consequences is needed to clarify the role of mitochondria in multistage skin tumorigenesis. These investigations could also lead to the development of new targets for skin cancer therapy.

Introduction

Malignant transformation of normal cells requires a number of characteristic alterations known as cancer hallmarks. These modifications enable cancer cells to survive under extreme conditions such as oxygen insufficiency and unlimited proliferation. In 2011, Hanahan and Weinberg suggested metabolism reprogramming as one of the hallmarks of tumorigenesis (Hanahan and Weinberg, 2011). Modified metabolism in cancer cells was recognized by Otto Warburg in 1930. He proposed that cancer cells shift their metabolism toward glycolysis with the production of more lactate even in conditions of oxygen sufficiency (Warburg, 1956). Metabolic reprogramming is an intelligent strategy used by malignant cells in order to support cell growth. Malignant cells are able to change their metabolism according to the requirements of the cell or tissue. All malignant cells are not necessarily glycolytic. For example, breast cancer cells enforce their metabolism towards OXPHOS whereas a large range of cancer types including colon, prostate and lung cancers are dependent on a glycolytic metabolism. Mitochondrial defects, hypoxia, oncogenes and altered metabolic enzymes are now characterized as the main cause of metabolic alteration (Pelicano et al., 2006). Understanding metabolism remodeling during the multistage process of carcinogenesis for developing new strategies is currently a main trend in cancer research, and we show in this review that UV-induced skin tumorigenesis is a good model to get novel mechanistic insights and to test drugs.

Ultraviolet Radiation and Skin Cancers

Skin cancers are classified into two main categories as non-melanoma (NMSC) and melanoma (MSC) skin cancers. There are two types of NMSCs including cutaneous basal cell carcinoma (BCC) and cutaneous squamous cell carcinoma (SCC). NMSCs account for more than 95% of all skin cancers. The rest 5% of incidence belongs to melanoma which is the most fatal form of skin cancers (Boukamp, 2005).

The most common lesion emerging in skin after exposure to solar irradiation is actinic keratosis which considered as a precancerous lesion (Goldenberg and Perl, 2014). Fair skin, cumulative sun exposure, immunosuppression and age are the major factors which affect the formation of AK.

Basal cell carcinomas originate from basal keratinocytes in the deeper layer of epidermis and account for 80% of NMSCs (Kasper et al., 2012). This type of cutaneous cancer is locally invasive but normally non-metastatic. Because of its pale color and lack of symptoms, BCC is misdiagnosed in most of the cases. Although excisional surgery is the main therapy for BCC, radiation therapy could a suitable alternative treatment in inoperable cases. In recent years, new therapeutic methods as topical treatments have been developed for BCC (Table 4)(Berking et al., 2014).

Cutaneous squamous cell carcinomas form 15% of NMSCs. Unlike BCC, SCC may metastasize to regions which are distant from the origin. Despite the wide range of therapies including excision, radiation therapy, cryosurgery, Mohs micrographic, electrodesiccation and curettage for SCC, fluorouracil accounts for the main current therapy for this disorder.

Meanwhile, the most fatal form of cutaneous cancers with 80% mortality is sporadic cutaneous melanoma which is derived from melanocytes. Melanoma harbors the potential of metastasis like SCC. Surgery and radiotherapy along with adjuvant therapy and chemotherapy are the main therapies for this type of cutaneous carcinomas.

Epidemiological studies reveal that intermittent exposure to sunlight is the major cause of BCC and melanoma whereas SCC appears as the result of chronic exposure.

As a mixture of electromagnetic spectrums including infrared, visible light and ultraviolet rays, sunlight is the best known cause of skin cancer. Exposure to sunlight can be classified into acute, intermittent and chronic exposure depending on daily activities and time of

exposure. Meanwhile, phototype is also an important predisposing factor to skin cancers. UV radiation is classified into three categories according to its wavelengths: UVA, UVB and UVC. Approximately 100% of UVC and 95% of UVB are absorbed by the ozone layer and do not reach the earth. Shorter wavelengths are more powerful, thus more harmful to the skin. Due to its shorter wavelength, UVB which accounts for less than 1% of the total solar radiation has more dangerous biological effects compared to UVA. It was once thought that skin cancers are caused only by exposure to UVB but several recent studies have shown the carcinogenic effects of UVA as well.

Generally UVA radiation penetrates deeply in the skin and involves in the generation of reactive oxygen species (ROS) which may cause damage to DNA, proteins, lipids and saccharides. Unlike UVA radiation, UVB has less penetrance but more genotoxic effects. UVB is absorbed by DNA especially aromatic rings of DNA bases. It has also been demonstrated that UVB can cause indirect damage through induction of ROS generation. The direct damage results in formation of DNA adducts such as cyclobutane pyrimidine dimers and pyrimidine pyrimidone dimers. Pyrimidine pyrimidone lesions are frequently repaired more efficiently and faster than cyclobutane dimers. Failure to repair UV-induced DNA damages results in specific types of mutation (i.e. C to T and CC to TT) named UV signature a marker of post irradiation mutation found in UV-induced precanceroses. In addition to affecting protein function, if these lesions occur in the promoter sequences, they strongly inhibit the binding of transcription factors (Tommasi et al., 1996).

Besides the direct damage to DNA, UVB deregulates different cell processes or pathways. In fact, UVB radiation disrupts redox homeostasis, by induction of ROS generation and/ or disabling the antioxidant systems. UVB could also lead to photoisomerisation of urocanic acid, induction of ornithine decarboxylase activity, cell cycle arrest, immune suppression, and impairment of DNA and RNA synthesis in the skin (Svobodova et al., 2006).

UV Irradiation and mtDNA Mutagenesis in Skin Cancers

Normally, in non-transformed cells, mitochondria play a crucial role in different processes such as energy production, biosynthesis, regulation of intracellular calcium signaling and apoptosis. In normal physiological conditions, mitochondria also produce reactive oxygen species (ROS) through three complexes of the respiratory chain (i.e. CI, CIII, and CIV). ROS result in dual central effects on cellular signaling pathways. On the one hand, increase in ROS

concentrations leads to cytotoxicity through oxidation of proteins, lipids, RNA and nuclear/mitochondrial DNA. On the other hand, ROS can also act as second-messengers which mediate the cell response to different stressors.

Alterations in quality or quantity of mitochondrial DNA have been reported as a possible contributor to neoplastic development. Unlike nucleus which has efficient DNA repair systems for removal of UV damages, mitochondria lacks this capacity (Mason et al., 2003; Ray et al., 2000). In fact, DNA repair systems in mitochondria are 10-17 times weaker than those of the nucleus leading to maintenance of the mutations for a long period in the mitochondrial DNA (Ames et al., 1993; Pesole et al., 1999). For this reason, mtDNA can be used as a first-rate biomarker of UV-induced DNA damage in early detection of skin cancers (Berneburg and Krutmann, 1998; Berneburg et al., 2006). mtDNA mutations have been observed in skin peritumoral (AK) and tumoral cells (SCC) (Birch-Machin et al, 1998; Ray et al, 2000). Study of sun-exposed skin revealed a 260 mtDNA tandem duplication in the regulatory site of mitochondrial DNA (D-loop) (Krishnan and Birch-machin, 2006; Krishnan et al., 2004).

In addition, two common mtDNA deletions including a 4,977 bp and a 3895 bp deletion have been reported in sun exposed human skin (Krishnan and Birch-machin, 2006; Krishnan et al., 2004). These common mtDNA deletions which remove the region encoding ND5, ATPase8, ATPase6, COXIII, ND3, ND4, ND4L and 6tRNA result in mitochondrial dysfunction. Krishnan and Birch-Machin (Krishnan and Birch-Machin, 2006) found a significant frequency of common mtDNA deletions and tandem duplication in chronically UV-exposed skin compared with acutely-exposed skin. While these mutations can serve as UV biomarkers (Krishnan and Birch-machin, 2006), their role in carcinogenesis remain to be clarified.

Table 1. Detected mitochondrial DNA mutations in several types of human cancers.

Cancer type	mtDNA mutation sites	Incidence (in patients)	Reference
Breast cancer	D-loop, 16S rRNA, ND2, and ATPase 6	74%	(Tan et al., 2002)
Colorectal	D-loop region	23%	(Alonso et al., 1997)

cancer			
Ovarian cancer	D-loop, 12S rRNA, 16S rRNA and cytochrome b	60%	(Liu et al., 2001)
Gastric carcinoma	D-loop region	48%	(Wu et al., 2005)
Hepatocellular cancer	D-loop region	68%	(Nomoto et al., 2002a, 2002b)
Prostate cancer	cytochrome oxidase subunit I (COX I)	11–12%	(Petros et al., 2005)
Lung cancer	D-loop region	20-61%	(Sanchez-Cespedes et al., 2001; Suzuki et al., 2003)
Renal cell carcinoma	D-loop region	28%	(Nagy et al., 2002)
Brain tumors	D-loop region	36%	(Montanini et al., 2005)

Table 2. List of mtDNA mutations in various types of cancers.

Cancer	mtDNA regional mutations	Reference
Breast cancer	ND4,ND5	(Sanchez-Cespedes et al., 2001)
Colorectal cancer	COX1, COX2, ND1, Cyt b, ND5, ND4L, COX3	(Habano et al., 1999; Polyak et al., 1998)
Ovarian cancer	Cyt b	(Liu et al., 2001)

Head and neck	ND4	(Fliss et al., 2000)
Bladder	Cyt b, ND3	(Fliss et al., 2000)
Prostate cancer	COX1, ND1, ND5	(Jerónimo et al., 2001)
Pancreas	COX1, COX2, ND1, ND2, Cyt b, ND6, ND3, COX3, ATP6	(Jones et al., 2001)
Thyroid	COX2, ND2, ND1, Cyt b, ND6, ND5, ND4, ND4L, ND3, COX3, ATP6	(Abu-Amero et al., 2005; Máximo et al., 2002)

UVB Irradiation and Energy Metabolism

UV irradiation in addition to induced damages in mtDNA and altered cellular energy metabolism could lead to mutations in oncogenes and tumor suppressors, thus exerting effects on cellular metabolism. Loss of P53 and PTEN as well as inactivation of hedgehog pathway or activation of BRAF, RAS and PI3K/AKT/mTOR have all been demonstrated to contribute in skin carcinogenesis, and potentially via altering cellular energy metabolism. For example, loss of P53 modulates cellular energy metabolism and also provides energy sources during starvation by promoting some pathways such as fatty acid oxidation and autophagy (Lee et al., 2014). P53 as a redox activated transcription factor regulates also ROS production through induction of tumor protein P53-induced nuclear protein 1 (TP53INP1), glutaminase 2 (GLS2), manganese superoxide dismutase (MnSOD)(reviewed by Lee et al., 2014b).

Metabolic alteration in BCC

Among different mutational causes of BCC, mutations in the hedgehog pathway, TP53 and RAS genes have been demonstrated in respectively 70-90% (Geeraert et al., 2013; Nitzki et al., 2012; Wang et al., 2013), 40-56% (Kim et al., 2002; Nitzki et al., 2012) and 30% (Alberts and Hess, 2014) of sporadic cases of cutaneous BCC. Based on a growing body of evidence the mutation of these genes could alter cellular energy metabolism.

Mutations in the hedgehog (Hh) pathway, including inactivating mutations in tumor suppressor gene PTCH and activating mutations of SMO have been reported in 70-90% and 10% of BCC cases, respectively (Geeraert et al., 2013; Nitzki et al., 2012; Wang et al., 2013).

Mutations in PTCH remove its inhibitory effect on SMO, resulting in translocation of SMO to the cell membrane. SMO then activates the final arbiter of Hh signaling, the Gli family of transcription factors. Finally activated Gli accumulates in the nucleus and controls the transcription of hedgehog target genes (Ciavardelli et al., 2014; Maiuri et al., 2007).

There is now growing evidence that activation of Hh signaling pathway is associated with altered energy metabolism. For instance, it has been shown that accumulation of Gli promotes Hif-1 α expression (Chen et al., 2012), which could in turn, switch metabolism towards aerobic glycolysis.

In 2012, Teperino et al (Teperino et al., 2014) have been shown that the hedgehog pathway could rewire the metabolism by mediating noncanonical cilium-dependent Smo-Ca²⁺-Ampk signaling. They have demonstrated that using smoothed agonist (SAG) as SMO activator induces a Warburg-like metabolic reprogramming. Increase of glycolysis level occurs by modulating of Pdh1, AMP-activated protein kinase (Ampk), and pyruvate kinase M1/M2 (Pkm2) (Teperino et al., 2014).

There is now overwhelming evidence that P53 could influence cellular energy metabolism by enhancing of OXPHOS and inhibition of glycolysis through several mechanisms. Numerous studies have been conducted in order to illustrate the importance of P53 functions in promotion of OXPHOS. P53 can localize also in mitochondria, where it can interact with the Bcl-2 family of proteins and VDAC (Ferecatu et al., 2009; Gottlieb and Vousden, 2010). The role of P53 in maintenance of mtDNA copy number and mitochondrial mass has also been demonstrated in several studies (Kulawiec et al., 2009; Lebedeva et al., 2009).

P53 also contributes to mitochondrial metabolism through transcriptional activation of some proteins, like synthesis of cytochrome c oxidase 2 (SCO2) (Matoba et al., 2006), subunit I of cytochrome c oxidase (Okamura et al., 1999), and p52R2, a subunit of ribonucleotide reductase (Bourdon et al., 2007). P53 also affects OXPHOS via posttranscriptional regulation of the COXII subunit by P53 (Zhou et al., 2003).

The inhibitory function of P53 on glycolysis has been ascribed to its ability to down-regulate the transcriptional expression of several glucose transporters such as GLUT1 and GLUT4 (Schwartzberg-bar-yoseph et al., 2004). P53 has been also shown to be capable to reduce GLUT3 expression through the inhibition of IKK (Kawauchi et al., 2008). The P53-mediated ubiquitination and inactivation of phosphoglycerate mutase (PGM) as an important glycolytic enzyme (Gottlieb and Vousden, 2010; Kondoh et al., 2005) leads to reduced glycolytic rate. The ability of P53 to regulate the expression of TIGAR, a protein that functions as a fructose

2,6 bisphosphatase (FBPase) to lower fructose 2,6-bisphosphate levels and glycolytic rate (Bensaad et al., 2006; Gottlieb and Vousden, 2010; Li and Jogl, 2009), is another mechanism by which P53 down-regulates glycolysis.

Moreover, mutations in RAS genes have been also reported in various cancers. Ras genes encode four homologous proteins; Harvey (Ha), N-ras, Kristen (Ki) and R-ras that encodes membrane-associated GTPases. HRAS and KRAS are the more important RAS mutations in BCC. In 2013 Zheng et al. have demonstrated that HRAS mutations result in glucose uptake and increased glycolytic metabolism through increased expression of glycolytic enzymes including PGK1, PKM1, LDHA, and PDK1. This study has also demonstrated a reduced TCA cycle flux from glucose via the decrease of PDH and mitochondrial complex I activity (Zheng et al., 2013).

In 2013, Son et al. (Son et al., 2013) have demonstrated that oncogenic KRAS mutations induce glycolysis as an intermediate pathway to promote the production of nucleotides through the non-oxidative arm of the pentose phosphate pathway (PPP). By measurement of NADPH produced by the oxidative arm of the PPP to maintain redox homeostasis they have shown that KRAS activates only the non-oxidative arm of the PPP (Son et al., 2013). Over expression of GLU1 in consequence of KRAS activation could increase glycolysis (Sasaki et al., 2012; Yun et al., 2009). It has been also shown that activation of KRAS could raise the glycolytic metabolism by upregulation of glutamine–fructose-6-phosphate transaminase1 (Gfpt1), ribose 5-phosphate isomerase A (Rpia) and ribulose-5-phosphate-3-epimerase (Rpe)(Martz, 2012).

Metabolic alteration in SCC

Mutations in the CDKN2A, HRAS, KNSTRN, NOTCH1, NOTCH2, FGFR3 and Fas genes are predisposing factors for SCC. Among them CDK2A, P53, and HRAS mutations have been identified, respectively, in 76% (Brown et al., 2004), 30-50% (Kubo et al., 1994; Ping et al., 2001), 3-30% (Oberholzer et al., 2012; Uribe and Gonzalez, 2011) of SCC.

CDKN2A encodes p16INK4a and p14ARF (Brown et al., 2004). According to recent investigations, deficiency in p16INK4a leads to phosphorylation of PKA regulatory subunits which subsequently activates the PKA-CREB-PGC1 α pathway, in turn would stimulate the expression of genes involved in gluconeogenesis, fatty acid oxidation, tricarboxylic acid (TCA) cycle flux, and mitochondrial oxidative phosphorylation (reviewed by Potthoff et al.,

2011). P16INK4a positively regulates cyclin D1-CDK4, which inhibits PGC-1 α and suppresses the glyconeogenesis.

Metabolic alteration in melanoma

According to the literature activating mutations in *NRAS* or *BRAF* proto-oncogenes are found, respectively, in ~13–25% (van 't Veer et al., 1989; Ball et al., 1994; Curtin et al., 2005) and ~50% (Davies et al., 2002; Maldonado et al., 2003; COSMIC) of cutaneous melanomas. Mutations in other genes such as PTEN (16%), ERK1/2 (8%), KIT (2-6%), CTNNB1 (2-3%), GNA11 (2%) and GNAQ (1%) are also reported in melanoma (<http://www.mycancergenome.org/content/disease/melanoma/>, 2014).

BRAF is mutated in early stage melanoma. It phosphorylates MEK1/2 which in turn phosphorylates and activates the MAPK ERK1 and ERK2 (Haq et al., 2013). The activation of oncogenic signaling pathways, such as the MAPK/ERK can promote HIF-1 α expression at the transcriptional and translational levels to increase the rate of glycolysis even in normoxia (Huang et al., 2014). Mutation in *BRAF* has been shown to be associated with increased glucose uptake and glycolysis which is mediated by up regulation of GLUT1 (Yun et al., 2009). Kluza et al. (Kluza et al., 2012) have shown an over expression of HIF1 α in melanoma cells which regulate the mitochondrial respiration. They have demonstrated that inhibition of the HIF-1 α /PDK3 axis by DCA restores mitochondrial respiration in melanoma cells. *BRAF* mutations in melanoma suppresses oxidative metabolism through inhibition of microphthalmia-associated transcription factor (MITF) and peroxisome proliferator-activated receptor γ , coactivator 1 α (PGC-1 α), which are master regulators of mitogenesis (Corzaorozas et al., 2013; Haq et al., 2013).

Over 95% of melanoma harboring *NRAS* activating mutations have an activated PI3K or MAPK pathway (Goel et al., 2006; Posch et al., 2013; Saldanha et al., 2006). Indeed, it has been shown that activation of the PI3K /mTOR/ AKT pathway in highly proliferative and malignant cells results in an increased glucose uptake and induction of the Warburg effect. Many studies have demonstrated that the PI3K/AKT/mTOR and RAS/RAF/MEK pathways are the major oncogenic pathways in human tumors (Ersahin et al., 2015). The AKT/mTOR/PI3K pathway regulates the expression of GLUT1, glucose-6-phosphatase (G6Pase), 6-phosphofructo-2-kinase/fructose-2,6-biphosphatase 2 (PFKFB2)(Bhatt et al.,

2012), peroxisome proliferator-activated receptor gamma, coactivator 1 alpha (PGC-1 α), phosphoenolpyruvate carboxykinase 2 (PEPCK), TIGAR and MnSOD (Ersahin et al., 2015). The activation of oncogenic signaling pathways, such as the PI3K/Akt, MAPK/ERK can promote HIF-1 α expression at the transcriptional and translational levels to increase the rate of glycolysis even in normoxia (Huang et al., 2014).

Loss of Phosphate and tensin homolog (PTEN) as a tumor suppressor has been reported in 19% of cutaneous melanomas (Goel et al., 2006). On the one hand, PTEN enhances oxidative phosphorylation and inhibits glycolysis (Ortega-molina and Serrano, 2013). Ortega-Molina and Serrano have been shown that Pten^{tg} MEFs present higher level of PGC1 α with an anti-Warburg effect (Ortega-molina and Serrano, 2013). On the other hand PTEN down regulates glycolysis by decreasing PFKFB stability which limits the Warburg effect in cells (Ortega-molina and Serrano, 2013). Loss of PTEN modulates also energy metabolism through affecting the PI3K/AKT pathway. Indeed, PTEN is negative regulator of AKT which, in turn, enhances glycolytic metabolism (Goel et al., 2006).

It appears that targeting the cellular metabolism could play an important role in preventing drug resistance and improving cellular responses to cancer treatments. For instance, the increase of lactate dehydrogenase A (LDHA) expression has been linked to elesclomol resistance in melanoma (Kluza et al., 2012). For the glutaminolysis pathway, activation of mTORC1 contributes to cisplatin resistance (Zhao et al., 2013). For this reason combination therapy targeting additionally cancer metabolism would theoretically improve efficacy in cancer therapy. Following this reasoning, Kluza et al. have demonstrated that combination of Dichloroacetate (DCA), an inhibitor of the HIF-1 α /PDK3 axis, with pro-oxidant drugs such as elesclomol restore sensitivity of malignant cells in melanoma (Kluza et al., 2012).

Metabolic profile in precancerous and developed forms of skin cancers

Data about the effect of UV on skin energy metabolism in different skin cancer types are scarce. In order to understand the metabolic change during carcinogenesis in different skin cancer, we have analyzed the Oncomine microarray database comparing normal skin, actinic keratosis, cutaneous squamous cell carcinomas, basal cell carcinoma and melanoma (Table 3). A significant increase in genes implicated in the glycolytic pathway during carcinogenesis is clearly demonstrated (apart from MSC). On the contrary, the mitochondria, oxidative

phosphorylation machinery, fatty acid beta oxidation and pentose phosphate pathway showed a dramatic reduction.

in ERK1 and ERK2 have been reported in approximately 8% of melanomas (Nikolaev et al., 2011). Since ERK signaling positively regulates PDH flux through decrease of PDK4 expression, any dysfunction in ERK could reduce OXPHOS (Grassian et al., 2011). Activation of ERK1/2 reduces NADPH oxidase activity which thereby leads to increased ROS levels and malignant cell invasiveness (Jajoo et al., 2009).

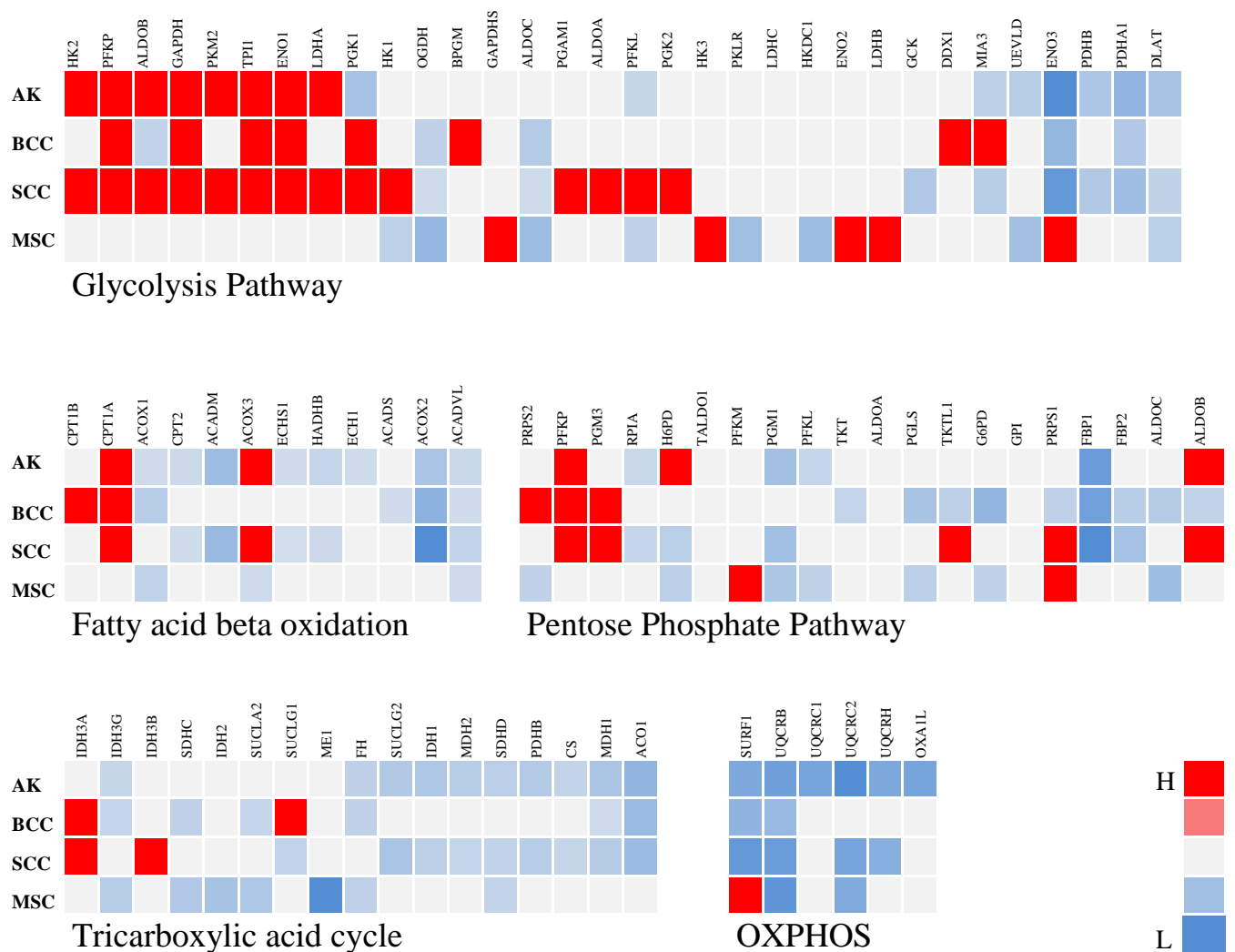
Altogether, all these data suggest an important role for energy metabolism in all type of skin cancers. Mechanistically, activation of oncogenes, increase of ROS production or inactivation of tumor suppressors could all rewire energy metabolism towards carcinogenesis.

The Link between Metabolism and Drug Resistance

Resistance to chemotherapy and molecularly targeted therapies is considered as the main challenge in cancer therapy. The metabolism in cancer cells unlike to normal cells rely mainly on glycolysis. In addition to glycolysis, the malignant cells have other particular metabolic characteristics such as increased fatty acid synthesis and increased level of glutamine metabolism.

A growing body of evidence on drug resistance indicates that dysregulation of Warburg-like glucose metabolism, fatty acid synthesis and glutaminolysis reduce drug efficacy in cancer.

Table 3. Microarray comparison of precancerous and major types of skin cancer vs normal skin (<https://www.oncomine.org>).



These preliminary data suggest that metabolism remodeling occur during skin carcinogenesis.

Treatments associated with skin cancer

Current options for treatment of skin cancer are:

- 1) **Excisional surgery** is the most common therapy for skin cancers. To remove the tumor, the surgical margins selected are usually from 4 mm to 10 mm, depending on the diameter of the tumor and its level of differentiation.
- 2) **Curettage and electrodesiccation** is used in general for small (<1 cm), well-defined, and well-differentiated tumors. It is not recommend for large tumors.

- 3) **Mohs surgery** is applied for skin tumors with a size larger than 2 cm with a high cure rate.
- 4) **Radiation therapy** is another form of treatment using ionizing radiation for killing the cancer cells by damaging their DNA directly or indirectly. In general, if the cell recognizes a high rate of damage in its DNA, activates the death programs instead of inducing their repair mechanism. Radiotherapy is an alternative therapy for tumors when surgery is not suitable or possible. Radiation therapy is an efficient method and can be combined with other type of therapies (such as Chemotherapy, immunotherapy, photodynamic therapy) for improving its efficiency.
- 5) **Cryosurgery** therapy is usually used for small and primary tumors in patients with medical conditions that preclude other types of surgery.
- 6) **Photodynamic therapy (PDT) and laser surgery** are also used as effective therapies to remove malignant cells.

Topical treatment

Since most therapies based on surgery result in scarring and esthetic disfigurement, topical medications or chemotherapies targeting damaged cells without impacting normal cells could be considered ideally as better methods of therapy. A large panel of topical drugs is available for different types of skin cancer for topical application or systemic administration. Most of these drugs target the immune system, cellular repair machinery and/or cellular growth and death (Table 4).

Table 4. List of common medications and their mechanism of action in skin cancers.

Drug	Official oncologic indications	Mechanism of action	cellular effect
5-fluorouracil (Adrucil, Efudex, Fluoroplex)	AK, BCC, SCC	DNA synthesis and RNA processing inhibition	cell growth arrest

Imiquimod (Aldara)	AK, BCC	immune response modifier	stimulates cytokine production
Vismodegib (Erivedge)	Advanced BCC	Hedgehog pathway inhibitor	embryo-fetal death
Diclofenac	AK, SCC invasiveness	upregulator of apoptosis	angiogenesis and cellular proliferation reduced
Ingenol mebutate	AK	swelling of mitochondria in dysplastic keratinocytes	cell death inducer by necrosis
Retinoids	AK, BCC	activator of the retinoic acid receptor	control of cell proliferation and differentiation
Resiquimod	AK	immune response modifier	Stimulator of immune responses
Piroxicam	AK	prostaglandins inhibitor	Increased apoptosis through cyclooxygenase
Dobesilate	AK, BCC, SCC	Inhibition of fibroblast growth factors	control of cell proliferation
Betulinic acid	AK	induction of mitochondrial pathway of apoptosis	cell death
Cetuximab (Erbitux)	SCC	inhibit dimerisation of EGFR	inhibit tumor growth and metastasis
Tretinoin	SCC, BCC	inhibitor of alpha, beta, and gamma retinoic acid receptors	control of cell proliferation, and differentiation
Aldesleukin (Proleukin)	Melanoma	stimulator of the immune system	induces lymphokine-activated killer (LAK) cell and natural killer

			(NK) cell activities
Dabrafenib			
(Tafinlar, vemurafenib, Sorafenib)	Melanoma	inhibitor of B-raf (BRAF)	anti-neoplastic activity
Dacarbazine			
(DTIC-Dome)	Melanoma	disruption of DNA function, cell cycle arrest, and apoptosis	Control of cell death
Intron A			
	Melanoma	binds to specific cell-surface receptors and mediate gene transcription and translation	regulation of cell proliferation and immune system
Ipilimumab			
(Yervoy)	Melanoma	blocks the CTLA-4 inhibitory signal	destroy the malignant cells
Keytruda			
	Melanoma	blocks of the immune response inhibitors	induces the cell proliferation and cytokine production
Peginterferon			
Alfa-2b	Melanoma,		
(Sylatron)	SCC,BCC	inhibits CYP1A2 and CYP2D6 activity	regulation of cell proliferation and immune system
Mekinist			
(Trametinib, Cobimetinib, Binimetinib, Selumetinib)	Melanoma	inhibitor of mitogen-activated protein kinase kinase(MEK)	inhibition of cellular proliferation
Vemurafenib			
(Zelboraf)	Melanoma	BRAF inhibitor	Programmed cell death
Axitinib			
	Melanoma	Inhibition of VEGFR	inhibition of vascularisation

Oblimersen	Melanoma	suppresses expression of Bcl-2	inducing the apoptosis
-------------------	----------	--------------------------------	------------------------

Energy metabolism remodeling in cancer therapy

If at energy level glycolysis is less efficient than oxidative phosphorylation for malignant cells, tumor cells choose this pathway for energy supplying. Firstly, due to the high rate of cell proliferation in malignant cells, they need a huge amount of energy as quickly as possible and glycolysis delivers energy very rapidly. Secondly, oxidative phosphorylation for generating ATP needs a high level of oxygen and malignant cells are often faced with the problem of hypoxia so glycolysis is a better survival option. Third, malignant cells by generating lactic and bicarbonic acids as by-products of glycolysis acidify their environment, promoting invasiveness. Fourth, glycolysis can be considered as an intermediate pathway that could supply the needs of other pathways such as pentose phosphate, fatty acid synthase and amino acid synthesis.

Metabolic targets for cancer therapy

Cancer cells change their metabolism to adapt with their microenvironment. Metabolism flexibility has been accepted as a hallmark of cancer. Targeting metabolism could therefore be a suitable strategy. In fact, several drugs targeting metabolism are being actually used in the therapy of some cancers (Figure 1). If altered metabolism is confirmed to be essential in development of skin cancer, these drugs could potentially applicable in this setting. Some pathways including AKT/mTOR/PI3K, AMPK, ERK, P53 and P21, are frequently mutated in skin cancers. Alterations in these pathways have been shown to modulate energy metabolism. Several drugs, which are currently used or proposed for skin cancer therapy owing to targeting these pathways (Table 5) in order to prevent the metabolic alterations. Investigation on the mechanisms of action of these inhibitors and their effects on metabolism could result in developing novel cancer therapies.

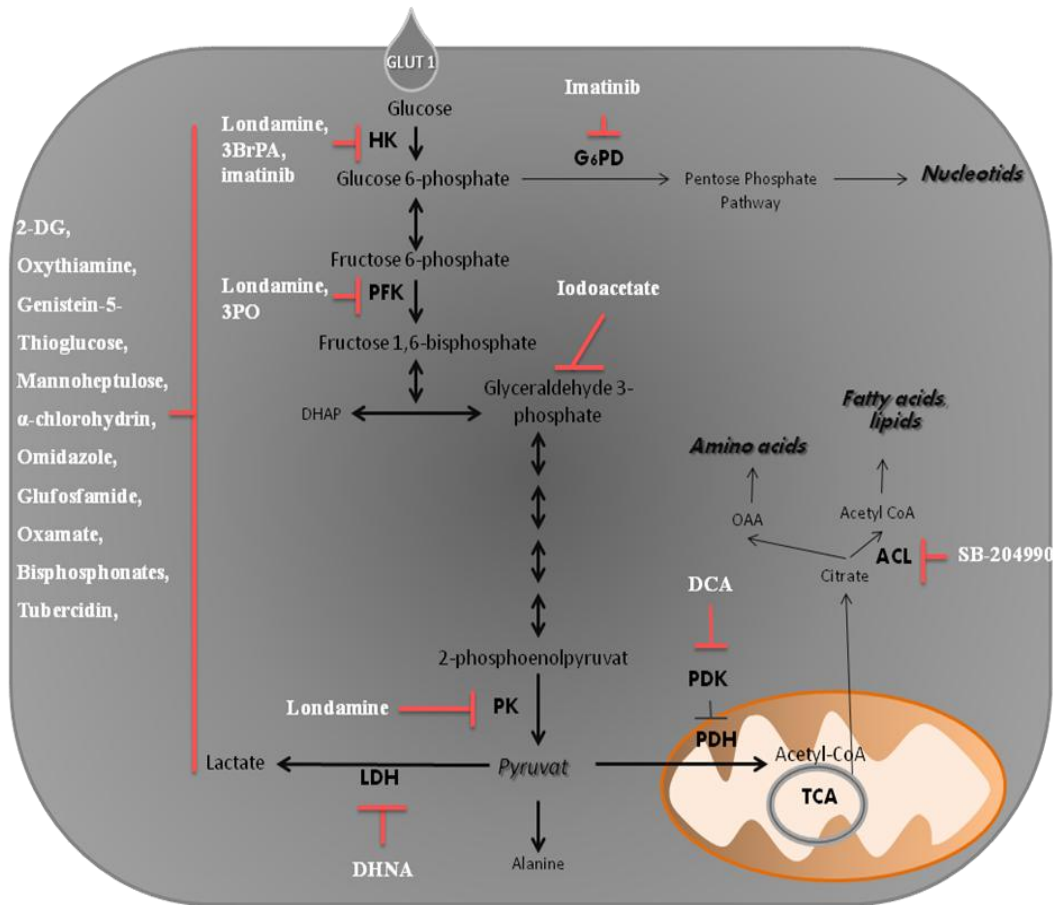


Fig.1. Potential metabolic inhibitors for skin cancer therapy.

Table 5. Potential pathways for skin cancer therapy in the future.

Drug	Potential pathways	Mechanism of action	Reference
CP-31398	P53 enhancer	restores the tumor suppressor functions	(Foster et al., 1999)
MK-2206	AKT inhibitor	induction of tumor cell apoptosis	(Hirai et al., 2010)
BEZ-235	PDK inhibitor, PI3K/mTOR inhibitor,	inhibitor of tumor cell growth	(Gong et al., 2011)
Dasatinib,	Tyrosine kinase	inhibits the growth-	(Crossman et al.,

Erlotinib,	inhibitor	promoting activities	2005)
Gefitinib			
MEK inhibitors			
Trametinib, Selumetinib, Binimetinib, PD-325901, Cobimetinib, CI-1040	ERK-1/2 inhibitor	Control of cell proliferation and apoptosis	(Zhao and Adjei, 2014)
HDACs inhibitors	inhibition of histone deacetylases	induction of apoptosis, DNA damage repair, cell cycle control, autophagy and senescence	(Rajendran et al., 2011; Ropero and Esteller, 2007)
CP-31398	P53 and P21 enhancer	Induction of apoptosis and inhibition of tumor proliferation	(Rao et al., 2009)
GSK-690693	pan-Akt inhibitor,	Induces growth inhibition and apoptosis	(Levy et al., 2009)
Tazarotene	mitochondrial caspase 9 enhancer	induction of apoptosis	(Wu et al., 2014)

Conclusion

Given the rising incidence of skin cancer across the world the effects of UV irradiation on energy metabolism deserve to be studied in more details. The efforts on this context could help us to understand the link between genetic modification and metabolism alteration. Energy metabolism shift in skin tumors can be envisaged as an adjunctive target for combined therapies but also for prognostic biomarkers applications. The metabolism profile of pre-cancer samples (i.e. AK) could be a diagnostic test to evaluate the risk of its tumoral transformation. Similarly, the metabolism profile of SCC and BCC could give an indication about their recurrence as well as their metastasis risks.

References

- Van 't Veer, L.J., Burgering, B.M., Versteeg, R., Boot, a J., Ruiter, D.J., Osanto, S., Schrier, P.I., and Bos, J.L. (1989). N-ras mutations in human cutaneous melanoma from sun-exposed body sites. *Mol. Cell. Biol.* *9*, 3114–3116.
- Abu-Amero, K.K., Alzahrani, A.S., Zou, M., and Shi, Y. (2005). High frequency of somatic mitochondrial DNA mutations in human thyroid carcinomas and complex I respiratory defect in thyroid cancer cell lines. *Oncogene* *24*, 1455–1460.
- Alberts, D., and Hess, L.M. (2014). *Fundamentals of Cancer Prevention* (Springer).
- Alonso, A., Martin, P., Albarran, C., Aquilera, B., Garcia, O., Guzman, A., Oliva, H., and Sancho, M. (1997). Detection of somatic mutations in the mitochondrial DNA control region of colorectal and gastric tumors by heteroduplex and single-strand conformation analysis. *Electrophoresis* *18*, 682–685.
- Ames, B.N., Shigenaga, M.K., and Hagen, T.M. (1993). Oxidants, antioxidants, and the degenerative diseases of aging. *Proc. Natl. Acad. Sci. U. S. A.* *90*, 7915–7922.
- Ball, N.J., Yohn, J.J., Morelli, J.G., Norris, D. a, Golitz, L.E., and Hoeffler, J.P. (1994). Ras mutations in human melanoma: a marker of malignant progression. *J. Invest. Dermatol.* *102*, 285–290.
- Bensaad, K., Tsuruta, A., Selak, M. a., Vidal, M.N.C., Nakano, K., Bartrons, R., Gottlieb, E., and Vousden, K.H. (2006). TIGAR, a P53-Inducible Regulator of Glycolysis and Apoptosis. *Cell* *126*, 107–120.
- Berneburg, M., and Krutmann, J. (1998). Mitochondrial DNA deletions in human skin reflect photo- rather than chronologic aging. *J. Invest. Dermatol.* *111*, 709–710.
- Berneburg, M., Kamenisch, Y., and Krutmann, J. (2006). Repair of mitochondrial DNA in aging and carcinogenesis. *Photochem. Photobiol. Sci.* *5*, 190–198.
- Bhatt, a. P., Jacobs, S.R., Freermerman, a. J., Makowski, L., Rathmell, J.C., Dittmer, D.P., and Damania, B. (2012). Dysregulation of fatty acid synthesis and glycolysis in non-Hodgkin lymphoma. *Proc. Natl. Acad. Sci.* *109*, 11818–11823.
- Bourdon, A., Minai, L., Serre, V., Jais, J.-P., Sarzi, E., Aubert, S., Chrétien, D., de Lonlay, P., Paquis-Flucklinger, V., Arakawa, H., et al. (2007). Mutation of RRM2B, encoding P53-controlled ribonucleotide reductase (P53R2), causes severe mitochondrial DNA depletion. *Nat. Genet.* *39*, 776–780.
- Brown, V.L., Harwood, ã.C.A., Crook, ã.T., Cronin, J.G., Kellsell, ã.D.P., and ã, C.M.P. (2004). p16 INK4a and p14 ARF Tumor Suppressor Genes Are Commonly Inactivated in Cutaneous Squamous Cell Carcinoma. 1284–1292.
- Chen, Y., Choi, S., Michelotti, G., Chan, I., Swiderska-Syn, M., Karaca, G., Xie, G., Moylan, C., Garibaldi, F., Premont, R., et al. (2012). Hedgehog Controls Hepatic Stellate Cell Fate by Regulating Metabolism. *Gastroenterology* *143*, 1319–1329.

- Ciavardelli, D., Bellomo, M., Crescimanno, C., and Vella, V. (2014). Type 3 Deiodinase: Role in Cancer Growth, Stemness, and Metabolism. *Front. Endocrinol. (Lausanne)*. 5, 1–7.
- Corazao-Rozas, P., Guerreschi, P., Jendoubi, M., André, F., Jonneaux, A., Scalbert, C., Garçon, G., Malet-Martino, M., Balayssac, S., Rocchi, S., et al. (2013). Mitochondrial oxidative stress is the Achilles's heel of melanoma cells resistant to Braf-mutant inhibitor. *Oncotarget* 4, 1986–1998.
- Crossman, L.C., O'Hare, T., Lange, T., Willis, S.G., Stoffregen, E.P., Corbin, a S., O'Brien, S.G., Heinrich, M.C., Druker, B.J., Middleton, P.G., et al. (2005). A single nucleotide polymorphism in the coding region of ABL and its effects on sensitivity to imatinib. *Leuk. Off. J. Leuk. Soc. Am. Leuk. Res. Fund, U.K* 19, 1859–1862.
- Curtin, J. a, Fridlyand, J., Kageshita, T., Patel, H.N., Busam, K.J., Kutzner, H., Cho, K.-H., Aiba, S., Bröcker, E.-B., LeBoit, P.E., et al. (2005). Distinct sets of genetic alterations in melanoma. *N. Engl. J. Med.* 353, 2135–2147.
- Davies, H., Bignell, G.R., Cox, C., Stephens, P., Edkins, S., Clegg, S., Teague, J., Woffendin, H., Garnett, M.J., Bottomley, W., et al. (2002). Mutations of the BRAF gene in human cancer. 949–954.
- Ersahin, T., Tuncbag, N., and Cetin-Atalay, R. (2015). The PI3K/AKT/mTOR interactive pathway. *Mol. BioSyst.*
- Ferecatu, I., Bergeaud, M., Rodríguez-Enfedaque, A., Le Floch, N., Oliver, L., Rincheval, V., Renaud, F., Vallette, F.M., Mignotte, B., and Vayssière, J.L. (2009). Mitochondrial localization of the low level P53 protein in proliferative cells. *Biochem. Biophys. Res. Commun.* 387, 772–777.
- Fliss, M.S., Usadel, H., Caballero, O.L., Wu, L., Buta, M.R., Eleff, S.M., Jen, J., and Sidransky, D. (2000). Facile detection of mitochondrial DNA mutations in tumors and bodily fluids. *Science* 287, 2017–2019.
- Foster, B. a, Coffey, H. a, Morin, M.J., and Rastinejad, F. (1999). Pharmacological rescue of mutant P53 conformation and function. *Science* 286, 2507–2510.
- Geeraert, P., Williams, J., and Brownell, I. (2013). Targeting the Hedgehog Pathway to Treat Basal Cell Carcinoma. *J. Drugs Dermatology* 10, 519.
- Goel, V.K., Lazar, A.J.F., Warneke, C.L., Redston, M.S., and Haluska, F.G. (2006). Examination of Mutations in BRAF , NRAS , and PTEN in Primary Cutaneous Melanoma. 126.
- Gong, H.C., Wang, S., Mayer, G., Chen, G., Leesman, G., Singh, S., and Beer, D.G. (2011). Signatures of Drug Sensitivity in Nonsmall Cell Lung Cancer. *Int. J. Proteomics* 2011, 1–13.
- Gottlieb, E., and Vousden, K.H. (2010). P53 Regulation of Metabolic Pathways. *Cold Spring Harb. Perspect. Biol.* 2, 1–11.

Grassian, A.R., Metallo, C.M., Coloff, J.L., Stephanopoulos, G., and Brugge, J.S. (2011). Erk regulation of pyruvate dehydrogenase flux through PDK4 modulates cell proliferation. *Genes Dev.* 25, 1716–1733.

Habano, W., Sugai, T., Yoshida, T., and Nakamura, S.I. (1999). Mitochondrial gene mutation, but not large-scale deletion, is a feature of colorectal carcinomas with mitochondrial microsatellite instability. *Int. J. Cancer* 83, 625–629.

Hanahan, D., and Weinberg, R. a (2011). Hallmarks of cancer: the next generation. *Cell* 144, 646–674.

Haq, R., Shoag, J., Andreu-Perez, P., Yokoyama, S., Edelman, H., Rowe, G.C., Frederick, D.T., Hurley, A.D., Nellore, A., Kung, A.L., et al. (2013). Oncogenic BRAF regulates oxidative metabolism via PGC1 α and MITF. *Cancer Cell* 23, 302–315.

Hirai, H., Sootome, H., Nakatsuru, Y., Miyama, K., Taguchi, S., Tsujioka, K., Ueno, Y., Hatch, H., Majumder, P.K., Pan, B.-S., et al. (2010). MK-2206, an allosteric Akt inhibitor, enhances antitumor efficacy by standard chemotherapeutic agents or molecular targeted drugs in vitro and in vivo. *Mol. Cancer Ther.* 9, 1956–1967.

<http://www.mycancergenome.org/content/disease/melanoma/> (2014). Molecular Profiling of Melanoma.

Huang, S., Kao, J., Wu, C., Wang, S., Lee, H., Liang, S., Chen, Y., and Shieh, J. (2014). Targeting Aerobic Glycolysis and HIF-1 α Expression Enhance Imiquimod-induced Apoptosis in Cancer Cells. *Oncotarget* 5, 1363–1381.

Jajoo, S., Mukherjea, D., Watabe, K., and Ramkumar, V. (2009). Adenosine A(3) receptor suppresses prostate cancer metastasis by inhibiting NADPH oxidase activity. *Neoplasia* 11, 1132–1145.

Jerónimo, C., Nomoto, S., Caballero, O.L., Usadel, H., Henrique, R., Varzim, G., Oliveira, J., Lopes, C., Fliss, M.S., and Sidransky, D. (2001). Mitochondrial mutations in early stage prostate cancer and bodily fluids. *Oncogene* 20, 5195–5198.

Jones, J.B., Song, J.J., Hempen, P.M., Parmigiani, G., Hruban, R.H., and Kern, S.E. (2001). Advances in Brief Detection of Mitochondrial DNA Mutations in Pancreatic Cancer Offers a “Mass”-ive Advantage over Detection of Nuclear DNA Mutations 1. *Pathology* 1299–1304.

Kawauchi, K., Araki, K., Tobiume, K., and Tanaka, N. (2008). P53 regulates glucose metabolism through an IKK-NF-kappaB pathway and inhibits cell transformation. *Nat. Cell Biol.* 10, 611–618.

Kim, M.Y., Park, H.J., Baek, S.C., Byun, D.G., and Houh, D. (2002). Mutations of the P53 and PTCH gene in basal cell carcinomas: UV mutation signature and strand bias. *J. Dermatol. Sci.* 29, 1–9.

Kluza, J., Corazao-Rozas, P., Touil, Y., Jendoubi, M., Maire, C., Guerreschi, P., Jonneaux, A., Ballot, C., Balayssac, S., Valable, S., et al. (2012). Inactivation of the HIF-1 α /PDK3

signaling axis drives melanoma toward mitochondrial oxidative metabolism and potentiates the therapeutic activity of pro-oxidants. *Cancer Res.* 72, 5035–5047.

Kondoh, H., Lleonart, M.E., Gil, J., Wang, J., Degan, P., Peters, G., Martinez, D., Carnero, A., and Beach, D. (2005). Glycolytic Enzymes Can Modulate Cellular Life Span Glycolytic Enzymes Can Modulate Cellular Life Span. 177–185.

Krishnan, K.J., and Birch-machin, M.A. (2006). The Incidence of Both Tandem Duplications and the Common Deletion in mtDNA from Three Distinct Categories of Sun-Exposed Human Skin and in Prolonged Culture of Fibroblasts. 126.

Krishnan, K.J., Harbottle, A., and Birch-machin, M.A. (2004). The Use of a 3895 bp Mitochondrial DNA Deletion as a Marker for Sunlight Exposure in Human Skin. 1020–1024.

Kubo, Y., Urano, Y., Yoshimoto, K., Iwahana, H., Fukuhara, K., Arase, S., and Itakura, M. (1994). P53 gene mutations in human skin cancers and precancerous lesions: comparison with immunohistochemical analysis. 440–444.

Kulawiec, M., Ayyasamy, V., and Singh, K. (2009). P53 regulates mtDNA copy number and mitochekpoint pathway. *J Carcinog.* 8.

Lebedeva, M. a., Eaton, J.S., and Shadel, G.S. (2009). Loss of P53 causes mitochondrial DNA depletion and altered mitochondrial reactive oxygen species homeostasis. *Biochim. Biophys. Acta - Bioenerg.* 1787, 328–334.

Lee, P., Vousden, K.H., and Cheung, E.C. (2014). TIGAR, TIGAR, burning bright. *Cancer Metab.* 2, 1.

Levy, D., Kahana, J., and Kumar, R. (2009). AKT inhibitor, GSK690693, induces growth inhibition and apoptosis in acute lymphoblastic leukemia cell lines. *Blood* 113, 1723–1729.

Li, H., and Jogl, G. (2009). Structural and biochemical studies of TIGAR (TP53-induced glycolysis and apoptosis regulator). *J. Biol. Chem.* 284, 1748–1754.

Liu, V.W., Shi, H.H., Cheung, a N., Chiu, P.M., Leung, T.W., Nagley, P., Wong, L.C., and Ngan, H.Y. (2001). High incidence of somatic mitochondrial DNA mutations in human ovarian carcinomas. *Cancer Res.* 61, 5998–6001.

Maiuri, M.C., Zalckvar, E., Kimchi, A., and Kroemer, G. (2007). Self-eating and self-killing: crosstalk between autophagy and apoptosis. *Nat. Rev. Mol. Cell Biol.* 8, 741–752.

Maldonado, J.L., Fridlyand, J., Patel, H., Jain, A.N., Busam, K., Kageshita, T., Ono, T., Albertson, D.G., Pinkel, D., and Bastian, B.C. (2003). Determinants of BRAF mutations in primary melanomas. *J. Natl. Cancer Inst.* 95, 1878–1890.

Martz, L. (2012). K-Ras in cancer metabolism. *Sci. Exch.* 5, 1–2.

Mason, P.A., Matheson, E.C., Hall, A.G., and Lightowlers, R.N. (2003). Mismatch repair activity in mammalian mitochondria. *Nucleic Acids Res.* 31, 1052–1058.

- Matoba, S., Kang, J., Patino, W., Wragg, A., Boehm, M., Gavrilova, O., Hurley, P., Bunz, F., and Hwang, P. (2006). P53 regulates mitochondrial respiration. *Science* (80-.). *312*, 1650–1653.
- Máximo, V., Soares, P., Lima, J., Cameselle-Teijeiro, J., and Sobrinho-Simões, M. (2002). Mitochondrial DNA somatic mutations (point mutations and large deletions) and mitochondrial DNA variants in human thyroid pathology: a study with emphasis on Hürthle cell tumors. *Am. J. Pathol.* *160*, 1857–1865.
- Montanini, L., Regna-Gladin, C., Eoli, M., Albarosa, R., Carrara, F., Zeviani, M., Bruzzone, M.G., Broggi, G., Boiardi, A., and Finocchiaro, G. (2005). Instability of mitochondrial DNA and MRI and clinical correlations in malignant gliomas. *J. Neurooncol.* *74*, 87–89.
- Nagy, A., Wilhelm, M., Sükösd, F., Ljungberg, B., and Kovacs, G. (2002). Somatic mitochondrial DNA mutations in human chromophobe renal cell carcinomas. *Genes. Chromosomes Cancer* *35*, 256–260.
- Nikolaev, S.I., Rimoldi, D., Iseli, C., Valsesia, A., Robyr, D., Gehrig, C., Harshman, K., Guipponi, M., Bukach, O., Zoete, V., et al. (2011). Exome sequencing identifies recurrent somatic MAP2K1 and MAP2K2 mutations in melanoma. *Nat. Genet.* *44*, 133–139.
- Nitzki, F., Becker, M., Frommhold, A., Schulz-Schaeffer, W., and Hahn, H. (2012). Patched Knockout Mouse Models of Basal Cell Carcinoma. *J. Skin Cancer* *2012*, 1–11.
- Nomoto, S., Sanchez-Cespedes, M., and Sidransky, D. (2002a). Identification of mtDNA mutations in human cancer. *Methods Mol Biol* *197*, 107–117.
- Nomoto, S., Yamashita, K., Koshikawa, K., Nakao, A., and Sidransky, D. (2002b). Mitochondrial D-loop mutations as clonal markers in multicentric hepatocellular carcinoma and plasma. *Clin. Cancer Res.* *8*, 481–487.
- Oberholzer, P., Kee, D., Dziunycz, P., Sucker, A., Kamsukom, N., Jones, R., Roden, C., Chalk, C., Ardlie, K., Palescandolo, E., et al. (2012). RAS Mutations Are Associated With the Development of Cutaneous Squamous Cell Tumors in Patients Treated With. *30*.
- Okamura, S., Ng, C., Koyama, K., Takei, Y., Arakawa, H., Monden, M., and Nakamura, Y. (1999). Identification of seven genes regulated by wild-type P53 in a colon cancer cell line carrying a well-controlled wild-type P53 expression system. *Oncol Res.* *11*, 281–285.
- Ortega-molina, A., and Serrano, M. (2013). PTEN in cancer , metabolism , and aging. *Trends Endocrinol. Metab.* *24*, 184–189.
- Pelicano, H., Martin, D.S., Xu, R.-H., and Huang, P. (2006). Glycolysis inhibition for anticancer treatment. *Oncogene* *25*, 4633–4646.
- Pesole, G., Gissi, C., De Chirico, A., and Saccone, C. (1999). Nucleotide substitution rate of mammalian mitochondrial genomes. *J. Mol. Evol.* *48*, 427–434.

Petros, J. a, Baumann, A.K., Ruiz-Pesini, E., Amin, M.B., Sun, C.Q., Hall, J., Lim, S., Issa, M.M., Flanders, W.D., Hosseini, S.H., et al. (2005). mtDNA mutations increase tumorigenicity in prostate cancer. *Proc. Natl. Acad. Sci. U. S. A.* *102*, 719–724.

Ping, X., Ratner, D., Zhang, H., Wu, X., Zhang, M., Chen, F., Silvers, D.N., Peacocke, M., and Tsou, H.C. (2001). PTCH Mutations in Squamous Cell Carcinoma of the Skin. 614–616.

Polyak, K., Li, Y., Zhu, H., Lengauer, C., Willson, J.K., Markowitz, S.D., Trush, M.A., Kinzler, K.W., and Vogelstein, B. (1998). Somatic mutations of the mitochondrial genome in human colorectal tumours. *Nat. Genet.* *20*, 291–293.

Posch, C., Moslehi, H., Feeney, L., Green, G., Ebaee, A., Feichtenschlager, V., and Al., E. (2013). mTORC1 Regulates Growth Factor-Induced Nucleotide Synthesis. *Cancer Discov.* *3*, 374–374.

Potthoff, M.J., Boney-Montoya, J., Choi, M., He, T., Sunny, N.E., Satapati, S., Suino-Powell, K., Xu, H.E., Gerard, R.D., Finck, B.N., et al. (2011). FGF15/19 regulates hepatic glucose metabolism by inhibiting the CREB-PGC-1 α pathway. *Cell Metab.* *13*, 729–738.

Rajendran, P., Williams, D.E., Ho, E., and Dashwood, R.H. (2011). Metabolism as a key to histone deacetylase inhibition. *Crit. Rev. Biochem. Mol. Biol.* *46*, 181–199.

Rao, C. V., Steele, V.E., Swamy, M. V., Patlolla, J.M.R., Guruswamy, S., and Kopelovic, L. (2009). Inhibition of AOM-Induced Colorectal Cancer by CP-31398, a TP53 modulator, Alone or in Combination with Low Doses of Celecoxib in Male F344 Rats. *69*, 8175–8182.

Ray, a J., Turner, R., Nikaido, O., Rees, J.L., and Birch-Machin, M. a (2000). The spectrum of mitochondrial DNA deletions is a ubiquitous marker of ultraviolet radiation exposure in human skin. *J. Invest. Dermatol.* *115*, 674–679.

Ropero, S., and Esteller, M. (2007). The role of histone deacetylases (HDACs) in human cancer. *Mol. Oncol.* *1*, 19–25.

Rowe, I., Chiaravalli, M., Mannella, V., Ulisse, V., Quilici, G., Pema, M., Song, X.W., Xu, H., Mari, S., Qian, F., et al. (2013). Defective glucose metabolism in polycystic kidney disease identifies a new therapeutic strategy. *Nat. Med.* *19*, 488–493.

Saldanha, G., Potter, L., Daforno, P., and Pringle, J.H. (2006). Human Cancer Biology Cutaneous Melanoma Subtypes Show Different BRAF and NRAS Mutation Frequencies. *12*, 4499–4506.

Sanchez-Cespedes, M., Parrella, P., Nomoto, S., Cohen, D., Xiao, Y., Esteller, M., Jeronimo, C., Jordan, R.C.K., Nicol, T., Koch, W.M., et al. (2001). Identification of a mononucleotide repeat as a major target for mitochondrial DNA alterations in human tumors. *Cancer Res.* *61*, 7015–7019.

Sasaki, H., Shitara, M., Yokota, K., Hikosaka, Y., Moriyama, S., Yano, M., and Fujii, Y. (2012). Overexpression of GLUT1 correlates with Kras mutations in lung carcinomas. *Mol. Med. Rep.* *5*, 599–602.

Schwartzberg-bar-yoseph, F., Armoni, M., and Karnieli, E. (2004). The Tumor Suppressor P53 Down-Regulates Glucose Transporters GLUT1 and GLUT4 Gene Expression The Tumor Suppressor P53 Down-Regulates Glucose Transporters GLUT1 and GLUT4 Gene Expression. *Cancer Res* 2627–2633.

Son, J., Lyssiotis, C. a, Ying, H., Wang, X., Hua, S., Ligorio, M., Perera, R.M., Ferrone, C.R., Mullarky, E., Shyh-Chang, N., et al. (2013). Glutamine supports pancreatic cancer growth through a KRAS-regulated metabolic pathway. *Nature* 496, 101–105.

Suzuki, M., Toyooka, S., Miyajima, K., Iizasa, T., Fujisawa, T., Bekele, N.B., and Gazdar, A.F. (2003). Alterations in the Mitochondrial Displacement Loop in Lung Cancers. *Clin. Cancer Res.* 9, 5636–5641.

Svobodova, A., Walterova, D., Vostalova, J., and Republic, C. (2006). ULTRAVIOLET LIGHT INDUCED ALTERATION TO THE SKIN. *150*, 25–38.

Tan, D., Bai, R., and Wong, L.C. (2002). Comprehensive Scanning of Somatic Mitochondrial DNA Mutations in Breast Cancer Advances in Brief Comprehensive Scanning of Somatic Mitochondrial DNA Mutations in Breast Cancer 1. 972–976.

Teperino, R., Aberger, F., Esterbauer, H., Riobo, N., and Pospisilik, A. (2014). Canonical and non-canonical Hedgehog signalling and the control of metabolis. *Semin Cell Dev Biol* 81–92.

Tommasi, S., Swiderski, P.M., Tu, Y., Kaplan, B.E., and Pfeifer, G.P. (1996). Inhibition of Transcription Factor Binding by Ultraviolet-Induced Pyrimidine. *2960*, 15693–15703.

Uribe, P., and Gonzalez, S. (2011). Epidermal growth factor receptor (EGFR) and squamous cell carcinoma of the skin: Molecular bases for EGFR-targeted therapy. *Pathol. Res. Pract.* 207, 337–342.

Wang, X. De, Inzunza, H., Chang, H., Qi, Z., Hu, B., Malone, D., and Cogswell, J. (2013). Mutations in the Hedgehog Pathway Genes SMO and PTCH1 in Human Gastric Tumors. *PLoS One* 8, 1–8.

Warburg, O. (1956). On the origin of cancer cells. *Science* 123, 309–314.

Wu, C., Chen, G., Lin, P., Pan, I., Wang, S., Lin, S., Yu, H., and Lin, C. (2014). Tazarotene induces apoptosis in human basal cell carcinoma via activation of caspase-8/t-Bid and the reactive oxygen species-dependent mitochondrial pathway. *DNA Cell Biol.* 33, 652–666.

Wu, C.-W., Yin, P.-H., Hung, W.-Y., Li, A.F.-Y., Li, S.-H., Chi, C.-W., Wei, Y.-H., and Lee, H.-C. (2005). Mitochondrial DNA mutations and mitochondrial DNA depletion in gastric cancer. *Genes. Chromosomes Cancer* 44, 19–28.

Yun, J., Rago, C., Cheong, I., Pagliarini, R., Angenendt, P., Schmidt, K., Wilson, J.K. V, Markowitz, S., Zhou, S., Jr, L. a D., et al. (2009). Glucose Deprivation Contributes to the Development of KRAS Pathway Mutations in Tumor Cells. *Science* (80-.). 325, 1555–1559.

Zhao, Y., and Adjei, A. a (2014). The clinical development of MEK inhibitors. *Nat. Rev. Clin. Oncol.* 11, 385–400.

Zhao, Y., Butler, E.B., and Tan, M. (2013). Targeting cellular metabolism to improve cancer therapeutics. *Cell Death Dis.* *4*, e532.

Zheng, W., Tayyari, F., Gowda, G. a N., Raftery, D., Mclamore, E.S., Porterfield, D.M., Donkin, S.S., Bequette, B., and Teegarden, D. (2013). Altered glucose metabolism in Harvey-ras transformed MCF10A cells. *Mol. Carcinog.* *120*, 111–120.

Zhou, S., Kachhap, S., and Singh, K.K. (2003). Mitochondrial impairment in P53-deficient human cancer cells malignancy remains unclear . *Mutagenesis* *18*, 287–292.

ARTICLE IN PREPARATION

UVB irradiation rewires cellular metabolism through over-activation of dihydroorotate dehydrogenase to coordinate DNA repair and ATP synthesis

Mohsen Hosseini^{1,2}, Lea Dousset^{1,2§}, Walid Mahfouf^{1,2§}, Martin Serrano-Sanchez^{1,2§}, Vanessa Bergeron^{1,2§}, Zeinab Kasraini^{1,2}, Doriane Bortolotto^{1,2}, Emilie Obre^{1,9}, Marc Bonneau⁵, Stephane Claverol⁵, Hubert de Verneuil^{1,2,3}, Marija Vlaski⁶, Zoran Ivanovic⁶, Walid Rachidi⁷, Thierry Douki⁷, Alain Taieb^{1,2,3,4}, Anne-Karine Bouzier-Sore⁸, Rodrigue Rossignol^{1,9}, Hamid Reza Rezvani^{1,2,3*}

1-Inserm U 1035, 33076 Bordeaux, France

2-Université de Bordeaux, 146 rue Léo Saignat, 33076 Bordeaux, France

3- Centre de Référence pour les Maladies Rares de la Peau, CHU de Bordeaux, France

4- Département de Dermatologie & Dermatologie Pédiatrique, CHU de Bordeaux, France

5- Centre Génomique Fonctionnelle de Bordeaux, Université de Bordeaux, Bordeaux, France

6- Etablissement français du sang aquitaine-limousin, Université Bordeaux, France

7- Nucleic Acids Lesions Laboratory, SCIB/INAC, CEA, Joseph Fourier University-Grenoble 1, 17 rue des Martyrs, 38054 Grenoble Cedex 9, France

8- Centre de Résonance Magnétique des Systèmes biologiques, CNRS-Université Bordeaux UMR 5536 Bordeaux, France

9- Université Bordeaux, Maladies Rares: Génétique et Métabolisme (MRGM), EA 4576, Bordeaux, France

§ These authors contributed equally to this work.

Running title: **Metabolism reprogramming upon UVB irradiation**

* Corresponding Author

INSERM U1035, Bordeaux, F-33000 France

Email address: hamid-reza.rezvani@u-bordeaux.fr

Phone: +33-557-575-683

Fax: +33-557-571-374

Abstract

Otto Warburg stated that cancer cells are impaired in respiratory chain function and depend predominantly on glycolysis. However, the relationship between the genomic instability and the Warburg effect during the tumoral transformation remains unclear. Recently, we demonstrated that accumulation of mutations in non-transcribed regions of the nuclear genome results in increased ROS levels which subsequently trigger bioenergetic alterations and tumoral transformation of normal human keratinocytes. Our studies showed that mutation accumulation is not alone sufficient for the induction of the tumoral transformation of the deficient keratinocytes and that the metabolic changes are essential for this process. Although growing evidence indicate that mitochondria-to-nucleus retrograde signaling has an important role in the progression stage of tumorigenesis, very little information is available on the contribution of reprogramming of energy metabolism in cancer initiation and promotion. To assess the role of metabolic reprogramming in different phases of carcinogenesis, we employed a multistage model of ultraviolet B (UVB) radiation-induced skin cancer. We showed that chronic UVB irradiation resulted in decreased glycolysis, TCA cycle and fatty acid β -oxidation, while at the same time mitochondrial ATP synthesis and a part of the electron transport chain (ETC) were up-regulated. The increased ETC was further found to be related to the over-activation of dihydroorotate dehydrogenase (DHODH). Decreased DHODH activity or ETC (chemically or genetically) led to hypersensitivity to UVB irradiation. In fact, following chronic UVB irradiation, *Tfam*-ablated or leflunomide-treated mice exhibited desquamative features with hyperkeratotic epidermis very early but they failed to develop actinic keratosis or squamous cell carcinoma. Our results indicated that DHODH pathway through induction of ETC and ATP synthesis represents a new and major link between DNA repair efficiency and metabolism reprogramming during UVB-induced carcinogenesis.

Introduction

The most common metabolic hallmark of malignant tumors, i.e. the so-called “Warburg effect”, is their propensity to metabolize glucose to lactic acid at a high rate even in the presence of oxygen (Gatenby and Gillies, 2004; Gottlieb and Tomlinson, 2005). Increased glucose uptake usually reflects an increased rate of glycolysis, with conversion of glucose to lactate and decreased conversion of pyruvate to acetyl-CoA, the substrate for mitochondrial oxidative phosphorylation (OXPHOS). Because of the relative inefficiency of glycolysis compared with that of oxidative phosphorylation as a means of generating ATP, flux through the glycolytic pathway must increase dramatically to maintain cellular homeostasis (Gatenby and Gillies, 2004; Gottlieb and Tomlinson, 2005). Because the dramatic reprogramming of energy metabolism is observed in more than 95% of advanced cancers, understanding the mechanisms and consequences of this energy metabolism alteration in cancer cells is an important challenge in cancer biology. However, almost a century after Warburg’s seminal finding, the metabolic transformation of cancer is still a mystery. Two scenarios for energy metabolism remodeling are still competing:

- 1) Mitochondrial dysfunction is a ‘second hit’ in the process of cancer metabolic transformation;
- 2) Mitochondria play a key role in tumorigenesis and their dysfunction is the driving cause of tumorigenesis.

The former scenario is supported by evidence showing that glucose metabolism is dramatically increased in most tumors while many of these tumor cells are still capable of OXPHOS when forced to. In these tumors, OXPHOS impairment could be the net outcome of accelerated glycolysis as the results of the loss of p53 or activation of PI3K, AKT, c-MYC, and HIF (hypoxia inducible factor), the most common alterations observed in human cancer (Bensaad and Vousden, 2007; Ward and Thompson, 2012; Yeung et al., 2008). Evidence for the second scenario comes from examples of tumors that exhibit inherent decreased mitochondrial functions caused by mutations in either the mitochondrial DNA (mtDNA) itself or in nuclear-encoded mitochondrial proteins such as succinate dehydrogenase (SDH) and fumarate hydratase (FH) (Baysal et al., 2000; Gottlieb and Tomlinson, 2005; King et al., 2006; Tomlinson et al., 2002). Besides these hereditary cancers, a large number of somatic mtDNA mutations are found in a variety of human cancers, which indicates a key role of mitochondria in oncology (Brandon et al., 2006; Modica-Napolitano and Singh, 2002). The cause of these mtDNA deletions and also their consequences are under investigation. Recent data suggest that oxidative stress, accumulation of damage during replication or during repair

of damaged mtDNA could lead to mtDNA deletions (Krishnan et al., 2008). It has been shown that mitochondrial deficiency can confer tumor cells resistance to mitochondrial-dependent apoptosis (Cai et al., 2005; Joshi et al., 1999) and enhances proliferation and/or an invasive phenotype (Amuthan et al., 2001; Liu et al., 2002; Petros et al., 2005).

Although growing evidence indicates that mitochondria-to-nucleus retrograde signaling has an important role in tumorigenesis, most published studies reveal the importance of the deficiency in mitochondrial energy metabolism in the progression stage of tumorigenesis using cancer cell lines (Petros et al., 2005; Singh et al., 2005). Indeed, very little information is available on the contribution of reprogramming of energy metabolism in cancer initiation and promotion. To rigorously assess the role of metabolic reprogramming in different phases of carcinogenesis, we employed a multistage model of ultraviolet B (UVB) radiation-induced skin cancer, a well-known model for the study of the initiation, promotion and progression stages of cancer (DiGiovanni, 1992). In fact, during chronic UVB irradiation of mice, mild nuclear atypia is initially seen within basal keratinocytes. These modifications are subtle and can only be identified histologically. Following extensive UV exposure, a greater cellular atypia occurs and identifiable pre-malignant actinic keratoses develop (promotion stage). Of these only 1-5 % will progress into squamous cell carcinoma (SCCs) (progression stage), with the potential for metastatic spread.

It worth mentioning that solar UVB radiation is the primary environmental risk factor responsible for induction of non-melanoma skin cancer which includes basal cell carcinomas (BCCs) and SCCs, the most common types of human malignancy worldwide. A major deleterious effect of UVB is the induction of well-defined structural alterations in DNA (Ravanat et al., 2001), which, in turn, trigger DNA repair, cell cycle delay, or apoptosis (Latonen and Laiho, 2005). The ultimate fate of cells with damaged DNA is dependent on the type and extent of damage, DNA repair capacity, and UVB-induced apoptotic signaling pathways (Assefa et al., 2005; Kulms and Schwarz, 2002). Understanding the interplay between various factors involved in the regulation of cellular responses to UVB could enhance current knowledge regarding cancer prevention, initiation, and therapy. Despite the functional importance of energy metabolism in maintaining genetic stability, little is known about the relationship among energy metabolism, the Warburg effect and DNA repair efficiency in UVB-induced tumorigenesis.

Our results showed that chronic UVB irradiation resulted in energy metabolism reprogramming through overactivation of dihydroorotate dehydrogenase (DHODH). Up-

regulated DHODH, in turn, triggered electron transport chain (ETC) activation and ATP production necessary for DNA repair activation and cell proliferation.

Results

Chronic UVB irradiation is associated with decreased glycolysis, TCA cycle and fatty acid β -oxidation

It is now widely accepted that tumorigenesis is associated with altered metabolism (Hanahan and Weinberg, 2011). We wondered whether metabolism reprogramming starts during the initial phase of carcinogenesis. To this end, SKH-1 hairless mice, that mimic UVB-induced photocarcinogenesis in humans, were exposed to 150 mJ/cm², corresponding to one minimal erythemal dose, three times per week. Mice started to develop pre-malignant actinic keratoses (AK)-like lesions (promotion stage) after 14 weeks of chronic irradiation. Of these, some progressed into small keratotic and large ulcerated tumors that have a similar appearance to human squamous cell carcinoma (SCCs) (progression stage), with the potential for metastatic spread after 20 weeks of UVB irradiation. To see whether altered energy metabolism occurs during the initiation phase of UVB-induced carcinogenesis, we first characterized the energy metabolism profile of mouse skin exposed to chronic UVB irradiation for 8 weeks. To delineate changes in the topology of the metabolic pathways involved in energy metabolism, we performed a quantitative label free differential proteomic analysis between irradiated versus non-irradiated skin. A detail of the function of those proteins was obtained by performing a KEGG pathway analysis of the data. We noted that the majority of enzymes implicated in glycolysis, TCA cycle and fatty acid β -oxidation were significantly down-regulated while the main proteins involved in fatty acid synthesis were up-regulated in irradiated skin compared with non-irradiated one (**Figure 1A and B**). As a striking result, it can be seen that 10 out of 13 enzymes of glycolysis were decreased from 50 to 80% following irradiation. Furthermore, the majority of proteins involved in TCA cycle and fatty acid β -oxidation were decreased, respectively, 36 to 58% and 28 to 84% in irradiated skin. On the contrary, irradiation increased fatty acid synthesis with overexpression of corresponding enzymes ranging from 2.25 to 6 fold.

In line with these topology data, biochemical functional analyses revealed decreased glucose consumption and lactate production in irradiated compared to non-irradiated skin (**Figure 2A, B**). Furthermore, irradiated skin was unable to mount a substantial switch to (a) glucose utilization when shifted from no-glucose to high glucose medium responding with a 1.72 fold smaller extracellular acidification rate (ECAR) burst than non-irradiated skin; (b) OXPHOS utilization when supplemented with succinate, reflected by a 1.53 fold smaller OCR burst compared with non-irradiated skin; or (c) fatty acid oxidation when shifted from no-glucose to

palmitate supplemented medium, reflected by a 1.22 fold smaller OCR burst than that of non-irradiated skin (**Figure 2C, D, E**). To evaluate the TCA flux efficiency, [1-¹³C] labeled glucose was injected intraperitoneally into two groups of mice. The signal intensities arising from the glutamate C4 and C3, which could be an index of TCA flux (**Figure 2F, peaks 8 and 5, respectively**), were compared between irradiated and non-irradiated skin. Results indicated a 56% reduction in the relative level of C3/C4 enrichment ratio in irradiated skin compared to non-irradiated ones (**Figure 2G**).

Altogether these results suggest that UVB irradiation results in downregulation of glycolysis, TCA cycle and fatty acid β -oxidation.

Chronic UVB irradiation leads to increased mitochondrial ATP synthesis

Whereas all our results suggested that mitochondrial metabolism was decreased in irradiated skin, basal oxygen consumption rates (OCR) were surprisingly higher in irradiated skin compared with non-irradiated one (**Figure 2D, 3A**). Since increased oxygen consumption can be related to ROS generation and because UVB has been already shown to induce ROS production (Rezvani et al., 2007; Rezvani et al., 2006), we then verified ROS levels. To this end, we measured both cytoplasmic and mitochondrial steady-state levels of ROS in keratinocytes isolated from irradiated and non-irradiated mice (**Figure 3B and C**). While a significant increase in cytoplasmic steady-state ROS levels occurred in irradiated mice compared with non-irradiated ones, variations in mitochondrial ROS were not statistically significant.

Numerous cytosolic enzymes including cyclooxygenase, nitric oxide synthase, xanthine oxidase, and the plasma membrane-bound NADPH oxidase can generate ROS. To determine whether cytoplasmic ROS generation was involved in the elevated basal OCR observed in irradiated skin, we treated skin samples with various inhibitors of cytosolic ROS-generating enzymes: NG-monomethyl-arginine (NMMA, 100 μ M), an inhibitor of nitric oxide synthase; allopurinol (100 μ M), an inhibitor of xanthine oxidase; hydroxyurea (1.5 mM), an inhibitor of ribonucleotide reductase; indomethacin (100 μ M), an inhibitor of cyclooxygenase (COX); diphenyl-iodonium (DPI, 2.5 μ M), an inhibitor of cytoplasmic NADPH oxidase, and a specific peptide inhibitor of NOX1 (InhNOX). We used in parallel inhibitors of mitochondrial respiratory chain complexes: rotenone (10 μ M), an inhibitor of complex I; malonate (10 μ M), an inhibitor of complex II; antimycin (10 μ M), an inhibitor of complex III; sodium azide (NaN₃, 5mM), an inhibitor of complex IV. Treatments of skin samples with the inhibitors of cytosolic ROS-generating enzymes did not suppress the difference between the basal OCR

level of irradiated and non-irradiated skin (**Figure 3D**). Treatment with rotenone, malonate, antimycin or NaN₃ led to, respectively, 42%, 35%, 46% and 49% reduction in the baseline oxygen consumption in non-irradiated skin. Interestingly, while rotenone and malonate decreased the baseline OCR level, respectively 14% and 18% in irradiated skin, antimycin and NaN₃ treatment reduced it about 71% and 62% (**Figure 3D**), suggesting a major role for complexes III and IV in elevated OCR in irradiated skin and a potential fueling of the respiratory chain between complex II and complex III in irradiated skin samples. To further investigate this difference in mitochondrial respiratory chain function, we evaluated the maximal activities of the different enzyme complexes. While the activity of complex II was significantly diminished following irradiation, the activities of complexes II+III and IV were markedly increased (**Figure 3E**), suggesting that complexes III and IV are over-activated in chronic irradiated skin.

We then examined whether this increase in the activities of complexes III and IV are coupled with mitochondrial ATP synthesis. Evaluation of ATP levels indicated that total ATP as well as ATP synthesized by mitochondria were significantly higher in irradiated skins compared with non-irradiated ones (**Figure 3F**). We noted that the ADP/ATP ratio in irradiated skin was also higher than non-irradiated mice, suggesting a higher cellular energy demand in irradiated skin (**Figure 3G**). Finally, the proportion of respiration used to produce ATP (ATP turnover) was increased in irradiated skin compared with non-irradiated skin (**Figure 3H**).

Altogether, these results reveal that a part of the electron transport chain (ETC) is up-regulated following chronic irradiation.

Increased ETC activity in chronic UVB irradiated skin is related to the activity of dihydroorotate dehydrogenase (DHODH)

Since glycolysis, TCA cycle and fatty acid β -oxidation, the three principal electron donors to coenzyme Q in the ETC, were decreased in irradiated skin, we wondered how complexes III, IV and V could be over-activated. Looking at proteomic data, we found that the enzymes implicated in purine and pyrimidine synthesis were markedly increased in irradiated skins compared to non-irradiated ones (**Figure 4A, B**). Indeed, the fourth step of the pyrimidine synthesis is catalyzed by dihydroorotate dehydrogenase (DHODH), the only mitochondrial enzyme of this pathway that converts dihydroorotate to orotate coupled with the reduction of ubiquinone to ubiquinol. Importantly, oxidation of ubiquinol in ETC is necessary to maintain an adequate supply of ubiquinone for DHODH activity. Thus, DHODH links cellular respiration and pyrimidine synthesis (Ahn and Metallo, 2015; Fang et al., 2013; Loffler et al.,

1997). We therefore measured the activity of DHODH in irradiated and non-irradiated groups. Activity of DHODH was about 5.4 times higher in irradiated skin than in non-irradiated skin ($P < 0.001$) (**Figure 4C**). To examine whether increased ATP synthesis in irradiated skin was dependent on the activity of DHODH, one group of chronic UVB-irradiated mice received intraperitoneally leflunomide (LFN), an inhibitor of DHODH, 2h prior to killing. Measurement of ATP revealed that the increased ATP production in irradiated skin is related to DHODH activity (**Figure 4D**). Furthermore, baseline OCR level was dramatically decreased when irradiated mice received LFN (**Figure 4E**). In contrast, a significant increase in ETC utilization was noted when irradiated skin was supplemented with dihydroorotic acid (**Figure 4F**).

Inhibition of DHODH activity or global down-regulation of ETC results in hypersensitivity to UVB exposure

To evaluate the impact of ETC activation on UVB-induced skin carcinogenesis, we used two following approaches: a) the inhibition of DHODH using LFN and b) a mouse model of inducible *Tfam* knockout targeted to keratinocytes (K14-Cre-ER^{T2}/*Tfam*^{flox/flox}). *Tfam* knockout model has been chosen because TFAM is the main regulator of mtDNA transcription and consequently mitochondrial genes encoding ETC subunits (Campbell et al., 2012; Kang et al., 2007). As seen in figure 5A, while the expression of mitochondrial-encoded NADH dehydrogenase 1 (MT-ND1), cytochrome c oxidase 1 (MT-CO1), and ATP synthase 6 (MT-ATP6) proteins were significantly reduced in *Tfam* ablated mice, the expression of nuclear-encoded mitochondrial complexes 1 subunit NDUFB8, II subunit SDHB, III subunit UQCRC2 and V subunit ATP5A did not change (**Figure 5A**). Moreover, we have noted a marked reduction in DHODH expression and activity in the skin of *Tfam*-ablated mice (**Figure 5A, B**). It is worth mentioning that we developed an inducible mouse model because mice with epidermal *Tfam* ablation (K14-Cre/*Tfam*^{flox/flox}) have been shown to have a short lifespan due to malnutrition (insufficient intake of milk) (Baris et al., 2011). To avoid the effect on nutrition, *Tfam* were ablated through topical skin application of tamoxifen in keratinocytes of K14-Cre-ER^{T2}/*Tfam*^{flox/flox} mice, hereinafter called K-*Tfam*^{-/-}. As controls, we used tamoxifen-treated K14-Cre-ER^{T2} mice, hereinafter referred to as K-*Tfam*^{+/+}. Since there were no meaningful differences in outcome between mice receiving LFN and K-*Tfam*^{-/-} mice, hereinafter only the results of K-*Tfam*^{+/+} and K-*Tfam*^{-/-} have been shown.

We first monitored LFN-treated, and K-*Tfam*^{-/-} mice and their control counterparts during the 4 first months of life. The mice developed normally and histological analysis of skin revealed

a normal epidermis with no obvious abnormality in epidermal differentiation or proliferation (**Figure 5C**). These mice were then exposed to chronic UVB irradiation. The LFN-treated and K-*Tfam*^{-/-} mice exhibited a UVB-related phenotype very early (**Figure 6A**). Indeed, 9 out of the 15 K-*Tfam*^{-/-}, 8 out of the 12 LFN-treated mice exhibited thick squamous hyperkeratic plaques 12 weeks after UVB irradiation. In 2 out of the 9, stratum corneum sloughing of a large part of dorsal skin was also noticed. All of these mice at 20 weeks after chronic irradiation presented desquamative features with hyperkeratotic epidermis (**Figure 6B**). However, none of these mice developed AK and/or keratotic tumors up to 30 weeks after irradiation (**Figure 6B, C**). In contrast, none of the control mice had any obvious abnormality up to week 12 after irradiation, and 8 out of the 15 K-*Tfam*^{+/+}, exhibited at least one AK lesion at 18 weeks (**Figure 6A-D**). Histological examination demonstrated that while K-*Tfam*^{+/+} mice at 12 weeks after irradiation presented moderate hyperplasia and no papillomatosis, K-*Tfam*^{-/-} mice presented a papillomatous epidermal hyperplasia, hyperkeratosis showing crusts and parakeratosis, and no dermal invasion. Twenty five weeks after irradiation, while K-*Tfam*^{+/+} mice presented typical small cell invasive and moderately differentiated SCC, K-*Tfam*^{-/-} presented papillomatous hyperplasia, hyperkeratosis with parakeratosis, without dermal invasion (**Figure 5C**).

Since DHODH is a key player in the pyrimidine *de novo* biosynthesis pathway, we wondered whether DHODH inhibition and *Tfam* ablation may affect DNA repair efficiency. In order to confirm this hypothesis, the level of cyclopyrimidine dimer (CPD) was first quantified by immuno-dot blot in DNA of the different groups of mice irradiated for 12 weeks. The CPD level was much higher in leflunomide-treated and K-*Tfam*^{-/-} mice than in K-*Tfam*^{+/+} mice (**Figure 7A**). Quantification of CPD in the genome of mice by HPLC-MS/MS revealed that CPD level was, respectively, 1.82 and 1.74 fold higher in leflunomide-treated and K-*Tfam*^{-/-} mice than in K-*Tfam*^{+/+} mice (**Figure 7B**). To determine whether the increased CPD level in *Tfam*-ablated or leflunomide-treated mice was directly related to reduced pyrimidine synthesis, we then measured the DNA repair capacity of skin mouse samples. To this end, we added the skin protein extracts on a fixed plasmid harboring defined quantity of CPD. In this assay, the capacity of CPD excision and the re-synthesis of the excised strand is directly correlated with the incorporation of labeled nucleotides. Results indicated a 40% and 54% reduction in CPD repair, respectively, in leflunomide-treated and K-*Tfam*^{-/-} mice as compared with K-*Tfam*^{+/+} mice (**Figure 7C**). Since in this assay, exogenous fluorescence nucleotides are added in reaction, we can conclude that decreased CPD repair capacity and consequently

increased CPD levels in *Tfam* ablated or LFN-treated mice are only partially dependent on pyrimidine synthesis (**Figure 7C vs 7B**).

We continuing to decipher this fascinating story:

- To investigate further this question, we are evaluating the expression of some NER proteins → XPC, DDB1 and XPA in LFN-treated, K-*Tfam*^{-/-} and K-*Tfam*^{+/+} mice
- To evaluate directly whether the effects of DHODH inhibition and *Tfam* ablation are dependent on pyrimidine synthesis, LFN-treated, K-*Tfam*^{-/-} and K-*Tfam*^{+/+} mice have been treated topically with exogenous uridine before each irradiation → we are waiting for the results
- We are also measuring the activity of DHODH in human BCC, SCC and melanoma samples.

Discussion

This study provides insights, which to our knowledge are previously unreported, in the understanding of UVB-induced keratinocyte carcinogenesis *in vivo*, emphasizing the role of energy metabolism. We demonstrate that UVB-induced DHODH overactivation participates in maintaining cell survival, thus favoring the development of SCCs. Our data clearly show that LFN-treated mice and TFAM-deficient mice manifest a specific type of hypersensitivity to UVB owing to the significant reduction in DNA repair capacity and subsequent increased apoptotic cell death. However, these mice do not develop actinic keratosis and keratotic tumors. Together, these observations support the possibility that UVB-induced DHODH activity protects UVB-exposed keratinocytes from DNA damage-mediated apoptotic cell death, thereby promoting the initiation of carcinogenesis. Beyond understanding of UVB-induced expression changes and tumoral transformation mechanisms, these demonstrations have substantial implications for the development of new therapeutics for skin SCC.

UVB-induced skin cancer and metabolism remodeling

In addition to involving in amino acid and lipid biosynthesis, mitochondrial metabolism affects nucleotide biosynthesis. Indeed, many components that contribute to both pyrimidine and purine bases are derived directly or indirectly from mitochondria. Besides glutamine and aspartate, which can be supplied by mitochondria, pyrimidine synthesis requires the activity of mitochondrial enzyme DHODH, linking directly cellular respiration and pyrimidine synthesis (Ahn and Metallo, 2015). Therefore, it is not surprising that the cells lacking functional mitochondrial DNA (such as ρ^0 cells) are addicted to uridine supplementation for their proliferation (Grassian et al., 2014; Mullen et al., 2014). Up-regulation and overactivation of DHODH have been reported in multiple types of cancers (Ahn and Metallo, 2015; He et al., 2014; Hu et al., 2013; White et al., 2011; Zhai et al., 2013). Inhibition of DHODH has been further shown to reduce tumor growth *in vitro* and in xenografted models (White et al., 2011; Zhai et al., 2013).

Reprogramming of the metabolic network is now considered to be a hallmark of neoplastic transformation (Hanahan and Weinberg, 2011). However, altered expressions of metabolic genes are very heterogeneous across different tumor types in that there is no uniform metabolic variation associated with all tumors (Hu et al., 2013). It is now widely accepted that OXPHOS and glycolysis cooperate to sustain energy demands of cancer cells (Smolkova et al., 2011; Ward and Thompson, 2012) and that cancer cell's metabolic reprogramming is further used to maintain anabolism through the deviation of glycolysis, Krebs cycle truncation

and OXPHOS redirection toward lipid and protein synthesis (DeBerardinis et al., 2007; Jose et al., 2011; Wise et al., 2008). Here, we showed that metabolism remodeling, which occur through DHODH upregulation-mediated ETC activation, in UVB-irradiated cells leads to ensuring the coordination among ATP generation, persistent nucleotide biosynthesis and repair of DNA damage. Therefore, metabolic signature of UVB-induced cells is in favor of repair of UVB-induced DNA damage. Consistently, inhibition of DHODH (through LFN treatment or *Tfam* ablation) results in decreased DNA repair efficiency and increased CPD levels.

It has been demonstrated that metabolic state alone can drive dramatic cell fate transitions and expression changes (e.g., immune cell polarity, activation state, cancer invasiveness) (Hitosugi et al., 2009; Hsu and Sabatini, 2008; Jeon et al., 2012; Shi et al., 2011). Our results indicate that rewiring of metabolism upon UVB exposure have an important role in defining of cell fate through modulation of apoptotic cell death and DNA repair capacity. Indeed, dependent on the type and extent of damage, DNA repair capacity, and UVB-induced apoptotic signaling pathways, UVB-induced DNA damage defines the ultimate fate of cells by triggering repair of DNA damage, cell cycle delay, or apoptosis (Assefa et al., 2005; Kulms and Schwarz, 2002; Latonen and Laiho, 2005). It is likely that both early UVB exposure phenotype and the absence of tumor formation in LFN treated and *Tfam* ablated mice could be related to persistence of UVB-induced DNA damage and subsequently increased apoptosis (**Figure 7**). The epidermis is a self-renewing tissue in which keratinocyte proliferation in the basal layer is followed by a series of well-orchestrated differentiation events which influence the production of dead squames and its barrier function. Following extensive damage, like that resulting from UV irradiation, many of the normal keratinocytes harboring DNA damage are eliminated via apoptosis. However, if the damage to a keratinocyte is marginal, this cell could persist and give rise later to patches of sun-damaged skin (Raj et al., 2006). It is likely that decreased DNA repair capacity in LFN treated and *Tfam* ablated mice results in accumulation of DNA damage in keratinocytes. Subsequent elimination of these cells harboring DNA damage by apoptosis finally prevents their tumoral transformation. However, further studies need to determine to what extent procancer effects of UVB depend on changes in metabolic state.

Materials and methods

Animals and experimental protocol

SKH-1 hairless mice were purchased at 4–6 weeks of age from Charles River (L'arbresle, France). *Tfam*^{flox/flox} mice were kindly provided by Dr. Nils-Göran Larsson, Max-Planck-Institute for Biology of Ageing, Cologne Germany. K14-Cre-ER^{T2} mice expressing inducible Cre recombinase under the control of the keratinocyte-specific K14 promoter (K14-Cre) were purchased from Jackson laboratory. Hairless *Tfam*^{flox/flox} mice and Hairless K14-Cre-ER^{T2} mice were generated by their cross breeding with hairless SKH-1 mice for 5 generations. The progeny was genotyped by PCR assays on tail DNA. Crossing these strains with together then generated the K14-Cre-ER^{T2}/*Tfam*^{flox/flox}. Mice in which TFAM deficiency was restricted to keratinocytes were then generated by topical application of 4-hydroxy-tamoxifen (OHT) at 1 mg kg⁻¹ for 5 consecutive days on these mice. *Tfam* ablation in keratinocytes was verified by PCR assays on skin DNA. Mice were bred and maintained in a pathogen-free mouse facility at Bordeaux University. All mouse experiments were carried out with the approval of Bordeaux University Animal Care and Use Committee.

Mouse genomic DNA isolation and genotyping

Mouse genomic DNA was obtained from tail clip or skin samples following their overnight digestion at 45°C with 100 µl of 100 mM Tris, pH 8.0, 5 mM EDTA, 0.2% SDS, 200 mM NaCl, 100 µg/ml proteinase K. Samples were then diluted with 300 µl of water and boiled for 5 min before use for PCR. *Tfam* genotyping was carried out using the following primers: *Tfam*-a: CGTCCTTCCTCTAGCCCGTG; *Tfam*-b: GTAACAGCAGACAACCTTGTG and *Tfam* C: CTCTGAAGCACATGGTCAAT. Cre-K14-ER^{T2} genotyping was carried out using the following primers: forward primer, CCTGGAAAATGCTTCTGTCCG; and reverse primer, CAGGGTGTTATAAGCAATCCC. Amplification products were detected on 2% agarose gel stained with ethidium bromide.

Isolation of Skin Samples and Keratinocytes

One part of the dorsal skin was excised and snap-frozen in liquid nitrogen for western blotting and measurement of enzymatic activities (Hosseini et al., 2015). The other part was used for isolation of keratinocytes. To this end, epidermis and dermis were separated by trypsinization

at 37°C for one hour. Keratinocyte suspensions were isolated from the epidermal sheet in HBSS on ice.

Western blotting procedure

Western blotting was performed as previously described (Rezvani et al., 2011b; Rezvani et al., 2011c). Briefly, equal amounts of total protein were resolved by SDS-polyacrylamide gel electrophoresis (SDS-PAGE) and electrophoretically transferred to PVDF membranes. The membranes were then incubated overnight at 4°C with a 1:1000 dilution of the anti-MT-ATP6, anti-MT-ND1, anti-DHODH (Abcam, Paris, France), anti- β -actin (Sigma, Saint Quentin Fallavier, France), antibodies or a total OXPHOS antibody cocktail (Abcam, Paris, France). After additional incubation with a 1:10,000 dilution of an anti-immunoglobulin horseradish peroxidase-linked antibody (Vector Laboratories, Biovalley S.A, Marne la Vallée, France) for 1 h, blots were developed using the chemiluminescence ECL reagent (Perkin Elmer, Courtaboeuf, France).

Assay of CPDs by immuno-dot blot analysis

The skin samples were incubated over night at 65°C in DirectPCR Lysis Reagent (Viagen, Euromedex, Mundolsheim, France) supplement with 2% proteinase K (Sigma). DNA was extracted using sodium acetate/ethanol precipitation protocol and then quantified by Nanodrop device. Equal amounts of genomic DNA (500 ng) were mixed with 1% SYBER green (*Brilliant III Ultra-Fast SYBR®*) and dot-blotted onto a Hybond N+ nitrocellulose membrane (Amersham,). The membrane was dried by baking at 80°C for 30 min. The SYBER green fluorescence were used to quantify the dot-blotted DNA for each sample. After incubation in blocking buffer in 20 mM TBS (pH 7.6) containing 5% non-fat dry milk and 1% Tween 20, the membrane was incubated overnight at 4°C with a 1:1000 dilution of the anti-CPD monoclonal antibody (Kamiya Biomedical). After additional incubation with a 1:10,000 dilution of an anti-immunoglobulin horseradish peroxidase-linked antibody (Vector Laboratories) for 1 h, blots developed using the chemiluminescence ECL reagent (Biorad, France). Fluorescence signals of SYBER green used as a loading control for normalization of chemiluminescence signals.

Quantification of DNA lesions by HPLC-MS/MS

DNAeasy Tissue kit (Qiagen) was used to extract DNA from whole skin samples following the manufacturer's instructions. Then, DNA was digested by incubation with nuclease P1,

phosphodiesterase II and buffer 10× (200 mM succinic acid, 100 mM CaCl₂, pH 6.0) altogether for 2h at 37°C. A second digestion step was realized with phosphodiesterase I and alkaline phosphatase in alkaline phosphatase buffer 10× (500 mM Tris, 1 mM EDTA, pH8) for 2 h at 37°C. At last, the solution was neutralized with 0.1 mM HCl and centrifuged for 5 min at 5000 g. The supernatant was collected for analysis by HPLC–MS/MS. The digested sample was then injected onto an HPLC system consisting in a Agilent series 1100 system equipped with a Uptisphere ODB reverse phase column (2x250 mm ID, particle size 5 µm; Interchim, Montluçon, France). The mobile phase was a gradient of acetonitrile in a 2 mM aqueous solution of triethylammonium acetate. A UV detector set at 260 nm was used to quantify normal nucleosides in order to determine the amount of analysed DNA. The HPLC flow was then directed toward an API 3000 electrospray triple quadrupole mass spectrometer operating in the negative ionization mode. Chromatographic conditions and mass spectrometry features were as described (Douki and Cadet, 2001). The signals used for detecting the bipyrimidine photoproducts, corresponding to conversion of the pseudomolecular ion into a specific daughter ion, were: m/z 545 → 447 for the TT cyclobutane dimer, m/z 545 → 432 for the TT (6-4) photoproduct, m/z 531 → 195 for the TC and the CT cyclobutane dimers, m/z 530 → 195 for the TC (6-4) photoproduct.

DNA excision/synthesis reaction. The excision/synthesis reaction was conducted on the modified plasmid arrays as described (Forestier et al., 2012; Millau et al., 2008) except that, to get a stronger signal, we used biotin-dCTP and biotin-dGTP instead of dCTP-Cy3. Custom reaction chambers (Grace Bio-Labs, USA) were set on the damaged plasmid microarray slides. 20 µL of the excision/synthesis mix composed of reaction buffer (5 µL of 5X ATG buffer (200 mM Hepes KOH pH 7.8, 35 mM MgCl₂, 2.5 mM DTT, 1.25 µM dATP, 1.25 µM dTTP, 17 % glycerol, 50 mM phosphocreatine (Sigma, USA), 10 mM EDTA, 250 µg/mL creatine phosphokinase, 0.5 mg/mL BSA)), 1 mM ATP (Amersham, England), 0.25 µM biotin-dCTP, 0.25 µM biotin-dGTP (Perkin Elmer, USA) and the nuclear extract at a final protein concentration of 0.1 mg/mL were injected into the reaction chambers. Each sample was tested in duplicate. The slides were incubated for 3h at 30°C in the dark. Subsequently, the reaction chambers were removed and the slides were washed for 2 x 3 min in PBS/Tween 0.05 %, and for 2 x 3 min in MilliQ water. The biotin incorporated into the plasmid DNA was revealed by incubation, 30 min at 30°C, in a solution of streptavidin-Cy5 (Jackson ImmunoResearch, UK) at 0.25 µg/mL diluted in PBS containing 0.1 mg/mL BSA. The slides were then washed as described before and dried for 5 min at 30°C in the dark. Total

fluorescence of each spot was quantified using the Mapix software (Innopsys), after scanning of the slides at 635 nm wavelength at a 10 µm resolution with the InnoScan710AL scanner (Innopsys, France). Duplicate data were normalized using NormalizeIt software (Millau et al., 2008). The fluorescence intensity of the CTRL plasmid was subtracted to the value obtained for each modified plasmid. Subsequently, the total fluorescence obtained for the repair of each lesion was calculated by adding the 3 values (dilution A, B and C) got for each type of lesion-containing plasmid.

Measurement of endogenous, cytoplasmic and mitochondrial ATP production and ADP/ATP ratio

The amount of intracellular ATP was measured by a luciferin/luciferase-based assay using an ATP bioluminescence assay kit HSII (Roche Applied Science, Meylan Cedex, France) in accordance with the manufacturer's instructions, as already explained (Hosseini et al., 2015; Rezvani et al., 2011a, b). In brief, skin samples were lysed with 0.2 ml of cell lysis reagent. ATP concentrations in the lysates were quantified. A standard curve for ATP concentration was plotted using standard ATP solution. ATP levels were calculated and normalized to protein lysate concentrations. The ADP/ATP ratio in the skin extract was measured by using ADP/ATP Ratio Assay Kit (abcam, ab65313) in accordance with the manufacturer's instructions. To assess the ATP levels produced by glycolysis or mitochondria the skin samples were incubated, respectively, with a cocktail containing 10 µM of rotenone, 10 µM antimycin and 4µM digitonin or a cocktail containing 1 mM of iodoacetate and 4µM digitonin for 5 minutes before they were lysed. Iodoacetate is an inhibitor of glycolysis, as it inhibits glyceraldehyde 3-phosphate dehydrogenase. Therefore, any ATP generation by the cells following this treatment must be a consequence of OXPHOS activity. After treatment, the skin samples were subjected to the same procedures as the untreated skin.

Cellular O₂/CO₂ Exchange

A Seahorse XF24 Extracellular Flux Analyzer (Seahorse Bioscience) was used to analyze bioenergetic function of skin samples. Results were normalized with weight of skin samples for potential differences in skin size. Slices on nylon inserts were individually inserted face down into 20 wells of 24-well XF Islet Capture Microplates that contained 500 µl of assay medium. The assay medium for measurement of glycolytic capacity XF Base medium (Sigma) supplemented with penicillin (100 IU/ml) and streptomycin (100 µg/ml) adjusted to pH 7.4. The assay medium for measurement of OXPHOS capacity consisted in XF Base

medium supplemented with D-glucose (11 mM), sodium pyruvate (1mM), penicillin (100 IU/ml) and streptomycin (100 µg/ml) adjusted to pH 7.4. For measurement of OCR or ECAR. For fatty acid β -oxidation, skin samples were put in a modified Krebs-Henseleit-bicarbonate buffer (KHB) supplemented with 2.5 mM glucose, 50 µM carnitine and 5 mM HEPES adjusted to pH 7.4. Four wells contained inserts but no skin samples to control for temperature-sensitive fluctuations in O₂ fluorophore emission. Once the transfer of inserts was complete, samples in XF Islet Capture Microplates were incubated in a CO₂-free incubator at 37°C for 1hr to allow temperature and pH equilibration. Slices were then loaded into the XF24 and further equilibrated for 15 min by three 3 min mix, 2 min wait cycles prior to the first measurement. XF assays consisted of 3 min mix, 3 min wait, and 2 min measurement cycles and were performed at 37°C as described (Wu et al., 2007). Using this protocol, it was possible to calculate an O₂ consumption rate every 8 min. Drugs of interest prepared in desired assay medium (75 µl) were preloaded into reagent delivery chambers A, B, C, and D at 10X, 11X, 12X, and 13X the final working concentration, respectively, and injected sequentially at intervals of 24 as indicated.

Dot-blot assays for quantifying the cytochrome c oxidase (COX) and succinate dehydrogenase (SDH) activities

The skin samples were homogenized in 0.1 M Tris-Cl (pH 7.5) buffer with CK-28 ceramic beads in a Precellysed ® 24 homogenizer 5500 rpm for 3 X 20-s. After sonication for two 30-s bursts, samples were centrifuged at 7500 rpm for 7min at 4°C. Total protein concentration in the supernatant was measured using BCA kit reagent (Pierce, Bezons, France). The equal amounts of protein (100µg) were dot-blotted onto a PVDF membrane by vacuum system. The membrane was subjected to staining for the activities of COX and SDH. Briefly, the membrane were incubated in COX staining solution (4mM diaminobenzidine tetrahydrochloride, 100µM cytochrome c and 20µg/ml catalase in 0.2 M phosphate buffer, pH 7) or SDH media (1.5mM nitroblue tetrazolium, 1mM sodium azide, 200µM phenazine methosulphate, 130mM sodium succinate in 0.2 M phosphate buffer, pH 7). The enzyme activities were monitored by taking a photo every minute.

Measurement of complexes II (succinate dehydrogenase) and IV (cytochrome c-oxidase) activities

Complexes II and IV activities were determined using Complexes II and IV enzyme activities assay kits (Abcam) in accordance with the manufacturer's instructions. Briefly, the homogenized skin samples were added on detergent solution and the incubated for 30 min on ice. After a centrifugation at 25,000 g for 20 min, the supernatants were put into the wells in which the monoclonal antibodies were bound. Concerning complex II activity, the activity of the immobilized enzyme in each sample was then measured by adding the activity solution containing ubiquinone, succinate and DCPIP (2,6-dichlorophenol-indophenol; used as an artificial electron acceptor) and monitoring spectrophotometrically the reduction of DCPIP to DCPIPH₂ at 600 nm at 37°C. Concerning complex IV activity, the activity of the immobilized enzyme in each sample was then measured by adding the activity solution containing reduced cytochrome c and monitoring the oxidation of cytochrome c spectrophotometrically at 550 nm at 30°C.

Measurement of complexes II+III activities

Activity of Complexes II+III was determined using MitoToxTM OXPHOS complex II+III activity kit (Abcam) in accordance with the manufacturer's instructions. Briefly, the homogenized skin samples were added on detergent solution and the incubated for 30 min on ice. After a centrifugation at 25,000 g for 20 min, the supernatants were put into the wells containing complex II+III activity solution. The reduction of cytochrome c was monitored spectrophotometrically at 550 nm at 30°C

Measurement of DHODH activity

The skin samples were put a hypotonic buffer (2.5 mM Tris/HCl, pH 7.5 and 2.5 mM MgCl₂) on ice for 15 min, homogenized and then sonicated for 15 s. The protein concentration for each reaction was measured by BCA protein assay. DHODH-dependent respiratory enzymatic activities were measured by spectrophotometry (U-3210; Hitachi) at 37°C by monitoring the decrease in absorbance at 600 nm of reduced DCPIP (2,6-dichlorophenol-indophenol; used as an artificial electron acceptor). Briefly, the reaction was initiated with 20 mM DHO in 1 ml of standard reaction buffer (contained 50 mM potassium phosphate, 5 mg/ml BSA and 2.5 mM MgCl₂) supplemented with 50 μM DCPIP, 2 μg of rotenone (a complex I inhibitor), 2 μg of antimycin A (a complex III inhibitor), 5 mM NaN₃ (a complex IV inhibitor) and 25 μg skin lysate. The data were expressed as nmol · min⁻¹ · μg⁻¹ of protein. The reaction was stopped by the addition of 2 μg of 50 μM terileflunomide.

Measurement of intracellular ROS

The intracellular production of ROS was assessed using a CM-H₂DCF-DA cytoplasmic probe or the MitoSOXTM red mitochondrial superoxide indicator (both from Molecular Probes, Invitrogen) as already described (Rezvani et al., 2007; Rezvani et al., 2006). Briefly, CM-H₂DCF-DA (5 μM) or MitoSOX (5 μM) were added onto keratinocytes immediately after their isolation from mouse skin. Keratinocytes were then incubated for 15 min at 37°C in the dark. After two washes with PBS, the cells were immediately analyzed by flow cytometry. Ten thousand individual data points were collected for each sample.

The reactions were cycled 40 times after initial polymerase activation (50°C, 2 minutes) and initial denaturation (95°C, 10 minutes) using the following parameters: denaturation at 95°C for 30 seconds; and annealing and extension at 60°C for 30 second. A final fusion cycle (95°C, 1 minute; 55°C, 30 seconds; 95°C, 30 seconds) terminated these reactions. The standard curve demonstrated a linear relationship between the Ct values and the cDNA concentration. The relative expression of each gene was assessed by considering the Ct and efficiency values and normalized according to the tubulin expression level.

Proteomic analysis

Sample preparation for proteomic analysis

Skin samples were lysed in RIPA buffer containing protease inhibitor cocktail (Sigma). Ten μg of each protein sample were solubilized in Laemlli buffer and were deposited onto SDS-PAGE gel for concentration and cleaning purpose. Separation was stopped after proteins have entered resolving gel. After colloidal blue staining, bands were cut out from the SDS-PAGE gel and subsequently cut in 1 mm x 1 mm gel pieces. Gel pieces were destained in 25 mM ammonium bicarbonate 50% ACN, rinsed twice in ultrapure water and shrunk in ACN for 10 min. After ACN removal, gel pieces were dried at room temperature, covered with the trypsin solution (10 ng/μl in 40 mM NH₄HCO₃ and 10% ACN), rehydrated at 4 °C for 10 min, and finally incubated overnight at 37 °C. Spots were then incubated for 15 min in 40 mM NH₄HCO₃ and 10% ACN at room temperature with rotary shaking. The supernatant was collected, and an H₂O/ACN/HCOOH (47.5:47.5:5) extraction solution was added onto gel slices for 15 min. The extraction step was repeated twice. Supernatants were pooled and concentrated in a vacuum centrifuge to a final volume of 40 μL. Digests were finally acidified by addition of 2.4 μL of formic acid (5%, v/v) and stored at -20 °C.

nLC-MS/MS analysis

Peptide mixture was analyzed on a Ultimate 3000 nanoLC system (Dionex, Amsterdam, The Netherlands) coupled to a Q-Exactive quadrupole Orbitrap benchtop mass spectrometer (Thermo Fisher Scientific, San Jose, CA). Ten microliters of peptide digests were loaded onto a 300- μm -inner diameter \times 5-mm C₁₈ PepMapTM trap column (LC Packings) at a flow rate of 30 $\mu\text{L}/\text{min}$. The peptides were eluted from the trap column onto an analytical 75-mm id \times 15-cm C18 Pep-Map column (LC Packings) with a 4–40% linear gradient of solvent B in 108 min (solvent A was 0.1% formic acid in 5% ACN, and solvent B was 0.1% formic acid in 80% ACN). The separation flow rate was set at 300 nL/min. The mass spectrometer operated in positive ion mode at a 1.8-kV needle voltage. Data were acquired in a data-dependent mode. MS scans (m/z 300-2000) were recorded at a resolution of $R = 70\,000$ (@ m/z 200) and an AGC target of 1×10^6 ions collected within 100 ms. Dynamic exclusion was set to 30 s and top 15 ions were selected from fragmentation in HCD mode. MS/MS scans with a target value of 1×10^5 ions were collected with a maximum fill time of 120 ms and a resolution of $R = 35\,000$. Additionally, only +2 and +3 charged ions were selected for fragmentation. Other settings were as follows: spray voltage, 1.8 kV, no sheath nor auxiliary gas flow, heated capillary temperature, 200 °C; normalized HCD collision energy of 25% and an isolation width of 3 m/z .

Database search and results processing

Data were searched by SEQUEST through Proteome Discoverer 1.4 (Thermo Fisher Scientific Inc.) against a subset of the 2013.08 version of UniProt database restricted to *Mus musculus* Reference Proteome Set (42,882 entries). Spectra from peptides higher than 5000 Da or lower than 350 Da were rejected. The search parameters were as follows: mass accuracy of the monoisotopic peptide precursor and peptide fragments was set to 10 ppm and 0.02 Da respectively. Only b- and y-ions were considered for mass calculation. Oxidation of methionines (+16 Da) was considered as variable modification and carbamidomethylation of cysteines (+57 Da) as fixed modification. Two missed trypsin cleavages were allowed. Peptide validation was performed using Percolator algorithm (Kall et al., 2007) and only “high confidence” peptides were retained corresponding to a 1% False Positive Rate at peptide level.

Label-Free Quantitative Data Analysis

Raw LC-MS/MS data were imported in Progenesis LC-MS 4.1 (Nonlinear Dynamics Ltd, Newcastle, U.K). Data processing includes the following steps: (i) Features detection, (ii) Features alignment across the 12 sample, (iii) Volume integration for 2-6 charge-state ions, (iv) Normalization on total protein abundance, (v) Import of sequence information, (vi) ANOVA test at peptide level and filtering for features $p < 0.05$, (vii) Calculation of protein abundance (sum of the volume of corresponding peptides), (viii) ANOVA test at protein level and filtering for features $p < 0.05$. Noticeably, only non-conflicting features and unique peptides were considered for calculation at protein level. Quantitative data were considered for proteins quantified by a minimum of 2 peptides.

NMR spectroscopy

Mice received an intraperitoneal injection of [1-¹³C]glucose solution (750mM). After 30min, mice were killed, skin was collected and dipped in liquid nitrogen for further NMR analysis. Perchloric acid extract of skin samples were analyzed by ¹³C-NMR HRMAS spectroscopy on a Bruker DPX 500MHz magnet. Proton-decoupled ¹³C-NMR spectra were acquired overnight using 60° flip angle, 10 s relaxation delay, 25063 Hz sweep width and 64 K memory size. Measurements were conducted under bi-level broad band gated proton decoupling and D₂O lock. From these spectra, the ¹³C content at the different carbon positions of compounds was determined as previously described (Bouzier et al., 1999). Briefly, incorporation of ¹³C into the different carbons in glutamate were determined from integrations of the observed resonances relative to the ethylene glycol peak (63 ppm, external reference, known amount). Perchloric acid extract spectra were normalized thanks to ethylene glycol and protein contents.

Statistics

Student's t-test was applied for statistical evaluation and a p-value < 0.05 (*) was considered significant. Results are presented as means +/- SD.

Acknowledgments

H.R.R gratefully acknowledges support from the ARC "Association pour la Recherche sur le Cancer" and the Institut National du Cancer "INCA_6654". AKBS is supported by the Labex TRAIL (ANR-10-LABX-57). The authors wish to thank P. Costet (University of Bordeaux)

and Véronique Guyonnet-Duperat (FR TransBioMed, Plateforme de vectorologie, University of Bordeaux) for their valuable expertise.

Conflict of interest:

None of the authors have a financial interest related to this work.

REFERENCES

- Ahn, C.S., and Metallo, C.M. (2015). Mitochondria as biosynthetic factories for cancer proliferation. *Cancer Metab* 3, 1.
- Amuthan, G., Biswas, G., Zhang, S.Y., Klein-Szanto, A., Vijayasarathy, C., and Avadhani, N.G. (2001). Mitochondria-to-nucleus stress signaling induces phenotypic changes, tumor progression and cell invasion. *EMBO J* 20, 1910-1920.
- Assefa, Z., Van Laethem, A., Garmyn, M., and Agostinis, P. (2005). Ultraviolet radiation-induced apoptosis in keratinocytes: on the role of cytosolic factors. *Biochim Biophys Acta* 1755, 90-106.
- Baris, O.R., Klose, A., Kloepper, J.E., Weiland, D., Neuhaus, J.F., Schauen, M., Wille, A., Muller, A., Merkwirth, C., Langer, T., *et al.* (2011). The mitochondrial electron transport chain is dispensable for proliferation and differentiation of epidermal progenitor cells. *Stem Cells* 29, 1459-1468.
- Baysal, B.E., Ferrell, R.E., Willett-Brozick, J.E., Lawrence, E.C., Myssiorek, D., Bosch, A., van der Mey, A., Taschner, P.E., Rubinstein, W.S., Myers, E.N., *et al.* (2000). Mutations in *SDHD*, a mitochondrial complex II gene, in hereditary paraganglioma. *Science (New York, NY)* 287, 848-851.
- Bensaad, K., and Vousden, K.H. (2007). p53: new roles in metabolism. *Trends Cell Biol* 17, 286-291.
- Bouzier, A.K., Quesson, B., Valeins, H., Canioni, P., and Merle, M. (1999). [1-(13)C]glucose metabolism in the tumoral and nontumoral cerebral tissue of a glioma-bearing rat. *J Neurochem* 72, 2445-2455.
- Brandon, M., Baldi, P., and Wallace, D.C. (2006). Mitochondrial mutations in cancer. *Oncogene* 25, 4647-4662.
- Cai, S., Xu, Y., Cooper, R.J., Ferkowicz, M.J., Hartwell, J.R., Pollok, K.E., and Kelley, M.R. (2005). Mitochondrial targeting of human O6-methylguanine DNA methyltransferase protects against cell killing by chemotherapeutic alkylating agents. *Cancer Res* 65, 3319-3327.
- Campbell, C.T., Kolesar, J.E., and Kaufman, B.A. (2012). Mitochondrial transcription factor A regulates mitochondrial transcription initiation, DNA packaging, and genome copy number. *Biochim Biophys Acta* 1819, 921-929.
- DeBerardinis, R.J., Mancuso, A., Daikhin, E., Nissim, I., Yudkoff, M., Wehrli, S., and Thompson, C.B. (2007). Beyond aerobic glycolysis: transformed cells can engage in glutamine metabolism that exceeds the requirement for protein and nucleotide synthesis. *Proceedings of the National Academy of Sciences of the United States of America* 104, 19345-19350.

DiGiovanni, J. (1992). Multistage carcinogenesis in mouse skin. *Pharmacol Ther* 54, 63-128.

Douki, T., and Cadet, J. (2001). Individual determination of the yield of the main UV-induced dimeric pyrimidine photoproducts in DNA suggests a high mutagenicity of CC photolesions. *Biochemistry* 40, 2495-2501.

Fang, J., Uchiumi, T., Yagi, M., Matsumoto, S., Amamoto, R., Takazaki, S., Yamaza, H., Nonaka, K., and Kang, D. (2013). Dihydro-orotate dehydrogenase is physically associated with the respiratory complex and its loss leads to mitochondrial dysfunction. *Biosci Rep* 33, e00021.

Forestier, A., Sarrazy, F., Caillat, S., Vandenbrouck, Y., and Sauvaigo, S. (2012). Functional DNA repair signature of cancer cell lines exposed to a set of cytotoxic anticancer drugs using a multiplexed enzymatic repair assay on biochip. *PLoS One* 7, e51754.

Gatenby, R.A., and Gillies, R.J. (2004). Why do cancers have high aerobic glycolysis? *Nat Rev Cancer* 4, 891-899.

Gottlieb, E., and Tomlinson, I.P. (2005). Mitochondrial tumour suppressors: a genetic and biochemical update. *Nat Rev Cancer* 5, 857-866.

Grassian, A.R., Parker, S.J., Davidson, S.M., Divakaruni, A.S., Green, C.R., Zhang, X., Slocum, K.L., Pu, M., Lin, F., Vickers, C., *et al.* (2014). IDH1 mutations alter citric acid cycle metabolism and increase dependence on oxidative mitochondrial metabolism. *Cancer research* 74, 3317-3331.

Hanahan, D., and Weinberg, R.A. (2011). Hallmarks of cancer: the next generation. *Cell* 144, 646-674.

He, T., Haapa-Paananen, S., Kaminsky, V.O., Kohonen, P., Fey, V., Zhivotovsky, B., Kallioniemi, O., and Perala, M. (2014). Inhibition of the mitochondrial pyrimidine biosynthesis enzyme dihydroorotate dehydrogenase by doxorubicin and brequinar sensitizes cancer cells to TRAIL-induced apoptosis. *Oncogene* 33, 3538-3549.

Hitosugi, T., Kang, S., Vander Heiden, M.G., Chung, T.W., Elf, S., Lythgoe, K., Dong, S., Lonial, S., Wang, X., Chen, G.Z., *et al.* (2009). Tyrosine phosphorylation inhibits PKM2 to promote the Warburg effect and tumor growth. *Sci Signal* 2, ra73.

Hosseini, M., Mahfouf, W., Serrano-Sanchez, M., Raad, H., Harfouche, G., Bonneau, M., Claverol, S., Mazurier, F., Rossignol, R., Taieb, A., *et al.* (2015). Premature skin aging features rescued by inhibition of NADPH oxidase activity in XPC-deficient mice. *The Journal of investigative dermatology* 135, 1108-1118.

Hsu, P.P., and Sabatini, D.M. (2008). Cancer cell metabolism: Warburg and beyond. *Cell* 134, 703-707.

Hu, J., Locasale, J.W., Bielas, J.H., O'Sullivan, J., Sheahan, K., Cantley, L.C., Vander Heiden, M.G., and Vitkup, D. (2013). Heterogeneity of tumor-induced gene expression changes in the human metabolic network. *Nat Biotechnol* 31, 522-529.

Jeon, S.M., Chandel, N.S., and Hay, N. (2012). AMPK regulates NADPH homeostasis to promote tumour cell survival during energy stress. *Nature* 485, 661-665.

Jose, C., Bellance, N., and Rossignol, R. (2011). Choosing between glycolysis and oxidative phosphorylation: a tumor's dilemma? *Biochim Biophys Acta* 1807, 552-561.

Joshi, B., Li, L., Taffe, B.G., Zhu, Z., Wahl, S., Tian, H., Ben-Josef, E., Taylor, J.D., Porter, A.T., and Tang, D.G. (1999). Apoptosis induction by a novel anti-prostate cancer compound, BMD188 (a fatty acid-containing hydroxamic acid), requires the mitochondrial respiratory chain. *Cancer Res* 59, 4343-4355.

Kall, L., Canterbury, J.D., Weston, J., Noble, W.S., and MacCoss, M.J. (2007). Semi-supervised learning for peptide identification from shotgun proteomics datasets. *Nat Methods* 4, 923-925.

Kang, D., Kim, S.H., and Hamasaki, N. (2007). Mitochondrial transcription factor A (TFAM): roles in maintenance of mtDNA and cellular functions. *Mitochondrion* 7, 39-44.

King, A., Selak, M.A., and Gottlieb, E. (2006). Succinate dehydrogenase and fumarate hydratase: linking mitochondrial dysfunction and cancer. *Oncogene* 25, 4675-4682.

Krishnan, K.J., Reeve, A.K., Samuels, D.C., Chinnery, P.F., Blackwood, J.K., Taylor, R.W., Wanrooij, S., Spelbrink, J.N., Lightowers, R.N., and Turnbull, D.M. (2008). What causes mitochondrial DNA deletions in human cells? *Nature genetics* 40, 275-279.

Kulms, D., and Schwarz, T. (2002). Independent contribution of three different pathways to ultraviolet-B-induced apoptosis. *Biochem Pharmacol* 64, 837-841.

Latonen, L., and Laiho, M. (2005). Cellular UV damage responses--functions of tumor suppressor p53. *Biochim Biophys Acta* 1755, 71-89.

Liu, S.L., Lin, X., Shi, D.Y., Cheng, J., Wu, C.Q., and Zhang, Y.D. (2002). Reactive oxygen species stimulated human hepatoma cell proliferation via cross-talk between PI3-K/PKB and JNK signaling pathways. *Arch Biochem Biophys* 406, 173-182.

Loffler, M., Jockel, J., Schuster, G., and Becker, C. (1997). Dihydroorotat-ubiquinone oxidoreductase links mitochondria in the biosynthesis of pyrimidine nucleotides. *Mol Cell Biochem* 174, 125-129.

Millau, J.F., Raffin, A.L., Caillat, S., Claudet, C., Arras, G., Ugolin, N., Douki, T., Ravanat, J.L., Breton, J., Oddos, T., *et al.* (2008). A microarray to measure repair of damaged plasmids by cell lysates. *Lab Chip* 8, 1713-1722.

Modica-Napolitano, J.S., and Singh, K.K. (2002). Mitochondria as targets for detection and treatment of cancer. *Expert Rev Mol Med* 4, 1-19.

Mullen, A.R., Hu, Z., Shi, X., Jiang, L., Boroughs, L.K., Kovacs, Z., Boriack, R., Rakheja, D., Sullivan, L.B., Linehan, W.M., *et al.* (2014). Oxidation of alpha-ketoglutarate is required for reductive carboxylation in cancer cells with mitochondrial defects. *Cell Rep* 7, 1679-1690.

Petros, J.A., Baumann, A.K., Ruiz-Pesini, E., Amin, M.B., Sun, C.Q., Hall, J., Lim, S., Issa, M.M., Flanders, W.D., Hosseini, S.H., *et al.* (2005). mtDNA mutations increase tumorigenicity in prostate cancer. *Proceedings of the National Academy of Sciences of the United States of America* 102, 719-724.

Raj, D., Brash, D.E., and Grossman, D. (2006). Keratinocyte apoptosis in epidermal development and disease. *The Journal of investigative dermatology* 126, 243-257.

Ravanat, J.L., Douki, T., and Cadet, J. (2001). Direct and indirect effects of UV radiation on DNA and its components. *J Photochem Photobiol B* 63, 88-102.

Rezvani, H.R., Dedieu, S., North, S., Belloc, F., Rossignol, R., Letellier, T., de Verneuil, H., Taieb, A., and Mazurier, F. (2007). Hypoxia-inducible factor-1alpha, a key factor in the keratinocyte response to UVB exposure. *The Journal of biological chemistry* 282, 16413-16422.

Rezvani, H.R., Kim, A.L., Rossignol, R., Ali, N., Daly, M., Mahfouf, W., Bellance, N., Taieb, A., de Verneuil, H., Mazurier, F., *et al.* (2011a). XPC silencing in normal human keratinocytes triggers metabolic alterations that drive the formation of squamous cell carcinomas. *Journal of Clinical Investigation* 121, 195-211.

Rezvani, H.R., Kim, A.L., Rossignol, R., Ali, N., Daly, M., Mahfouf, W., Bellance, N., Taieb, A., de Verneuil, H., Mazurier, F., *et al.* (2011b). XPC silencing in normal human keratinocytes triggers metabolic alterations that drive the formation of squamous cell carcinomas. *The Journal of clinical investigation* 121, 195-211.

Rezvani, H.R., Mazurier, F., Cario-Andre, M., Pain, C., Ged, C., Taieb, A., and de Verneuil, H. (2006). Protective effects of catalase overexpression on UVB-induced apoptosis in normal human keratinocytes. *The Journal of biological chemistry* 281, 17999-18007.

Rezvani, H.R., Rossignol, R., Ali, N., Benard, G., Tang, X., Yang, H.S., Jouary, T., de Verneuil, H., Taieb, A., Kim, A.L., *et al.* (2011c). XPC silencing in normal human keratinocytes triggers metabolic alterations through NOX-1 activation-mediated reactive oxygen species. *Biochim Biophys Acta* 1807, 609-619.

Shi, L.Z., Wang, R., Huang, G., Vogel, P., Neale, G., Green, D.R., and Chi, H. (2011). HIF1alpha-dependent glycolytic pathway orchestrates a metabolic checkpoint for the differentiation of TH17 and Treg cells. *J Exp Med* 208, 1367-1376.

Singh, K.K., Kulawiec, M., Still, I., Desouki, M.M., Geradts, J., and Matsui, S. (2005). Inter-genomic cross talk between mitochondria and the nucleus plays an important role in tumorigenesis. *Gene* 354, 140-146.

Smolkova, K., Plecita-Hlavata, L., Bellance, N., Benard, G., Rossignol, R., and Jezek, P. (2011). Waves of gene regulation suppress and then restore oxidative phosphorylation in cancer cells. *Int J Biochem Cell Biol* 43, 950-968.

Tomlinson, I.P., Alam, N.A., Rowan, A.J., Barclay, E., Jaeger, E.E., Kelsell, D., Leigh, I., Gorman, P., Lamlum, H., Rahman, S., *et al.* (2002). Germline mutations in FH predispose to dominantly inherited uterine fibroids, skin leiomyomata and papillary renal cell cancer. *Nature genetics* 30, 406-410.

Ward, P.S., and Thompson, C.B. (2012). Metabolic reprogramming: a cancer hallmark even warburg did not anticipate. *Cancer cell* 21, 297-308.

White, R.M., Cech, J., Ratanasirintrawoot, S., Lin, C.Y., Rahl, P.B., Burke, C.J., Langdon, E., Tomlinson, M.L., Mosher, J., Kaufman, C., *et al.* (2011). DHODH modulates transcriptional elongation in the neural crest and melanoma. *Nature* 471, 518-522.

Wise, D.R., DeBerardinis, R.J., Mancuso, A., Sayed, N., Zhang, X.Y., Pfeiffer, H.K., Nissim, I., Daikhin, E., Yudkoff, M., McMahon, S.B., *et al.* (2008). Myc regulates a transcriptional program that stimulates mitochondrial glutaminolysis and leads to glutamine addiction. *Proceedings of the National Academy of Sciences of the United States of America* 105, 18782-18787.

Wu, M., Neilson, A., Swift, A.L., Moran, R., Tamagnine, J., Parslow, D., Armistead, S., Lemire, K., Orrell, J., Teich, J., *et al.* (2007). Multiparameter metabolic analysis reveals a close link between attenuated mitochondrial bioenergetic function and enhanced glycolysis dependency in human tumor cells. *Am J Physiol Cell Physiol* 292, C125-136.

Yeung, S.J., Pan, J., and Lee, M.H. (2008). Roles of p53, MYC and HIF-1 in regulating glycolysis - the seventh hallmark of cancer. *Cell Mol Life Sci* 65, 3981-3999.

Zhai, H., Song, B., Xu, X., Zhu, W., and Ju, J. (2013). Inhibition of autophagy and tumor growth in colon cancer by miR-502. *Oncogene* 32, 1570-1579.

Figure legends

Figure 1. UVB irradiation down-regulates the majority of proteins implicated in glycolysis, TCA cycle and fatty acid β -oxidation. Proteomic analysis was used to investigate the effects of chronic UVB irradiation on profile expression of several proteins in skin biopsies of SKH-1 mice. To this end, skin biopsies of mice irradiated for 2 months (Ir) and non-irradiated (nIr) counterparts were subjected to proteomic analysis. The quantity of each protein implicated in glycolysis, TCA cycle (**A**), fatty acid β -oxidation or fatty acid synthesis (**B**) was compared between Ir and nIr groups and the results are expressed as mean fold change of expression of each protein.

Figure 2. UVB irradiation results in a metabolic remodeling. SKH-1 mice exposed to chronic UVB irradiation for 8 weeks.

(**A-C**) Skin biopsies of irradiated mice consume less glucose (**A**), produce less lactate (**B**) and exhibit lack of increased extracellular acidification rate (ECAR) upon glucose exposure, reflecting absence of glycolytic flexibility (**C**).

(**D**) UVB-irradiated skin samples display increased basal oxygen consumption but are incapable of mounting oxygen consumption rate (OCR) upon supplementation with succinate.

(**E**) Kinetics of OCR response to palmitate indicates a significant decrease of fatty acid oxidation in irradiated skin biopsies.

(**F-G**) [$1-^{13}\text{C}$] labeled glucose has been injected into irradiated and non-irradiated mice. While glutamate is labeled at carbon 4 in the first TCA cycle turn, carbons 2 and 3 are labeled in the second turn (**F**). C3/C4 ratio enrichment ratio, which is an indicator of TCA flux, is decreased in irradiated mice (**G**).

N=15 mice for each group [(A-E)] and 4 mice [(G)] . *P< 0.05 and **<0.01 for irradiated versus non-irradiated mice.

Dig, Digitonin; Oligo, oligomycin; DNP, 2,4-dinitrophenol; E, etomoxir.

Figure 3. UVB irradiation leads to the activation of OXPHOS complexes III, IV and V.

(**A**) UVB irradiation is associated with an increased basal oxygen consumption rate (OCR) and a decreased ECAR.

(**B-C**) ROS levels in irradiated and non-irradiated skin samples were measured by flow cytometry using cytoplasmic- (**B**) and mitochondrial-specific probes (**C**). The mean of ROS level in the non-irradiated samples was arbitrarily set to 100. Results are then assessed and expressed as the mean \pm SD.

(D) Increased OCR in UVB-irradiated skin samples is blocked when samples are treated with inhibitors of complexes III and IV (i.e antimycin and sodium azide).

(E-H) UVB irradiation results in over-activation of complex III and IV **(E)**, increased ATP synthesis **(F)**, elevation of ADP/ATP ratio **(G)** and increased proportion of oxygen used for ATP synthesis (ATP turnover).

N=15 for each group. *P< 0.05 and **<0.01 for irradiated versus non-irradiated mice.

Figure 4. UVB irradiation leads to the overactivation of dihydroorotate dehydrogenase (DHODH) which triggers increased ETC activation and ATP synthesis

(A-B) Skin biopsies of mice irradiated for 2 months (Ir) and non-irradiated (nIr) counterparts were subjected to proteomic analysis. The quantity of each protein implicated in de novo pyrimidine synthesis **(A)** and de novo purine synthesis **(B)** was compared between nIr and Ir groups and the results are expressed as mean fold change of expression of each protein.

(C) UVB irradiation leads to upregulation of DHODH. Treatment of mice with leflunomide (LFN), an inhibitor of DHPDH, blocks this overactivation.

(D-E) LFN treatment blocks UVB exposure-mediated increased ATP synthesis **(D)** and basal OCR **(E)** in mouse skin.

(F) UVB-irradiated skin samples display increased OCR level upon supplementation with dihydroorotic acid.

N=6 mice per group [(A-B)] and 12 per group [(C-F)]. *P< 0.05 and **<0.01 for irradiated versus non-irradiated mice.

Figure 5. UVB exposure-mediated DHODH overactivation is blocked upon epidermal ablation of mitochondrial transcription factor A (*Tfam*)

(A-B) Epidermal ablation of *Tfam* results in downregulation of mitochondrial-encoded enzymes, DHODH expression **(A)** as well as DHODH activity **(B)**.

(C) *Tfam* ablated mice (K-*Tfam*^{-/-}) and their control counterparts (K-*Tfam*^{+/+}) were subjected to chronic UVB irradiation and skin biopsies were done at indicated times. Histopathology of epidermis was evaluated with H&E staining. Differentiation status of epidermis was assessed using immunofluorescence staining of K10, filaggrin, loricrin. Proliferation was evaluated by Ki67 immunostaining. The nuclei were marked in blue with DAPI.

Figure 6. A keratinocyte-specific knockout of *Tfam* results in early UVB exposure phenotype without tumor formation

(A-D) *Tfam* ablated mice (K-*Tfam*^{-/-}) and their control counterparts (K-*Tfam*^{+/+}) were subjected to chronic UVB irradiation. On K-*Tfam*^{+/+} mice, variable number of tumors of variable size mostly ulcerated are seen. Some mild pigmentation of UV treated areas are also observed on some mice. The back of K-*Tfam*^{-/-} mice is covered by a large squame with evidence of peripheral desquamation and there is also evidence of punctiform or larger erosions in the larger squamous lesion. Mild erythema and pigmentation are also observed on squamous area (A). The number of mice harbouring desquamative features or tumors (B), the number (C), and the volume (D) of tumors per mouse have been assessed (mean±SD) at indicated times.

N=15 for each group. *P< 0.05 and **<0.01 for irradiated versus non-irradiated mice.

Figure 7. *Tfam* ablation or leflunomide treatment results in downregulation of DNA repair capacity

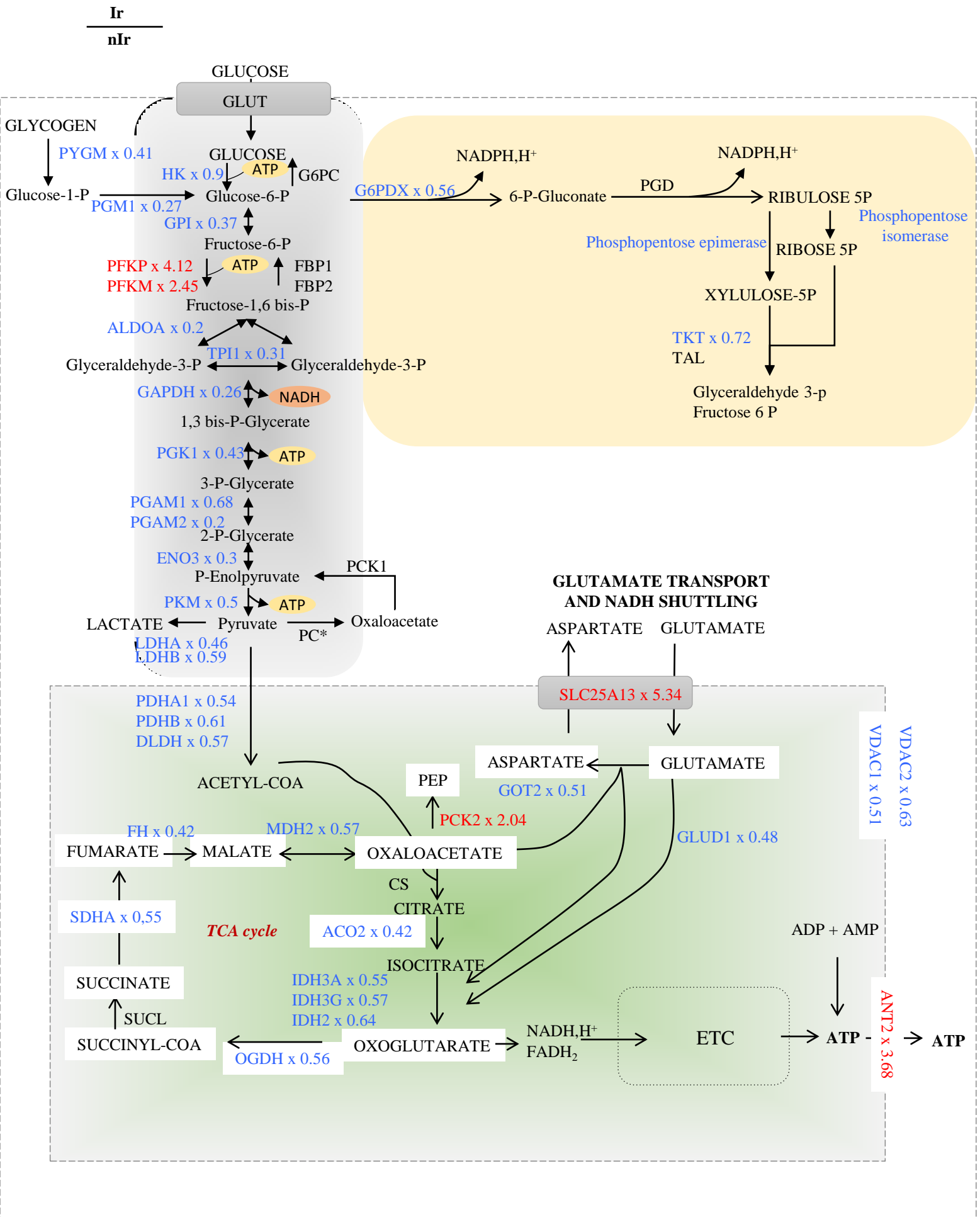
(A-B) Immuno-dot blot (A) and HPLC-MS/MS (B) analysis indicate that the quantity of cyclopyrimidine dimer (CPD) is higher in skin samples of *Tfam*-ablated mice and LFN-treated mice upon chronic UVB irradiation compared with control mice.

(C) The capacity of CPD excision and the re-synthesis is lower in *Tfam*-ablated or LFN-treated mice than control mice.

Error bars are SD from 6 mice per group [(B) to (C)], three experiments [(D) to (F)], or two experiments (H). *P < 0.05 by t test are for the difference between the *Tfam* ablated or LFN-treated mice with control mice.

Glycolysis, PPP pathway and TCA cycle

Figure 1A



β oxidation & fatty acid synthesis

Figure 1B

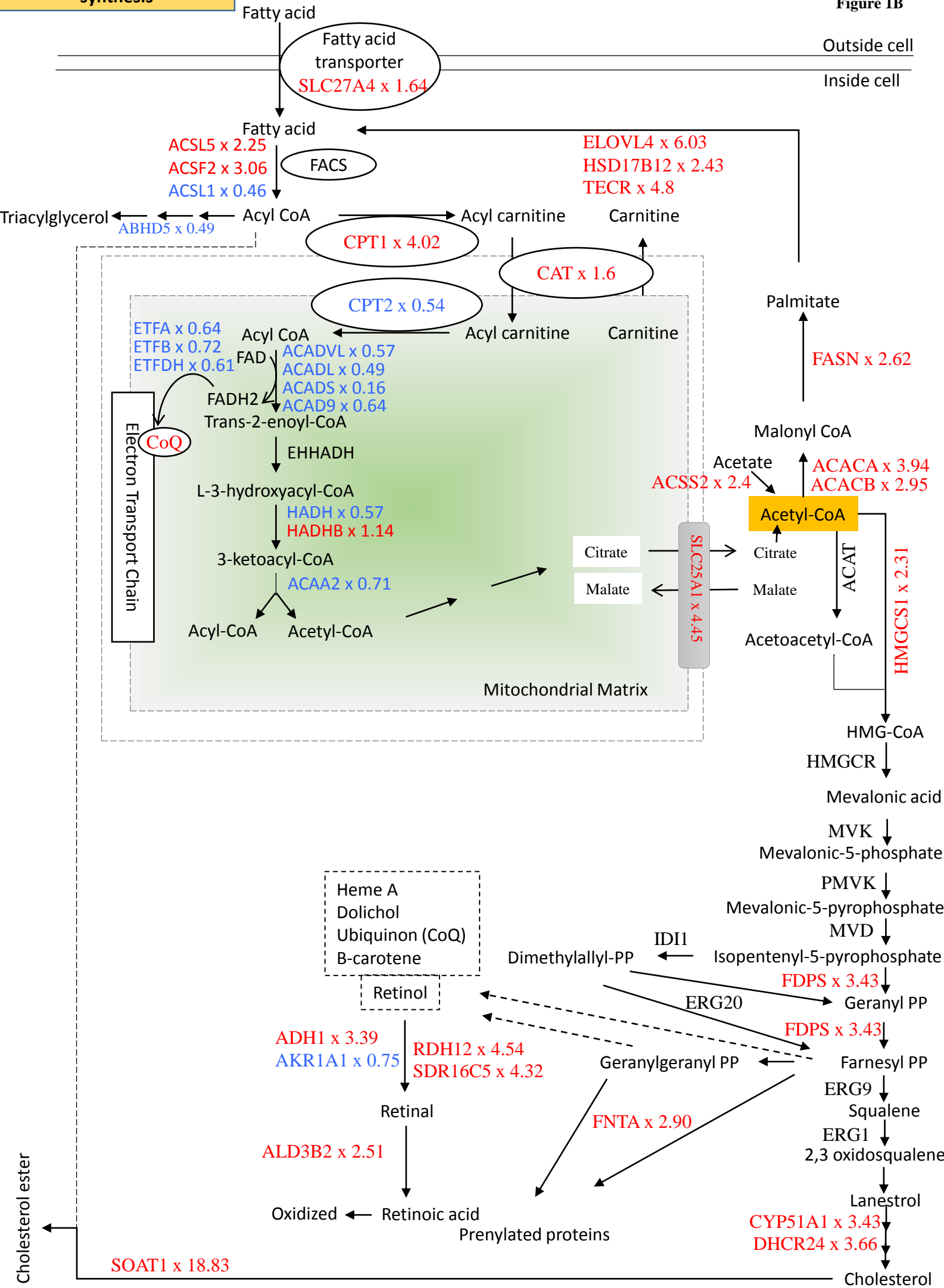
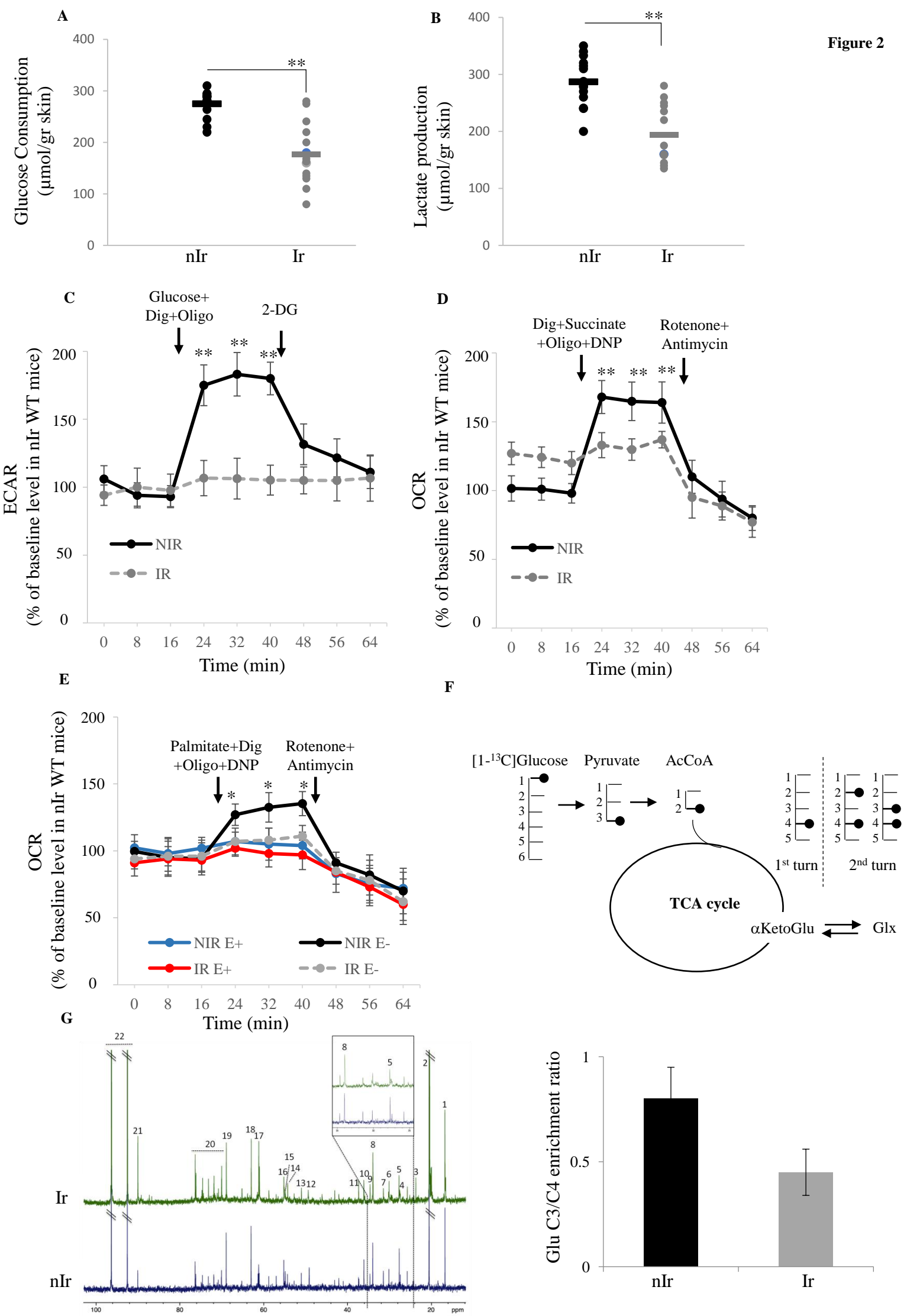
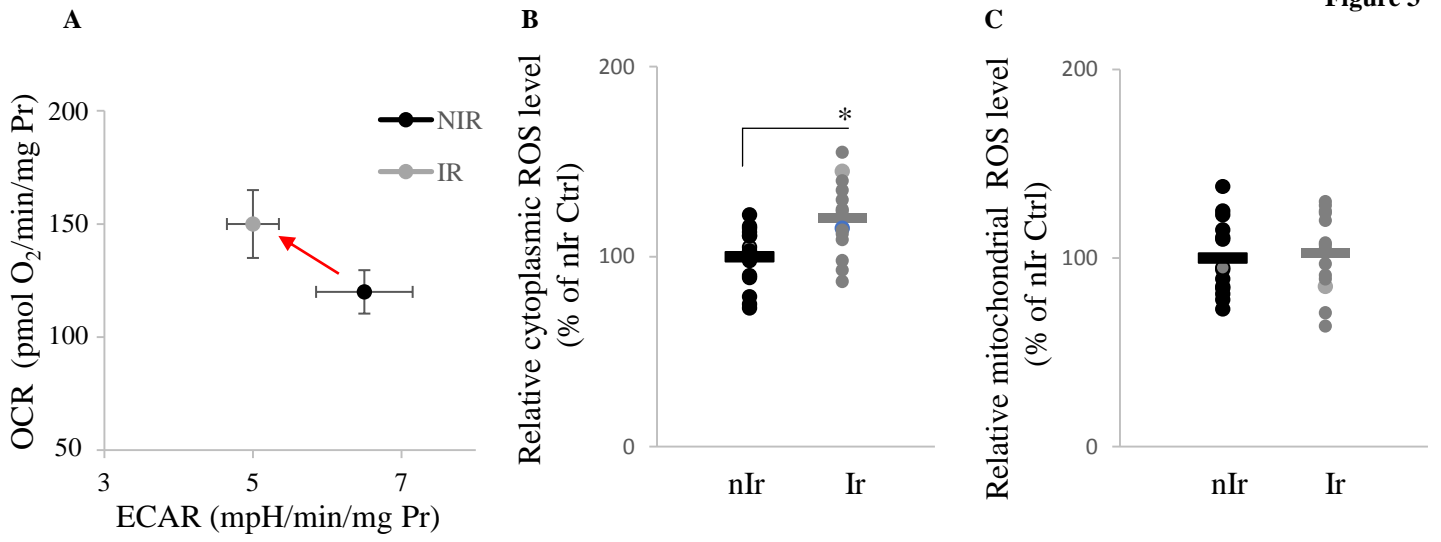
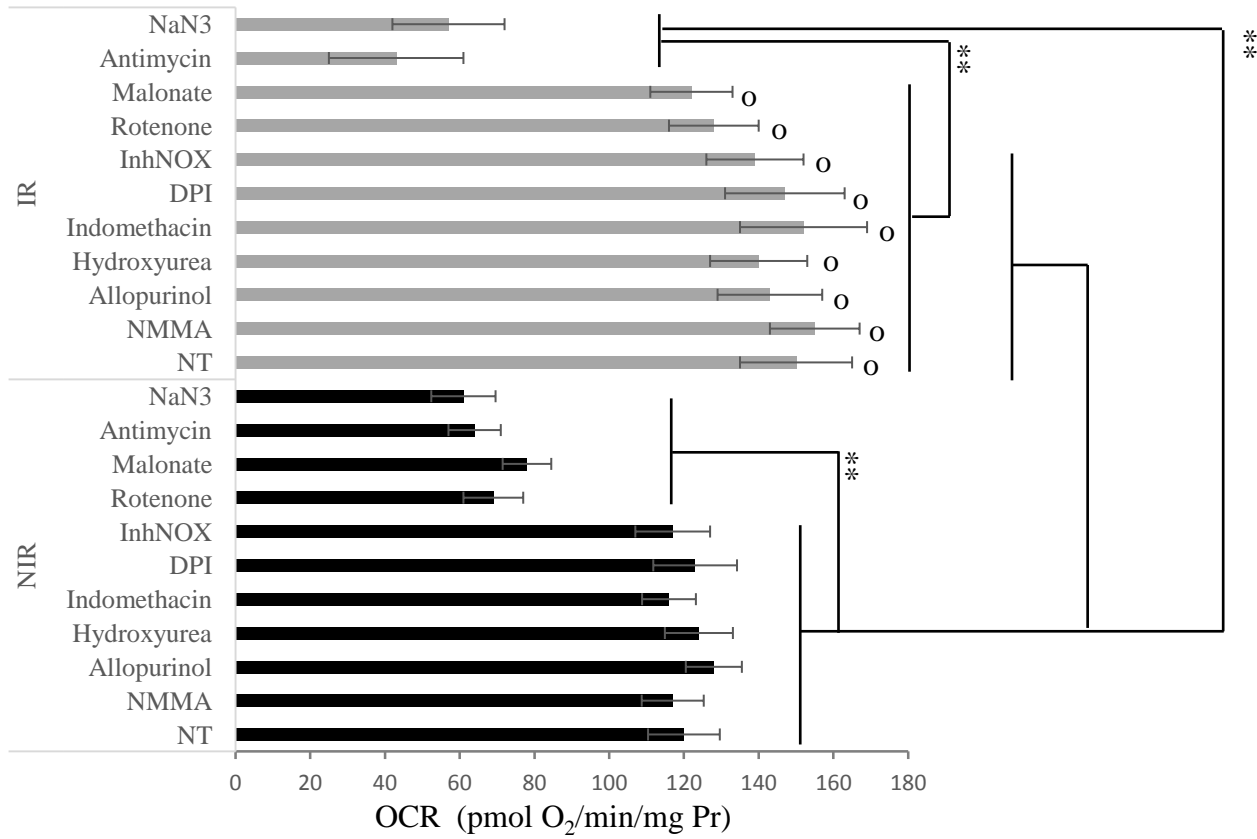


Figure 2

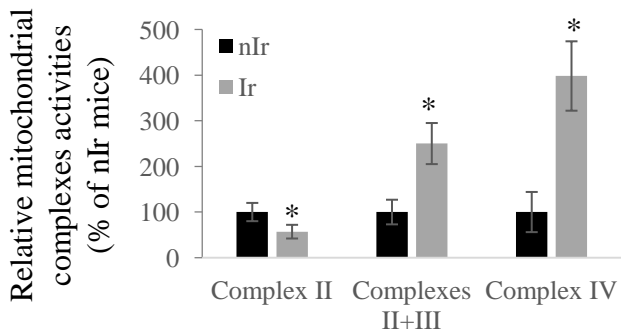




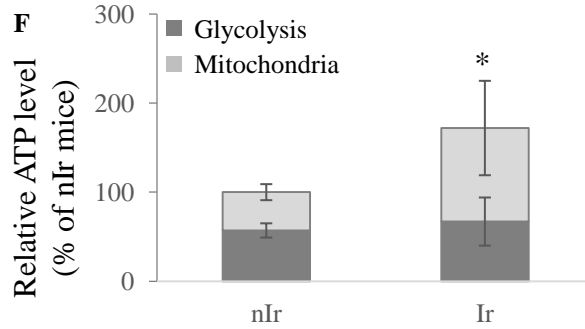
D



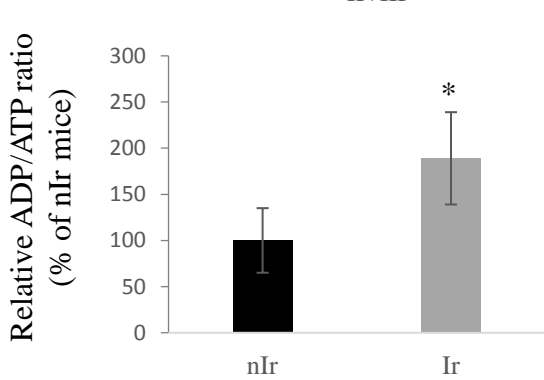
E



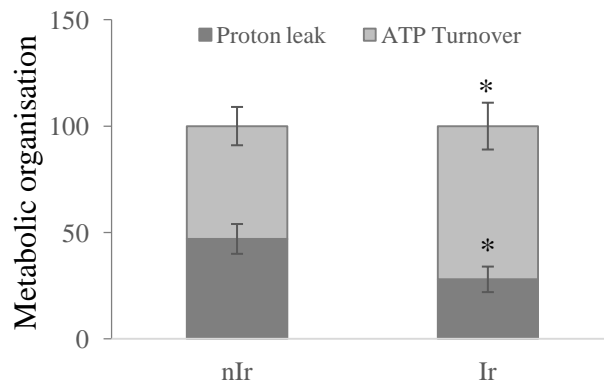
F



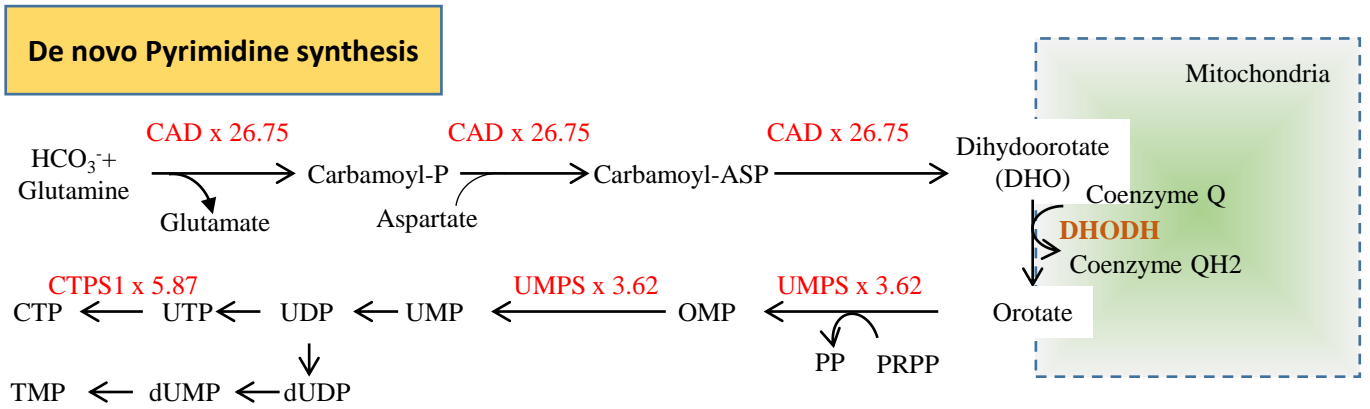
G



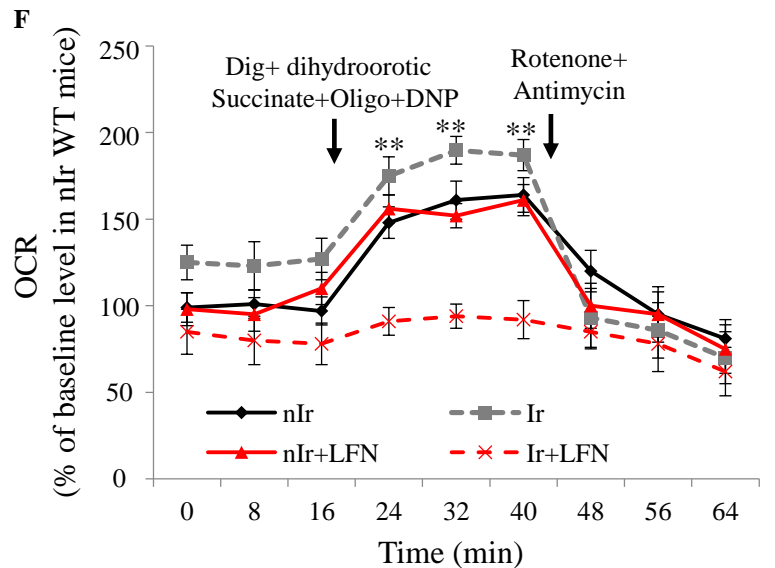
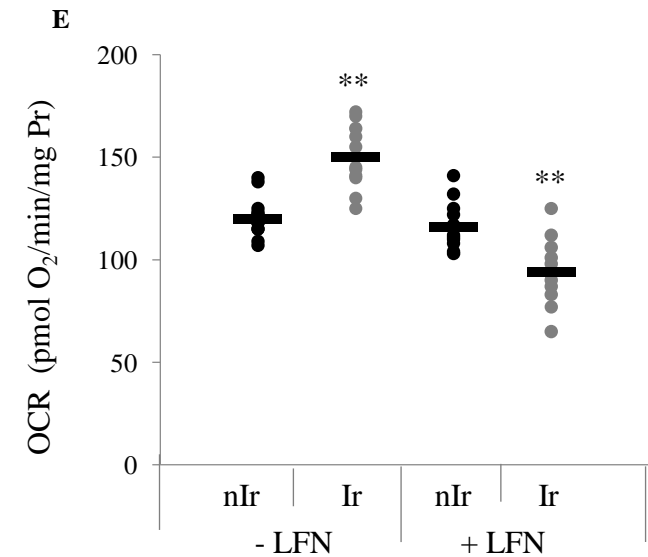
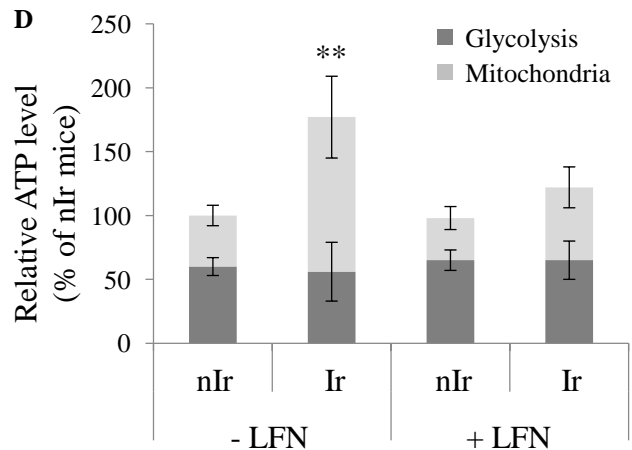
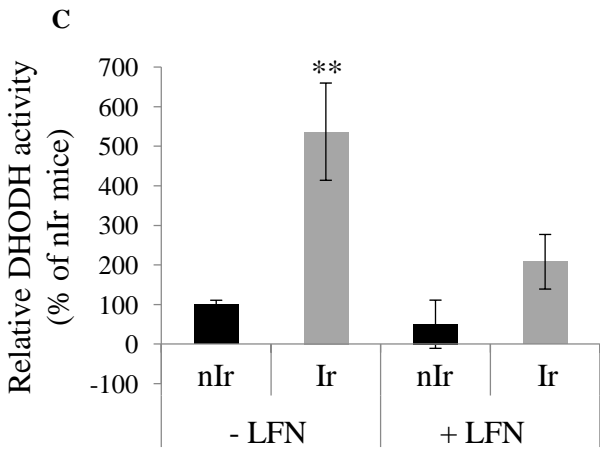
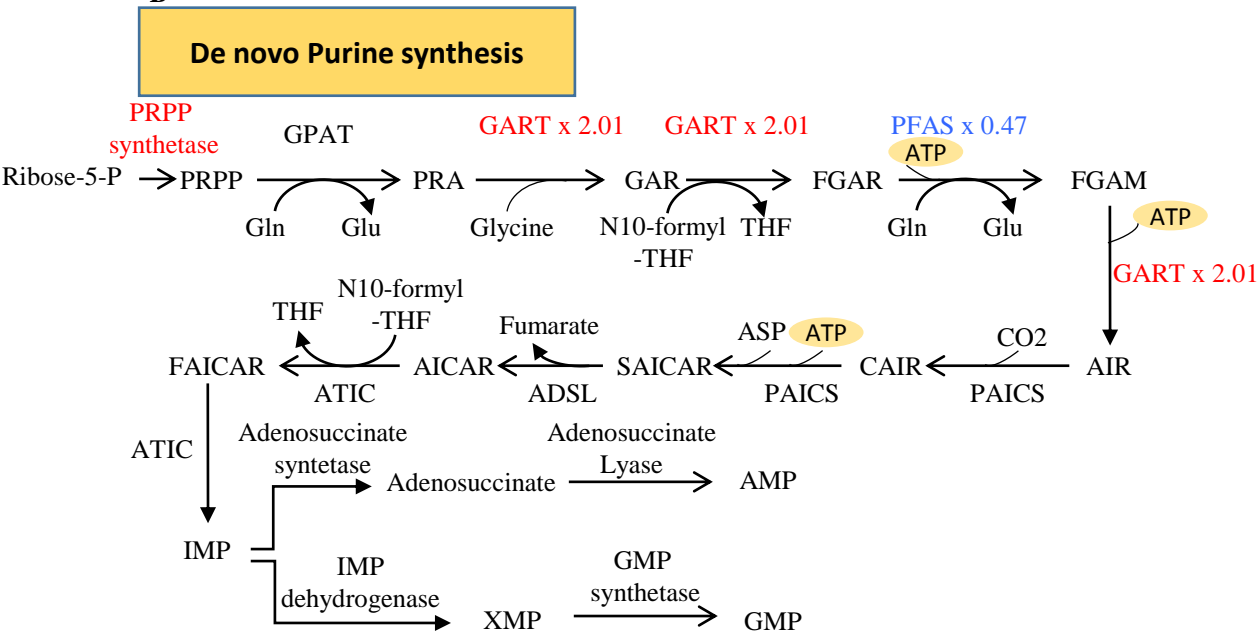
H



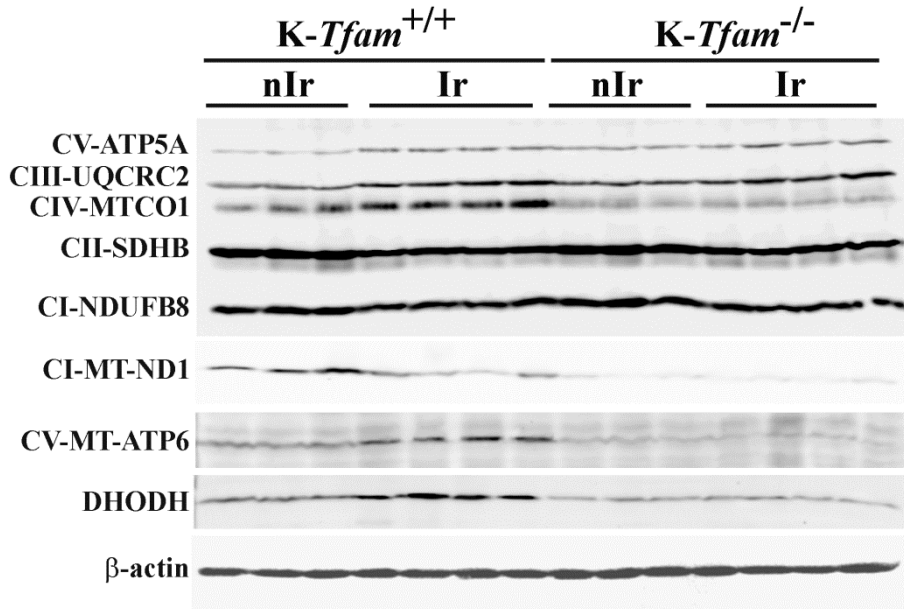
A



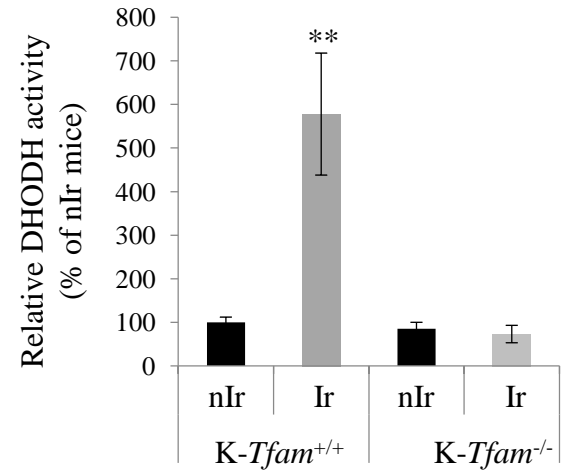
B



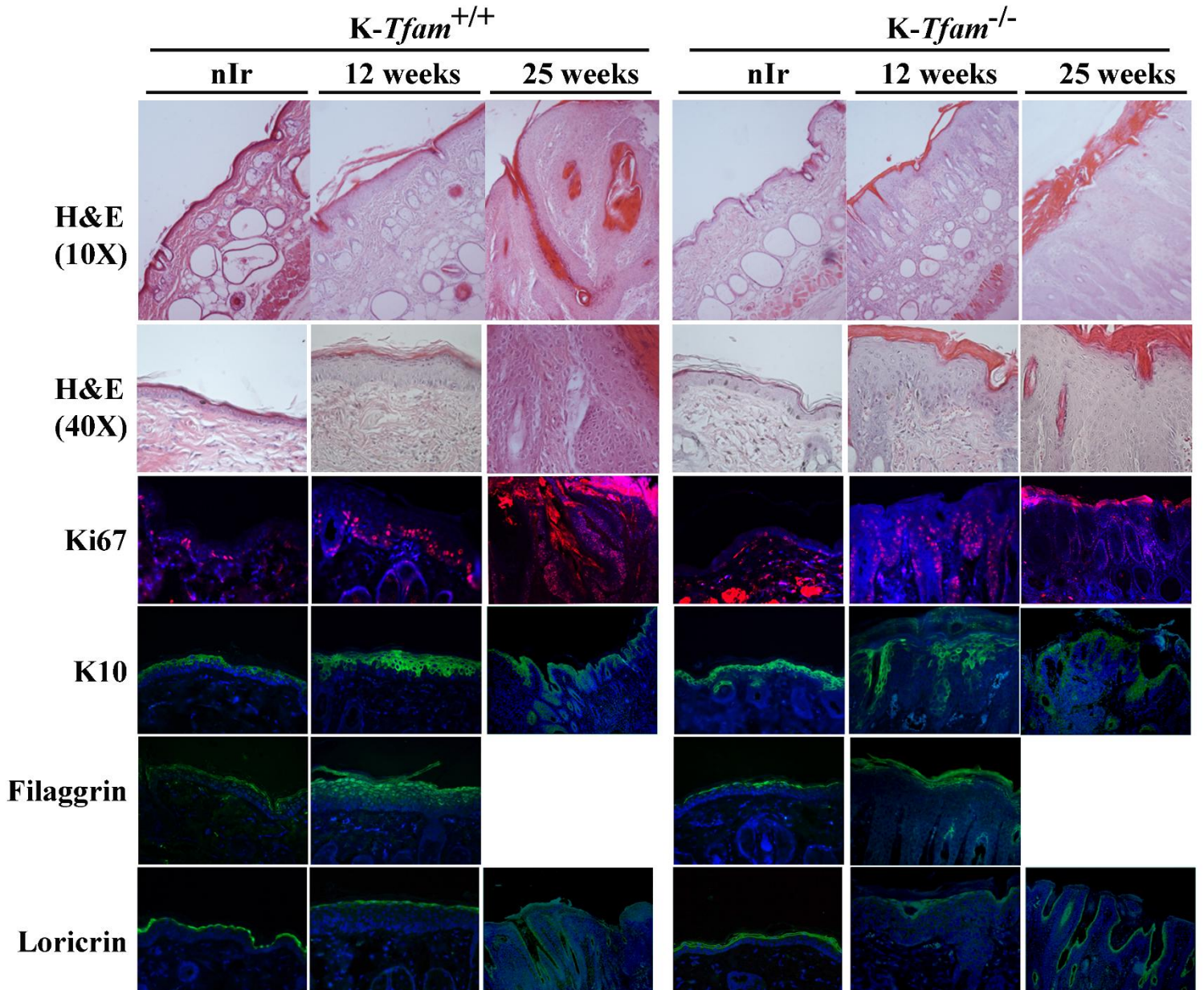
A



B



C



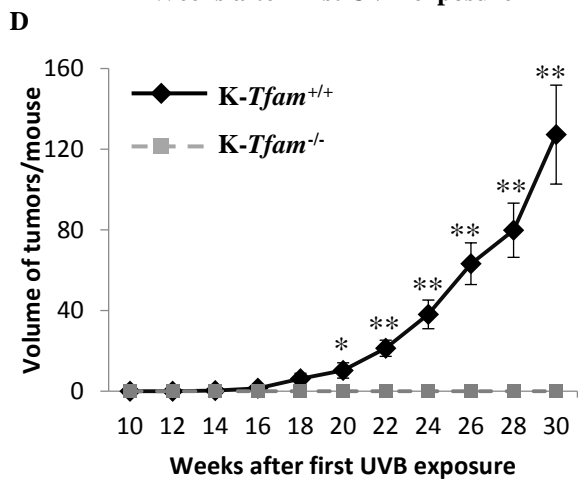
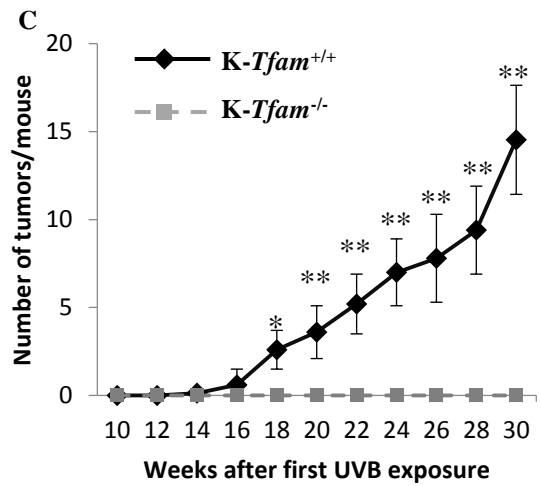
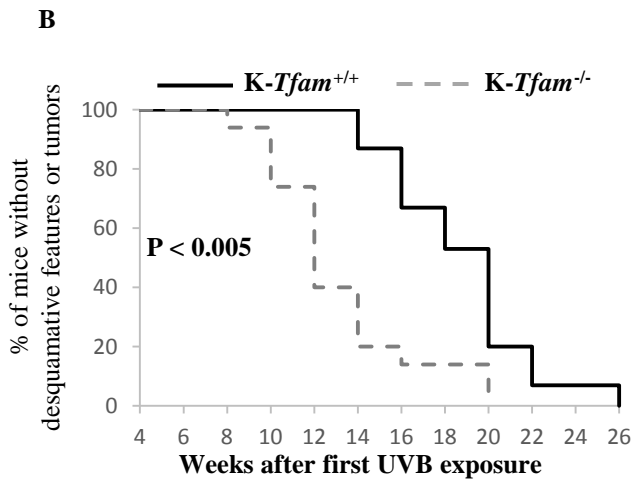
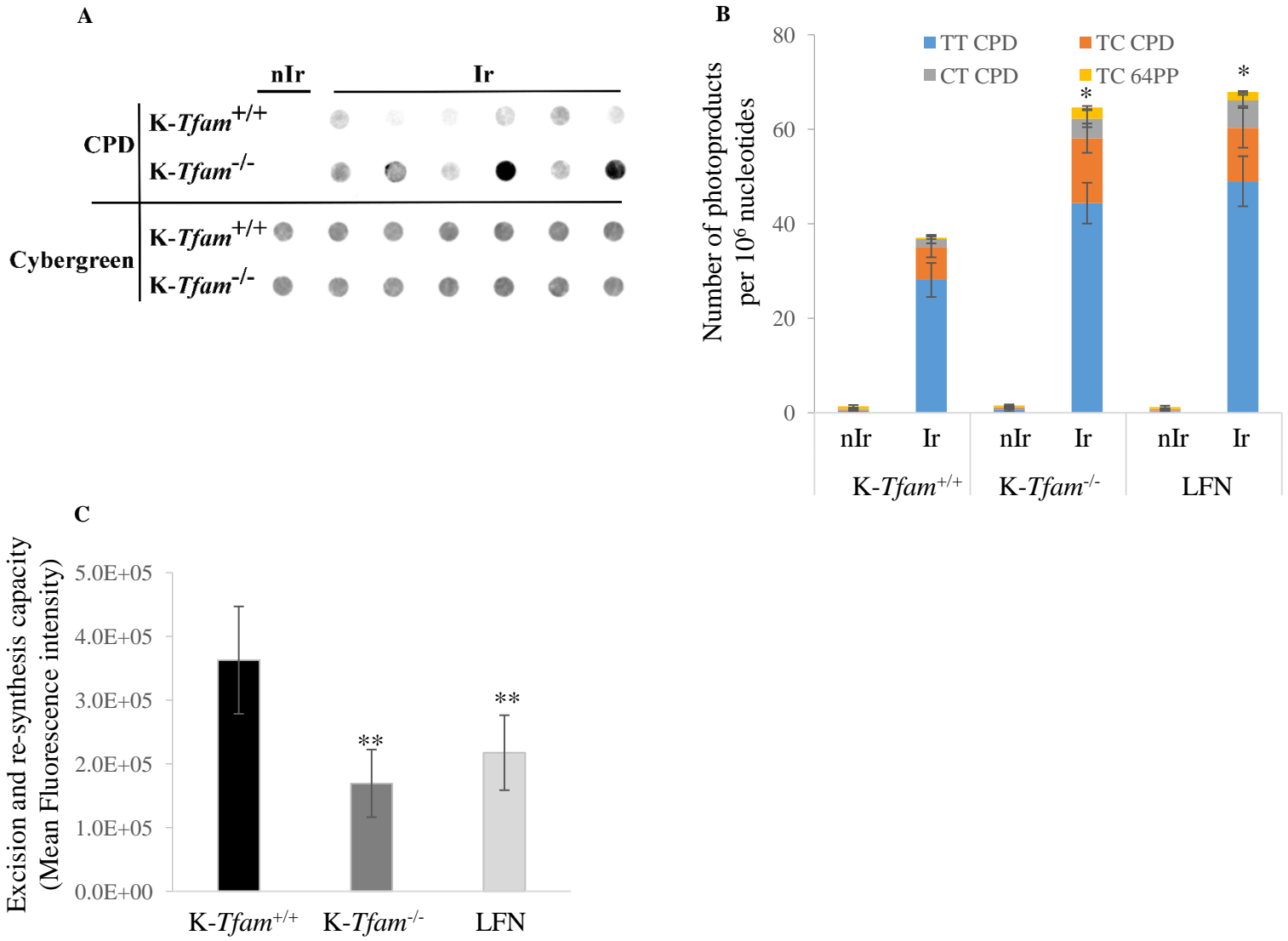


Figure 7



Article 5

Skin reconstruction

In the light of the work we did on metabolism and UV, we got curious to examine the effect of other metabolism modulators on UV-induced carcinogenesis. However, as preparing transgenic mice model in SKH-1 genetic background is completely time-consuming, we sought to find an alternative model for SKH-1 models as a valuable tool in skin cancer studies. To this end, all existing models were reviewed and the results are discussed in the following review article.

Skin equivalents: skin from reconstructions as models to study skin development and diseases

N. Ali,^{1,2,3} M. Hosseini,^{2,3} S. Vainio,¹ A. Taïeb,^{2,3,4,5} M. Cario-André^{2,3,4} and H.R. Rezvani^{2,3,4}

¹Laboratory of Developmental Biology, Faculty of Biochemistry and Molecular Medicine, University of Oulu and Biocenter Oulu, Aapistie 5A, 90220 Oulu, Finland

²Inserm U 1035, 33076 Bordeaux, France

³Université de Bordeaux, 146 rue Léo Saignat, 33076 Bordeaux, France

⁴Centre de Référence pour les Maladies Rares de la Peau, Bordeaux, France

⁵Département de Dermatologie & Dermatologie Pédiatrique, CHU de Bordeaux, Bordeaux, France

Summary

Correspondence

Hamid Reza Rezvani.

E-mail: hamid-reza.rezvani@u-bordeaux.fr

Accepted for publication

1 April 2015

Funding sources

H.R.R. gratefully acknowledges support from the Association pour la Recherche sur le Cancer and the Institut National du Cancer 'INCA_6654'.

Conflicts of interest

None declared.

DOI 10.1111/bjd.13886

While skin is readily available for sampling and direct studies of its constituents, an important intermediate step is to design *in vitro* and/or *in vivo* models to address scientific or medical questions in dermatology and skin biology. Pioneered more than 30 years ago, human skin equivalents (HSEs) have been refined with better cell culture techniques and media, together with sophisticated cell biology tools including genetic engineering and cell reprogramming. HSEs mimic key elements of human skin biology and have been instrumental in demonstrating the importance of cell–cell interactions in skin homeostasis and the role of a complex cellular microenvironment to coordinate epidermal proliferation, differentiation and pigmentation. HSEs have a wide field of applications from cell biology to dermocosmetics, modelling diseases, drug development, skin ageing, pathophysiology and regenerative medicine. In this article we critically review the major current approaches used to reconstruct organotypic skin models and their application with a particular emphasis on skin biology and pathophysiology of skin disorders.

What's already known about this topic?

- Human skin equivalents are being used for different purposes from cell–cell interactions to modelling diseases.

What does this study add?

- We have critically reviewed the various methods for the reconstruction of epidermis.
- We provide an update of the different applications of skin equivalents in skin biology and dermatology.

The skin is the largest organ in humans and serves as a major barrier that, among other functions, prevents the invasion of pathogens, limits chemical and physical aggressions and regulates the loss of water and electrolytes.¹ It is a complex organ composed of the epidermis and its appendages (hair follicles, sebaceous glands and sweat glands), which are separated from the dermis by a basement membrane (BM) consisting primarily of laminins and collagens.² The epidermis is a highly dynamic stratified epithelium made principally from ectodermal-derived keratinocytes, which constitute about 90% of

epidermal cells. New differentiating keratinocytes continuously emerge from the proliferative basal layer of the epidermis to replenish the upper layers, progressively differentiating into the external cornified and desquamating dead envelope. In addition to keratinocytes, the epidermis contains a minority of functionally important cells of nonectodermal origin, including neural crest melanocytes, bone marrow-derived Langerhans cells (antigen-presenting cells) and Merkel cells.

The dermis is a thick connective tissue providing tension, strength and elasticity to the skin through an extracellular

matrix (collagen, elastin and extracellular matrix). In addition to nerve terminations and vessels, the dermis is composed of three major cell types: fibroblasts, macrophages and adipocytes. It also contains epidermal appendages (hair follicles, sebaceous gland and sweat glands).³

Various cell types constituting the skin have been studied individually using two-dimensional (2D) monolayer cultures. However, these monolayer tissue cultures fail to capture the relevant complexity of the *in vivo* microenvironment and cell–cell interactions that considerably affect the responses of cells to different stimuli. In fact, growing evidence indicates that there are significant differences in phenotype, cell migration, proliferative capacity, cell surface receptor expression, extracellular matrix synthesis, cellular signalling, metabolic functions and responses to various stimuli when the same cells are grown under 2D or three-dimensional (3D) culture conditions.^{4–11} To approach *in vivo* conditions, skin histocultures (also called skin explants), which are obtained by putting the intact skin samples containing all resident skin cells (such as immune and neuronal cells) into growth medium either with a collagen gel support or simply free-floating, have been widely used and improved over time (e.g. histocultures that allow longer experimentation time than traditional explants).

Skin histocultures have many uses, ranging from testing drug sensitivity to designing effective individualized therapies for each patient.^{12–19} However, this model has several drawbacks including (i) a limitation in the number and size of skin histocultures, (ii) the complexity owing to the presence of all resident skin cells resulting in their inherent heterogeneity, which cannot be experimentally controlled and (iii) difficulties in the uniform genetic manipulation. These limitations restrict the use of these models and indicate the need to develop a new 3D *in vitro* system that allows a more detailed study of the basic molecular processes affecting skin physiology and pathophysiology. Therefore, the reconstitution of 3D human skin equivalents (HSEs) using both dermal and epidermal components is a relevant strategy to answer the physiological questions that cannot be solved solely in the context of monolayer tissue culture or skin explants/histocultures. Furthermore, HSEs, which have been developed and improved over the last 30 years, present time- and cost-effective alternatives to the use of laboratory animals, especially mice, which have a skin architecture that is ill-suited to human studies. Indeed, mouse epidermis is much thinner than human epidermis (only three layers in adult murine epidermis compared with generally six to 10 layers in human epidermis). Secondly, mouse epidermis is densely packed with hair follicles, whereas human epidermis possesses larger interfollicular regions. Thirdly, mouse melanocytes reside mainly in dermal hair follicles, while human melanocytes are located in the basal layer of the epidermis. Fourthly, a cutaneous muscle layer (i.e. the panniculus carnosus) is present in mouse skin but absent from human dermis.²⁰

In this article we critically review the various techniques for human skin reconstruction and their current and future fields of application to skin physiology and diseases.

Aims to constitute human skin *in vivo*

In vitro reconstruction of human skin

In 1960, Cruickshank *et al.* demonstrated that when the epidermal keratinocytes of adult guinea pig were seeded at high density, they grew in culture even in the absence of the normal underlying dermal connective tissue.²¹ However, in subculture the cells had a tendency to differentiate. A critical step forward was made in 1975 when Rheinwald and Green generated cell colonies that had originated from an isolated founder keratinocyte. This was achieved by using lethally irradiated 3T3 fibroblasts as feeders.²² This technology enabled the production of large quantities of keratinocytes and their expansion in *in vitro* cell culture conditions. Pioneering 3D epidermal reconstruction, Freeman *et al.* developed a method in which human epidermal cells were cultured on decellularized pig dermis.²³ A small piece of human skin containing both epidermis and superficial dermis was put on the top of the dead pig dermis used as dermal substrate. Only epidermal keratinocytes attached to the dermis, allowing the growth of pure keratinocytes associated with a good level of differentiation. A better differentiated epidermis was then produced by Lillie *et al.* and Fusenig *et al.* when they placed the cultured keratinocytes on collagen membranes at the air–liquid interface.^{24,25} More complete differentiation was obtained by Prunieras *et al.* using human de-epidermized dermis (DED)²⁶ rather than dead pig dermis.²³

Since then, the production of skin equivalents (SEs) at the air–liquid interface has been achieved by different methods in which the principal difference is the dermal equivalents, which can be acellular or cellular structures. An inert filter^{27–30} or DED can be used as acellular dermal substrate.^{26,31–36} Reconstruction of epidermis using acellular DED requires the removal of the epidermis that preserves the BM, followed by dermal sterilization with glycerol, ethylene oxide, alcohol or gamma irradiation. After sterilization, the formerly epidermal side of the DED is seeded with keratinocytes. Following an immersion period during which the cells proliferate, the dermis is placed at the air–liquid interface, thereby inducing keratinocyte differentiation and the formation of a stratified epidermis (Fig. 1a).^{26,31–36} In the alternative techniques, a cellular substrate composed of fibroblast-populated DED or collagen matrix can be used as dermal equivalents.^{37–41} With this technique, the dermal equivalent is prepared by mixing a collagen solution with human dermal fibroblasts or by seeding fibroblasts on the subcutaneous side of the DED. After contraction, this support is seeded with normal human epidermal keratinocytes. The culture is initially maintained in submerged conditions allowing the proliferation of cells, before being placed on a grid at the air–liquid interface resulting in keratinocyte differentiation and the formation of a horny layer (Fig. 1a). It should be noted that other cell types can be incorporated into the epidermal (including melanocytes and Langerhans cells) or the dermal compartments (including fibroblasts and lymphocytes) to obtain a more complete physiological system.^{35,36,42–45} However, the

incorporation of immune cells is poorly reproducible. It is worth mentioning that epidermis reconstructed on an acellular dermal substrate contains only three to four viable stratified epidermal layers, so a successful reconstruction by this system needs the supplementation of medium with various growth factors including epidermal growth factor (EGF), keratinocyte growth factor, and/or insulin-like growth factor. The presence of fibroblasts in the dermal substrate stimulates the proliferation of keratinocytes, improves the epidermal morphology and enhances the formation of BM proteins.^{41,46,47}

The dermal substrate used in the reconstructed epidermis (RE) has an important impact on experimental studies. One of the main differences between epidermis reconstructed on DED or collagen matrix is the way in which the BM is formed. In skin reconstructed with DED, an intact BM and a papillary morphology of the epidermal–dermal junction (EDJ) zone is preserved, whereas in skin reconstructed with collagen matrix, a BM is produced by the fibroblasts and keratinocytes during the culture process⁴⁸ and the EDJ zone remains horizontal without rete ridges. Another important difference is that the composition of DED (which may contain various growth factors, proteases and cytokines) is not clearly defined and differences among individual donors need to be considered, thereby justifying the use of a similar dermis for a set of experiments.

Long-term maintenance of human skin equivalents and humanized mouse models

Following the seminal discovery of the method allowing the growth of keratinocytes as stratified cultures,²² their use as grafts was suggested⁴⁹ and they were introduced in 1981 for burn therapy.⁵⁰ Grafting epidermal sheets enriched in holoclone-forming keratinocytes provided evidence of the long-term survival of the grafts but failed to provide an immediate dermal replacement, resulting in possible wound contraction and graft fragility.⁵¹ To solve this problem, grafting of SEs was promoted for the therapy of burns, but no real breakthrough has been made.^{52–54}

In an attempt to maintain epidermal homeostasis and increase the lifespan of SE beyond 2–3 weeks, researchers implemented humanized skin mouse models. They consist of chimeric models in which skin of human origin is regenerated, vascularized and innervated by mouse vessels and nerves. For this purpose, two experimental protocols have been developed. The first is based on grafting either the RE (performed as described above)^{55–57} or split-thickness human skin obtained from volunteers^{58,59} on the back of athymic mice (Fig. 1b). The second is based on seeding cells directly on the back of mice. A silicon chamber is implanted on the back of severe combined immunodeficiency mice, then a slurry of keratinocytes and fibroblasts is placed in the chamber.^{25,26,60} The chamber is removed 1 week after grafting and humanized skin is formed at the grafting site in 2 weeks (Fig. 1c).⁶⁰

The main difference between these models lies in the development of BM. Compared with the RE engrafted onto the

back of mice, the human skin reconstructed by an injection of slurry cells has greater numbers of keratin intermediate filaments within the basal keratinocytes that are connected to hemidesmosomes, and more numerous connections of collagen filaments and anchoring fibrils to the lamina densa on the dermal side.⁶⁰ While the grafting of human skin samples has the advantage of maintaining BM, the EDJ zone and rete ridges, its implementation is technically difficult for the following reasons: (i) establishing the model requires large keratome sheets or multiple punch biopsies from volunteers or patients; (ii) the grafting needs to be performed quickly in order to minimize graft ischemia and (iii) uniform genetic manipulation of grafts is difficult. Indeed, humanized skin mouse models that use an isolation step and cell amplification offer the possibility of using *in vitro* genetically manipulated human keratinocytes, fibroblasts and/or melanocytes, thus generating transgenic or knockout humanized skin.

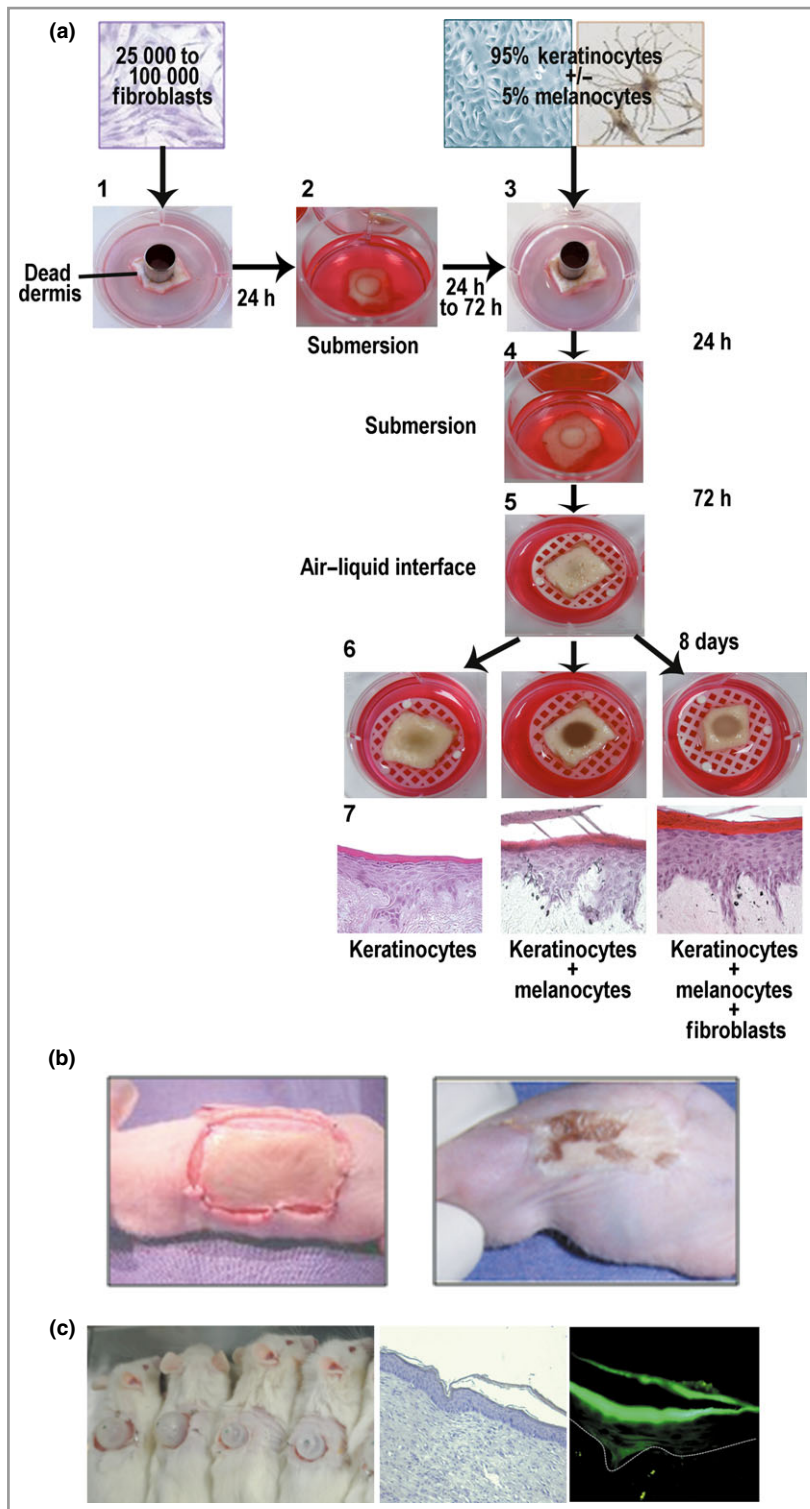
Applications of human skin reconstruction

The reconstruction of artificial HSEs has become an important tool for investigating skin physiology and pathophysiology. These models supply critical information about cell–cell interactions, the effects of the stromal environment on cell proliferation, differentiation and pigmentation. SEs are relevant models for testing dermocosmetics and drugs topically, and also for investigating photoageing and cancer. Furthermore, specific genetic alterations in either dermal or epidermal compartments, which can easily be achieved, facilitate mechanistic and signal transduction studies. These skin models also provide suitable alternatives to the use of laboratory animals. As a consequence, increasing numbers of commercially available skin models have reached the market, such as EpiDerm[®] (MatTek, Ashland, MA, U.S.A.), Episkin[®] (L’Oreal; SkinEthic, Nice, France), Apligraf[®] (Organogenesis Inc., Canton, MA, U.S.A.) and Labskin (Innovenn, Dublin, Ireland). The latter model uses a dermal component consisting of fibroblasts incorporated into a fibrin matrix and allows microorganisms to be grown on its surface, mimicking infection or the skin’s natural microflora.

Skin equivalents as a model for studying the effects of cell–cell interactions on skin homeostasis

Keratinocyte–fibroblast interactions and skin homeostasis

Fibroblasts influence skin homeostasis by affecting BM formation, in addition to keratinocyte proliferation and differentiation. The EDJ zone, which provides an adhesive and dynamic interface, is composed primarily of laminin, collagen, nidogen and perlecan. Studies of BM formation during skin reconstitution have shown that keratinocytes alone are capable of synthesizing the major components of BM (such as type IV collagen, type VII collagen and laminin) and depositing them in a polarized manner into the EDJ zone.^{48,61–63}



Fibroblasts affect BM formation through three mechanisms. Firstly, they secrete cytokines such as transforming growth factor (TGF)- β , which stimulates keratinocytes to synthesize BM components.⁴⁶ Secondly, fibroblasts are necessary for the assembly of an ultrastructurally complete BM. Thirdly, fibroblasts are capable of producing type IV collagen and type VII collagen, laminin-5 and

nidogen, which also contribute to BM formation.^{46,64} In addition to being involved in BM formation, fibroblasts are able to affect keratinocyte proliferation and differentiation.^{46,64,65} This effect is based on fibroblast density where an increase in fibroblast numbers in dermal equivalents with a minimal and maximal threshold leads to an improvement in epidermal architecture.⁴¹

Fig 1. *In vitro* and *in vivo* reconstruction of epidermis. (a) *In vitro* reconstruction of epidermis. (1) Dermal equivalent is prepared by seeding fibroblasts on the subcutaneous side of the dead dermis. (2) Twenty-four hour later, culture is immersed for a few days (24–72 h) to allow contraction. (3) Following immersion, the formerly epidermal side of the dead dermis is seeded with keratinocytes and melanocytes. (4) Culture is then immersed for a few days (up to 72 h) to allow cell proliferation. (5) Epidermis is then placed on grid at air–liquid interface resulting in keratinocyte differentiation and formation of horny layers. (6) As seen macroscopically, if melanocytes are included in reconstruction, the reconstructed epidermis (RE) is more pigmented. (7) Histology and immunohistology can be done on formalin-fixed, paraffin-embedded RE to verify the architecture of the epidermis or assess the expression of various proteins/markers. The panels show the general morphology of epidermis reconstructed with keratinocytes, keratinocytes + melanocytes and keratinocytes + melanocytes + fibroblasts following staining with haematoxylin and eosin. (b, c) Skin humanized mouse models. (b) *In vivo* human epidermal reconstruction can be carried out by grafting either human skin samples or skin equivalents reconstituted using the methods explained above onto the back of mice. The left panel shows the graft of human skin samples on the back of mice. The right panel indicates the macroscopic aspect of chimeric skin 1 month after graft. (c) *In vivo* human epidermal reconstruction can also be performed by adding a slurry containing human keratinocytes and fibroblasts into a silicone chamber implanted on the back of severe combined immunodeficiency mouse muscle fascia (left panel). The middle panel shows histology of humanized epidermis formed on the back of mice. In this experiment human keratinocytes transduced with a viral vector expressing green fluorescent protein (GFP) have been used. GFP expression is detected in epidermal part of regenerated human skin (right panel).

Keratinocyte–melanocyte interactions and their effects on pigmentation

Melanocytes, which are responsible for skin colour, are maintained in the basal layer through their interactions with (i) BM components owing to the presence of discoidin domain receptor (DDR)1 and integrin $\alpha 6\beta 1$ receptors (in the BM, these receptors interact with type IV collagen and laminins, respectively)^{66,67} and (ii) keratinocytes owing to the presence of E-cadherin.⁶⁷ These interaction leads to the transfer of melanosomes into the keratinocytes via the melanocyte dendrites.

When skin melanocytes are incorporated into SEs, they are spontaneously located in the basal layer in close contact with multiple keratinocytes, a localization similar to that in normal human skin. Detection of the melanosomes in different layers of the RE, and notably in the granular layer when dark melanocytes are used, further indicates that melanocytes are functional in RE.^{68,69} Using chimeric reconstructs (keratinocytes and melanocytes derived from phototypes II, III, IV, V or VI), melanocytes have been identified as the cells responsible for skin phototypes. Indeed, epidermal pigmentation is dependent on the phototype of melanocytes and is independent of the origin of keratinocytes.^{36,45,70–72} Stimulation of the RE by applying pigment modifiers such as 3-isobutyl-1-methyl-xanthine, α -melanocyte-stimulating hormone or ultraviolet (UV) irradiation has shown that the epidermal melanin unit in pigmented reconstructs function exactly as in the *in vivo* situation in terms of pigment production.^{73–78} Several studies have characterized the biological behaviour of melanocytes in skin reconstructs by focusing on melanin transfer, response to UV radiation exposure and DNA damage.^{36,70,76,79}

Fibroblast–melanocyte interactions and their effects on pigmentation

Direct evidence of dermal influence on pigmentation comes from clinical observations of the outcome of epidermal suspension transplantation surgery in vitiligo in autologous recipient

skin of different colours (e.g. nipple).⁷¹ When incorporated into pigmented SEs, fibroblasts have been found to play a key role in the control of pigmentation.^{71,80} In fact, when pigmented epidermal reconstructs are grafted onto the backs of mice, they develop a nonregular pigmentation pattern that is dependent on the presence of colonizing human or mouse fibroblasts.⁷¹ In agreement with this finding, treatment of pigmented epidermal reconstructs with conditioned medium from UVA-irradiated aged fibroblasts mimicked senile lentigo pathology, a disorder characterized by hyperpigmented areas in photo-exposed skin.⁸¹ Fibroblasts have been shown to affect pigmentation via various mechanisms. Fibroblasts secrete hepatocyte growth factor, basic fibroblast growth factor and stem cell factor, which bind to their receptors (i.e. c-Met, FGF-R and c-Kit, respectively) located on the plasma membrane of melanocytes, resulting in the activation of microphthalmia-associated transcription factor (MITF), the master regulator of pigmentation.^{82–85} Fibroblasts can also play an inhibitory role in pigmentation via the secretion of TGF- $\beta 1$ or Dickkopf1, a fibroblastic secreted factor that suppresses melanocyte growth and melanogenesis.^{84,86,87} More recently, neuregulin-1, which is specifically expressed by fibroblasts from dark-skinned subjects, has been identified as a melanogenic dermal factor.⁸⁸

Skin equivalents in studies of epidermal and dermal stem cells

Several studies in various tissues suggest that stem cell regeneration largely depends on the interactions between these cells and the environment where they reside and function. Specialized niches for various types of stem cells have been characterized in mammalian epidermis and dermis. These stem cells, which are distinct in marker expression patterns and growth properties, contribute differently to the homeostasis of epidermal and dermal compartments.^{89–91} RE (*in vitro* or humanized mouse model) can be used to identify the stem cell populations and their localization. Moreover, it can be used to determine whether the epidermal and dermal cells derived from induced pluripotent stem cells (iPSCs) and embryonic stem

cells (ESCs) are morphologically and functionally similar to those of mature skin cells.

Epidermal stem cells and their regulation

At least three major stem cell populations are involved in epidermo-annexial regeneration: the hair follicle bulge, the sebaceous gland and the basal layer of interfollicular epithelium.^{92–94} They can be distinguished on the basis of their marker expression patterns. Briefly, hair follicle bulge stem cells express K15, CD34, Lgr5 and K19, in addition to transcription factors Sox9 and Lhx2;⁹¹ sebaceous gland stem cells express the transcriptional repressor, Blimp1⁹⁵ and interfollicular epithelium stem cells express elevated levels of $\alpha 6$ and $\beta 1$ integrins and EGF receptor.⁸⁹ Because these stem cells are responsible for maintaining skin integrity and hair folliculogenesis,^{92,96} the focus of recent studies has been the identification of stem cell populations and characterization of the molecular signals that govern regeneration of the epidermis and hair follicles. To this end, *ex vivo* transplant and grafting experiments on the backs of mice have been widely used. These experiments showed that the bulge area contains different stem cell populations that are able to generate hair follicles, sebaceous glands and epidermis.^{97–99} Concerning the molecular regulation of hair stem cells, transplanted skin graft methods uncovered intrafollicular (short-distance niche) and interfollicular (long-distance niche including dermis, subcutaneous fat and adjacent follicles) microenvironments affecting the activity of these cells. In fact, stem cells are regulated by interaction between activators as well as inhibitors arising from the interfollicular and intrafollicular environment. Specifically, components of the wingless-type/ β -catenin, sonic hedgehog, and TGF- β /bone morphogenetic protein pathways appear to be particularly relevant to epidermal stem cell function.^{92,96,98,100–103} These experiments also showed that hair cycling in transplanted hair follicles was affected by the surrounding host skin, indicating that an interaction occurs between grafted skin, donor and host skin.¹⁰⁰

Dermal stem cells

Recent studies suggest that a cell population within the dermal papilla of hair follicles, which expresses somatic stemness marker SOX2, may function as adult dermal stem cells (DSCs).^{104–109} Rodent hair follicle-derived dermal cells can interact with local epithelia and induce *de novo* hair follicles in a variety of hairless recipient skin sites.^{110–114} However, human dermal papilla cells failed to recapitulate this procedure under the same conditions, suggesting that human cells lose some key properties during the culture period. Recently, it was shown that if human dermal papilla cells are grown as spheroids, they can induce *de novo* hair follicles in human skin.¹¹⁵ This study suggests novel treatment possibilities for cicatricial alopecia.

Li *et al.* have demonstrated a direct differentiation of DSCs into melanocytes. These melanocytes act in the same way as mature epidermal melanocytes upon incorporation into RE.

They are able to migrate to the BM, produce pigment and express appropriate melanocytic markers such as MITF, tyrosinase, tyrosinase-related protein 1, gp100 (human melanoma black 45) and E-cadherin.^{116,117}

Researchers have also demonstrated that perivascular sites in the dermis may act as a mesenchymal stem cell (MSC)-like niche in human skin.¹¹⁸ SE models have been used to define the role of MSCs in epidermal regeneration. Ma *et al.* have reported that MSCs are able to proliferate and form a multilayered epidermis when seeded on top of a contractible fibroblast-embedded collagen gel.¹¹⁹ Expression of two major epidermal markers (keratin 10 and filaggrin) revealed further similarity to epidermal lineage.¹¹⁹ When incorporated into a dermal substitute, it has been shown that skin-derived MSCs are able to grow and proliferate efficiently¹²⁰ and provide a microenvironment that supports keratinocyte attachment, proliferation and differentiation similar to normal fibroblasts. However, these cells failed to transdifferentiate into epidermal lineages.¹²¹

Skin cells derived from induced pluripotent stem cells and/or embryonic stem cells

It has been shown that iPSCs and ESCs can be differentiated into keratinocytes, fibroblasts or melanocytes.^{122–128} Seeded on dermal substitutes, ESC- and iPSC-derived keratinocytes have been shown to form a pluristratified epidermis.^{124–126} Hewitt *et al.* have shown that iPSC-derived fibroblasts are similar to dermal fibroblasts in the establishment of the BM, which supports keratinocyte proliferation and differentiation upon incorporation into SE.¹²⁷ Both human ESC- and iPSC-derived melanocytes are able to migrate to the BM and produce melanin upon incorporation in RE.¹²⁸

Skin equivalents in wound healing and clinical applications for patients with burns

SEs can be used to characterize some aspects of the wound-healing process. *In vitro* 'scratch' wound models using 2D monolayer cultures are, in fact, very limited for such studies. These cultures are helpful for studying only keratinocyte proliferation and migration in response to wounding, but cannot be used to investigate epidermal–dermal or epithelial–mesenchymal cross-talk during wound repair.^{129–131} Growing evidence indicates that *in vitro* wound-healing models are similar to *in vivo* models in many aspects, including proliferation, migration and expression of growth factors (e.g. TGF- $\beta 1$ and platelet-derived growth factor- β) in addition to cytokine secretion [e.g. interleukin (IL)-1 α , IL-6, tumour necrosis factor- α].^{129,132–136} Collectively, these results indicate that REs are valuable models for studying the chronology of re-epithelialization, cell proliferation, migration, differentiation and cell–cell cross-talk. Because these models can be used to modify various factors (e.g. medium components and types of incorporated cells),¹³⁷ they are very useful for understanding the roles played by individual cellular processes and the signalling pathways that drive tissue repair.

Although very valuable models, *in vitro* SEs lack the complexity associated with wound-healing mechanisms in native tissues. To study molecular mechanisms of tissue regeneration in a complex system, many researchers are now using rat and mouse models with limitations.¹³⁸ Several lines of evidence indicate that SEs grafted or implanted onto athymic mice represent more appropriate models for studying wound healing. Indeed, data obtained with this system showed that re-epithelialization progressed at a similar rate to human wounds^{139–141} and that the phenotype of wounded keratinocytes is consistent with human wound-healing physiology.¹⁴²

Covering the wound area as quickly as possible is one of the most crucial issues in improving the treatment of patients with deep burns. Acellular cadaver skin and fresh porcine skin have been used to treat large burn injuries.^{143,144} However, the drawbacks of these strategies, notably the difficulties associated with their handling and disease transmission in addition to the possible risk of rejection and infection, have limited their use.^{44,46,145} The application of skin reconstructs using collagen alone or collagen with skin cells has been shown to be of some benefit for patients with burns.^{146–148} Guenou *et al.* reported that RE with human ESCs have a structure consistent with that of mature human skin 12 weeks after grafting onto immunodeficient mice, suggesting that this resource could be developed to provide temporary skin substitutes for patients awaiting autologous grafts.¹²⁴ Several studies have demonstrated that grafts of skin substitutes populated with MSCs accelerate wound healing.^{149,150}

Skin equivalents in photodamage and photoprotection studies

As a relatively simple model that could mimic the *in vivo* situation, SEs are used to investigate skin responses to UV irradiation. As with human skin, the major effect of UVB on RE is the formation of sunburn cells,¹⁵¹ while the disappearance of superficial fibroblasts due to the UVA-induced cell death is the major effect of UVA on dermis.^{152,153} It has also been shown that keratinocyte differentiation markers are downregulated at early time points after UVB exposure. These downregulated markers are restored when SEs are maintained in culture for a longer period.¹⁵³ The involvement of melanocytes in photoprotection has been widely studied by using SE technology.^{36,154,155} The possibility of using genetically modified keratinocytes, melanocytes and fibroblasts renders these SEs powerful tools for studying cell signalling pathways in addition to autocrine and paracrine factors regulating skin responses to UV irradiation.^{33,156–160} SEs are also a resource for evaluating the protective effects of topically applied products such as sunscreens.^{76,152,161–163} A point that should be considered, especially when the aim of study is the evaluation of a topical application or a repetitive treatment, is the absence of desquamation in *in vitro* SEs.¹⁶⁴

One of the consequences of chronic UV irradiation is photoageing. SEs have been used to reveal biological modifications in epidermal and dermal compartments during this

process. For instance, RE using preglycated collagen as a dermal substitute led to an increased expression of extracellular matrix molecules (e.g. type III procollagen), the synthesis of metalloproteinases [e.g. matrix metalloproteinase (MMP)-1, MMP-2, MMP-9] and BM molecules (e.g. type IV collagen), in addition to the modification of the expression patterns of $\alpha 6$ and $\beta 1$ integrins in epidermis, which are highly relevant for the *in vivo* study of aged skin.^{165,166} Interestingly, glycation is a nonenzymatic reaction that takes place between free amino groups in a protein and a reducing sugar, such as glucose or ribose. The formation of these bridges between dermal molecules is thought to be responsible for loss of elasticity and other properties of the dermis observed during ageing.^{165,166} In agreement with this finding, when using *in vitro* skin reconstructed with keratinocytes derived from several human donors of different ages, the age of the donor was found to have a significant effect on the epidermal architecture and the expression pattern of p16INK4A, a biomarker of cellular ageing in human skin.^{167–169}

Skin equivalents and modelling of diseases

Human reconstructed skin, which mimics many morphological and molecular characteristics of normal human skin, has been used for modelling various skin diseases such as psoriasis, genodermatoses (e.g. epidermolysis bullosa and xeroderma pigmentosum) and vitiligo.

- Psoriasis has been modelled by using keratinocytes from patients with psoriasis,^{170,171} inhibition of transglutaminase,¹⁷² addition of lymphocytes¹⁷³ or stimulation using pro-inflammatory cytokines.^{174,175} Results indicate that *in vitro* reconstructed skin models, which display the molecular characteristics of psoriatic epidermis, are relevant for studying the biology of this disease and for screening anti-psoriatic drugs.^{170,174,175} Future studies including incorporation of other cell types such as T cells could provide important insights into the interactions between cell types in psoriasis.
- In recessive dystrophic epidermolysis bullosa, which is due to mutations in the COL7A1 gene, *in vitro* REs composed of patient-derived keratinocytes and/or fibroblasts have been proposed for modelling this disease.¹⁷⁶ Patient-specific induced iPSCs have also been used for this purpose.^{125,126} These SEs provide significant advantages for testing preclinical strategies including cell- and gene-based therapy.^{177,178}
- For xeroderma pigmentosum (XP), a rare autosomal recessive disorder of DNA repair, SEs reconstituted with keratinocytes and/or fibroblasts taken from patients with XP mimic features of the disease (i.e. DNA repair deficiency, UV sensitivity, predisposition to cancer and deficiency in catalase activity).^{160,179,180} Indeed, the XP model displayed repair deficiency with long-lasting persistence of UV-induced DNA damage and p53-positive nuclei upon exposure to UVB, unlike the normal SE, which efficiently repaired UVB-induced DNA lesions.¹⁸⁰ Furthermore, *ex vivo*

gene therapy for XP-C cells has been tested using *in vitro* SEs and SEs grafted onto mice. Results showed that corrected XP-C keratinocytes exhibited efficient DNA repair capacity and normal features of epidermal differentiation in both models.¹⁸¹

- Vitiligo, the most common depigmenting disorder, is an acquired disease characterized by progressive loss of melanocytes.¹⁸² RE reconstructed with normal keratinocytes and melanocytes from vitiligo showed that vitiligo melanocytes present a defect in adhesion and that this deficiency is amplified if vitiligo keratinocytes are also incorporated into reconstructs.¹⁸³ This suggests an intrinsic defect in melanocytes and possibly in the keratinocytes of patients. Furthermore, some stress conditions (e.g. adrenaline or oxidative stress) could trigger the transepidermal loss of normal and vitiligo melanocytes.¹⁸³ As already mentioned, one of the mechanisms by which melanocyte basal location is ensured is DDR1–type IV collagen interactions. To test whether deficiency in DDR1 or the connective tissue growth factor (CCN)3, which regulates DDR1,⁶⁶ is implicated in vitiligo, their endogenous protein expression was inhibited using lentivirus-mediated expression of shRNA against DDR1 or CCN3. CCN3 downregulation prevented melanocyte attachment, unlike inhibition of DDR1 expression.¹⁸⁴ This model can reproduce hypo- and hyperpigmentary disorders associated with melanocyte defects and can highlight dermal influences on the pigmentary phenotype. SEs have been used in our laboratory for modelling *in vitro* the hypo- and hyperpigmentary disorders associated with lentigo senilis,⁸¹ systemic scleroderma and melasma (Y. Gauthier, S. Lepreux, A. Taïeb, M. Cario-André, unpublished data).

Limitations of human *in vitro* and *in vivo* reconstructed epidermis and perspectives

With the improvements achieved in recent years, SEs have become an indispensable tool for investigative dermatology, especially for addressing (i) skin homeostasis and the molecular mechanisms that govern different cell types and their interactions, (ii) skin repair, specifically the signalling pathways that drive this process, (iii) skin regeneration, by understanding the properties and the behaviour of the skin stem cells residing in various niches and (iv) skin diseases, by modelling these diseases using cells from patients or genetically engineered ones to reproduce molecular defects.

However, these models are still perfectible for several essential reasons:

- As blood flow is not present in *in vitro* reconstructs, this negatively influences cell nutrition and metabolism, a bias limited by optimal medium composition and renewal. However, securing a vascular bed would provide an optimal environment for immune cells, which are difficult to maintain in SEs. Lastly, this vascular bed would facilitate the incorporation of MSCs in order to study their effects in skin biology.

- Having a functional immune system in RE remains a major objective. Although mouse models have efficiently advanced our knowledge about basic immunological mechanisms, they cannot address all questions concerning human skin immunology. Despite the many preserved features between the human and mouse immune systems, several studies have highlighted important differences.^{185,186} This could explain why some protocols for treating autoimmune diseases or cancer immunotherapy work well in mice but have not been successful in human trials.¹⁸⁷ The incorporation of immune cells in *in vitro* RE has been tried with some success by various groups,^{163,188–190} but a well-established and reproducible protocol is not currently available. Therefore we need to make greater efforts to overcome this obstacle in the future.
- Epidermal reconstructs lack neuronal cells. The sensitivity of the skin is due to the presence of sensory neurons that transmit tactile, proprioceptive, chemical and nociceptive sensations. Several reports have shown that the density of sensory neurons ending in the epidermis is increased in immune skin diseases such as psoriasis and atopic dermatitis.^{191–194} Therefore, incorporation of neurons would be of great benefit for investigating skin reactions in detail after specific stimulation and the interconnection between all resident skin cells.

As humanized mouse models will not be useable for many research aspects for ethical reasons, cell-scaffold technology with its new generation of skin substitutes is an emerging field. This technology has the potential to meet the engineering challenges posed by the complexity of skin.

References

- 1 Proksch E, Brandner JM, Jensen JM. The skin: an indispensable barrier. *Exp Dermatol* 2008; **17**:1063–72.
- 2 Burgeson RE, Christiano AM. The dermal-epidermal junction. *Curr Opin Cell Biol* 1997; **9**:651–8.
- 3 Tobin DJ. Biochemistry of human skin—our brain on the outside. *Chem Soc Rev* 2006; **35**:52–67.
- 4 Grinnell F. Biochemical analysis of cell adhesion to a substratum and its possible relevance to cell metastasis. *Prog Clin Biol Res* 1976; **9**:227–36.
- 5 Bissell MJ, Hall HG, Parry G. How does the extracellular matrix direct gene expression? *J Theor Biol* 1982; **99**:31–68.
- 6 Yang J, Balakrishnan A, Hamamoto S *et al.* Different mitogenic and phenotypic responses of human breast epithelial cells grown in two versus three dimensions. *Exp Cell Res* 1986; **167**:563–9.
- 7 Lin CQ, Bissell MJ. Multi-faceted regulation of cell differentiation by extracellular matrix. *FASEB J* 1993; **7**:737–43.
- 8 Smalley KS, Lioni M, Herlyn M. Life isn't flat: taking cancer biology to the next dimension. *In Vitro Cell Dev Biol Anim* 2006; **42**:242–7.
- 9 Grinnell F. Fibroblast mechanics in three-dimensional collagen matrices. *J Bodyw Mov Ther* 2008; **12**:191–3.
- 10 Horning JL, Sahoo SK, Vijayaraghavalu S *et al.* 3-D tumor model for *in vitro* evaluation of anticancer drugs. *Mol Pharm* 2008; **5**:849–62.

- 11 Mazzoleni G, Di Lorenzo D, Steimberg N. Modelling tissues in 3D: the next future of pharmaco-toxicology and food research? *Genes Nutr* 2009; **4**:13–22.
- 12 Lu Z, Hasse S, Bodo E *et al.* Towards the development of a simplified long-term organ culture method for human scalp skin and its appendages under serum-free conditions. *Exp Dermatol* 2007; **16**:37–44.
- 13 Yano S, Miwa S, Mii S *et al.* Cancer cells mimic in vivo spatial-temporal cell-cycle phase distribution and chemosensitivity in 3-dimensional gelfoam histoculture but not 2-dimensional culture as visualized with real-time FUCCI imaging. *Cell Cycle* 2015; **14**:808–19.
- 14 Li LN, Margolis LB, Hoffman RM. Skin toxicity determined in vitro by three-dimensional, native-state histoculture. *Proc Natl Acad Sci USA* 1991; **88**:1908–12.
- 15 Hoffman RM. The clinical benefit of the histoculture drug response assay. *Gan To Kagaku Ryoho* 2000; **27**(Suppl. 2):321–2.
- 16 Hoffman RM. Three-dimensional histoculture: origins and applications in cancer research. *Cancer Cells* 1991; **3**:86–92.
- 17 Hoffman RM, Connors KM, Meerson-Monosov AZ *et al.* A general native-state method for determination of proliferation capacity of human normal and tumor tissues in vitro. *Proc Natl Acad Sci USA* 1989; **86**:2013–17.
- 18 Li L, Paus R, Slominski A *et al.* Skin histoculture assay for studying the hair cycle. *In Vitro Cell Dev Biol* 1992; **28A**:695–8.
- 19 Bagabir R, Syed F, Paus R, Bayat A. Long-term organ culture of keloid disease tissue. *Exp Dermatol* 2012; **21**:376–81.
- 20 Wong VW, Sorkin M, Glotzbach JP *et al.* Surgical approaches to create murine models of human wound healing. *J Biomed Biotechnol* 2011; **2011**:969618.
- 21 Cruickshank CN, Cooper JR, Hooper C. The cultivation of cells from adult epidermis. *J Invest Dermatol* 1960; **34**:339–42.
- 22 Rheinwald JG, Green H. Serial cultivation of strains of human epidermal keratinocytes: the formation of keratinizing colonies from single cells. *Cell* 1975; **6**:331–43.
- 23 Freeman AE, Igel HJ, Herrman BJ, Kleinfeld KL. Growth and characterization of human skin epithelial cell cultures. *In Vitro* 1976; **12**:352–62.
- 24 Lillie JH, MacCallum DK, Jepsen A. Fine structure of subcultivated stratified squamous epithelium grown on collagen rafts. *Exp Cell Res* 1980; **125**:153–65.
- 25 Fusenig NE, Amer SM, Boukamp P, Worst PK. Characteristics of chemically transformed mouse epidermal cells in vitro and in vivo. *Bull Cancer* 1978; **65**:271–9.
- 26 Prunieras M, Regnier M, Woodley D. Methods for cultivation of keratinocytes with an air-liquid interface. *J Invest Dermatol* 1983; **81**:28s–33s.
- 27 Gazel A, Ramphal P, Rosdy M *et al.* Transcriptional profiling of epidermal keratinocytes: comparison of genes expressed in skin, cultured keratinocytes, and reconstituted epidermis, using large DNA microarrays. *J Invest Dermatol* 2003; **121**:1459–68.
- 28 Poumay Y, Dupont F, Marcoux S *et al.* A simple reconstructed human epidermis: preparation of the culture model and utilization in in vitro studies. *Arch Dermatol Res* 2004; **296**:203–11.
- 29 Poumay Y, Leclercq-Smekens M. In vitro models of epidermal differentiation. *Folia Med (Plovdiv)* 1998; **40**:5–12.
- 30 Rosdy M, Clauss LC. Terminal epidermal differentiation of human keratinocytes grown in chemically defined medium on inert filter substrates at the air-liquid interface. *J Invest Dermatol* 1990; **95**:409–14.
- 31 Asselineau D, Prunieras M. Reconstruction of 'simplified' skin: control of fabrication. *Br J Dermatol* 1984; **111**(Suppl. 27):219–22.
- 32 Bernerd F, Vioux C, Lejeune F, Asselineau D. The sun protection factor (SPF) inadequately defines broad spectrum photoprotection: demonstration using skin reconstructed in vitro exposed to UVA, UVB or UV-solar simulated radiation. *Eur J Dermatol* 2003; **13**:242–9.
- 33 Rezvani HR, Cario-André M, Pain C *et al.* Protection of normal human reconstructed epidermis from UV by catalase overexpression. *Cancer Gene Ther* 2007; **14**:174–86.
- 34 Prunieras M, Regnier M, Schlotterer M. [New procedure for culturing human epidermal cells on allogenic or xenogenic skin: preparation of recombined grafts]. *Ann Chir Plast* 1979; **24**:357–62 (in French).
- 35 Cario-André M, Briganti S, Picardo M *et al.* Epidermal reconstructs: a new tool to study topical and systemic photoprotective molecules. *J Photochem Photobiol, B* 2002; **68**:79–87.
- 36 Cario-André M, Pain C, Gall Y *et al.* Studies on epidermis reconstructed with and without melanocytes: melanocytes prevent sunburn cell formation but not appearance of DNA damaged cells in fair-skinned caucasians. *J Invest Dermatol* 2000; **115**:193–9.
- 37 Tinois E, Tiollier J, Gaucherand M *et al.* In vitro and post-transplantation differentiation of human keratinocytes grown on the human type IV collagen film of a bilayered dermal substitute. *Exp Cell Res* 1991; **193**:310–19.
- 38 Ponc M, Weerheim A, Kempenaar J *et al.* The formation of competent barrier lipids in reconstructed human epidermis requires the presence of vitamin C. *J Invest Dermatol* 1997; **109**:348–55.
- 39 Hull BE, Sher SE, Rosen S *et al.* Fibroblasts in isogenic skin equivalents persist for long periods after grafting. *J Invest Dermatol* 1983; **81**:436–8.
- 40 Pigeon H, Bakala H, Monnier VM, Asselineau D. Collagen glycation triggers the formation of aged skin in vitro. *Eur J Dermatol* 2007; **17**:12–20.
- 41 el-Ghalebzouri A, Gibbs S, Lamme E *et al.* Effect of fibroblasts on epidermal regeneration. *Br J Dermatol* 2002; **147**:230–43.
- 42 Régnier M, Staquet MJ, Schmitt D, Schmidt R. Integration of Langerhans cells into a pigmented reconstructed human epidermis. *J Invest Dermatol* 1997; **109**:510–12.
- 43 Régnier M, Patwardhan A, Scheynius A, Schmidt R. Reconstructed human epidermis composed of keratinocytes, melanocytes and Langerhans cells. *Med Biol Eng Comput* 1998; **36**:821–4.
- 44 Phillips TJ. New skin for old: developments in biological skin substitutes. *Arch Dermatol* 1998; **134**:344–9.
- 45 Régnier M, Duval C, Schmidt R. Potential cosmetic applications of reconstructed epidermis. *Int J Cosmet Sci* 1999; **21**:51–8.
- 46 Wong T, McGrath JA, Navsaria H. The role of fibroblasts in tissue engineering and regeneration. *Br J Dermatol* 2007; **156**:1149–55.
- 47 Cooper ML, Hansbrough JF, Spielvogel RL *et al.* In vivo optimization of a living dermal substitute employing cultured human fibroblasts on a biodegradable polyglycolic acid or polyglactin mesh. *Biomaterials* 1991; **12**:243–8.
- 48 Smola H, Stark HJ, Thiekotter G *et al.* Dynamics of basement membrane formation by keratinocyte-fibroblast interactions in organotypic skin culture. *Exp Cell Res* 1998; **239**:399–410.
- 49 Green H, Kehinde O, Thomas J. Growth of cultured human epidermal cells into multiple epithelia suitable for grafting. *Proc Natl Acad Sci USA* 1979; **76**:5665–8.
- 50 O'Connor N, Mulliken JB, Banks-Schlegel S *et al.* Grafting of burns with cultured epithelium prepared from autologous epidermal cells. *Lancet* 1981; **317**:75–8.
- 51 Herzog SR, Meyer A, Woodley D, Peterson HD. Wound coverage with cultured autologous keratinocytes: use after burn wound excision, including biopsy followup. *J Trauma* 1988; **28**:195–8.

- 52 Bell E, Ehrlich HP, Buttle DJ, Nakatsuji T. Living tissue formed *in vitro* and accepted as skin-equivalent tissue of full thickness. *Science* 1981; **211**:1052–4.
- 53 Burke JF, Yannas IV, Quinby WC Jr *et al.* Successful use of a physiologically acceptable artificial skin in the treatment of extensive burn injury. *Ann Surg* 1981; **194**:413–28.
- 54 Hansbrough JF, Boyce ST, Cooper ML, Foreman TJ. Burn wound closure with cultured autologous keratinocytes and fibroblasts attached to a collagen-glycosaminoglycan substrate. *JAMA* 1989; **262**:2125–30.
- 55 Krejci NC, Cuono CB, Langdon RC, McGuire J. *In vitro* reconstitution of skin: fibroblasts facilitate keratinocyte growth and differentiation on acellular reticular dermis. *J Invest Dermatol* 1991; **97**:843–8.
- 56 Medalie DA, Eming SA, Tompkins RG *et al.* Evaluation of human skin reconstituted from composite grafts of cultured keratinocytes and human acellular dermis transplanted to athymic mice. *J Invest Dermatol* 1996; **107**:121–7.
- 57 Ben-Bassat H, Eldad A, Chaouat M *et al.* Structural and functional evaluation of modifications in the composite skin graft: cryopreserved dermis and cultured keratinocytes. *Plast Reconstr Surg* 1992; **89**:510–20.
- 58 Gilhar A, Keren A, Paus R. A new humanized mouse model for alopecia areata. *J Investig Dermatol Symp Proc* 2013; **16**:S37–8.
- 59 Gilhar A, Ullmann Y, Berkutzi T *et al.* Autoimmune hair loss (alopecia areata) transferred by T lymphocytes to human scalp explants on SCID mice. *J Clin Invest* 1998; **101**:62–7.
- 60 Wang CK, Nelson CF, Brinkman AM *et al.* Spontaneous cell sorting of fibroblasts and keratinocytes creates an organotypic human skin equivalent. *J Invest Dermatol* 2000; **114**:674–80.
- 61 Marinkovich MP, Keene DR, Rimberg CS, Burgeson RE. Cellular origin of the dermal-epidermal basement membrane. *Dev Dyn* 1993; **197**:255–67.
- 62 Fleischmajer R, Kuhn K, Sato Y *et al.* There is temporal and spatial expression of alpha1 (IV), alpha2 (IV), alpha5 (IV), alpha6 (IV) collagen chains and beta1 integrins during the development of the basal lamina in an “*in vitro*” skin model. *J Invest Dermatol* 1997; **109**:527–33.
- 63 Latijnhouwers M, Bergers M, Ponc M *et al.* Human epidermal keratinocytes are a source of tenascin-C during wound healing. *J Invest Dermatol* 1997; **108**:776–83.
- 64 Nolte SV, Xu W, Rennekampff HO, Rodemann HP. Diversity of fibroblasts – a review on implications for skin tissue engineering. *Cells Tissues Organs* 2008; **187**:165–76.
- 65 El Ghalbzouri A, Lamme E, Ponc M. Crucial role of fibroblasts in regulating epidermal morphogenesis. *Cell Tissue Res* 2002; **310**:189–99.
- 66 Fukunaga-Kalabis M, Martinez G, Liu ZJ *et al.* CCN3 controls 3D spatial localization of melanocytes in the human skin through DDR1. *J Cell Biol* 2006; **175**:563–9.
- 67 Santiago-Walker A, Li L, Haass NK, Herlyn M. Melanocytes: from morphology to application. *Skin Pharmacol Physiol* 2009; **22**:114–21.
- 68 Valyi-Nagy IT, Murphy GF, Mancianti ML *et al.* Phenotypes and interactions of human melanocytes and keratinocytes in an epidermal reconstruction model. *Lab Invest* 1990; **62**:314–24.
- 69 Meier F, Nesbit M, Hsu MY *et al.* Human melanoma progression in skin reconstructs: biological significance of bFGF. *Am J Pathol* 2000; **156**:193–200.
- 70 Bessou S, Surleve-Bazeille JE, Pain C *et al.* *Ex vivo* study of skin phototypes. *J Invest Dermatol* 1996; **107**:684–8.
- 71 Cario-André M, Pain C, Gauthier Y *et al.* *In vivo* and *in vitro* evidence of dermal fibroblasts influence on human epidermal pigmentation. *Pigment Cell Res* 2006; **19**:434–42.
- 72 Okazaki M, Suzuki Y, Yoshimura K, Harri K. Construction of pigmented skin equivalent and its application to the study of congenital disorders of pigmentation. *Scand J Plast Reconstr Surg Hand Surg* 2005; **39**:339–43.
- 73 Ni-Komatsu L, Tong C, Chen G *et al.* Identification of quinolines that inhibit melanogenesis by altering tyrosinase family trafficking. *Mol Pharmacol* 2008; **74**:1576–86.
- 74 Jain P, Sonti S, Garruto J *et al.* Formulation optimization, skin irritation, and efficacy characterization of a novel skin-lightening agent. *J Cosmet Dermatol* 2012; **11**:101–10.
- 75 Wang Z, Li X, Yang Z *et al.* Effects of aloesin on melanogenesis in pigmented skin equivalents. *Int J Cosmet Sci* 2008; **30**:121–30.
- 76 Duval C, Schmidt R, Regnier M *et al.* The use of reconstructed human skin to evaluate UV-induced modifications and sunscreen efficacy. *Exp Dermatol* 2003; **12**(Suppl. 2):64–70.
- 77 Duval C, Chagnoleau C, Pouradier F *et al.* Human skin model containing melanocytes: essential role of keratinocyte growth factor for constitutive pigmentation-functional response to alpha-melanocyte stimulating hormone and forskolin. *Tissue Eng Part C Methods* 2012; **18**:947–57.
- 78 Bernerd F, Marionnet C, Duval C. Solar ultraviolet radiation induces biological alterations in human skin *in vitro*: relevance of a well-balanced UVA/UVB protection. *Indian J Dermatol Venereol Leprol* 2012; **78**(Suppl. 1):S15–23.
- 79 Archambault M, Yaar M, Gilchrist BA. Keratinocytes and fibroblasts in a human skin equivalent model enhance melanocyte survival and melanin synthesis after ultraviolet irradiation. *J Invest Dermatol* 1995; **104**:859–67.
- 80 Hedley SJ, Layton C, Heaton M *et al.* Fibroblasts play a regulatory role in the control of pigmentation in reconstructed human skin from skin types I and II. *Pigment Cell Res* 2002; **15**:49–56.
- 81 Salducci M, André N, Guere C *et al.* Factors secreted by irradiated aged fibroblasts induce solar lentigo in pigmented reconstructed epidermis. *Pigment Cell Melanoma Res* 2014; **27**:502–4.
- 82 Imokawa G, Yada Y, Morisaki N, Kimura M. Biological characterization of human fibroblast-derived mitogenic factors for human melanocytes. *Biochem J* 1998; **330**(Pt. 3):1235–9.
- 83 Kondo T, Hearing VJ. Update on the regulation of mammalian melanocyte function and skin pigmentation. *Expert Rev Dermatol* 2011; **6**:97–108.
- 84 Yamaguchi Y, Itami S, Watabe H *et al.* Mesenchymal-epithelial interactions in the skin: increased expression of dickkopf1 by palmar fibroblasts inhibits melanocyte growth and differentiation. *J Cell Biol* 2004; **165**:275–85.
- 85 Choi W, Miyamura Y, Wolber R *et al.* Regulation of human skin pigmentation *in situ* by repetitive UV exposure: molecular characterization of responses to UVA and/or UVB. *J Invest Dermatol* 2010; **130**:1685–96.
- 86 Yamaguchi Y, Passeron T, Hoashi T *et al.* Dickkopf 1 (DKK1) regulates skin pigmentation and thickness by affecting Wnt/beta-catenin signaling in keratinocytes. *FASEB J* 2008; **22**:1009–20.
- 87 Yamaguchi Y, Hearing VJ. Physiological factors that regulate skin pigmentation. *BioFactors* 2009; **35**:193–9.
- 88 Choi W, Wolber R, Gerwat W *et al.* The fibroblast-derived paracrine factor neuregulin-1 has a novel role in regulating the constitutive color and melanocyte function in human skin. *J Cell Sci* 2010; **123**:3102–11.
- 89 Watt FM, Jensen KB. Epidermal stem cell diversity and quiescence. *EMBO Mol Med* 2009; **1**:260–7.
- 90 Driskell RR, Clavel C, Rendl M, Watt FM. Hair follicle dermal papilla cells at a glance. *J Cell Sci* 2011; **124**:1179–82.

- 91 Liu S, Zhang H, Duan E. Epidermal development in mammals: key regulators, signals from beneath, and stem cells. *Int J Mol Sci* 2013; **14**:10869–95.
- 92 Tadeu AM, Horsley V. Epithelial stem cells in adult skin. *Curr Top Dev Biol* 2014; **107**:109–31.
- 93 Fuchs E, Horsley V. More than one way to skin. *Genes Dev* 2008; **22**:976–85.
- 94 Fuchs E. Skin stem cells: rising to the surface. *J Cell Biol* 2008; **180**:273–84.
- 95 Horsley V, O'Carroll D, Tooze R *et al.* Blimp1 defines a progenitor population that governs cellular input to the sebaceous gland. *Cell* 2006; **126**:597–609.
- 96 Blanpain C, Fuchs E. Epidermal stem cells of the skin. *Annu Rev Cell Dev Biol* 2006; **22**:339–73.
- 97 Morris RJ, Liu Y, Marles L *et al.* Capturing and profiling adult hair follicle stem cells. *Nat Biotechnol* 2004; **22**:411–17.
- 98 Blanpain C, Lowry WE, Geoghegan A *et al.* Self-renewal, multipotency, and the existence of two cell populations within an epithelial stem cell niche. *Cell* 2004; **118**:635–48.
- 99 Oshima H, Rochat A, Kedzia C *et al.* Morphogenesis and renewal of hair follicles from adult multipotent stem cells. *Cell* 2001; **104**:233–45.
- 100 Plikus MV, Mayer JA, de la Cruz D *et al.* Cyclic dermal BMP signalling regulates stem cell activation during hair regeneration. *Nature* 2008; **451**:340–4.
- 101 Myung PS, Takeo M, Ito M, Atit RP. Epithelial Wnt ligand secretion is required for adult hair follicle growth and regeneration. *J Invest Dermatol* 2013; **133**:31–41.
- 102 Blanpain C, Fuchs E. Epidermal homeostasis: a balancing act of stem cells in the skin. *Nat Rev Mol Cell Biol* 2009; **10**:207–17.
- 103 Yang L, Peng R. Unveiling hair follicle stem cells. *Stem Cell Rev* 2010; **6**:658–64.
- 104 Kellner JC, Coulombe PA. Preview. SKPing a hurdle: Sox2 and adult dermal stem cells. *Cell Stem Cell* 2009; **5**:569–70.
- 105 Driskell RR, Giangreco A, Jensen KB *et al.* Sox2-positive dermal papilla cells specify hair follicle type in mammalian epidermis. *Development* 2009; **136**:2815–23.
- 106 Biernaskie J, Paris M, Morozova O *et al.* SKPs derive from hair follicle precursors and exhibit properties of adult dermal stem cells. *Cell Stem Cell* 2009; **5**:610–23.
- 107 Toma JG, Akhavan M, Fernandes KJ *et al.* Isolation of multipotent adult stem cells from the dermis of mammalian skin. *Nat Cell Biol* 2001; **3**:778–84.
- 108 Fernandes KJ, McKenzie IA, Mill P *et al.* A dermal niche for multipotent adult skin-derived precursor cells. *Nat Cell Biol* 2004; **6**:1082–93.
- 109 Toma JG, McKenzie IA, Bagli D, Miller FD. Isolation and characterization of multipotent skin-derived precursors from human skin. *Stem Cells* 2005; **23**:727–37.
- 110 Cohen J. The transplantation of individual rat and guinea-pig whisker papillae. *J Embryol Exp Morphol* 1961; **9**:117–27.
- 111 Oliver RF. The induction of hair follicle formation in the adult hooded rat by vibrissa dermal papillae. *J Embryol Exp Morphol* 1970; **23**:219–36.
- 112 Jahoda CA, Horne KA, Oliver RF. Induction of hair growth by implantation of cultured dermal papilla cells. *Nature* 1984; **311**:560–2.
- 113 Kishimoto J, Burgeson RE, Morgan BA. Wnt signaling maintains the hair-inducing activity of the dermal papilla. *Genes Dev* 2000; **14**:1181–5.
- 114 Rendl M, Polak L, Fuchs E. BMP signaling in dermal papilla cells is required for their hair follicle-inductive properties. *Genes Dev* 2008; **22**:543–57.
- 115 Higgins CA, Chen JC, Cerise JE *et al.* Microenvironmental reprogramming by three-dimensional culture enables dermal papilla cells to induce de novo human hair-follicle growth. *Proc Natl Acad Sci USA* 2013; **110**:19679–88.
- 116 Li L, Fukunaga-Kalabis M, Yu H *et al.* Human dermal stem cells differentiate into functional epidermal melanocytes. *J Cell Sci* 2010; **123**:853–60.
- 117 Li L, Fukunaga-Kalabis M, Herlyn M. Isolation and cultivation of dermal stem cells that differentiate into functional epidermal melanocytes. *Methods Mol Biol* 2012; **806**:15–29.
- 118 Yamanishi H, Fujiwara S, Soma T. Perivascular localization of dermal stem cells in human scalp. *Exp Dermatol* 2012; **21**:78–80.
- 119 Ma K, Laco F, Ramakrishna S *et al.* Differentiation of bone marrow-derived mesenchymal stem cells into multi-layered epidermis-like cells in 3D organotypic coculture. *Biomaterials* 2009; **30**:3251–8.
- 120 Jeremias T da S, Machado RG, Visoni SB *et al.* Dermal substitutes support the growth of human skin-derived mesenchymal stromal cells: potential tool for skin regeneration. *PLoS One* 2014; **9**:e89542.
- 121 Ojeh NO, Navsaria HA. An in vitro skin model to study the effect of mesenchymal stem cells in wound healing and epidermal regeneration. *J Biomed Mater Res A* 2014; **102**:2785–92.
- 122 Bilousova G, Chen J, Roop DR. Differentiation of mouse induced pluripotent stem cells into a multipotent keratinocyte lineage. *J Invest Dermatol* 2011; **131**:857–64.
- 123 Tolar J, Xia L, Riddle MJ *et al.* Induced pluripotent stem cells from individuals with recessive dystrophic epidermolysis bullosa. *J Invest Dermatol* 2011; **131**:848–56.
- 124 Guenou H, Nissan X, Larcher F *et al.* Human embryonic stem-cell derivatives for full reconstruction of the pluristratified epidermis: a preclinical study. *Lancet* 2009; **374**:1745–53.
- 125 Itoh M, Kiuru M, Cairo MS, Christiano AM. Generation of keratinocytes from normal and recessive dystrophic epidermolysis bullosa-induced pluripotent stem cells. *Proc Natl Acad Sci USA* 2011; **108**:8797–802.
- 126 Itoh M, Umegaki-Arao N, Guo Z *et al.* Generation of 3D skin equivalents fully reconstituted from human induced pluripotent stem cells (iPSCs). *PLoS One* 2013; **8**:e77673.
- 127 Hewitt KJ, Shamis Y, Hayman RB *et al.* Epigenetic and phenotypic profile of fibroblasts derived from induced pluripotent stem cells. *PLoS One* 2011; **6**:e17128.
- 128 Nissan X, Larr이버 L, Saidani M *et al.* Functional melanocytes derived from human pluripotent stem cells engraft into pluristratified epidermis. *Proc Natl Acad Sci USA* 2011; **108**:14861–6.
- 129 Safferling K, Sutterlin T, Westphal K *et al.* Wound healing revised: a novel reepithelialization mechanism revealed by in vitro and in silico models. *J Cell Biol* 2013; **203**:691–709.
- 130 Garlick JA, Taichman LB. Fate of human keratinocytes during reepithelialization in an organotypic culture model. *Lab Invest* 1994; **70**:916–24.
- 131 Garlick JA, Parks WC, Welgus HG, Taichman LB. Re-epithelialization of human oral keratinocytes in vitro. *J Dent Res* 1996; **75**:912–18.
- 132 Hu T, Khambatta ZS, Hayden PJ *et al.* Xenobiotic metabolism gene expression in the EpiDerm in vitro 3D human epidermis model compared to human skin. *Toxicol In Vitro* 2010; **24**:1450–63.
- 133 Hayden PJ, Petrali JP, Stolper G *et al.* Microvesicating effects of sulfur mustard on an in vitro human skin model. *Toxicol In Vitro* 2009; **23**:1396–405.
- 134 Mallampati R, Patlolla RR, Agarwal S *et al.* Evaluation of EpiDerm full thickness-300 (EFT-300) as an in vitro model for skin

- irritation: studies on aliphatic hydrocarbons. *Toxicol In Vitro* 2010; **24**:669–76.
- 135 Black AT, Hayden PJ, Casillas RP *et al.* Expression of proliferative and inflammatory markers in a full-thickness human skin equivalent following exposure to the model sulfur mustard vesicant, 2-chloroethyl ethyl sulfide. *Toxicol Appl Pharmacol* 2010; **249**:178–87.
- 136 Falanga V, Isaacs C, Paquette D *et al.* Wounding of bioengineered skin: cellular and molecular aspects after injury. *J Invest Dermatol* 2002; **119**:653–60.
- 137 Egles C, Garlick JA, Shamis Y. Three-dimensional human tissue models of wounded skin. *Methods Mol Biol* 2010; **585**:345–59.
- 138 Sullivan TP, Eaglstein WH, Davis SC, Mertz P. The pig as a model for human wound healing. *Wound Repair Regen* 2001; **9**:66–76.
- 139 Amendt C, Mann A, Schirmacher P, Blessing M. Resistance of keratinocytes to TGF β -mediated growth restriction and apoptosis induction accelerates re-epithelialization in skin wounds. *J Cell Sci* 2002; **115**:2189–98.
- 140 Grose R, Hutter C, Bloch W *et al.* A crucial role of β 1 integrins for keratinocyte migration in vitro and during cutaneous wound repair. *Development* 2002; **129**:2303–15.
- 141 Yoshida S, Yamaguchi Y, Itami S *et al.* Neutralization of hepatocyte growth factor leads to retarded cutaneous wound healing associated with decreased neovascularization and granulation tissue formation. *J Invest Dermatol* 2003; **120**:335–43.
- 142 Mansbridge JN, Knapp AM. Changes in keratinocyte maturation during wound healing. *J Invest Dermatol* 1987; **89**:253–63.
- 143 Obeng MK, McCauley RL, Barnett JR *et al.* Cadaveric allograft discards as a result of positive skin cultures. *Burns* 2001; **27**:267–71.
- 144 Garfein ES, Orgill DP, Pribaz JJ. Clinical applications of tissue engineered constructs. *Clin Plast Surg* 2003; **30**:485–98.
- 145 Hansen SL, Voigt DW, Wiebelhaus P, Paul CN. Using skin replacement products to treat burns and wounds. *Adv Skin Wound Care* 2001; **14**:37–44.
- 146 Wisser D, Rennekampff HO, Schaller HE. Skin assessment of burn wounds covered with a collagen based dermal substitute in a 2 year-follow-up. *Burns* 2004; **30**:399–401.
- 147 Still J, Glat P, Silverstein P *et al.* The use of a collagen sponge/living cell composite material to treat donor sites in burn patients. *Burns* 2003; **29**:837–41.
- 148 Hohlfeld J, de Buys Roessingh A, Hirt-Burri N *et al.* Tissue engineered fetal skin constructs for paediatric burns. *Lancet* 2005; **366**:840–2.
- 149 Ichioka S, Kouraba S, Sekiya N *et al.* Bone marrow-impregnated collagen matrix for wound healing: experimental evaluation in a microcirculatory model of angiogenesis, and clinical experience. *Br J Plast Surg* 2005; **58**:1124–30.
- 150 Vojtassak J, Danisovic L, Kubes M *et al.* Autologous biograft and mesenchymal stem cells in treatment of the diabetic foot. *Neuro Endocrinol Lett* 2006; **27**(Suppl. 2):134–7.
- 151 Bernerd F, Asselineau D. Successive alteration and recovery of epidermal differentiation and morphogenesis after specific UVB-damages in skin reconstructed in vitro. *Dev Biol* 1997; **183**:123–38.
- 152 Bernerd F, Asselineau D. An organotypic model of skin to study photodamage and photoprotection in vitro. *J Am Acad Dermatol* 2008; **58**:S155–9.
- 153 Bernerd F, Asselineau D. UVA exposure of human skin reconstructed in vitro induces apoptosis of dermal fibroblasts: subsequent connective tissue repair and implications in photoaging. *Cell Death Differ* 1998; **5**:792–802.
- 154 Bessou S, Surlève-Bazeille JE, Sorbier E, Taïeb A. *Ex vivo* reconstruction of the epidermis with melanocytes and the influence of UVB. *Pigment Cell Res* 1995; **8**:241–9.
- 155 Cario-André M, Bessou S, Gontier E *et al.* The reconstructed epidermis with melanocytes: a new tool to study pigmentation and photoprotection. *Cell Mol Biol (Noisy-le-grand)* 1999; **45**:931–42.
- 156 Javeri A, Huang XX, Bernerd F *et al.* Human 8-oxoguanine-DNA glycosylase 1 protein and gene are expressed more abundantly in the superficial than basal layer of human epidermis. *DNA Repair (Amst)* 2008; **7**:1542–50.
- 157 Kurdykowski S, Mine S, Bardey V *et al.* Ultraviolet-B irradiation induces epidermal up-regulation of heparanase expression and activity. *J Photochem Photobiol, B* 2012; **106**:107–12.
- 158 Fagot D, Asselineau D, Bernerd F. Matrix metalloproteinase-1 production observed after solar-simulated radiation exposure is assumed by dermal fibroblasts but involves a paracrine activation through epidermal keratinocytes. *Photochem Photobiol* 2004; **79**:499–505.
- 159 Marionnet C, Pierrard C, Lejeune F *et al.* Different oxidative stress response in keratinocytes and fibroblasts of reconstructed skin exposed to non extreme daily-ultraviolet radiation. *PLoS One* 2010; **5**:e12059.
- 160 Rezvani HR, Ged C, Bouadjar B *et al.* Catalase overexpression reduces UVB-induced apoptosis in a human xeroderma pigmentosum reconstructed epidermis. *Cancer Gene Ther* 2008; **15**:241–51.
- 161 Bernerd F, Vioux C, Asselineau D. Evaluation of the protective effect of sunscreens on in vitro reconstructed human skin exposed to UVB or UVA irradiation. *Photochem Photobiol* 2000; **71**:314–20.
- 162 Monti D, Brini I, Tampucci S *et al.* Skin permeation and distribution of two sunscreens: a comparison between reconstituted human skin and hairless rat skin. *Skin Pharmacol Physiol* 2008; **21**:318–25.
- 163 Facy V, Flouret V, Régnier M, Schmidt R. Reactivity of Langerhans cells in human reconstructed epidermis to known allergens and UV radiation. *Toxicol In Vitro* 2005; **19**:787–95.
- 164 Ponec M, Kempenaar J, Weerheim A. Lack of desquamation – the Achilles heel of the reconstructed epidermis. *Int J Cosmet Sci* 2002; **24**:263–72.
- 165 Pigeon H. Reaction of glycation and human skin: the effects on the skin and its components, reconstructed skin as a model. *Pathol Biol (Paris)* 2010; **58**:226–31.
- 166 Pigeon H, Zucchi H, Rousset F *et al.* Skin aging by glycation: lessons from the reconstructed skin model. *Clin Chem Lab Med* 2014; **52**:169–74.
- 167 Krishnamurthy J, Torrice C, Ramsey MR *et al.* Ink4a/Arf expression is a biomarker of aging. *J Clin Invest* 2004; **114**:1299–307.
- 168 Ressler S, Bartkova J, Niederegger H *et al.* p16INK4A is a robust in vivo biomarker of cellular aging in human skin. *Aging Cell* 2006; **5**:379–89.
- 169 Adamus J, Aho S, Meldrum H *et al.* p16INK4A influences the aging phenotype in the living skin equivalent. *J Invest Dermatol* 2014; **134**:1131–3.
- 170 Barker CL, McHale MT, Gillies AK *et al.* The development and characterization of an in vitro model of psoriasis. *J Invest Dermatol* 2004; **123**:892–901.
- 171 Amigo M, Schalkwijk J, Olthuis D *et al.* Identification of avarol derivatives as potential antipsoriatic drugs using an in vitro model for keratinocyte growth and differentiation. *Life Sci* 2006; **79**:2395–404.
- 172 Harrison CA, Layton CM, Hau Z *et al.* Transglutaminase inhibitors induce hyperproliferation and parakeratosis in tissue-engineered skin. *Br J Dermatol* 2007; **156**:247–57.
- 173 Engelhart K, El Hindi T, Biesalski HK, Pfitzner I. In vitro reproduction of clinical hallmarks of eczematous dermatitis in organotypic skin models. *Arch Dermatol Res* 2005; **297**:1–9.

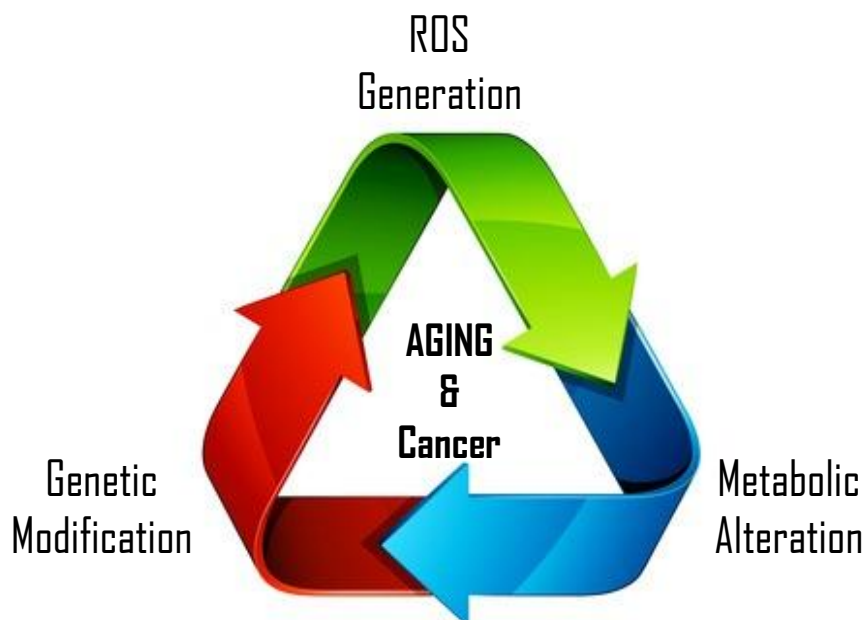
- 174 Tjabringa G, Bergers M, van Rens D *et al.* Development and validation of human psoriatic skin equivalents. *Am J Pathol* 2008; **173**:815–23.
- 175 Jansen PA, Rodijk-Olthuis D, Hollox EJ *et al.* β -defensin-2 protein is a serum biomarker for disease activity in psoriasis and reaches biologically relevant concentrations in lesional skin. *PLoS One* 2009; **4**:e4725.
- 176 Woodley DT, Krueger GG, Jorgensen CM *et al.* Normal and gene-corrected dystrophic epidermolysis bullosa fibroblasts alone can produce type VII collagen at the basement membrane zone. *J Invest Dermatol* 2003; **121**:1021–8.
- 177 Siprashvili Z, Nguyen NT, Bezchinsky MY *et al.* Long-term type VII collagen restoration to human epidermolysis bullosa skin tissue. *Hum Gene Ther* 2010; **21**:1299–310.
- 178 Baldeschi C, Gache Y, Rattenholl A *et al.* Genetic correction of canine dystrophic epidermolysis bullosa mediated by retroviral vectors. *Hum Mol Genet* 2003; **12**:1897–905.
- 179 Rezvani HR, Kim AL, Rossignol R *et al.* XPC silencing in normal human keratinocytes triggers metabolic alterations that drive the formation of squamous cell carcinomas. *J Clin Invest* 2011; **121**:195–211.
- 180 Bernerd F, Asselineau D, Frechet M *et al.* Reconstruction of DNA repair-deficient xeroderma pigmentosum skin in vitro: a model to study hypersensitivity to UV light. *Photochem Photobiol* 2005; **81**:19–24.
- 181 Warrick E, Garcia M, Chagnoleau C *et al.* Preclinical corrective gene transfer in xeroderma pigmentosum human skin stem cells. *Mol Ther* 2012; **20**:798–807.
- 182 Taïeb A, Picardo M; VETF Members. The definition and assessment of vitiligo: a consensus report of the Vitiligo European Task Force. *Pigment Cell Res* 2007; **20**:27–35.
- 183 Cario-André M, Pain C, Gauthier Y, Taïeb A. The melanocytorrhagic hypothesis of vitiligo tested on pigmented, stressed, reconstructed epidermis. *Pigment Cell Res* 2007; **20**:385–93.
- 184 Ricard AS, Pain C, Daubos A *et al.* Study of CCN3 (NOV) and DDR1 in normal melanocytes and vitiligo skin. *Exp Dermatol* 2012; **21**:411–16.
- 185 Mestas J, Hughes CC. Of mice and not men: differences between mouse and human immunology. *J Immunol* 2004; **172**:2731–8.
- 186 Shay T, Jojic V, Zuk O *et al.* Conservation and divergence in the transcriptional programs of the human and mouse immune systems. *Proc Natl Acad Sci USA* 2013; **110**:2946–51.
- 187 Davis MM. A prescription for human immunology. *Immunity* 2008; **29**:835–8.
- 188 Chau DY, Johnson C, MacNeil S *et al.* The development of a 3D immunocompetent model of human skin. *Biofabrication* 2013; **5**:035011.
- 189 Thode C, Woetmann A, Wandall HH *et al.* Malignant T cells secrete galectins and induce epidermal hyperproliferation and disorganized stratification in a skin model of cutaneous T-cell lymphoma. *J Invest Dermatol* 2015; **135**:238–46.
- 190 van den Bogaard EH, Tjabringa GS, Joosten I *et al.* Crosstalk between keratinocytes and T cells in a 3D microenvironment: a model to study inflammatory skin diseases. *J Invest Dermatol* 2014; **134**:719–27.
- 191 Botchkarev VA, Yaar M, Peters EM *et al.* Neurotrophins in skin biology and pathology. *J Invest Dermatol* 2006; **126**:1719–27.
- 192 Tominaga M, Tengara S, Kamo A *et al.* Psoralen-ultraviolet A therapy alters epidermal Sema3A and NGF levels and modulates epidermal innervation in atopic dermatitis. *J Dermatol Sci* 2009; **55**:40–6.
- 193 Yamaguchi J, Aihara M, Kobayashi Y *et al.* Quantitative analysis of nerve growth factor (NGF) in the atopic dermatitis and psoriasis horny layer and effect of treatment on NGF in atopic dermatitis. *J Dermatol Sci* 2009; **53**:48–54.
- 194 Harvima IT, Nilsson G, Naukkarinen A. Role of mast cells and sensory nerves in skin inflammation. *G Ital Dermatol Venerol* 2010; **145**:195–204.

CONCLUSION AND PERSPECTIVES

Conclusion and Perspectives

Growing body of evidence suggests a key role for cellular energy balance in the process of aging and carcinogenesis as well. Since mitochondria generate a large amount of energy by oxidizing nutritional carbohydrates (TCA cycle) and fats (β -oxidation), any dysfunction in this machinery may eventually lead to a variety of diseases in particular age-related disorders and cancers.

As discussed in previous sections, a wide variety of factors including extrinsic and intrinsic stressors such as ROS, oncogenes, tumor suppressors (intrinsic) and UV irradiation and chimio-physical stress (extrinsic) as well can influence mitochondrial metabolism. In this regard, numerous protective mechanisms have been evolved for eliminating the extra and intracellular damages. Endogenous metabolizing and antioxidant enzymes, DNA repair, cell cycle checkpoints, apoptosis, autophagy and immune system are among those mechanisms which all attempt to minimize damage effects. Any disruption or escape from these cellular defense systems could bring various disorders such as premature aging and cancer. In the present research project, we aimed to investigate the role of oxidative and energy metabolism in skin aging and UVB-induced skin cancer.



1. NOX, NOX inhibitor and Aging

To better understand the impact of oxidative and energy metabolism on aging, in the first part of my work we used a transgenic mice model (XPC knockout mice) to find a link between genetic instability, ROS generation and metabolism alteration in process of aging in particular premature skin aging.

Several studies have reported a decline in mitochondrial respiration and mitochondrial energy metabolism, increased steady-state of ROS levels and abundance of mtDNA damages during aging processes (Hosseini et al. 2014a, 2014b; Sanches Silveira and Pedroso 2014).

There are two main accepted theories on aging known as programmed and damage/ error theories. The programmed theory explains that aging follows a biological timetable with linking aging to the length of telomeres and telomerase activity as well (JIN 2010). The damage or error theory elucidates how environmental assaults result in progressive accumulation of damages at various levels. Among five sub-categories of damage theory, theory of free radicals is considered as the most important according to the role of these agents in cellular signaling pathways. This theory proposes that superoxide anion and other free radicals induce damage to macromolecules. Excessive amount of oxidative damages can lead to the failure of cellular repair and maintenance systems (JIN 2010).

Igor Afanas'ev in his review suggests that ROS signaling pathway is possibly the most important enzyme/ gene pathway responsible for the development of cellular senescence and aging (Wallace 2005; Wei et al. 2009; Afanas 2010; Rezvani et al. 2011a).

As described in the first chapter, among several pathways involved in ROS generation NADPH oxidases (NOX_S) are the only known enzymes which are dedicated solely to ROS generation. The expression of these families of oxidases is tissue specific.

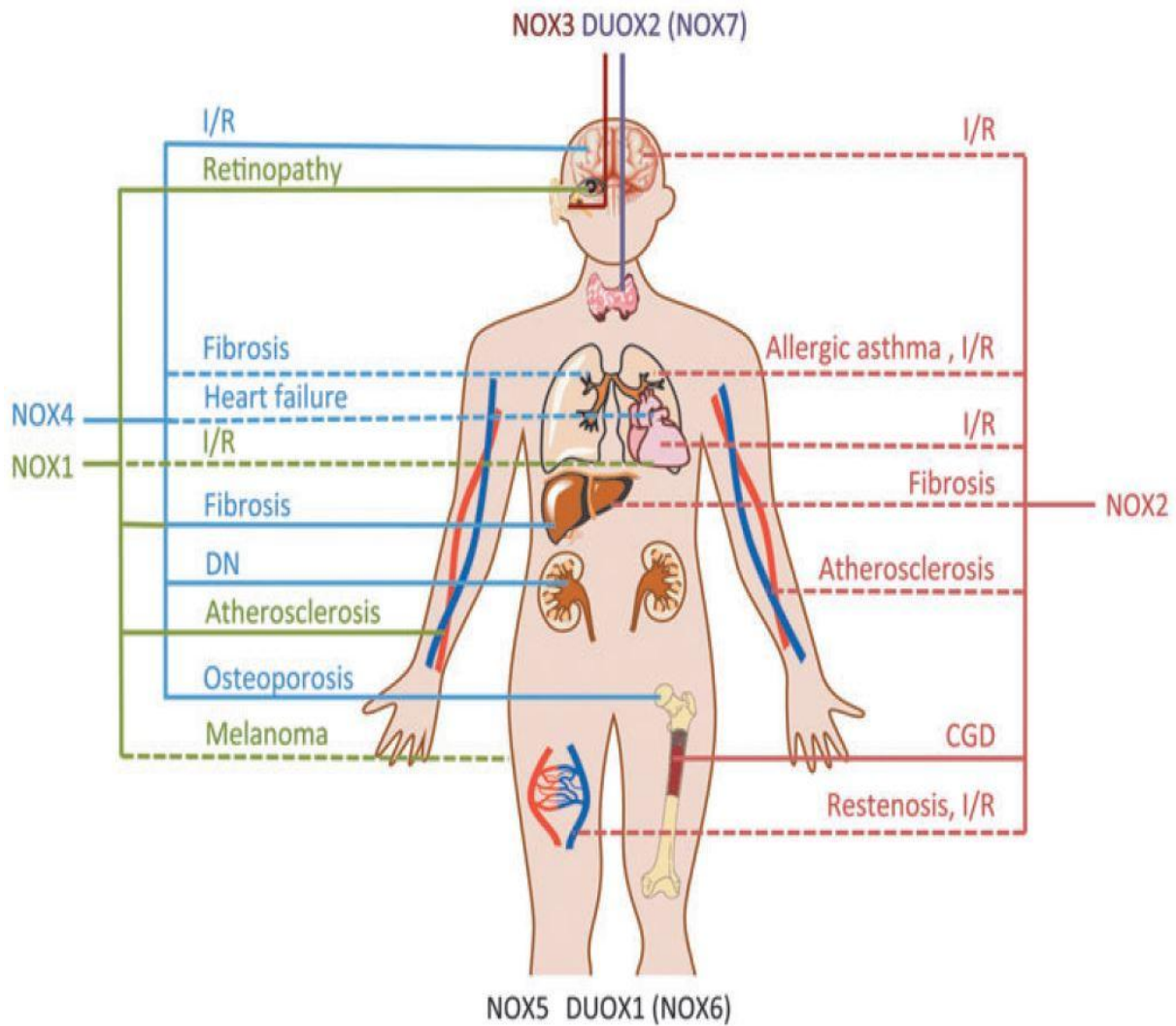


Fig.24. NOX enzymes as validated therapeutic targets (Altenhöfer et al. 2014). The role of each NOX has been shown in mentioned diseases. Partial validation of the mentioned disease model in knockout animals or by using NOX inhibitors (dashed lines). Full validation based on both knockout animals and NOX inhibition or knowledge on mutations leading to human disease (full lines). CGD, chronic granulomatous disease; I/R, ischemia-reperfusion (Altenhöfer et al. 2014).

As previously explained, NOX family members are different in tissue distribution and function (Figure 24, Table3). Thus, developing specific inhibitors for these members would be of benefit in clinical applications.

1.1. NOX Activity in Carcinogenesis

Multiple genetic and epigenetic alterations (HITS) are the major causes of cellular transformation. These processes could lead to over expression of NOX complexes and subsequently increase the NOX-derived reactive oxygen species (ROS). It has been shown that excess in ROS can lead to an uncontrolled cell proliferation and decreased apoptosis (Block and Gorin 2012a). Afterwards, increase in uncontrolled cell proliferation gradually would build the tumor mass. In tumors with a diameter between 1-2 mm, NOX complexes sense a reduced level of oxygen level. Accordingly, in order to supply the required cellular oxygen, NOXs would mediate the activation of angiogenesis. NOX complexes can facilitate tumor invasion and metastasis by regulating the extracellular fluid surrounding the tumor environment.

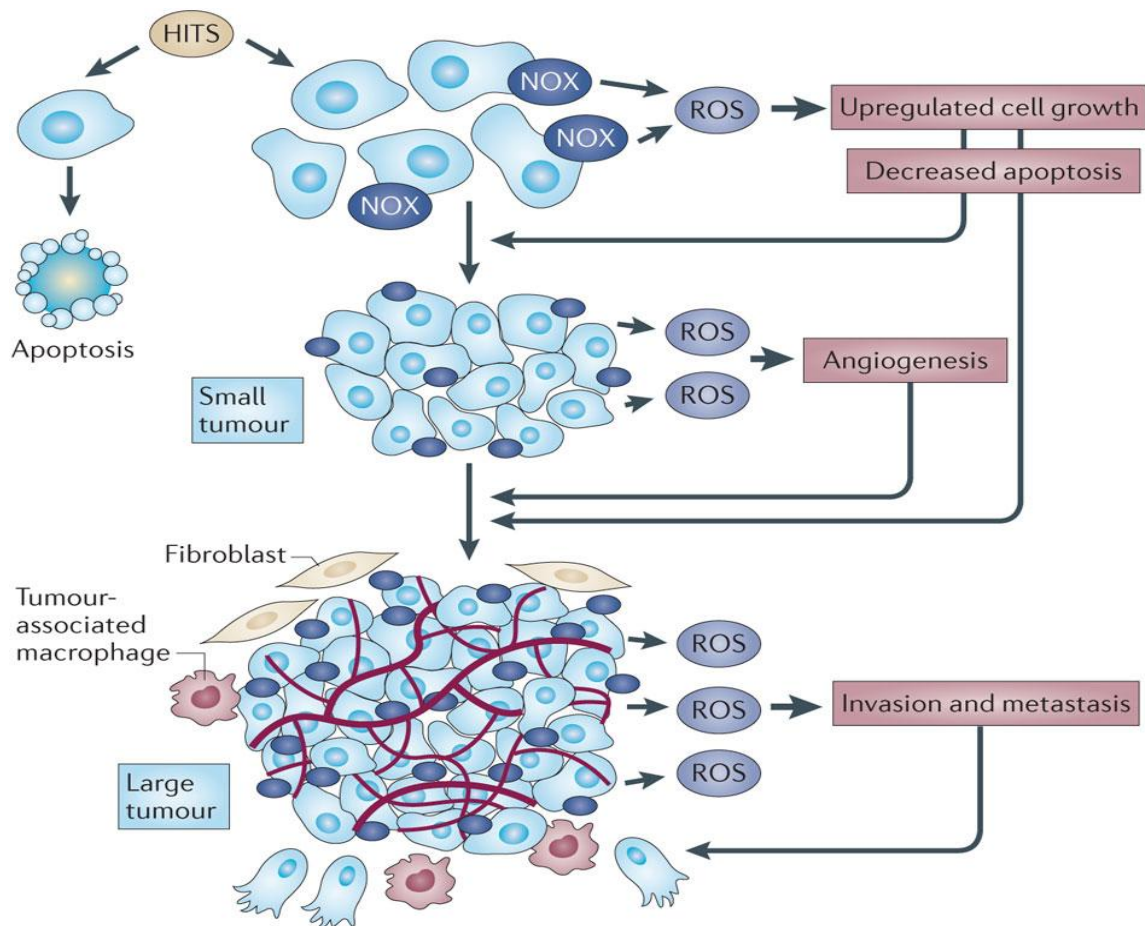
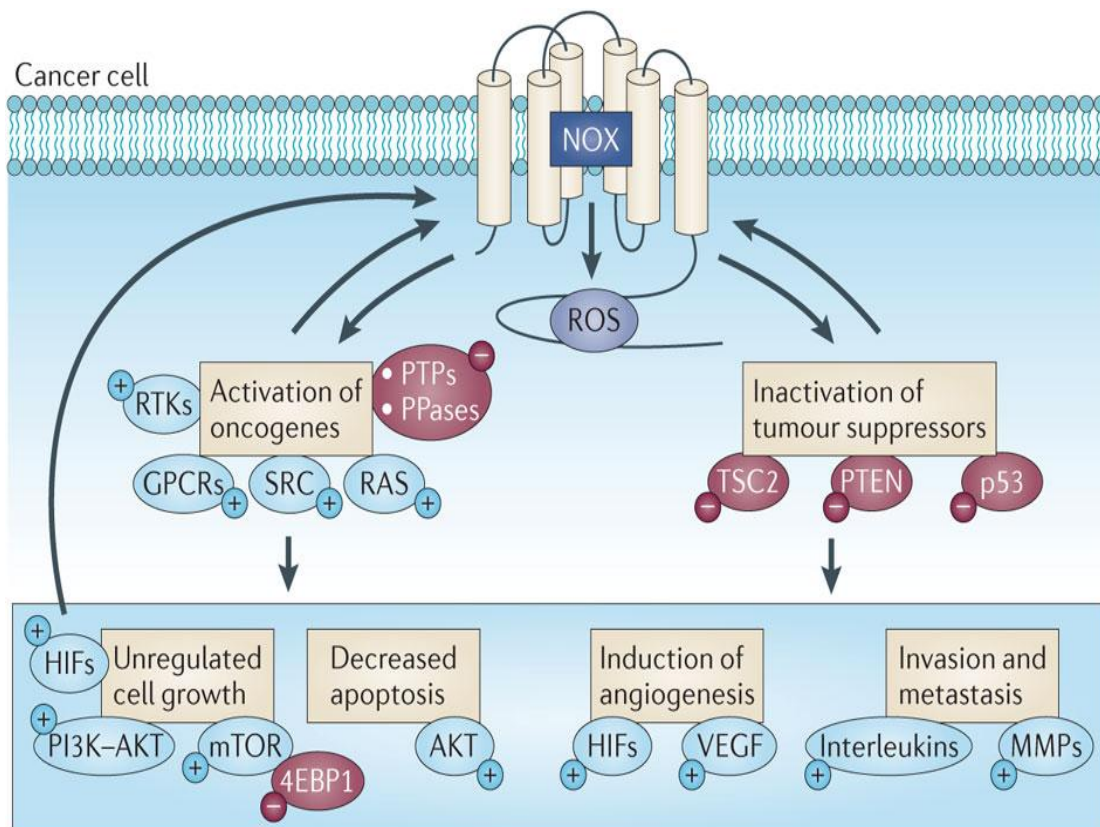


Fig.25. The role of NOX complexes and NOX-derived ROS in the progression of carcinogenesis (Block and Gorin 2012a).

Signaling pathways associated with upregulation of NOX are demonstrated in figure 26. The link between NOX activity and activation of oncogenesis or inactivation of tumor suppressors has been confirmed in several studies (Block and Gorin 2012b; Altenhöfer et al. 2014). These studies have shown that any alterations in oncogenes or tumor suppressors influence NOX activity and lead to tumorigenesis by deregulation of cell growth, angiogenesis and apoptosis pathways, afterwards.



Nature Reviews | Cancer

Fig.26. Integration of NOX oxidase-derived ROS with the hallmarks of cancer (Block and Gorin 2012a).

1.2. NOX Inhibitors

After failure in most of the antioxidant clinical trials, NOX inhibitors appear to be the most promising therapeutic option for disorders associated with oxidative stress such as aging (Altenhöfer et al. 2014).

The potential of NOX inhibitors as a real therapeutic target has been determined following construction of the first NOX knockout (KO) mice model. This mice model was a NOX2 KO with more susceptibility to infections as a result of the loss of oxygen-dependent killer mechanism (Pollock et al. 1995). Later, other NOX KO models were created in order to better understand the role of each complex on clinical disorders.

DPI (diphenyleneiodonium) and Apocynin are widely used as NOX inhibitors to inhibit these enzymes in several disorders. Due to their non-specific effects, it is not possible to determine the specific role of each complex separately after the administration of the drug.

Following scheme presents the current inhibitors of NOX_s and their specific inhibition sites. Non-specific inhibitors of NOX are illustrated in red font, recommended inhibitors in white on a red background and partly recommended inhibitors in red on a pale red background (Altenhöfer et al. 2014; Hosseini et al. 2014b).

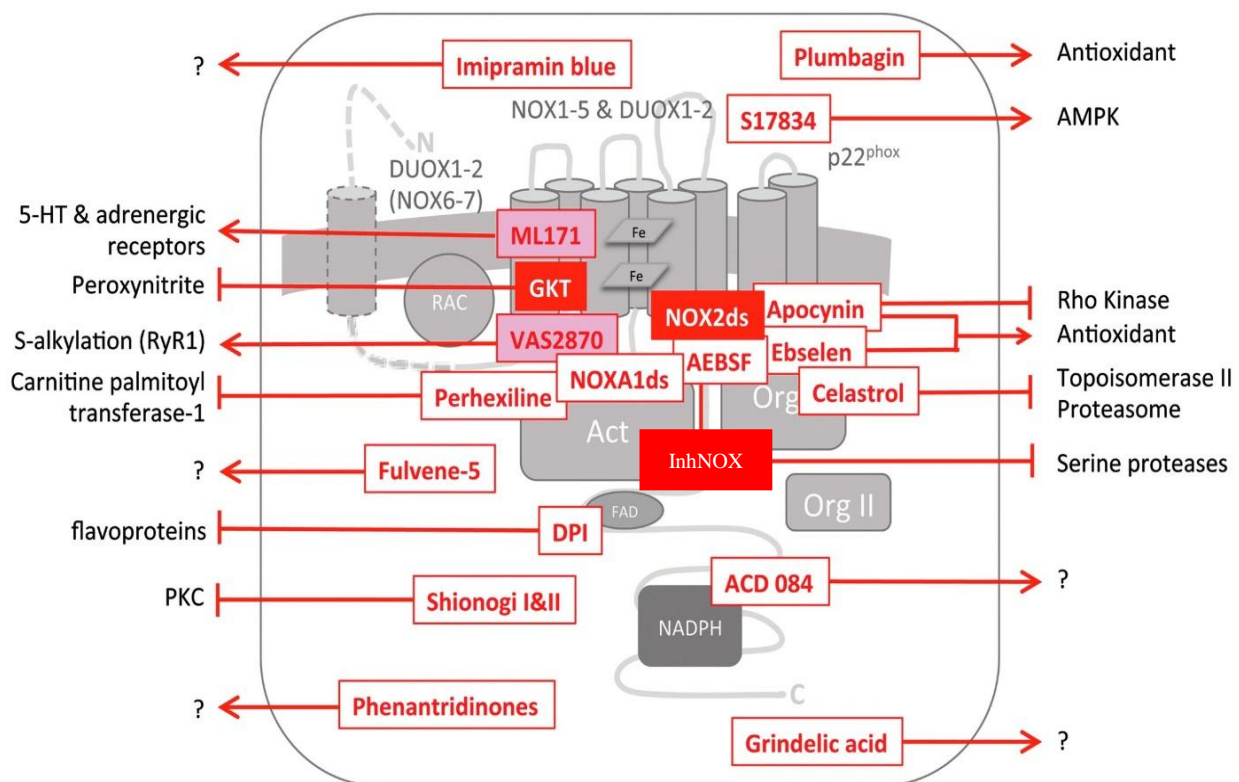


Fig.27. Different Types of NOX Inhibitors and their Specific Site of Action (Altenhöfer et al. 2014).

Our team has already demonstrated that over expression of NOX1 is the principle responsible element for excess of ROS generation in XPC deficient cells (Rezvani et al. 2011b; Hosseini et al. 2014b). NOX1 over-expression has been also reported in various cultured cancer cell lines and many disorders such as cardiovascular diseases. Application of the current inhibitors of NOX1 had any significant inhibitory effect on ROS generation.

In order to reduce NOX1-mediated ROS generation and their respective damage in XPC deficient cells, our team used to investigate the development of a specific inhibitor against NOX1. Following examination of several different peptides, we pinpointed one efficient peptide inhibitor which impedes the assembly of NOX1A subunit (Activator) to NOX1O (Organizer). This novel peptide is considered to be helpful in prevention and/or treatment of cancer, atherosclerosis, angiogenesis and aging as well. In our recent study we showed that topic application of InhNOX prevents premature skin aging in XPC-KO mice through inhibition of ROS generation and alteration of metabolism (Hosseini et al. 2014b).

1.3. InhNOX for Cancer Therapy

Rezvani and colleagues in 2011 demonstrated that NOX1 is the major source of ROS production in human keratinocytes XPC^{KD} (Rezvani et al. 2011b). To determine whether increased ROS generation in XPC^{KD} cells can lead to tumorigenesis, cells were subcutaneously injected to immunodeficient NOD/ SCID. Cells formed SCC tumors 17 weeks after the injection. In previous investigations of the tem, significant increase in NOX1-mediated ROS levels and an alteration in metabolism had been identified as the main cause of skin carcinogenesis (Rezvani et al. 2011b).

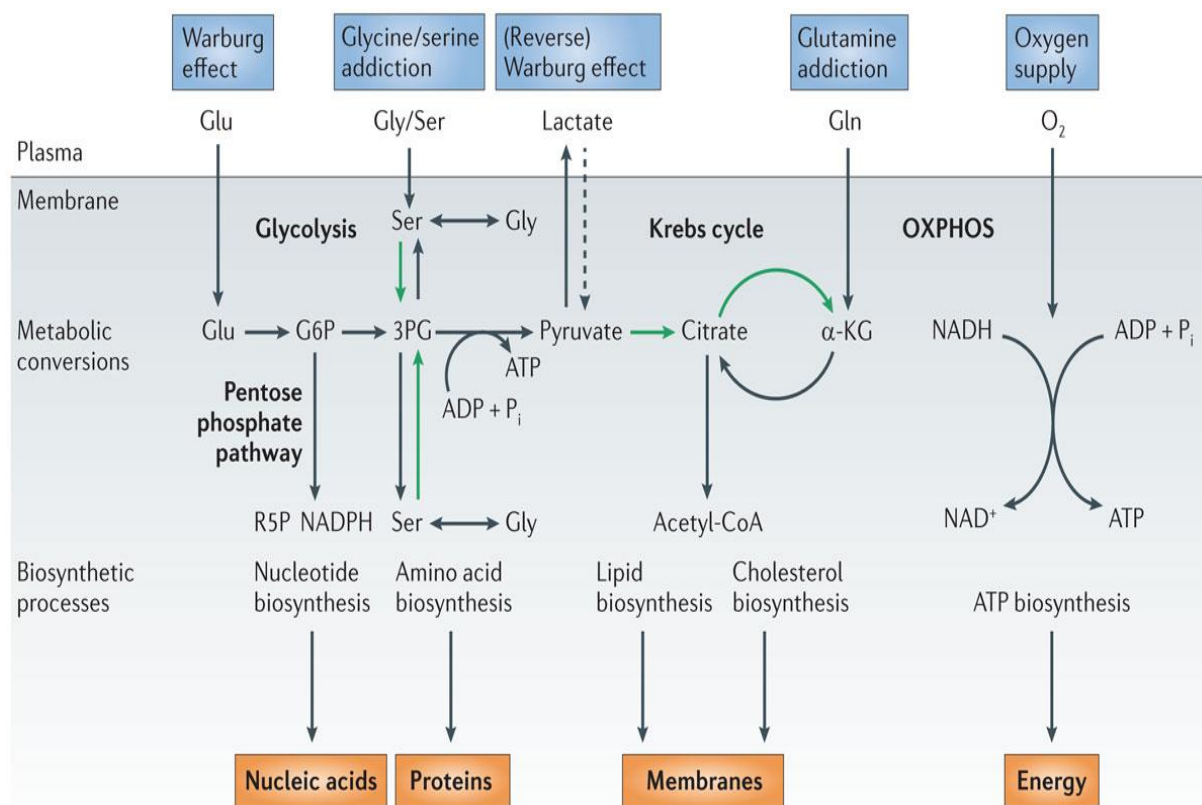
To find out if InhNOX could reduce the UVB-induced tumorigenesis in XPC deficient mice, we used to administer the inhibitor on the back of the mice before each irradiation. As expected, InhNOX significantly reduced UV-induced carcinogenesis in SKH mice model. The reduced NOX-1 activity in InhNOX-treated mice also led to alteration of several pathways in specific metabolism and DNA repair pathways (unpublished data).

Our published and unpublished data on the role of NOX in skin aging and carcinogenesis suggest that NOX1 complex can be considered as a promising target in cancer therapy and prevention of premature aging. Moreover, InhNOX as a specific inhibitor for NOX1 activity

presents great therapeutic potential in the treatment of disorders associated with NOX1-related oxidative stress.

2. Energy Metabolism in UVB-induced Skin Cancer

In the latter part of the thesis, the focus was on the relationship between metabolism remodeling and carcinogenesis. Based on Warburg effect, malignant cells have an increased rate of glycolysis. In addition, a large number of studies have confirmed an elevated flux in the pentose phosphate pathway, high rates of glutamine consumption and reduction of autophagy and apoptosis levels in transformed cells as well. Beside changes in catabolic pathways, malignant cells (as highly proliferative normal cells) also develop a few anabolic pathways including biosynthesis of fatty acids, nucleic acids and proteins (Galluzzi et al. 2013).



Nature Reviews | Drug Discovery

Fig.28. Overview of metabolic alterations in malignant cells (Galluzzi et al. 2013).

Excessive rate of lipid synthesis has been reported in a wide variety of precursor lesions and tumors. Fatty acid synthase (FASN) is one of the most important key metabolic enzymes involved in this path. This enzyme catalyzes the synthesis of palmitate and the last step of FA synthesis as well. Alteration of FASN function has been indicated in almost all malignant cells. Recent studies suggest that evaluation of FASN over expression can be used as a diagnostic test in estimating the recurrence risk of human cancers. Inhibition of FASN is identified as an effective strategy to reduce the cancer development (Dang 2012).

As already mentioned, the pathway of nucleic acid biosynthesis is another anabolic pathway which increases during carcinogenesis. Inhibition of nucleic acid synthesis in malignant cells is considered as an effective strategy in cancer therapy. The known molecules used for reducing nucleic acid synthesis in this regard include: i) Methotrexate and pemetrexed which inhibits folate metabolism, ii) 5-Fluorouracil which acts through the inhibition of thymidine synthesis, iii) Hydroxyurea which blocks deoxynucleotide synthesis, iv) Gemcitabine and Fludarabine which are inhibitors of nucleic acid elongation.

These molecules reduce carcinogenesis but also affect highly proliferative cells by their toxicity.

According to the literature, a part of *de novo* synthesis of pyrimidines is dependent on the mitochondrial respiratory chain since dehydroorotic acid dehydrogenase (DHODH) reduces CoQ which is located on ETC. Therefore any change in ETC activity can directly influence the biosynthesis of nucleic acids. In 2013, Fang et al. (Fang et al. 2013) showed that knockdown of DHODH leads to the cell growth retardation and deficiency in pyrimidine synthesis. They found that depletion of DHODH ultimately results in mitochondrial dysfunction.

Since damaged cells need a large amount of energy in order to serve various cellular pathways such as defense mechanisms including DNA repair system, apoptosis, autophagy, mitophagy and many others, ETC is considered as the best supplier of ATP. Accordingly, Over-activation of ETC and higher production of ATP as the result could increase the rate of *de novo* synthesis of pyrimines.

Up-regulation of DHODH has been reported in many disorders such as cancer, autoimmunity, malaria, rheumatoid arthritis and psoriasis. DHODH has been shown to be an ideal target for cancer therapy (Vyas and Ghate 2011). In this study, we depleted DHODH activity by using *Tfam* mice model. Our results have shown that deficiency in DNA repair or other defense

mechanisms as a result of ETC deficiency ultimately lead to a dramatic rise in UVB-induced precancerous lesions in *Tfam* deficient mice.

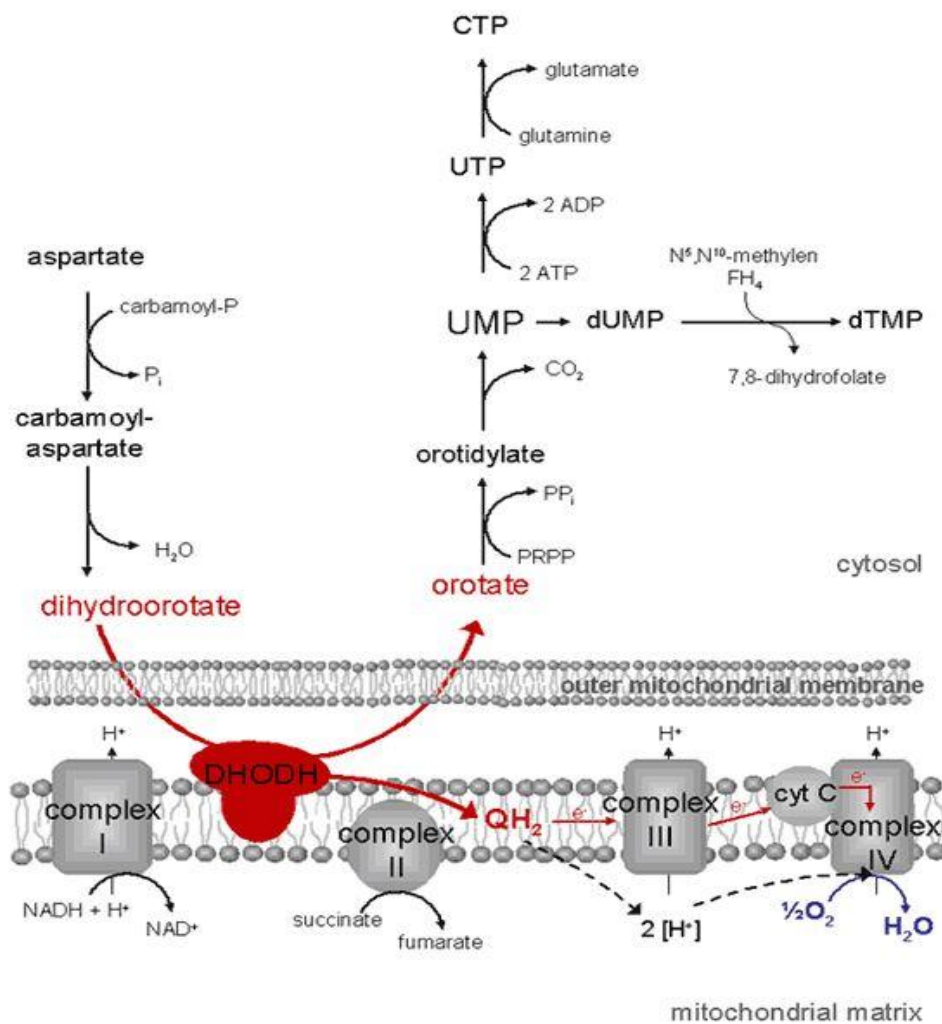


Fig.29. Nucleogenesis: Dihydroorotate dehydrogenase(from <http://www.metabolicdatabase.com>)

2.1. Targeting Cancer Metabolism

In the last two decades, a great deal of research has been conducted to understand the link between metabolic alterations and tumorigenesis. As detailed in my review article on metabolism and cancer, activating or deactivating bioenergetic pathways and anabolic metabolism are ideal targets for cancer therapy as they are the main affected pathways in carcinogenesis. Promising metabolic targets for cancer therapy are depicted in figure 30 and my review article on metabolism and skin cancer.

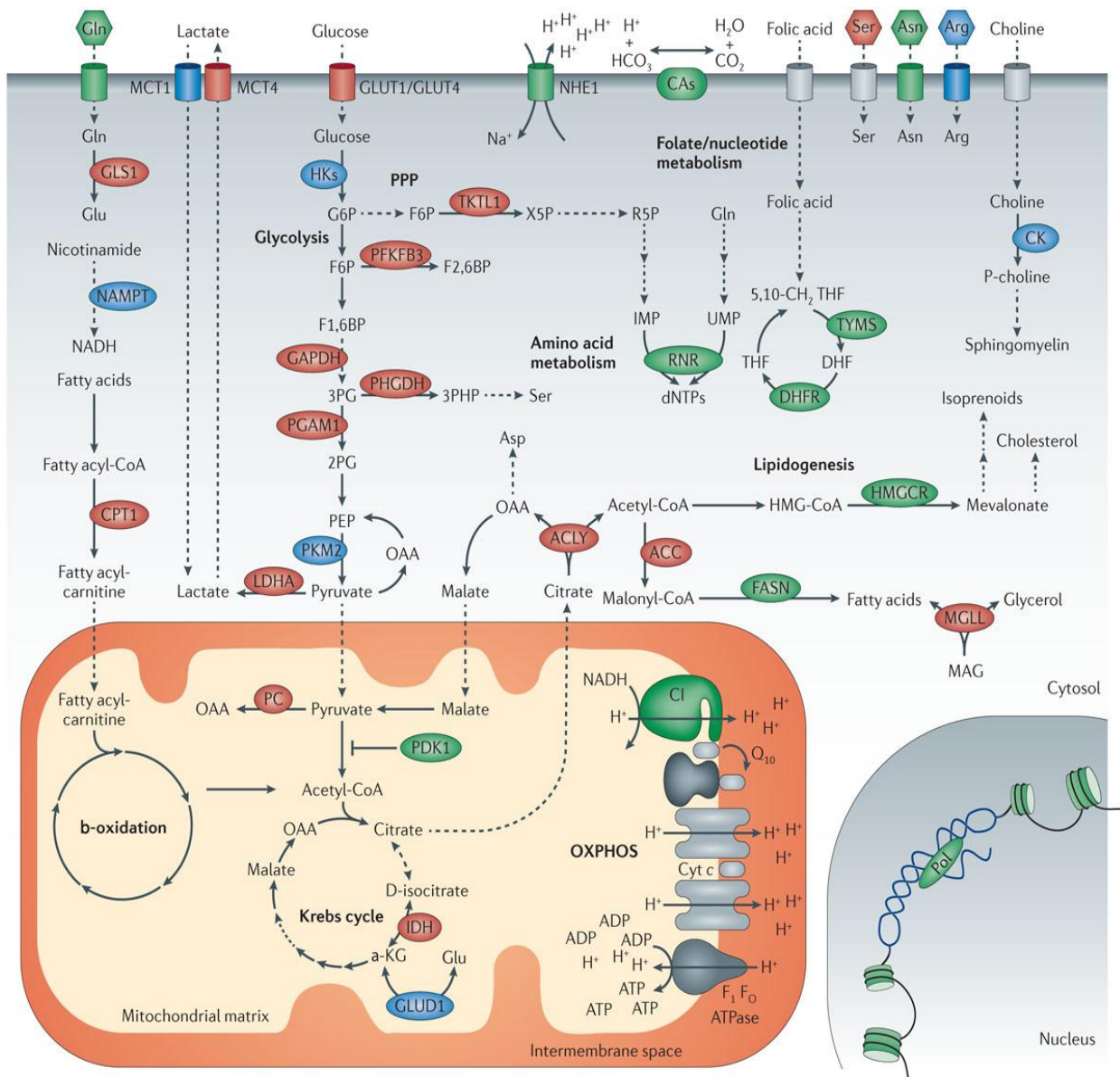


Fig.30. Metabolic Targets for Cancer Therapy. Green: Targets in clinical phase, Blue: Targets in preclinical, Red: To be considered as future targets (Galluzzi et al. 2013).

2.2. Combination Therapy

As suggested by Hanahan and Weinberg (Hanahan and Weinberg 2011), inhibition of metabolism alteration can be considered as a therapy for cancer. In the present study, we

report that UVB irradiation would promote metabolic alterations. In fact, irradiated cells reprogram their energy metabolism systems in order to adapt themselves to new conditions.

Evidently, cells discover new ways to respond thoroughly to the UVB-induced damage by; i) induction of nucleotide synthesis to boost DNA repair, ii) triggering lipid synthesis to induce cell differentiation and membrane synthesis and iii) supplying energy demands of the cell for clearance of the damage. These results indicate that cells have a huge capacity in adapting new conditions. Certainly, this adaptive capacity should be considered in cancer therapy. Indeed, due to the high degree of cancer clonal heterogeneity, cell signal complexity and intra-tumor genetic heterogeneity, inhibition of a single target alone, cannot be the best solution for the treatment of cancer. Cancer cells in case of abnormalities or blocked pathways have this potential to find other pathways for respond to their needs.

Recently some research work using a combination of molecular-targeted agents (MATs) showed a great potential in this strategy in regard to cancer therapy. Advantage for this type of therapy is sure a definite reduced resistance to drug. Accordingly, in investigating effective combination treatment of cancer therapy, the most important cellular signaling pathways (i.e. VEGF, EGFR, MAPK, PI3K and mTOR) could be sure taken into account.

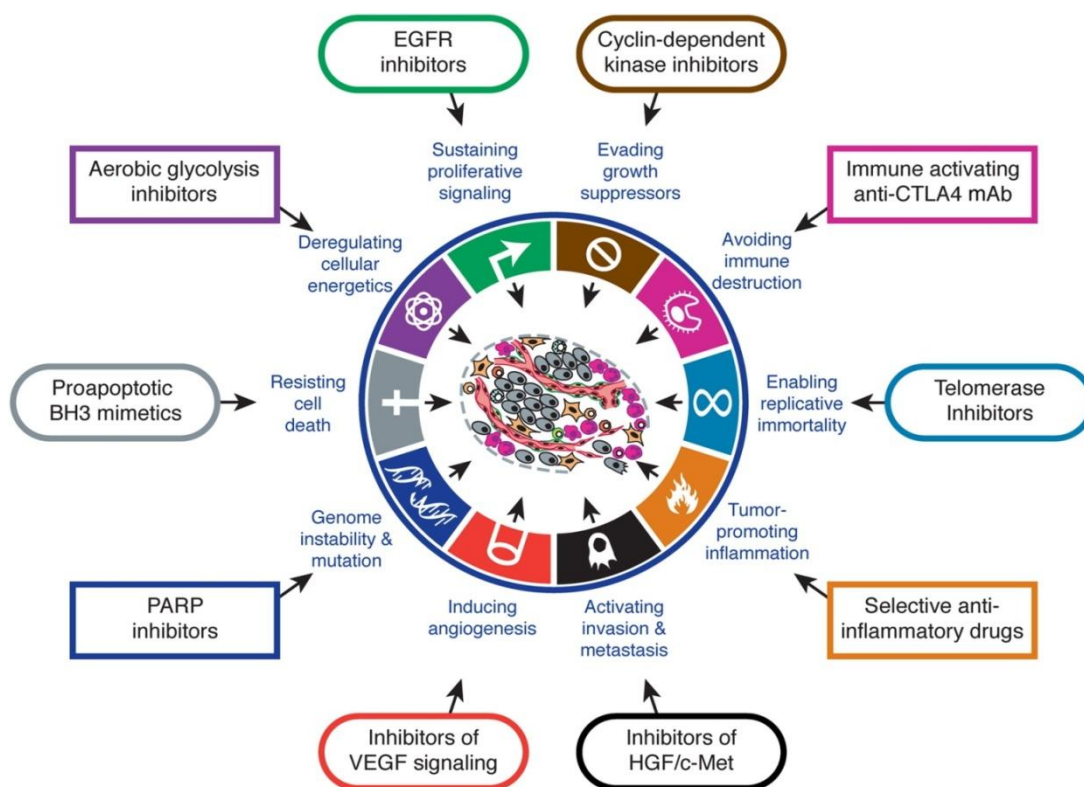


Fig.31. The main pathways involved in carcinogenesis (Hanahan and Weinberg 2011).

Perspectives

In general, over 10% of untreated Actinic Keratosis can develop into skin cancer. Currently in most of the cases, AK is treated with available therapies without taking any biopsy. Patients with multiple and confluent actinic keratoses (AKs) are highly susceptible to non-melanoma skin cancer. In order to estimate the recurrence rate of AK or evaluate the risk of tissue tumorigenesis for this purpose, we propose to measure the metabolic rate in biopsy samples as a diagnosis test. Moreover, we suggest to measure the metabolic rate in cancer biopsies. Having skin cancer can raise the risk for developing other cancers as well. In a small number of patients, cancer comes back either in the same skin area or nearby. It is noteworthy that, by measuring metabolic factors in cancer biopsies, we can prevent and treat cancer recurrences and estimate the recurrence rate of tumorigenesis in patients as well.

APPENDIX

Article 6



Inhibition of p38 MAPK Signaling Augments Skin Tumorigenesis via NOX2 Driven ROS Generation

Liang Liu¹, Hamid Reza Rezvani^{2,3}, Jung Ho Back¹, Mohsen Hosseini^{2,3}, Xiuwei Tang¹, Yucui Zhu¹, Walid Mahfouf^{2,3}, Houssam Raad^{2,3}, Grace Raji¹, Mohammad Athar⁴, Arianna L. Kim^{1*}, David R. Bickers^{1*}

1 Department of Dermatology, Columbia University Medical Center, New York, New York, United States of America, **2** Biothérapies des maladies génétiques et cancers, Univ. de Bordeaux, Bordeaux, France, **3** INSERM, Biothérapies des maladies génétiques et cancers, Bordeaux, France, **4** Department of Dermatology, University of Alabama at Birmingham, Birmingham, Alabama, United States of America

Abstract

p38 mitogen-activated protein kinases (MAPKs) respond to a wide range of extracellular stimuli. While the inhibition of p38 signaling is implicated in the impaired capacity to repair ultraviolet (UV)-induced DNA damage—a primary risk factor for human skin cancers—its mechanism of action in skin carcinogenesis remains unclear, as both anti-proliferative and survival functions have been previously described. In this study, we utilized cultured keratinocytes, murine tumorigenesis models, and human cutaneous squamous cell carcinoma (SCC) specimens to assess the effect of p38 in this regard. UV irradiation of normal human keratinocytes increased the expression of all four p38 isoforms ($\alpha/\beta/\gamma/\delta$); whereas irradiation of p53-deficient A431 keratinocytes derived from a human SCC selectively decreased p38 α , without affecting other isoforms. p38 α levels are decreased in the majority of human cutaneous SCCs assessed by tissue microarray, suggesting a tumor-suppressive effect of p38 α in SCC pathogenesis. Genetic and pharmacological inhibition of p38 α and in A431 cells increased cell proliferation, which was in turn associated with increases in NADPH oxidase (NOX2) activity as well as intracellular reactive oxygen species (ROS). These changes led to enhanced invasiveness of A431 cells as assessed by the matrigel invasion assay. Chronic treatment of p53^{-/-}/SKH-1 mice with the p38 inhibitor SB203580 accelerated UV-induced SCC carcinogenesis and increased the expression of NOX2. NOX2 knockdown suppressed the augmented growth of A431 xenografts treated with SB203580. These findings indicate that in the absence of p53, p38 α deficiency drives SCC growth and progression that is associated with enhanced NOX2 expression and ROS formation.

Citation: Liu L, Rezvani HR, Back JH, Hosseini M, Tang X, et al. (2014) Inhibition of p38 MAPK Signaling Augments Skin Tumorigenesis via NOX2 Driven ROS Generation. PLoS ONE 9(5): e97245. doi:10.1371/journal.pone.0097245

Editor: Andrzej T. Slominski, University of Tennessee, United States of America

Received: October 31, 2013; **Accepted:** April 16, 2014; **Published:** May 13, 2014

Copyright: © 2014 Liu et al. This is an open-access article distributed under the terms of the Creative Commons Attribution License, which permits unrestricted use, distribution, and reproduction in any medium, provided the original author and source are credited.

Funding: This work was supported in part by a pilot grant from the Center for Environmental Health in Northern Manhattan (P30 ES009089), Columbia University Skin Disease Research Center grant P30AR44535, R01ES020344, and R01CA130998. The funders had no role in study design, data collection and analysis, decision to publish, or preparation of the manuscript.

Competing Interests: Arianna Kim currently serves an Academic Editor for PLOS ONE. This does not alter the authors' adherence to all the PLOS ONE policies on sharing data and materials. The authors have declared that no other competing interests exist.

* E-mail: ak309@columbia.edu; ak309@columbia.edu

Introduction

Exposure to solar ultraviolet (UV) radiation is a primary risk factor for human skin carcinogenesis. In addition to its ability to induce mutagenic DNA damage, UV radiation induces extensive cellular damage through a variety of mechanisms, including augmented production of intracellular reactive oxygen species (ROS) [1]. Augmented ROS and consumption of physiological antioxidants drive signaling mechanisms involved in tumor promotion and progression [1–3]. Intracellular ROS are primarily generated through aerobic metabolism or through a specialized group of enzymes, known as the NADPH oxidases, in which NOX is the catalytic subunit [4,5]. NADPH oxidase activity is associated with several characteristic features of cancer, including genomic instability, cell proliferation, survival, invasion, and metastasis [6–8]. Of the seven distinct NOX enzymes (NOX1–NOX5, Duox1, and Duox2) that are known to exist in humans, NOX1-induced ROS has been implicated in oncogenic signaling in Ras-transformed NIH3T3 cells [9]. Moreover, increases in NADPH oxidase activity and NOX1 levels are observed in human cutaneous squamous cell carcinomas (SCCs) and keratinocytes of

individuals affected with xeroderma pigmentosum C (XPC), an autosomal recessive disorder that is associated with compromised nucleotide excision repair that leads to accelerated development of multiple types of skin cancer [10,11]. Despite the evidence supporting the role of oxidative stress in skin cancer, the molecular pathways involved in skin carcinogenesis are not fully understood.

p38 mitogen-activated protein kinases (MAPKs) are activated in response to a wide range of extracellular stimuli, including among others osmotic and thermal stress, growth factors, inflammatory cytokines, and UV radiation. p38 influences various cellular processes, including proliferation, differentiation, apoptosis, and inflammation [12]. Four p38 MAPK isoforms have been identified, including α , β , γ , and δ . Among these four isoforms, p38 α and p38 β have overlapping functions; meanwhile, p38 γ and p38 δ are structurally similar to each other, but distantly related to both p38 α and p38 β [13] [14]. Furthermore, p38 α and p38 δ are abundantly expressed in epidermis, whereas p38 β or p38 γ are virtually undetectable in normal epidermis [15,16]. p38 α has also been shown to be responsive to UV irradiation and plays an important role in the regulation of cell-cycle arrest and apoptosis [17]. The exact role of p38 α in cancer, however, remains

controversial. Both anti-proliferative and survival functions of p38 α have been described [18–21]. For example, p38 α can negatively regulate cell cycle progression at both the G1/S and G2/M transitions, via downregulation of cyclins and upregulation of cyclin-dependent kinase inhibitors [18,19]. In contrast, pro-survival roles of p38 have also been observed during the G2 DNA damage checkpoint response, through the upregulation of the Bcl2 family proteins [20], or via induction of a quiescent state known as cancer dormancy, which may be an important mechanism for acquisition of drug resistance by cancer cells [21]. These dualistic effects of p38 α also occur in skin carcinogenesis. Autophagy-associated decreased p38 phosphorylation enhances cell survival and UVB-induced SCC carcinogenesis in murine models [22]. In contrast, chronic UV irradiation of p38 α -dominant negative (p38 α DN) mice diminished the growth of skin tumors [23]. The cause of these disparate effects are not clear but interplay with other signaling pathways, as well as the nature of p38 MAPK substrates, could account for them [24]. For example, p38 activates the p53 tumor suppressor, and the p53 pathway is known to synergize p38 MAPK signaling, suggesting cross-talk between these two pathways [25]. Nonetheless, UV-induced mutational inactivation of p53 is a common finding in sun-exposed skin, and the majority of human SCCs harbor p53 mutations. Using p53-deficient SCC keratinocytes and p53^{-/-}/SKH-1 mice, we assessed the role of p38 α to explore the connection between p38 α and NOX-mediated ROS generation. Our results indicate that chemical inhibition of p38 activity enhances UV-induced SCC growth in p53^{-/-}/SKH-1 mice, which is accompanied by increased NOX2 expression and elevated intracellular ROS levels.

Materials and Methods

Cells and Reagents

A431 human epidermoid squamous cell carcinoma (SCC) cells were obtained from the American Type Culture Collection (ATCC, Manassas, VA) and maintained according to ATCC guidelines. Primary human keratinocytes isolated from neonatal foreskin were obtained from Columbia University Skin Disease Research Center (SDRC) tissue culture core facility and cultured in 154CF medium supplemented with human keratinocyte growth supplement (Life Technologies, Grand Island, NY). SB203580, a pyridinyl imidazole inhibitor widely used to inhibit the biological function of p38 α / β [26–28], and diphenyleneiodonium (DPI), an inhibitor of NADPH oxidase-mediated ROS formation, were purchased from Sigma-Aldrich (St. Louis, MO). siRNA targeting p38 α coding regions and scrambled siRNA controls (con) were obtained from Santa Cruz Biotechnology (Santa Cruz, CA). SB203580 was dissolved in DMSO for cell culture or in 0.5% methylcellulose (Sigma-Aldrich) for oral administration to mice. DPI was dissolved in dimethyl sulfoxide (DMSO) and added to cell cultures at a final concentration of 2.5 μ M. SCC tissue microarrays (TMAs) were obtained from Imgenex (San Diego, CA).

siRNA transfection

A431 cells were transfected with 40 nM of p38 α MAPK siRNA or scrambled siRNAs using Lipofectamine RNAiMax (Santa Cruz Biotechnology, Santa Cruz, CA). The efficiency of p38 α downregulation was assessed by RT-PCR and Western blotting 24 h–48 h after transfection.

qRT-PCR and Western blotting

Total RNA was isolated from whole skin or cultured cells using the RNeasy Kit (Qiagen, Gaithersburg, MD) and treated with DNase I (Life Technologies, Grand Island, NY) according to the

manufacturers' protocols. Total RNA (2 μ g) was then reverse transcribed by Superscript III using random hexamer primers according to the manufacturer's instructions. Primers for each gene are listed in Table 1. For Western blotting, protein was isolated from whole skin or cultured cells following established procedures [29]. Proteins were resolved on 4–15% SDS-PAGE gels and blotted according to standard procedures using the following primary antibodies: p38 α , p38 β , p38 γ , p38 δ , p-p38 and cyclin D1 (Cell Signaling Technology, Danvers, MA), Cdc25C, and phospho-c-Jun (Santa Cruz Biotechnology, Dallas, TX), NOX2 (Abcam, Cambridge, MA), tubulin and β -actin (Sigma-Aldrich, St. Louis, MO).

BrdU incorporation assay

A431 cell growth and proliferation following p38 α siRNA-treatment or scramble siRNA control (scr)-treatment were analyzed by BrdU incorporation, following the manufacturer's instructions (BD Biosciences, San Jose, CA). For labeling, 24 h after transfection, BrdU was added directly to the cell culture to a final concentration of 100 μ M, and cultures were incubated for another 24 h, at which point cells were harvested, fixed, permeabilized, treated with DNase I, and stained with a FITC-conjugated anti-BrdU antibody (BD Biosciences, San Jose, CA). Fluorescence intensity was measured using a fluorescence plate reader.

Cell invasion assay

The invasiveness of p38 α -depleted and control SCC cells was assessed using BD BioCoat Matrigel Invasion Chambers, following the manufacturer's instructions (BD Biosciences, San Jose, CA). Briefly, 1×10^5 cells/well were plated onto the six-well plate and allowed to grow overnight at 37°C. Cells invading the matrigel were stained and counted.

Measurement of intracellular ROS

Intracellular ROS was assessed using a cell-permeable fluorogenic probe, 2',7'-dichlorofluorescein diacetate (CM-H2DCF-DA) dye (Life Technologies), which detects hydrogen peroxide production. Briefly, 48 h following transfection of the p38 α siRNA or scrambled siRNA into A431 cells, CM-H2DCF-DA was added to the cells at a final concentration of 5 μ M and incubated for 15 min at 37°C in the dark. CM-H2DCF-DA is oxidized by cytoplasmic ROS to a green fluorescent CM-DCF compound. After 2 washes with PBS, cells were detached by trypsin-EDTA and immediately analyzed by flow cytometry; 1×10^4 cells were collected and analyzed for each sample.

Measurement of NADPH oxidase activity

NADPH oxidase activity was measured in plasma membranes obtained from A431 cells or tumor tissues. Specimens were incubated in hypotonic buffer supplemented with protease inhibitor cocktails (Sigma-Aldrich, St. Louis, MO) for 30 min on ice. Following sonication, the homogenate was centrifuged at $1000 \times g$ for 15 min at 4°C. The supernatant was collected and centrifuged at $12,000 \times g$ for 1 h at 4°C. The pellet consisting of crude membranes was resuspended in 50 μ l $1 \times$ PBS supplemented with 0.9 mM CaCl₂ and 0.5 mM MgCl₂. After adding 200 μ l of solution containing 0.8 mM glucose, 2 mM luminol and 500 U/ml horseradish peroxidase, the reaction mixture was incubated for 1 min at 37°C. Following the addition of 10 ng/ml of phorbol myristate acetate (PMA), the RLU of chemiluminescence were recorded every 30 seconds for a total of 90 minutes at 37°C using a luminometer.

Table 1. Primer sequences for real-time PCR.

	Forward (5'-3')	Reverse (5'-3')
GAPDH (human)	AATGAAGGGTCATTGATGG	AAGGTGAAGGTCGGAGTCAA
p38 α (human)	TCAGTCCATCATTATGCGAAA	AACGTCCAACAGACCAATCAC
p38 β (human)	AAGCACGAGAACGTCATCGG	TCACCAAGTACACTTCGCTGA
p38 γ (human)	CATGAGAAGCTAGGCGAGGAC	CAGCGTGGATATACCTCAGCC
p38 δ (human)	GCCGAGATGACTGGCTACG	TGGTCCAGGTAATCTTTCCCC
Nox2-1st (mouse)	ACCCCTTGGTACGCCAGTG	TTGCAATGGTCTTGAACCTCG
Nox2-2nd (mouse)	CCTTGGCTCCATTCTCAAG	GTGCACAGCAAAGTGATTGG

doi:10.1371/journal.pone.0097245.t001

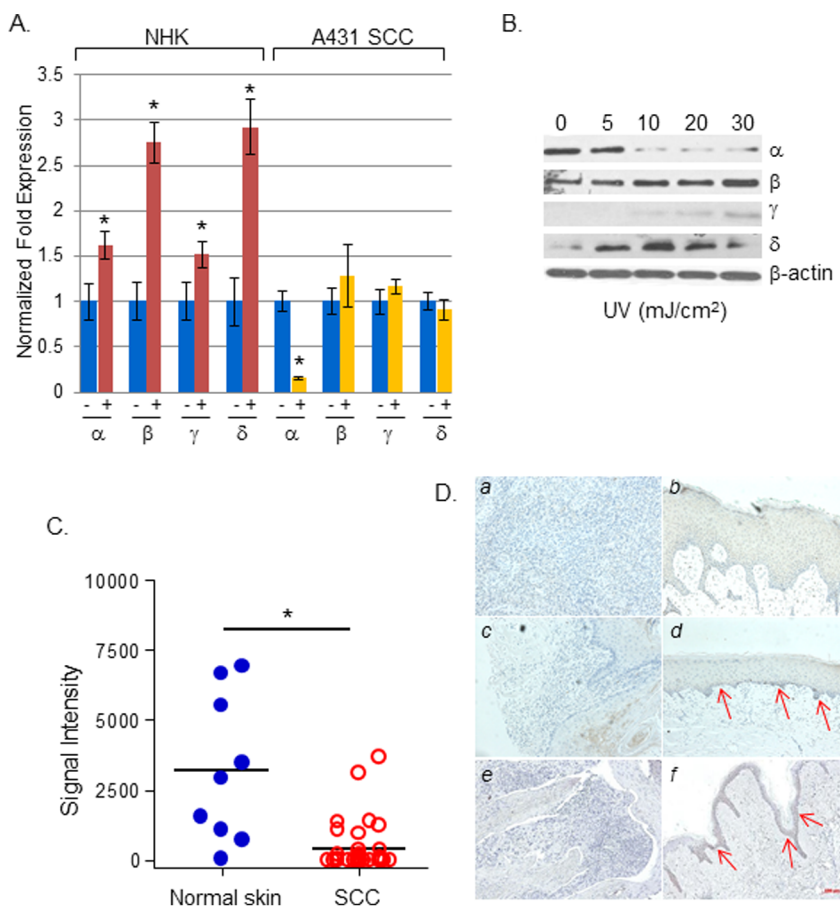


Figure 1. p38 α MAPK expression is diminished in UV-irradiated A431 SCC keratinocytes and human SCCs. UV decreases p38 α expression in A431 cells. The mRNA levels of p38 α , β , γ , and δ were determined by real-time qRT-PCR in normal human keratinocytes (NHK) and human A431 cells, 24 h after UV irradiation (30 mJ/cm²); The data shown are from a representative experiment of three different sets of independent experiments using keratinocytes derived from independent donors. * $p < 0.05$. (B) The levels of p38 isoforms in A431 cells were assessed by Western blotting, 24 h after UV irradiation at the indicated UV doses. β -actin was used as an internal loading control; 50 μ g protein was loaded per lane. (C) Immunohistochemical analyses of p38 α in human cutaneous SCCs. p38 α expression in cutaneous SCC tissue arrays containing 35 SCC sections and nine normal skin sections was analyzed by immunohistochemical staining. The signal intensity and the extent of staining were quantified using the pixel analysis function of Adobe Photoshop. Two SCC samples were excluded from the following statistical analysis, due to excessive infiltrations of p38 α -positive lymphocytes in the tumor tissues. The resulting pixel values from each image were subjected to an unpaired t-test with Welch's correction by using GraphPad Prism software, to determine the statistical significance of the difference between the SCC sample and normal skin sample groups. *: $p = 0.014$. (D) Representative immunohistochemical staining of p38 α . (a) Moderately differentiated and (c) well-differentiated cutaneous SCCs; (b and d) tumor-adjacent skin of (a) and (c), respectively; Representative immunohistochemical staining of phospho-p38. SCC (e) and its tumor-adjacent skin (f). Arrows indicate positive staining.

Immunohistochemical (IHC) staining and quantification

Skin SCC tissue arrays (TMAs, Imgenex, IMH-323) were used in the immunohistochemical assessment of p38 α . Sections were treated with Antigen Unmasking Solution (Vector Labs, Burlingame, CA) prior to incubation with primary antibodies and detection with DAB, as previously described [29] [30]. Images were obtained using an Axioplan2 microscope. The signal intensity and the extent of staining were quantified using the pixel analysis function of Adobe Photoshop. The resulting pixel values from each image were subjected to an unpaired t-test with Welch's correction by using GraphPad Prism software, to determine statistical significance.

UV light source

A UV Irradiation Unit (Daavlin, Bryan, OH), equipped with an electronic controller to regulate the dosage, was used. The UV source consisted of eight FS72T12-UVB-HO lamps that emit UVB (290–320 nm, 75–80% of total energy) and UVA (320–380 nm, 20–25% of total energy). A UVC sensor (Goldilux UVC Probe, Oriel, Stratford, CT) was routinely used during each exposure to confirm lack of UVC emission. The UV dose was quantified with a UVB Spectrum 305 Dosimeter obtained from Daavlin. The radiation was further calibrated with an IL1700 Research Radiometer/Photometer from International Light (Newburyport, MA).

Tumor study in p53^{-/-}/SKH-1 mice

p53^{-/-}/SKH-1 mice were generated as previously described [31] by crossing eight-week-old female non-agouti p53^{-/-} mice (B6/C57BL/6J-Trp53^{-/-}, Jackson Laboratories, Bar Harbor, ME) with SKH-1 males (Charles River Laboratories, Wilmington, MA) to generate littermates heterozygous for p53. These mice were then backcrossed for 11 generations to SKH-1 mice to minimize the C57BL/6 genetic background, and a colony of p53^{-/-}/SKH-1 mice (F14–F16) were utilized for the tumorigenesis studies. Male or female 8–9 week-old p53^{-/-}/SKH-1 mice were divided into four groups: Mice in Groups I and II received either 0.5% methylcellulose by gavage or UV irradiation (180 mJ/cm²), respectively. Mice in Group III received SB203580 (50 mg/kg body weight in 0.5% methylcellulose, gavage) and mice in Group IV received both UV irradiation and SB203580. SB203580 and/or UV irradiation were applied twice per week for a total of 22 weeks. Tumors were counted weekly once they reached 2 mm in diameter. At week 22, all mice were sacrificed, their dorsal skin removed, and tumors were harvested and collected for analysis.

Xenografts of A431 cells

NOD/Shi-scid IL2rgamma(null) (NOG) mice were divided into four groups of six mice each. Groups I and II received 0.5% methylcellulose by gavage. Mice in Group III and IV received SB203580 by gavage (50 mg/kg body weight in 0.5% methylcellulose, three times per week for six weeks). Three days after starting the drug administration, A431 cells transduced with control vector (shCTRL) (3×10^4 cells in 100 μ l matrigel) were subcutaneously injected into mice in groups I and III, while mice in groups II and IV received NOX2 knockdown A431 cells (shNOX2). Tumor growth was measured every five days for 40 days.

Ethics Statement

The tumor study in p53^{-/-}/SKH-1 mice was carried out in strict accordance with the recommendations in the Guide for the Care and Use of Laboratory Animals of the National Institutes of

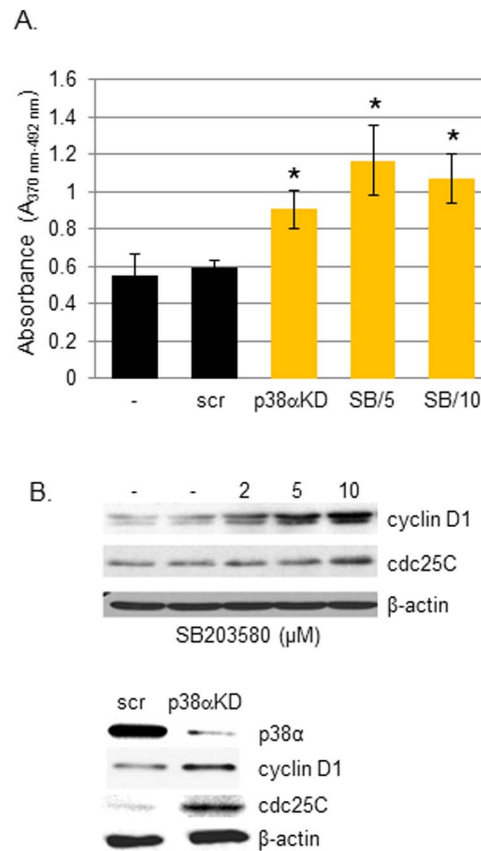


Figure 2. p38 α inhibition enhances proliferative capacity of A431 SCC keratinocytes. (A) The effects of p38 α inhibition were assessed by BrdU incorporation in A431 cells transfected with p38 α siRNA (p38 α KD), or treated with SB203580 (5 μ M (SB/5), 10 μ M (SB/10)) for 24 h. Each histogram represents the results from triplicate cultures; * $p < 0.05$. scr, scrambled control siRNA. The levels of cyclin D1 and cdc25C in A431 cells treated with the indicated concentrations of SB203580 for 24 h (B), or following p38 α knockdown (C) were assessed by Western blotting (50 μ g protein loaded per lane). β -actin was used as an internal loading control. doi:10.1371/journal.pone.0097245.g002

Health. The protocol was approved by Columbia University Institutional Animal Care and Use. The xenograft study was performed at the University de Bordeaux; the protocol was approved by the animal ethics committee there. All efforts were made to minimize suffering in experimental animals.

Statistics

Statistical analyses were performed using the Student's t test (two-tailed) or 1-way ANOVA tests, followed by post-hoc Tukey's tests. $P < 0.05$ was considered significant. Results are presented as mean \pm SD. Statistical analyses for TMAs were performed using an unpaired t-test with Welch's correction by using GraphPad Prism software, to determine the statistical significance of the difference between the SCC sample and the normal skin sample groups.

Results

Differential regulation of p38 α MAPK expression in normal human keratinocytes (NHK) and A431 SCC cells following UV irradiation

In previous studies, we showed that acute UV irradiation of the skin of SKH-1 mice activates p38 MAPK signaling, which

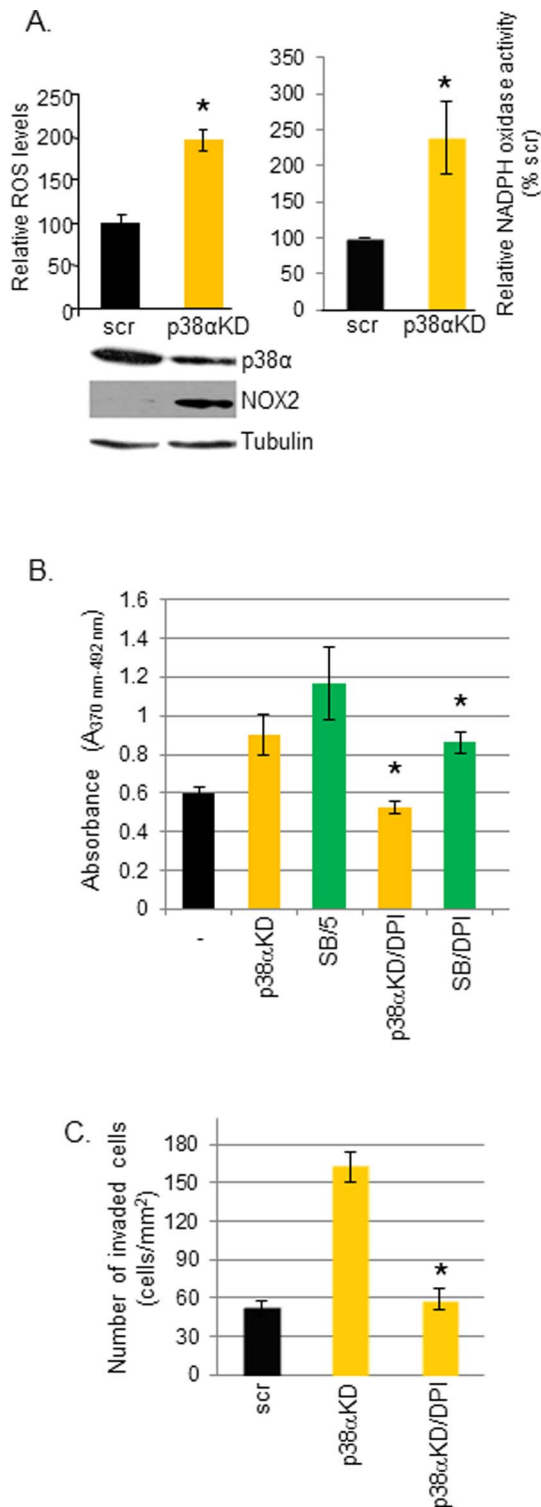


Figure 3. Inhibition of NADPH oxidase activity reduces the cellular proliferation and invasiveness of p38 α -deficient A431 SCC keratinocytes. (A) p38 α downregulation increases NADPH oxidase activity and generates intracellular ROS. Intracellular ROS levels were measured using a cell-permeable fluorogenic probe, 2',7'-dichlorofluorescein diacetate (DCFDA) dye, which detects hydrogen peroxide production, following siRNA-mediated p38 α knockdown in A431 cells. NOX2 levels were assessed by Western blotting in extracts prepared from p38 α knockdown (p38 α KD) A431 cells. NADPH oxidase activity was determined as previously described [11]. scr, scrambled

control siRNA. Presence of NADPH oxidase inhibitor, DPI (2.5 μ M), inhibits the proliferation (B) and cellular invasiveness (C) of A431 cells treated with SB203580 or p38 α KD A431 cells. Proliferation was measured by BrdU incorporation assay, and invasiveness was assessed in matrigel-coated chambers. Each histogram represents results from triplicate cultures; * p <0.05. doi:10.1371/journal.pone.0097245.g003

transiently increases the local pro-inflammatory response [32]. p38 α was recently shown to be the dominantly phosphorylated p38 isoform in response to UV in hTERT-immortalized human keratinocytes [23], suggesting a role in UV-induced skin carcinogenesis. We first assessed the effect of UV irradiation on p38 isoforms in NHK and A431 SCC cells. In Fig. 1A, we show that acute UV irradiation of NHK increased the expression of all four p38 isoforms ($\alpha/\beta/\gamma/\delta$), but particularly p38 β and p38 δ . In A431 cells, p38 α showed a selective reduction in response to UV (Figs. 1A, 1B), whereas p38 β showed a slight increase, as assessed by Western blotting (Fig. 1B). The level of p38 δ substantially increased in UV-irradiated A431 cells compared to non-irradiated controls, while the levels of p38 γ were relatively low in both the non-irradiated and UV-irradiated A431 cells. Additionally, while the siRNA-mediated knockdown of p38 α had no significant effects on other p38 isoforms in NHK, p38 α knockdown in A431 cells led to the upregulation of p38 β and p38 δ , as determined by real-time PCR (Fig. S1). These data suggest that the decrease in p38 α causes compensatory increases in p38 β and p38 δ in A431 cells. Taken together, our results indicate that p38 isoforms are differentially regulated in response to UV irradiation, in which p38 α is selectively downregulated in A431 cells.

p38 α is downregulated in human SCCs

The immunohistochemical assessment of human cutaneous SCC tissue microarrays demonstrated that the majority of SCCs either lacked or had reduced p38 α expression (Fig. 1C, normal vs. SCCs, p = 0.014). Representative pictures of p38 α immunohistochemical staining in paired tumor and tumor-adjacent skin (Fig. 1D) indicate that p38 α is present in both the basal and suprabasal layers of non-tumor bearing epidermis (b, d), whereas it was substantially reduced in SCCs (a, c). Furthermore, phosphorylated p38 levels were substantially diminished in SCCs (e, f).

Pharmacological inhibition of p38 α MAPK enhances proliferation of A431 SCC cells lacking functional p53

p38 α influences UV stress responses by several pathways, including its effects on p53. It is known that p53 mutations occur early during the induction of UV-induced SCCs in humans as well as in murine models [33,34]. To determine the effects of p38 α deficiency in the absence of p53, we used p38 α -expressing A431 cells harboring mutant p53. Both genetic inhibition of p38 α via siRNA-mediated p38 α knockdown and chemical inhibition of p38 activity using SB203580 resulted in significant increases in the proliferation of A431 cells, as measured by BrdU incorporation (Fig. 2A). This was associated with increased cyclin D1 and cdc25C (Fig. 2B), which are cell cycle regulators known to be upregulated in SCC carcinogenesis [30]. These results suggest that inhibition of the p38 signaling pathway, which likely involves p38 α , drives cell proliferation.

Inhibition of NADPH oxidase decreases proliferation and invasiveness of p38 α -deficient A431 SCC cells

We previously showed that NOX1 is overexpressed in human SCCs [10]. In A431 cells, p38 α knockdown increased NOX2 expression and NADPH oxidase activity that was associated with

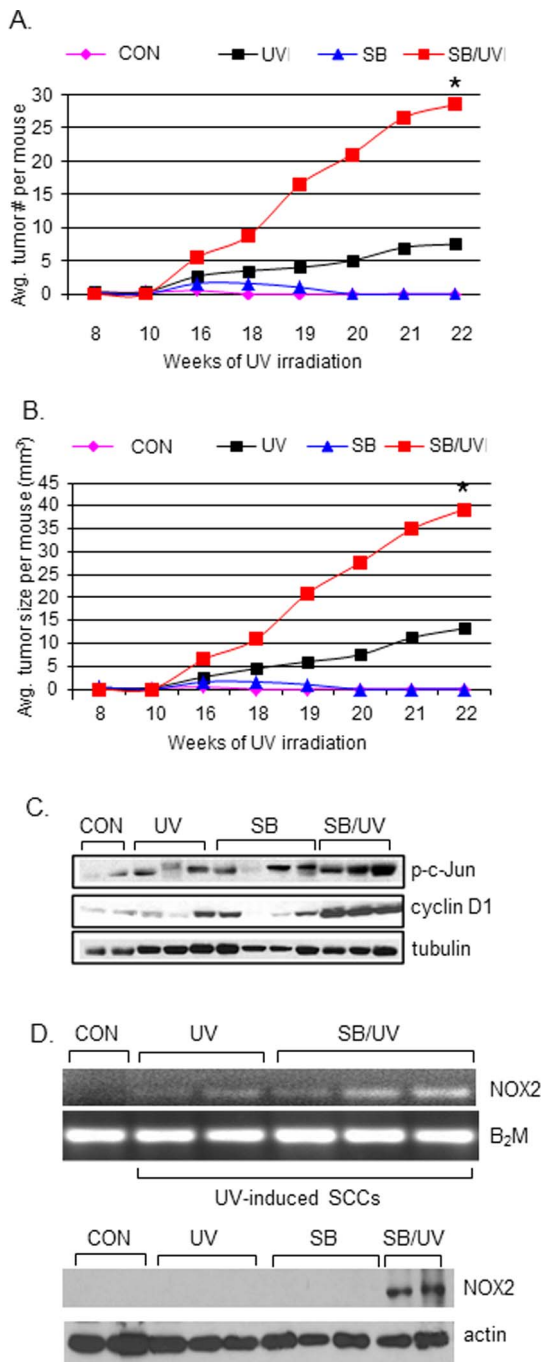


Figure 4. The p38 MAPK inhibitor SB203580 accelerates UV-induced skin carcinogenesis and increases NOX2 levels in p53^{-/-}/SKH-1 mice. The number of skin tumors (A) and tumor size (B) at week 22 in UV-irradiated p53^{-/-}/SKH-1 mice (UV) were compared to mice that had received SB203580 alone (SB) or received both SB203580 and UV irradiation (SB/UV), control, non-irradiated, non-treated mice; * $p < 0.05$, UV vs. SB/UV. (C) The levels of phospho-c-Jun and cyclin D1 in tissue extracts, assessed by Western blotting. 60 μ g total protein per lane; β -actin was used as an internal loading control. (D) SB203580 administration leads to the upregulation of NOX2 in UV-induced SCCs in p53^{-/-}/SKH-1 mice. NOX2 levels were detected by RT-PCR (top panel) and Western blotting (bottom panel). B₂M and actin were used as internal controls for RT-PCR and Western blotting, respectively. doi:10.1371/journal.pone.0097245.g004

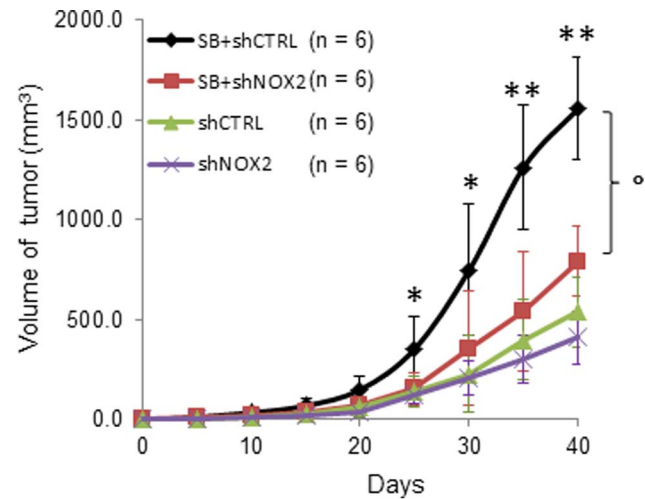


Figure 5. NOX2 silencing suppresses the growth of A431 xenografts treated with SB203580. The *in vivo* tumor growth of NOX2 knockdown A431 cells subcutaneously injected into NOG mice, which were either treated or not treated with SB203580 (SB+shNOX2 or shNOX2, respectively). A431 cells were transfected three days prior to injection. shCTRL, A431 cells transfected with control shRNA; SB+shCTRL, A431 cells transfected with control shRNA and treated with SB203580. Results are presented as mean \pm SD. * $p < 0.05$, ** $p < 0.001$ SB+shCtrl vs. shCtrl; \circ $p = 0.032$, SB+shCtrl vs. SB+shNOX2. doi:10.1371/journal.pone.0097245.g005

increased ROS production (Fig. 3A). Pretreatment of A431 cells with DPI, a NADPH oxidase inhibitor, abolished the increased cell proliferation and invasiveness observed in p38 α knockdown and SB203580-treated A431 cells (Fig. 3B, C) suggesting a link between NOX2-dependent ROS generation and cell proliferation and *in vivo* invasiveness.

Oral administration of the p38 MAPK inhibitor SB203580 enhances UV-induced skin carcinogenesis in p53^{-/-}/SKH-1 mice.

To elucidate the role of p38 in the pathogenesis of SCCs in the absence of p53, we utilized our p53^{-/-}/SKH-1 mouse model in a standard photocarcinogenesis protocol. SB203580 was administered orally (50 mg/kg) prior to each UV irradiation (180 mJ/cm², twice per week for a total of 22 weeks). As compared to UV-irradiated mice, SB203580-treated UV-irradiated mice showed a four-fold increase in the number of skin tumors (Fig. 4A) and a three-fold increase in average tumor size (Fig. 4B). No tumors developed in unirradiated SB203580-treated mice. Interestingly, liver-specific deletion of p38 α is known to enhance JNK activity and the levels of c-Jun, leading to hepatocyte proliferation and hepatic tumorigenesis [35]. Similarly, we found elevated phosphorylated c-Jun and cyclin D1 in SCCs harvested from the UV-irradiated, SB203580-treated mice (Fig. 4C). Importantly, SB203580 administration augmented the mRNA and protein levels of NOX2 (Fig. 4D) and NADPH oxidase activity (Fig. 4E), suggesting that inhibition of p38 may exacerbate the carcinogenic effects of UV by driving NOX2-dependent ROS signaling.

NOX2 downregulation suppresses the growth of SB203580-treated A431 xenograft tumors

To determine whether NOX2 influences tumor growth, A431 cells transfected with shRNA targeting NOX2 (shNOX2) or control shRNA (shCTRL) were subcutaneously injected into

immunodeficient NOG mice ($n = 12$ each group). These mice were further divided into two groups of six mice each, of which one group received SB203580 (50 mg/kg, gavage, three times per week for six weeks), while the other groups received a methylcellulose vehicle. Consistent with the data observed in UV-irradiated p53^{-/-}/SKH-1 mice in Fig. 4, the growth of A431 xenografts were substantially enhanced in mice treated with SB203580 (Fig. 5; shCTRL vs. SB+shCTRL). NOX2 silencing suppressed this growth by 50% (SB+shCTRL vs. SB+shNOX2). Interestingly, NOX2 silencing alone did not significantly affect the growth of A431 xenografts (shNOX2; Fig. 5). These data indicate a direct relationship between p38 and NOX2 and suggest NOX2 as a potential therapeutic target for SCCs with diminished p38 activity.

Discussion

p38 α is generally considered to be a tumor suppressor; however, studies performed in various model systems suggest that p38 α may have dualistic or context-dependent effects in regulating cell death and survival, in part due to substrate specificity and sensitivity in response to specific stimuli. Because UV-induced mutational inactivation of p53 is an important driver of cutaneous SCCs, we employed p53-deficient A431 SCC cells and a p53^{-/-}/SKH-1 mouse model to assess the p53-independent role of p38 α in skin carcinogenesis. Genetic inhibition of p38 α or pharmacological inhibition of p38 activity with SB203580 increased the proliferation and invasiveness of A431 cells (Figs. 2, 3), and the oral administration of SB203580 augmented the growth of UV-induced SCCs in p53^{-/-}/SKH-1 mice (Fig. 4). Further confirmation of our results comes from our observation that p38 α is decreased in human primary SCCs compared to non-tumor bearing skin and in UV-irradiated A431 cells (Fig. 1), suggesting its role in tumor suppression. Our results are consistent with those of Qiang et al [22], who showed that autophagy-associated decreases in p38 phosphorylation enhances cell survival [22]. p38 activity was also found to be reduced in human SCCs, compared to normal human skin [22]. Moreover, inhibition of p38 signaling was associated with a defect in global genome nucleotide excision repair (GG-NER), a vitally important tumor protective pathway that recognizes and excises UVB-induced CPDs (cyclobutane pyrimidine dimers) and 6-4PPs (pyrimidine (6-4) pyrimidone photoproducts) that would otherwise be mutagenic [36]. These data indicate that p38 α loss can promote UV-induced skin tumorigenesis. Our results, however, differ from those of Dickinson et al. who reported that a dominant negative mutant of p38 α (p38 α DN) SKH-1 mice, consisting of T180A and Y182F point mutations at the Thr-Gly-Tyr activation site [26,37], were resistant to UV-induced skin carcinogenesis [37]. Similarly, using the same p38 α DN model, Dong et al demonstrated that p38 blockade resulted in fewer and smaller tumors in response to ultraviolet radiation [38]. The explanation for these conflicting results is unclear, but several possibilities can be considered. For example, our study utilized p53^{-/-}/SKH mice and cultured p53-mutant human cells. Given the synergistic interaction between p38 and p53 in cell-cycle regulation [25], we postulate that, in the absence of p53, p38 α could compensate for the loss of the p53 tumor-suppression function; this may explain the augmented UV-induced skin carcinogenesis observed in SB203580-treated p53^{-/-}/SKH mice. In addition to the p53 functional status, other factors could contribute to the observed discrepancy: differential modes of p38 inhibition, the role of other p38 isoforms, differential inflammatory responses, and the source of UV (i.e., the UV radiation employed in our study comprised 75–80% UVB and 20–

25% UVA of total energy, whereas Dong and colleagues used 95% UVA and 5% UVB [38]).

While p38 α has been shown to be predominantly sensitive to SB203580 in certain cases—for example, in primary fibroblast [27]—SB203580 is known to target both p38 α and p38 β isoforms. Coupled with our data showing the presence of p38 β and its UV-induced increase in A431 cells (Fig. 1), as well as a compensatory increase of p38 β following p38 α knockdown (Fig. S1), it is possible that the effect of SB203580 can be attributed to the inhibition of both p38 α and p38 β , and not solely p38 α . Additionally, it is interesting to note that the p38 δ level increased in p38 α knockdown A431 cells; no such effects were seen in normal human keratinocytes (Fig. S1). The p38 δ level was also increased in UV-irradiated A431 cells (Fig. 1B). In a study that employed two-stage 7,12-dimethylbenz(a)anthracene/12-O-tetradecanoylphorbol-13-acetate chemical skin carcinogenesis, mice lacking p38 δ were resistant to the development of benign papillomas [39]; this suggests that p38 δ promotes tumorigenesis. Whether p38 δ indeed promotes SCC tumorigenesis and whether it plays a similar role in UV-induced skin carcinogenesis remains unknown. Nonetheless, these data collectively suggest a complex interplay among p38 isoforms during skin responses to UV radiation and warrant further investigation, if we are to understand the functional relevance of these compensatory increases in UV carcinogenesis and the specific contribution of the individual p38 isoforms that underlie skin cancer pathogenesis.

Immunohistochemical assessments of p38 α in human cutaneous SCC tissue arrays indicate that p38 α levels are reduced in tumors, compared to non-tumor-bearing skin (Fig. 1). The mechanism underlying p38 α downregulation is not clear. Recently, it was shown that UV irradiation of HaCaT cells, a spontaneously immortalized skin keratinocyte cell line, harboring mutant p53 induces NF- κ B-mediated miR-125b expression, which repressed p38 α levels by targeting its 3'-UTR [17]. miR-125b-mediated p38 α repression was also shown to protect cells against UV-induced apoptosis, thereby promoting cell survival [17]. The combination of the absence of functional p53 and UV-induced p38 α repression likely provide a survival advantage that accelerates tumor promotion and progression. Further research assessing the status of p38 α and p53 in tumors developed in p38 α DN mice and p53^{-/-}/SKH-1 and p53^{+/-}/SKH-1 mice in response to UV may help clarify the relationship between p38 α and p53 in skin carcinogenesis.

It is important to note, however, that a previous study using high-density oligonucleotide arrays identified p38 α expression as being moderately increased (1.4-fold) at the mRNA level in human cutaneous SCCs [40]. Junttila and colleagues also reported that p38 α mRNA is expressed in head and neck SCC (HNSCC) cell lines at levels comparable to that in normal squamous epithelial cells [15]. Since our results were based on IHC—to facilitate comparisons of protein levels between cutaneous SCCs and normal skin—the lack of p38 α protein in our study could indicate a possible post-transcriptional control of p38 α during SCC tumorigenesis.

Our results indicate that p38 α loss during SCC pathogenesis is accompanied by enhanced NOX2 expression leading to increased intracellular ROS levels and that NOX2 downregulation suppresses the growth of A431 xenografts (Figs. 3, 5). Given that the p38 α protein does not possess DNA-binding activity, its role in NOX2 regulation is likely to be indirect and perhaps involves transcription factors known to be direct targets of p38 [41]. Additionally, p38 α phosphorylates serine residues in the N-terminal tail of histone H3 (Ser10 and Ser28) [42] [43], suggesting a potential for epigenetic reversible regulation of gene expression

[44] [45]. In A431 cells, p38 α knockdown increased the DNA-binding activity of the transcription factor AP-1, and we have identified putative AP-1 recognition sites in the NOX2 promoter (data not shown). Further studies are needed to define the mechanisms by which p38 α regulates NOX2 expression and the relevance to UV-induced skin tumorigenesis. Identification of UV-specific p38 α substrates, as well as modulation of p38 α expression in genetically modified murine skin cancer models in a time- and tissue-specific manner, will aid in understanding its effects on signaling pathways that are relevant to skin carcinogenesis and may also help to determine whether restoration of p38 α expression can prevent the development of these tumors.

Supporting Information

Figure S1 siRNA-mediated knockdown of p38 α has no significant effects on other p38 isoforms in NHKs (left

panel), but led to compensatory upregulation of p38 β and p38 δ in SCC cells (right panel).

(TIF)

Acknowledgments

We thank Fatimatou Diallo and Vivek Raj for technical assistance, and Dr. Annemieke de Jong for the statistical analyses.

Author Contributions

Conceived and designed the experiments: ALK MA DRB. Performed the experiments: LL HRR JB MH XT YZ WM HR GR ALK. Analyzed the data: LL HRR JB MH ALK. Contributed reagents/materials/analysis tools: HRR MH WM HR MA. Wrote the paper: LL ALK DRB.

References

1. Bito T, Nishigori C (2012) Impact of reactive oxygen species on keratinocyte signaling pathways. *Journal of Dermatological Science* 68: 3–8.
2. Bossi O, Gartsbein M, Leitges M, Kuroki T, Grossman S, et al. (2008) UV irradiation increases ROS production via PKC δ signaling in primary murine fibroblasts. *J Cell Biochem* 105: 194–207.
3. Scharfetter-Kochanek K, Wlaschek M, Brenneisen P, Schauen M, Blandschun R, et al. (1997) UV-induced reactive oxygen species in photocarcinogenesis and photoaging. *Biol Chem* 378: 1247–1257.
4. Bedard K, Krause KH (2007) The NOX family of ROS-generating NADPH oxidases: physiology and pathophysiology. *Physiol Rev* 87: 245–313.
5. Kang MA, So EY, Simons AL, Spitz DR, Ouchi T (2012) DNA damage induces reactive oxygen species generation through the H2AX-Nox1/Rac1 pathway. *Cell Death Dis* 3: e249.
6. Maraldi T, Prata C, Vieceli Dalla Sega F, Caliceti C, Zamboni L, et al. (2009) NAD(P)H oxidase isoform Nox2 plays a prosurvival role in human leukaemia cells. *Free Radic Res* 43: 1111–1121.
7. Block K, Gorin Y (2012) Aiding and abetting roles of NOX oxidases in cellular transformation. *Nat Rev Cancer* 12: 627–637.
8. Kamata T (2009) Roles of Nox1 and other Nox isoforms in cancer development. *Cancer Sci* 100: 1382–1388.
9. Mitsuhashi J, Lambeth JD, Kamata T (2004) The superoxide-generating oxidase Nox1 is functionally required for Ras oncogene transformation. *Cancer Res* 64: 3580–3585.
10. Rezvani HR, Rossignol R, Ali N, Benard G, Tang X, et al. (2011) XPC silencing in normal human keratinocytes triggers metabolic alterations through NOX-1 activation-mediated reactive oxygen species. *Biochim Biophys Acta* 1807: 609–619.
11. Rezvani HR, Kim AL, Rossignol R, Ali N, Daly M, et al. (2011) XPC silencing in normal human keratinocytes triggers metabolic alterations that drive the formation of squamous cell carcinomas. *J Clin Invest* 121: 195–211.
12. Cuadrado A, Nebreda AR (2010) Mechanisms and functions of p38 MAPK signalling. *Biochem J* 429: 403–417.
13. Wagner EF, Nebreda AR (2009) Signal integration by JNK and p38 MAPK pathways in cancer development. *Nat Rev Cancer* 9: 537–549.
14. Cuenda A, Rousseau S (2007) p38 MAP-kinases pathway regulation, function and role in human diseases. *Biochim Biophys Acta* 1773: 1358–1375.
15. Junttila MR, Ala-Aho R, Jokilehto T, Peltonen J, Kallajoki M, et al. (2007) p38 α and p38 δ mitogen-activated protein kinase isoforms regulate invasion and growth of head and neck squamous carcinoma cells. *Oncogene* 26: 5267–5279.
16. Dashti SR, Efimova T, Eckert RL (2001) MEK7-dependent activation of p38 MAP kinase in keratinocytes. *J Biol Chem* 276: 8059–8063.
17. Tan G, Niu J, Shi Y, Ouyang H, Wu ZH (2012) NF- κ B-dependent microRNA-125b up-regulation promotes cell survival by targeting p38 α upon ultraviolet radiation. *J Biol Chem* 287: 33036–33047.
18. Ambrosino C, Nebreda AR (2001) Cell cycle regulation by p38 MAP kinases. *Biol Cell* 93: 47–51.
19. Thornton TM, Rincon M (2009) Non-classical p38 map kinase functions: cell cycle checkpoints and survival. *Int J Biol Sci* 5: 44–51.
20. Phong MS, Van Horn RD, Li S, Tucker-Kellogg G, Surana U, et al. (2010) p38 mitogen-activated protein kinase promotes cell survival in response to DNA damage but is not required for the G2 DNA damage checkpoint in human cancer cells. *Mol Cell Biol* 30: 3816–3826.
21. Aguirre-Ghiso JA (2007) Models, mechanisms and clinical evidence for cancer dormancy. *Nat Rev Cancer* 7: 834–846.
22. Qiang L, Wu C, Ming M, Viollet B, He YY (2013) Autophagy controls p38 activation to promote cell survival under genotoxic stress. *J Biol Chem* 288: 1603–1611.
23. Liu K, Yu D, Cho YY, Bode AM, Ma W, et al. (2013) Sunlight UV-induced skin cancer relies upon activation of the p38 α signaling pathway. *Cancer Res*.
24. Cuadrado A, Nebreda AR (2010) Mechanisms and functions of p38 MAPK signalling. *Biochemical Journal* 429: 403–417.
25. Chen Y, Miao Z-H, Zhao W-M, Ding J (2005) The p53 pathway is synergized by p38 MAPK signaling to mediate 11,11'-dideoxyverticillin-induced G2/M arrest. *FEBS Letters* 579: 3683–3690.
26. Raingeaud J, Gupta S, Rogers JS, Dickens M, Han J, et al. (1995) Pro-inflammatory Cytokines and Environmental Stress Cause p38 Mitogen-activated Protein Kinase Activation by Dual Phosphorylation on Tyrosine and Threonine. *Journal of Biological Chemistry* 270: 7420–7426.
27. Xu J, Clark RA, Parks WC (2001) p38 mitogen-activated kinase is a bidirectional regulator of human fibroblast collagenase-1 induction by three-dimensional collagen lattices. *Biochem J* 355: 437–447.
28. Cuenda A, Rouse J, Doza YN, Meier R, Cohen P, et al. (1995) SB 203580 is a specific inhibitor of a MAP kinase homologue which is stimulated by cellular stresses and interleukin-1. *FEBS Lett* 364: 229–233.
29. Kim H, Casta A, Tang X, Luke CT, Kim AL, et al. (2012) Loss of hairless confers susceptibility to UVB-induced tumorigenesis via disruption of NF- κ B signaling. *PLoS One* 7: e39691.
30. Kim AL, Athar M, Bickers DR, Gautier J (2002) Stage-specific alterations of cyclin expression during UVB-induced murine skin tumor development. *Photochem Photobiol* 75: 58–67.
31. Kim KH, Back JH, Zhu Y, Arbesman J, Athar M, et al. (2011) Resveratrol targets transforming growth factor- β 2 signaling to block UV-induced tumor progression. *J Invest Dermatol* 131: 195–202.
32. Kim AL, Labasi JM, Zhu Y, Tang X, McClure K, et al. (2005) Role of p38 MAPK in UVB-induced inflammatory responses in the skin of SKH-1 hairless mice. *J Invest Dermatol* 124: 1318–1325.
33. Brash DE, Rudolph JA, Simon JA, Lin A, McKenna GJ, et al. (1991) A role for sunlight in skin cancer: UV-induced p53 mutations in squamous cell carcinoma. *Proc Natl Acad Sci U S A* 88: 10124–10128.
34. Black AP, Ogg GS (2003) The role of p53 in the immunobiology of cutaneous squamous cell carcinoma. *Clin Exp Immunol* 132: 379–384.
35. Hui L, Bakiri L, Mairhorfer A, Schweifer N, Haslinger C, et al. (2007) p38 α suppresses normal and cancer cell proliferation by antagonizing the JNK-c-Jun pathway. *Nat Genet* 39: 741–749.
36. Ming M, Feng L, Shea CR, Soltani K, Zhao B, et al. (2011) PTEN positively regulates UVB-induced DNA damage repair. *Cancer Res* 71: 5287–5295.
37. Dickinson SE, Olson ER, Zhang J, Cooper SJ, Melton T, et al. (2011) p38 MAP kinase plays a functional role in UVB-induced mouse skin carcinogenesis. *Mol Carcinog* 50: 469–478.
38. Liu K, Yu D, Cho YY, Bode AM, Ma W, et al. (2013) Sunlight UV-induced skin cancer relies upon activation of the p38 α signaling pathway. *Cancer Res* 73: 2181–2188.
39. Schindler EM, Hinds A, Gribben EL, Burns CJ, Yin Y, et al. (2009) p38 δ Mitogen-Activated Protein Kinase Is Essential for Skin Tumor Development in Mice. *Cancer Research* 69: 4648–4655.
40. Haider AS, Peters SB, Kaporis H, Cardinale I, Fei J, et al. (2006) Genomic analysis defines a cancer-specific gene expression signature for human squamous cell carcinoma and distinguishes malignant hyperproliferation from benign hyperplasia. *J Invest Dermatol* 126: 869–881.
41. Trempele N, Dave-Coll N, Nebreda AR (2013) Snapshot: p38 MAPK Substrates. *Cell* 152: 924–924.e921.
42. Zhong SP, Ma WY, Dong Z (2000) ERKs and p38 kinases mediate ultraviolet B-induced phosphorylation of histone H3 at serine 10. *J Biol Chem* 275: 20980–20984.

43. Zhong S, Zhang Y, Jansen C, Goto H, Inagaki M, et al. (2001) MAP kinases mediate UVB-induced phosphorylation of histone H3 at serine 28. *J Biol Chem* 276: 12932–12937.
44. Nowak SJ, Corces VG (2004) Phosphorylation of histone H3: a balancing act between chromosome condensation and transcriptional activation. *Trends Genet* 20: 214–220.
45. James TT, Aroor AR, Lim RW, Shukla SD (2012) Histone H3 phosphorylation (Ser10, Ser28) and phosphoacetylation (K9S10) are differentially associated with gene expression in liver of rats treated in vivo with acute ethanol. *J Pharmacol Exp Ther* 340: 237–247.

LIST OF PUBLICATIONS

Mohsen Hosseini^{1,2}, Zeinab Kasraian^{1,2}, Hamid Reza Rezvani^{1,2,3*}. *UV, Mutations and Metabolism in Skin Cancers: A Therapeutic Perspective*; In preparation

Mohsen Hosseini^{1,2}, Lea Dousset^{1,2§}, Walid Mahfouf^{1,2§}, Martin Serrano-Sanchez^{1,2§}, Vanessa Bergeron^{1,2§}, Zeinab Kasraian^{1,2}, Marc Bonneu⁵, Stephane Claverol⁵, Alain Taieb^{1,2,3,4}, Anne-Karine Bouzior-Sore⁷, Rodrigue Rossignol^{1,6}, Hamid Reza Rezvani^{1,2,3*}. *UVB irradiation rewires cellular metabolism through over-activation of dihydroorotate dehydrogenase to coordinate DNA repair and ATP synthesis*; In preparation

Ali N, **Hosseini M**, Vainio S, Taïeb A, Cario-André M, Rezvani HR. *Skin Equivalent: Skin from Reconstructions as Models to Study Skin Development & Diseases. British journal of Dermatology. Br J Dermatol. 2015 /bjd.13886*

Hosseini M, Mahfouf W, Serrano-Sanchez M, Raad H, Harfouche G, Bonneu M, Claverol S, Mazurier F, Rossignol R, Taïeb A, Rezvani HR. *Premature aging features rescue by inhibition of NADPH oxidase activity in XPC deficient mice. J Invest Dermatol. 1Dec. jid.2014.511.*

Hosseini M, Ezzedine K, Taïeb A, Rezvani HR. *Oxidative and energy metabolism as potential clues for clinical heterogeneity in nucleotide excision repair disorders. J Invest Dermatol. 9 Oct. jid.2014.365.*

Liu L, Rezvani HR, Back JH, **Hosseini M**, Tang X, Zhu Y, Mahfouf W, Raad H, Raji G, Athar M, Kim AL, Bickers DR. *Inhibition of p38 MAPK Signaling Augments Skin Tumorigenesis via NOX2 Driven ROS Generation. PLoS One. 2014 May 13;9(5):e97245.*

LIST OF PRESENTATIONS

- Talk

19 June 2014 **Hosseini M**, Mahfouf W, Serrano-Sanchez M, Raad H, , Harfouche G, Bonneu M, Claverol S, Mazurier F, Rossignol R, Taieb A, Rezvani HR. *Premature aging features rescue by inhibition of NADPH oxidase activity in XPC deficient mice / FR TransBioMed-Young Researchers' Day/Bordeaux-France (FR TransBioMed)*

11 May 2013 **Hosseini M**, Mahfouf W, Serrano-Sanchez M, Rossignol R, Taieb A, Rezvani HR. *Immediate HIF-1 α down-regulation following UVB irradiation is triggered by NOX1-mediated ROS/ International Investigative Dermatology meeting (IID2013)/Edinburgh-Scotland*

- Poster

19 June 2014 **Hosseini M**, Mahfouf W, Serrano-Sanchez M, Raad H, , Harfouche G, Bonneu M, Claverol S, Mazurier F, Rossignol R, Taieb A, Rezvani HR. *Premature aging features rescue by inhibition of NADPH oxidase activity in XPC deficient mice / FR TransBioMed-Young Researchers' Day/Bordeaux-France (FR TransBioMed)*

11 May 2013 **Hosseini M**, Mahfouf W, Serrano-Sanchez M, Rossignol R, Taieb A, Rezvani HR. *Immediate HIF-1 α down-regulation following UVB irradiation is triggered by NOX1-mediated ROS/ International Investigative Dermatology meeting (IID2013)/Edinburgh-Scotland*

13 September 2014 **Hosseini M**, Mahfouf W, Serrano-Sanchez M, Raad H, , Harfouche G, Bonneu M, Claverol S, Mazurier F, Rossignol R, Taieb A, Rezvani HR. *Premature aging features rescue by inhibition of NADPH oxidase activity in XPC deficient mice/44th annual of the European Society for Dermatological Research –meeting(SID and JSID2014)/Copenhagen- Denmark*

- 10 April 2014** **Hosseini M**, Mahfouf W, Serrano-Sanchez M, Raad H, , Harfouche G, Bonneu M, Claverol S, Mazurier F, Rossignol R, Taieb A, Rezvani HR. *Premature aging features rescue by inhibition of NADPH oxidase activity in XPC deficient mice/ Doctoral School Day/ Arcachon-France*
- 8- 11 May 2013** **Hosseini M**, Mahfouf W, Rossignol R, Taieb A, Rezvani HR. *Energy metabolism affects keratinocyte responses to UVB irradiation/ International Investigative Dermatology meeting (IID2013)/Edinburgh-Scotland*
- 8-11 May 2013** **Hosseini M**, Mahfouf W, Serrano-Sanchez M, Rossignol R, Taieb A, Rezvani HR. *Immediate HIF-1 α down-regulation following UVB irradiation is triggered by NOX1-mediated ROS/ International Investigative Deramatology meeting (IID2013)/Edinburgh-Scotland*
- 11 April 2013** **Hosseini M**, Mahfouf W, Serrano-Sanchez M, Rossignol R, Taieb A, Rezvani HR. *Immediate HIF-1 α down-regulation following UVB irradiation is triggered by NOX1-mediated ROS/ Doctoral School Day/ Arcachon-France*
- 11 April 2012** **Hosseini M**, Mahfouf W, Rossignol R, Taieb A, Rezvani HR. *Energy metabolism affects keratinocyte responses to UVB irradiation /Cancer Cell Metabolism: Beyond Warburg /Toulouse-France*
- 4 December 2012** **Hosseini M**, Mahfouf W, Rossignol R, Taieb A, Rezvani HR. *Energy metabolism affects keratinocyte responses to UVB irradiation/ Doctoral School Day/ Arcachon-France*
- 22 October 2008** **Hosseini M**, Lellahi SM, Dorraji SE. *Early detection of cancer cells by Quantum dots. 11th annual congress of pathology and 5th annual congress of Iranian cancer association. Tehran, Iran.*
- 22 November 2004** **Hosseini M**, Dorraji SE, Lellahi SM. *Application of nano in medicine and drug delivery. First student's seminar of application of nanotechnology in medicine. Tehran, Iran.*

REFERENCES

REFERENCES

- Afanas, I (2010). Signaling and Damaging Functions of Free Radicals in Aging — Free Radical Theory , Hormesis , and TOR 1.
- Altenhöfer, S, Radermacher, K a, Kleikers, PWM, *et al.* (2014). Evolution of NADPH Oxidase Inhibitors: Selectivity and Mechanisms for Target Engagement. *Antioxid Redox Signal* 00: 1–64.
- Aragane, Y, Kulms, D, Metze, D, *et al.* (1998). Ultraviolet light induces apoptosis via direct activation of CD95 (Fas/APO-1) independently of its ligand CD95L. *J Cell Biol* 140: 171–82.
- Barnard, S, Bouffler, S, Rothkamm, K (2013). The shape of the radiation dose response for DNA double-strand break induction and repair. *Genome Integr* 4: 1.
- Barrett, K, Brooks, H, Boitano, S, *et al.* (2010). *Ganong's review of medical physiology*.
- Barzilai, N, Huffman, DM, Muzumdar, RH, *et al.* (2012). The critical role of metabolic pathways in aging. *Diabetes* 61: 1315–22.
- Bauer, DE, Harris, MH, Plas, DR, *et al.* (2004). Cytokine stimulation of aerobic glycolysis in hematopoietic cells exceeds proliferative demand. *FASEB J* 18: 1303–5.
- Baysal, BE, Ferrell, RE, Willett-Brozick, JE, *et al.* (2000). Mutations in SDHD, a mitochondrial complex II gene, in hereditary paraganglioma. *Science* 287: 848–51.
- Bedard, K, Krause, K-H (2007). The NOX Family of ROS-Generating NADPH Oxidases: Physiology and Pathophysiology. *Physiol Rev* 87: 245–313.
- Bedogni, B, Welford, SM, Cassarino, DS, *et al.* (2005). The hypoxic microenvironment of the skin contributes to Akt-mediated melanocyte transformation. *Cancer Cell* 8: 443–54.
- Bender, K, Blattner, C, Knebel, A, *et al.* (1997). UV-induced signal transduction. *J Photochem Photobiol B* 37: 1–17.
- Bernhardt, D, Müller, M, Reichert, AS, *et al.* (2015). Simultaneous impairment of mitochondrial fission and fusion reduces mitophagy and shortens replicative lifespan. *Sci Rep* 5: 7885.
- Bernstein, C, Bernstein, H, Payne, CM, *et al.* (2002). *DNA repair/pro-apoptotic dual-role proteins in five major DNA repair pathways: Fail-safe protection against carcinogenesis. Mutat Res - Rev Mutat Res*.
- Bess, AS, Leung, MCK, Ryde, IT, *et al.* (2013). Effects of mutations in mitochondrial dynamics-related genes on the mitochondrial response to ultraviolet C radiation in developing *Caenorhabditis elegans*. *Worm* 2: e23763.

- Bizik, J, Kankuri, E, Ristimäki, a, *et al.* (2004). Cell-cell contacts trigger programmed necrosis and induce cyclooxygenase-2 expression. *Cell Death Differ* 11: 183–95.
- Block, K, Gorin, Y (2012a). Aiding and abetting roles of NOX oxidases in cellular transformation. *Nat Rev Cancer* 12: 627–37.
- Block, K, Gorin, Y (2012b). Aiding and abetting roles of NOX oxidases in cellular transformation. *Nat Rev Cancer* 12: 627–37.
- Bode, AM, Dong, Z (2003). Mitogen-activated protein kinase activation in UV-induced signal transduction. *Sci STKE* 2003: RE2.
- Boedeker, CC, Neumann, HPH, Maier, W, *et al.* (2007). Malignant head and neck paragangliomas in SDHB mutation carriers. *Otolaryngol - Head Neck Surg* 137: 126–9.
- De Boer, J, Andressoo, JO, de Wit, J, *et al.* (2002). Premature aging in mice deficient in DNA repair and transcription. *Science* 296: 1276–9.
- De Boer, J, Hoeijmakers, JH (2000). Nucleotide excision repair and human syndromes. *Carcinogenesis* 21: 453–60.
- Boland, ML, Chourasia, AH, Macleod, KF (2013). Mitochondrial Dysfunction in Cancer. *Front Oncol* 3: 292.
- Boya, P, Reggiori, F, Codogno, P (2013). Emerging regulation and functions of autophagy. *Nat Cell Biol* 15: 713–20.
- Bustamante, E, Pedersen, PL (1977). High aerobic glycolysis of rat hepatoma cells in culture: role of mitochondrial hexokinase. *Proc Natl Acad Sci U S A* 74: 3735–9.
- Bustamante, E, Pedersen, PL (1980). Mitochondrial hexokinase of rat hepatoma cells in culture: solubilization and kinetic properties. *Biochemistry* 19: 4972–7.
- Butterworth, J, Yates, CM, Reynolds, GP (1985). Distribution of phosphate-activated glutaminase, succinic dehydrogenase, pyruvate dehydrogenase and ??-glutamyl transpeptidase in post-mortem brain from Huntington's disease and agonal cases. *J Neurol Sci* 67: 161–71.
- Cadet, J, Sage, E, Douki, T (2005). Ultraviolet radiation-mediated damage to cellular DNA. *Mutat Res - Fundam Mol Mech Mutagen* 571: 3–17.
- Campisi, J, d'Adda di Fagagna, F (2007). Cellular senescence: when bad things happen to good cells. *Nat Rev Mol Cell Biol* 8: 729–40.
- Cantor, JR, Sabatini, DM (2012). Cancer cell metabolism: One hallmark, many faces. *Cancer Discov* 2: 881–98.
- Cao, K, Blair, CD, Faddah, D a., *et al.* (2011). Progerin and telomere dysfunction collaborate to trigger cellular senescence in normal human fibroblasts. *J Clin Invest* 121: 2833–44.

- Carracedo, A, Cantley, LC, Pandolfi, PP (2013). Cancer metabolism: fatty acid oxidation in the limelight. *Changes* 13: 227–32.
- Cha, MK, Kim, HK, Kim, IH (1995). Thioredoxin-linked “thiol peroxidase” from periplasmic space of *Escherichia coli*. *J Biol Chem* 270: 28635–41.
- Cheeseman, KH (1993). Tissue injury by free radicals. *Toxicol Ind Heal* 9: 39–51.
- Chin-Chan, M, Navarro-Yepes, J, Quintanilla-Vega, B (2015). Environmental pollutants as risk factors for neurodegenerative disorders: Alzheimer and Parkinson diseases. *Front Cell Neurosci* 9: 1–22.
- Cooper, K, Neises, G, Katz, S (1986). Antigen-presenting OKM5+ melanophages appear in human epidermis after ultraviolet radiation. *J Invest Dermatol* 86: 363–70.
- Corominas-faja, B, Cuyàs, E, Gumuzio, J, *et al.* (2014). Chemical inhibition of acetyl-CoA carboxylase suppresses self-renewal growth of cancer stem cells 5.
- Corre, S, Primot, A, Sviderskaya, E, *et al.* (2004). UV-induced expression of key component of the tanning process, the POMC and MC1R genes, is dependent on the p-38-activated upstream stimulating factor-1 (USF-1). *J Biol Chem* 279: 51226–33.
- Cuervo, AM (2009). NIH Public Access. *Aging (Albany NY)* 24: 604–12.
- Currie, E, Schulze, A, Zechner, R, *et al.* (2013). Cellular fatty acid metabolism and cancer. *Cell Metab* 18: 153–61.
- D’Atri, S, Aquino, A, Graziani, G, *et al.* (2011). Exogenous control of the expression of group I CD1 molecules competent for presentation of microbial nonpeptide antigens to human T lymphocytes. *Clin Dev Immunol* 2011: 10–2.
- D’Orazio, J a, Jarrett, S, Marsch, A, *et al.* (2013). Melanoma — Epidemiology, Genetics and Risk Factors. *Intech* 3–36.
- D’Orazio, J, Marsch, A, Veith, J (2010). Skin Pigmentation and Melanoma Risk. *CdnIntechwebOrg*.
- Dang, C V. (2012). Links between metabolism and cancer. *Genes Dev* 26: 877–90.
- Dasika, GK, Lin, SC, Zhao, S, *et al.* (1999). DNA damage-induced cell cycle checkpoints and DNA strand break repair in development and tumorigenesis. *Oncogene* 18: 7883–99.
- DeBerardinis, RJ, Lum, JJ, Hatzivassiliou, G, *et al.* (2008). The biology of cancer: metabolic reprogramming fuels cell growth and proliferation. *Cell Metab* 7: 11–20.
- Dechat, T, Pflieger, K, Sengupta, K, *et al.* (2008). Nuclear lamins: Major factors in the structural organization and function of the nucleus and chromatin. *Genes Dev* 22: 832–53.
- Van Deursen, J (2014). The role of senescent cells in ageing. *Nature* 509: 439–46.

- Dhup (2012). Multiple Biological Activities of Lactic Acid in Cancer: Influences on Tumor Growth, Angiogenesis and Metastasis. *Curr Pharm Des* 1319–30.
- Ding, WX, Yin, XM (2012). Mitophagy: Mechanisms, pathophysiological roles, and analysis. *Biol Chem* 393: 547–64.
- Domingo, DS, Baron, ED (2008). Melanoma and Nonmelanoma Skin Cancers and the Immune System. *Adv Exp Med Biol* 624: 187–202.
- Donati, A (2006). The involvement of macroautophagy in aging and anti-aging interventions. *Mol Aspects Med* 27: 455–70.
- Donawho, CK, Kripke, ML (1991). Evidence that the local effect of ultraviolet radiation on the growth of murine melanomas is immunologically mediated. *Cancer Res* 51: 4176–81.
- Donawho, CK, Muller, HK, Bucana, CD, *et al.* (1996). Enhanced growth of murine melanoma in ultraviolet-irradiated skin is associated with local inhibition of immune effector mechanisms. *J Immunol* 157: 781–6.
- Drummond, GR, Selemidis, S, Griendling, KK, *et al.* (2011). Combating oxidative stress in vascular disease: NADPH oxidases as therapeutic targets. *Nat Rev Drug Discov* 10: 453–71.
- Van Dyck, E, Stasiak, a Z, Stasiak, a, *et al.* (1999). Binding of double-strand breaks in DNA by human Rad52 protein. *Nature* 398: 728–31.
- Eisen, J, Hanawalt, P (1999). A phylogenomic study of DNA repair genes, proteins, and processes. *Mutat Res Repair* 435: 171–213.
- El-abaseri, TB, Hammiller, B, Repertinger, SK, *et al.* (2013). The Epidermal Growth Factor Receptor Increases Cytokine Production and Cutaneous Inflammation in Response to Ultraviolet Irradiation. *ISRN Dermatol* 2013.
- Escobar, J, Rubio, M, Lissi, E (1996). Sod and catalase inactivation by singlet oxygen and peroxy radicals. *Free Radic Biol Med* 20: 285–90.
- Fan, J, Wilson, DM (2005). Protein-protein interactions and posttranslational modifications in mammalian base excision repair. *Free Radic Biol Med* 38: 1121–38.
- Fang, J, Uchiumi, T, Yagi, M, *et al.* (2013). Dihydro-orotate dehydrogenase is physically associated with the respiratory complex and its loss leads to mitochondrial dysfunction. *Biosci Rep* 33: e00021.
- Faubert, B, Boily, G, Izreig, S, *et al.* (2013). AMPK is a negative regulator of the Warburg effect and suppresses tumor growth in vivo. *Cell Metab* 17: 113–24.
- Favaudon, V (2000). Mise au point Régulation du cycle cellulaire et de la mort cellulaire radio-induite. *CancerRadiothérapie* 4: 355–68.

- Featherstone, C, Jackson, SP (1999). Ku, a DNA repair protein with multiple cellular functions? *Mutat Res* 434: 3–15.
- Fernández-mejía, C (2013). Oxidative Stress in Diabetes Mellitus and the Role Of Vitamins with Antioxidant Actions. *Agric Biol Sci*.
- Feuerhahn, S, Egly, J-M (2008). Tools to study DNA repair: what's in the box? *Trends Genet* 24: 467–74.
- Fisher, GJ, Choi, HC, Bata-Csorgo, Z, *et al.* (2001). Ultraviolet irradiation increases matrix metalloproteinase-8 protein in human skin in vivo. *J Invest Dermatol* 117: 219–26.
- Fitzpatrick, T (1986). Ultraviolet-induced pigmentary changes: benefits and hazards. *Curr Probl Dermatol* 15: 25–38.
- Fletcher, L a (2004). The influence of relative humidity on the UV susceptibility of airborne gram negative bacteria. *IUVA News* 6: 7.
- Fletcher, MJ, Sanadi, DR (1961). Turnover of rat-liver mitochondria [WWW Document]. *Biochim Biophys Acta*. 356-360
- Frank, M, Duvezin-Caubet, S, Koob, S, *et al.* (2012). Mitophagy is triggered by mild oxidative stress in a mitochondrial fission dependent manner. *Biochim Biophys Acta - Mol Cell Res* 1823: 2297–310.
- Fridman, A, Tainsky, M (2008). Critical pathways in cellular senescence and immortalization revealed by gene expression profiling. *Oncogene* 29: 997–1003.
- Friedrich, T, van Heek, P, Leif, H, *et al.* (1994). Two binding sites of inhibitors in NADH: ubiquinone oxidoreductase (complex I). Relationship of one site with the ubiquinone-binding site of bacterial glucose:ubiquinone oxidoreductase. *Eur J Biochem* 219: 691–8.
- Frit, P, Kwon, K, Coin, F, *et al.* (2002). Transcriptional activators stimulate DNA repair. *Mol Cell* 10: 1391–401.
- Gabriel, D, Roedl, D, Gordon, LB, *et al.* (2015). Sulforaphane enhances progerin clearance in Hutchinson-Gilford progeria fibroblasts. *Aging Cell* 14: 78–91.
- Galluzzi, L, Kepp, O, Vander Heiden, MG, *et al.* (2013). Metabolic targets for cancer therapy. *Nat Rev Drug Discov* 12: 829–46.
- Game, J (1993). DNA double-strand breaks and the RAD50-RAD57 genes in *Saccharomyces*. *Semin Cancer Biol* 4: 73–83.
- Gibbs, NK, Tye, J, Norval, M (2008). Recent advances in urocanic acid photochemistry, photobiology and photoimmunology. *Photochem Photobiol Sci* 7: 655–67.
- Gimenez-Roqueplo, a P, Favier, J, Rustin, P, *et al.* (2001). The R22X mutation of the SDHD gene in hereditary paraganglioma abolishes the enzymatic activity of complex II in the

- mitochondrial respiratory chain and activates the hypoxia pathway. *Am J Hum Genet* 69: 1186–97.
- Goldstein, JC, Waterhouse, NJ, Juin, P, *et al.* (2000). The coordinate release of cytochrome c during apoptosis is rapid, complete and kinetically invariant. *Nat Cell Biol* 2: 156–62.
- Gradin, K, McGuire, J, Wenger, RH, *et al.* (1996). Functional interference between hypoxia and dioxin signal transduction pathways: competition for recruitment of the Arnt transcription factor. *Mol Cell Biol* 16: 5221–31.
- Grether-Beck, S, Bonizzi, G, Schmitt-Brenden, H, *et al.* (2000). Non-enzymatic triggering of the ceramide signalling cascade by solar UVA radiation. *EMBO J* 19: 5793–800.
- Ha, HY, Kim, Y, Ryoo, ZY, *et al.* (2006). Inhibition of the TPA-induced cutaneous inflammation and hyperplasia by EC-SOD. *Biochem Biophys Res Commun* 348: 450–8.
- Hachiya, a., Kobayashi, a., Ohuchi, a., *et al.* (2001). The paracrine role of stem cell factor/c-kit signaling in the activation of human melanocytes in ultraviolet-B-induced pigmentation. *J Invest Dermatol* 116: 578–86.
- Halliday, GM, Zhou, Y, Sou, PW, *et al.* (2012). The absence of Brm exacerbates photocarcinogenesis 599–604.
- Hanada, K, Baba, T, Hashimoto, I, *et al.* (1993). Possible role of cutaneous metallothionein in protection against photo-oxidative stress--epidermal localization and scavenging activity for superoxide and hydroxyl radicals. *Photodermatol Photoimmunol Photomed* 9: 209–13.
- Hanahan, D, Weinberg, R a (2011). Hallmarks of cancer: the next generation. *Cell* 144: 646–74.
- Hang, B (2010). Formation and repair of tobacco carcinogen-derived bulky DNA adducts. *J Nucleic Acids* 2010: 709521.
- Hardie, DG, Ross, F a., Hawley, S a. (2012). AMPK: a nutrient and energy sensor that maintains energy homeostasis. *Nat Rev Mol Cell Biol* 13: 251–62.
- Haupt, S, Berger, M, Goldberg, Z, *et al.* (2003). Apoptosis - the p53 network. *J Cell Sci* 116: 4077–85.
- Heck, DE, Gerecke, DR, Vetrano, AM, *et al.* (2004). Solar ultraviolet radiation as a trigger of cell signal transduction. *Toxicol Appl Pharmacol* 195: 288–97.
- Hemmings, BA, Restuccia, DF (2012). PI3K-PKB / Akt Pathway 3–5.
- Herst, PM, Berridge, M V. (2007). Cell surface oxygen consumption: A major contributor to cellular oxygen consumption in glycolytic cancer cell lines. *Biochim Biophys Acta - Bioenerg* 1767: 170–7.

- Hervouet, E, Cízková, A, Demont, J, *et al.* (2008). HIF and reactive oxygen species regulate oxidative phosphorylation in cancer. *Carcinogenesis* 29: 1528–37.
- Hill, LL, Ouhtit, A, Loughlin, SM, *et al.* (1999). Fas Ligand: A Sensor for DNA Damage Critical in Skin Cancer Etiology. *Science* (80-) 285: 898–900.
- Hiona, A, Sanz, A, Kujoth, GC, *et al.* (2010). Mitochondrial DNA mutations induce mitochondrial dysfunction, apoptosis and sarcopenia in skeletal muscle of mitochondrial DNA mutator mice. *PLoS One* 5.
- Hirst, J, Carroll, J, Fearnley, IM, *et al.* (2003). The nuclear encoded subunits of complex I from bovine heart mitochondria. *Biochim Biophys Acta - Bioenerg* 1604: 135–50.
- Hitomi, J, Christofferson, DE, Ng, A, *et al.* (2009). Screen. *Cell* 135: 1311–23.
- Hoeijmakers, JHJ (1993). Nucleotide excision repair II: From yeast to mammals. *Trends Genet* 9: 211–7.
- Hoekstra, AS, Bayley, JP (2013). The role of complex II in disease. *Biochim Biophys Acta - Bioenerg* 1827: 543–51.
- Hojyo-Tomoka, MT, Vega-Memije, ME, Cortes-Franco, R, *et al.* (2003). Diagnosis and treatment of actinic prurigo. *Dermatol Ther* 16: 40–4.
- Horton, T, Petros, J, Heddi, A, *et al.* (1996). Novel mitochondrial DNA deletion found in a renal cell carcinoma. *Genes Chromosom Cance* 15: 95–101.
- Hosseini, M, Ezzedine, K, Taieb, A, *et al.* (2014a). Oxidative and Energy Metabolism as Potential Clues for Clinical Heterogeneity in Nucleotide Excision Repair Disorders 1–11.
- Hosseini, M, Mahfouf, W, Serrano-Sanchez, M, *et al.* (2014b). Premature Skin Aging Features Rescued by Inhibition of NADPH Oxidase Activity in XPC-Deficient Mice. *J Invest Dermatol* 1–11.
- Hunt, G, Kyne, S, Ito, S, *et al.* (1995). Eumelanin and pheomelanin contents of human epidermis and cultured melanocytes. *Pigment Cell Res* 8: 202–8.
- Ichihashi, M, Ueda, M, Budiyo, a., *et al.* (2003). UV-induced skin damage. *Toxicology* 189: 21–39.
- Ikeda, Y, Sciarretta, S, Nagarajan, N, *et al.* (2014). New Insights into the Role of Mitochondrial Dynamics and Autophagy during Oxidative Stress and Aging in the Heart. *Oxid Med Cell Longev* 2014: 210934.
- Imokawa, G (2004). Autocrine and Paracrine Regulation of Melanocytes in Human Skin and in Pigmentary Disorders. *Pigment Cell Res* 17: 96–110.
- Imokawa, G, Kobayashi, T, Miyagishi, M, *et al.* (1997). The role of endothelin-1 in epidermal hyperpigmentation and signaling mechanisms of mitogenesis and melanogenesis. *Pigment Cell Res* 10: 218–28.

- Jaskelioff, M, Muller, FL, Paik, J-H, *et al.* (2011). Telomerase reactivation reverses tissue degeneration in aged telomerase-deficient mice. *Nature* 469: 102–6.
- Jeggo, P (1998). Identification of genes involved in repair of DNA double-strand breaks in mammalian cells. *Radiat Res* 150: S80–91.
- Jeggo, P, Taccioli, G, Jackson, S (1995). Menage à trois: double strand break repair, V(D)J recombination and DNA-PK. *Bioessays* 17: 949–57.
- Jenner, T, Cunniffe, S, Stevens, D, *et al.* (1998). Induction of DNA-protein crosslinks in Chinese hamster V79-4 cells exposed to high- and low-linear energy transfer radiation. *Radiat Res* 150: 593–9.
- JIN, K (2010). Modern biological theories of aging. *Aging Dis* 1: 72–4.
- Jiricny, J (2000). Mediating mismatch repair. *Nat Genet* 24: 6–8.
- Jornayvaz, F, Shulman, G (2010). Regulation of mitochondrial biogenesis. *Essays Biochem* 47: 69–84.
- Kaneko, N, Vierkoetter, A, Kraemer, U, *et al.* (2012). Mitochondrial common deletion mutation and extrinsic skin ageing in German and Japanese women. *Exp Dermatol* 21: 26–30.
- Kang, X, Li, J, Zou, Y, *et al.* (2010). PIASy stimulates HIF1 α SUMOylation and negatively regulates HIF1 α activity in response to hypoxia. *Oncogene* 29: 5568–78.
- Karran, P (2000). DNA double strand break repair in mammalian cells. *Curr Opin Genet Dev* 10: 144–50.
- Kawaguchi, M, Hearing, VJ (2011). The Roles of ADAMs Family Proteinases in Skin Diseases. *Enzyme Res* 2011: 482498.
- Kemp, LM, Jeggo, P a (1986). Radiation-induced chromosome damage in X-ray-sensitive mutants (xrs) of the Chinese hamster ovary cell line. *Mutat Res* 166: 255–63.
- Van der kemp, P, Thomas, D, Barbey, R, *et al.* (1996). Cloning and expression in Escherichia coli of the OGG1 gene of Saccharomyces cerevisiae, which codes for a DNA glycosylase that excises 7,8-dihydro-8-oxoguanine and 2,6-diamino-4-hydroxy-5-N-methylformamidopyrimidine. *Proc Natl Acad Sci U S A* 93: 5197–202.
- Kim, JW, Tchernyshyov, I, Semenza, GL, *et al.* (2006). HIF-1-mediated expression of pyruvate dehydrogenase kinase: A metabolic switch required for cellular adaptation to hypoxia. *Cell Metab* 3: 177–85.
- Kitanaka, C, Kuchino, Y (1999). Caspase-independent programmed cell death with necrotic morphology. *Cell Death Differ* 6: 508–15.
- Kluck, RM, Bossy-Wetzels, E, Green, DR, *et al.* (1997). The release of cytochrome c from mitochondria: a primary site for Bcl-2 regulation of apoptosis. *Science* 275: 1132–6.

- Koenig, U, Eckhart, L, Tschachler, E (2001). Evidence that caspase-13 is not a human but a bovine gene. *Biochem Biophys Res Commun* 285: 1150–4.
- Kolodner, RD, Marsischky, GT (1999). Eukaryotic DNA mismatch repair. *Curr Opin Genet Dev* 9: 89–96.
- Kondo, S, Sauder, DN, McKenzie, RC, *et al.* (1995). The role of cis-urocanic acid in UVB-induced suppression of contact hypersensitivity. *Immunol Lett* 48: 181–6.
- Kuhajda, FP, Jenner, K, Wood, FD, *et al.* (1994). Fatty acid synthesis: a potential selective target for antineoplastic therapy. *Proc Natl Acad Sci U S A* 91: 6379–83.
- Van Kuilenburg, a. BP, Van Lenthe, H, Löffler, M, *et al.* (2004). Analysis of pyrimidine synthesis “de novo” intermediates in urine and dried urine filter-paper strips with HPLC-electrospray tandem mass spectrometry. *Clin Chem* 50: 2117–24.
- Kullavanijaya, P, Lim, HW (2005). Photoprotection. *J Am Acad Dermatol* 52: 937–58; quiz 959–62.
- Kulms, D, Zeise, E, Pöppelmann, B, *et al.* (2002). DNA damage, death receptor activation and reactive oxygen species contribute to ultraviolet radiation-induced apoptosis in an essential and independent way. *Oncogene* 21: 5844–51.
- Kurimoto, I, Streilein, J (1992). Deleterious effects of cis-urocanic acid and UVB radiation on Langerhans cells and on induction of contact hypersensitivity are mediated by tumor necrosis factor- α . *J Invest Dermatol* 99: 69S – 70S.
- Kwon, OS, Yoo, HG, Han, JH, *et al.* (2008). Photoaging-associated changes in epidermal proliferative cell fractions in vivo. *Arch Dermatol Res* 300: 47–52.
- Lamkanfi, M, Declercq, W, Kalai, M, *et al.* (2002). Alice in caspase land. A phylogenetic analysis of caspases from worm to man. *Cell Death Differ* 9: 358–61.
- Langhoff, E, Kalland, KH, Haseltine, W a (1993). Early molecular replication of human immunodeficiency virus type 1 in cultured-blood-derived T helper dendritic cells. *J Clin Invest* 91: 2721–6.
- Leadon, SA, Avrutskaya, A V (1997). Differential involvement of the human mismatch repair proteins, hMLH1 and hMSH2, in transcription-coupled repair. *Cancer Res* 57: 3784–91.
- Lehmann, a R, Kirk-Bell, S, Arlett, CF, *et al.* (1975). Xeroderma pigmentosum cells with normal levels of excision repair have a defect in DNA synthesis after UV-irradiation. *Proc Natl Acad Sci U S A* 72: 219–23.
- Lehtonen, HJ, Kiuru, M, Ylisaukko-Oja, SK, *et al.* (2006). Increased risk of cancer in patients with fumarate hydratase germline mutation. *J Med Genet* 43: 523–6.
- Li, WW, Li, J, Bao, JK (2012). Microautophagy: Lesser-known self-eating. *Cell Mol Life Sci* 69: 1125–36.

- Lindahl, T, Wood, R (1999). Quality Control by DNA Repair. *Science* (80-) 286: 1897–905.
- Locasale, JW, Cantley, LC (2010). Altered metabolism in cancer. *BMC Biol* 8: 88.
- Lombard, DB, Chua, KF, Mostoslavsky, R, *et al.* (2005). DNA repair, genome stability, and aging. *Cell* 120: 497–512.
- Maiuri, MC, Zalckvar, E, Kimchi, A, *et al.* (2007). Self-eating and self-killing: crosstalk between autophagy and apoptosis. *Nat Rev Mol Cell Biol* 8: 741–52.
- Mangoni, a. a., Jackson, SHD (2004). Age-related changes in pharmacokinetics and pharmacodynamics: Basic principles and practical applications. *Br J Clin Pharmacol* 57: 6–14.
- Marchetti, P, Susin, S a, Decaudin, D, *et al.* (1996). Apoptosis-associated Derangement of Mitochondrial Function in Cells Lacking Mitochondrial DNA Apoptosis-associated Derangement of Mitochondrial Function in Cells Lacking 2033–8.
- Masaki, H, Okano, Y, Sakurai, H (1998). Differential role of catalase and glutathione peroxidase in cultured human fibroblasts under exposure of H₂O₂ or ultraviolet B light. *Arch Dermatol Res* 290: 113–8.
- Masutani, C, Araki, M, Yamada, A, *et al.* (1999a). Xeroderma pigmentosum variant (XP-V) correcting protein from HeLa cells has a thymine dimer bypass DNA polymerase activity. *EMBO J* 18: 3491–501.
- Masutani, C, Kusumoto, R, Yamada, a, *et al.* (1999b). The XPV (xeroderma pigmentosum variant) gene encodes human DNA polymerase eta. *Nature* 399: 700–4.
- Matés, JM (2000). Effects of antioxidant enzymes in the molecular control of reactive oxygen species toxicology. *Toxicology* 163: 219.
- Mathupala, SP, Ko, YH, Pedersen, PL (2009). Hexokinase-2 bound to mitochondria: cancer's stygian link to the “Warburg Effect” and a pivotal target for effective therapy. *Semin Cancer Biol* 19: 17–24.
- Matsumura, Y, Ananthaswamy, HN (2004). Toxic effects of ultraviolet radiation on the skin. *Toxicol Appl Pharmacol* 195: 298–308.
- McLelland, J, Chu, A (1990). Multi-system Langerhans-cell histiocytosis in adults. *Clin Exp Dermatol* 15: 79–82.
- Medema, RH, Herrera, RE, Lam, F, *et al.* (1995). Growth suppression by p16ink4 requires functional retinoblastoma protein. *Proc Natl Acad Sci U S A* 92: 6289–93.
- Meneghini, R (1997). Iron homeostasis, oxidative stress, and DNA damage. *Free Radic Biol Med* 23: 783–92.
- Milane, L, Trivedi, M, Singh, A, *et al.* (2015). Mitochondrial Biology, Targets, and Drug Delivery. *J Control Release* 207: 40–58.

- Millington, GWM (2006). Proopiomelanocortin (POMC): The cutaneous roles of its melanocortin products and receptors. *Clin Exp Dermatol* 31: 407–12.
- Min, KS, Nishida, K, Onosaka, S (1999). Protective effect of metallothionein to ras DNA damage induced by hydrogen peroxide and ferric ion-nitrilotriacetic acid. *Chem Biol Interact* 122: 137–52.
- Miquel, J, Economos, a. C, Fleming, J, *et al.* (1980). Mitochondrial role in cell aging. *Exp Gerontol* 15: 575–91.
- Mitchell, P (1961). Coupling of phosphorylation to electron and hydrogen transfer by a chemi-osmotic type of mechanism. *Nature* 191: 144–8.
- Mizumura, K, Choi, AMK, Ryter, SW (2014). Emerging role of selective autophagy in human diseases. *Front Pharmacol* 5: 1–8.
- Modrich, P (1997). Minireview Strand-specific Mismatch Repair in Mammalian Cells *. *Biochemistry* 272: 24727–30.
- Montague, J, Cidlowski, J (1996). Cellular catabolism in apoptosis: DNA degradation and endonuclease activation. *Experientia* 52: :957–62.
- Moodycliffe, a M, Kimber, I, Norval, M (1994). Role of tumour necrosis factor-alpha in ultraviolet B light-induced dendritic cell migration and suppression of contact hypersensitivity. *Immunology* 81: 79–84.
- Morel, Y, Barouki, R (1998). Down-regulation of cytochrome P450 1A1 gene promoter by oxidative stress: Critical contribution of nuclear factor 1. *J Biol Chem* 273: 26969–76.
- Morliere, P, Moysan, A, Tirache, I (1995). Action Spectrum For Uv-Induced Lipid Peroxidation In Cultured Human Skin Fibroblasts. *Free Radic Biol Med* 19: 365–71.
- Moslehi, J, Depinho, R a., Sahin, E (2012). Telomeres and mitochondria in the aging heart. *Circ Res* 110: 1226–37.
- Motegi, S, Yokoyama, Y, Uchiyama, A, *et al.* (2014). First Japanese case of atypical progeroid syndrome/atypical Werner syndrome with heterozygous *LMNA* mutation. *J Dermatol* 41: 1047–52.
- Murphy, GM (2001). Diseases associated with photosensitivity. *J Photochem Photobiol B Biol* 64: 93–8.
- Myllyharju, J (2013). Prolyl 4-hydroxylases, master regulators of the hypoxia response. *Acta Physiol* 208: 148–65.
- Nakamoto, R, Baylis, JA, Al-Shawi, M (2009). NIH Public Access. *Arch Biochem Biophys* 476: 43–50.
- Neckelmann, N, Li, K, Wade, RP, *et al.* (1987). cDNA sequence of a human skeletal muscle ADP/ATP translocator: lack of a leader peptide, divergence from a fibroblast

- translocator cDNA, and coevolution with mitochondrial DNA genes. *Proc Natl Acad Sci U S A* 84: 7580–4.
- Nijhawan, D, Fang, M, Traer, E, *et al.* (2003). Elimination of Mcl-1 is required for the initiation of apoptosis following ultraviolet irradiation. *Genes Dev* 17: 1475–86.
- Nishigori, C, Yarosh, D, Donawho, C, *et al.* (1996). The immune system in ultraviolet carcinogenesis. *J Invest Dermatol Symp Proc* 1: 143–6.
- Norval, M, Gibbs, NK, Gilmour, J (1995). The role of urocanic acid in UV-induced immunosuppression: recent advances (1992-1994). *Photochem Photobiol* 62: 209–17.
- Ohlrogge, J, Browse, J (1995). Lipid biosynthesis. *Plant Cell* 7: 957–70.
- Ohnishi, Y, Tajima, S, Akiyama, M, *et al.* (2000). Expression of elastin-related proteins and matrix metalloproteinases in actinic elastosis of sun-damaged skin. *Arch Dermatol Res* 292: 27–31.
- Ou-Yang, H, Stamatias, G, Kollias, N (2004). Spectral Responses of Melanin to Ultraviolet a Irradiation. *J Invest Dermatol* 122: 492–6.
- Palade, GE (1952). The Fine Structure Of Mitochondria. *Anat Rec* 114: 427–51.
- Palade, GE (1953). An Electron Microscope Study Of The Mitochondrial Structure. *J Histochem Cytochem* 1: 188–211.
- Papandreou, I, Cairns, R a., Fontana, L, *et al.* (2006). HIF-1 mediates adaptation to hypoxia by actively downregulating mitochondrial oxygen consumption. *Cell Metab* 3: 187–97.
- Parat, MO, Richard, MJ, Meplan, C, *et al.* (1999). Impairment of cultured cell proliferation and metallothionein expression by metal chelator NNN'N'-tetrakis-(2-pyridylmethyl)ethylene diamine. *Biol Trace Elem Res* 70: 51–68.
- Philips, N, Auler, S, Hugo, R, *et al.* (2011). Beneficial regulation of matrix metalloproteinases for skin health. *Enzyme Res* 2011: 427285.
- Pollock, JD, Williams, D a, Gifford, M a, *et al.* (1995). Mouse model of X-linked chronic granulomatous disease, an inherited defect in phagocyte superoxide production. *Nat Genet* 9: 202–9.
- Porstmann, T, Griffiths, B, Chung, Y-L, *et al.* (2005). PKB/Akt induces transcription of enzymes involved in cholesterol and fatty acid biosynthesis via activation of SREBP. *Oncogene* 24: 6465–81.
- Pospisilova, J (2013). Resistance to TRAIL in mantle cell lymphoma cells is associated with the decreased expression of purine metabolism enzymes. *Int J Mol Med* 1273–9.
- Qiang, L, Wu, C, Ming, M, *et al.* (2013). Autophagy controls p38 activation to promote cell survival under genotoxic stress. *J Biol Chem* 288: 1603–11.

- Qin, Z, Voorhees, JJ, Fisher, GJ, *et al.* (2014). Age-associated reduction of cellular spreading/mechanical force up-regulates matrix metalloproteinase-1 expression and collagen fibril fragmentation via c-Jun/AP-1 in human dermal fibroblasts. *Aging Cell* 13: 1028–37.
- Quan, T, Fisher, GJ (2015). Role of Age-Associated Alterations of the Dermal Extracellular Matrix Microenvironment in Human Skin Aging: A Mini-Review. *Gerontology* 48:109.
- Rana, S, Byrne, SN, MacDonald, LJ, *et al.* (2008). Ultraviolet B suppresses immunity by inhibiting effector and memory T cells. *Am J Pathol* 172: 993–1004.
- Rapp, A, Greulich, KO (2004). After double-strand break induction by UV-A, homologous recombination and nonhomologous end joining cooperate at the same DSB if both systems are available. *J Cell Sci* 117: 4935–45.
- Rastogi, RP, Richa, Kumar, A, *et al.* (2010). Molecular mechanisms of ultraviolet radiation-induced DNA damage and repair. *J Nucleic Acids* 2010: 592980.
- Ravanat, JL, Douki, T, Cadet, J (2001). Direct and indirect effects of UV radiation on DNA and its components. *J Photochem Photobiol* 63: 88–102.
- Rehemtulla, a, Hamilton, C a, Chinnaiyan, a M, *et al.* (1997). Ultraviolet radiation-induced apoptosis is mediated by activation of CD-95 (Fas/APO-1). *J Biol Chem* 272: 25783–6.
- Reimann, V, Krämer, U, Sugiri, D, *et al.* (2008). Sunbed use induces the photoaging-associated mitochondrial common deletion. *J Invest Dermatol* 128: 1294–7.
- Reitzer, L, Wice, B, Kennell, D (1979). Evidence that glutamine, not sugar, is the major energy source for cultured HeLa cells. *J Biol Chem* 254: 2669–76.
- Remacle, C, Barbieri, MR, Cardol, P, *et al.* (2008). Eukaryotic complex I: Functional diversity and experimental systems to unravel the assembly process. *Mol Genet Genomics* 280: 93–110.
- Rezvani, HR, Dedieu, S, North, S, *et al.* (2007). Hypoxia-inducible factor-1 α , a key factor in the keratinocyte response to UVB exposure. *J Biol Chem* 282: 16413–22.
- Rezvani, HR, Kim, AL, Rossignol, R, *et al.* (2011a). XPC silencing in normal human keratinocytes triggers metabolic alterations that drive the formation of squamous cell carcinomas. *J Clin Invest* 121: 195–211.
- Rezvani, HR, Kim, AL, Rossignol, R, *et al.* (2011b). XPC silencing in normal human keratinocytes triggers metabolic alterations that drive the formation of squamous cell carcinomas 121: 195–211.
- Rezvani, HR, Mazurier, F, Cario-André, M, *et al.* (2006). Protective effects of catalase overexpression on UVB-induced apoptosis in normal human keratinocytes. *J Biol Chem* 281: 17999–8007.

- Rosette, C, Karin, M (1996). Ultraviolet light and osmotic stress: activation of the JNK cascade through multiple growth factor and cytokine receptors. *Science* (80-) 274: 1194–7.
- Rossignol, R, Gilkerson, R, Aggeler, R, *et al.* (2004). Energy Substrate Modulates Mitochondrial Structure and Oxidative Capacity in Cancer Cells. *Cancer Res* 64: 985–93.
- Rötig, a, de Lonlay, P, Chretien, D, *et al.* (1997). Aconitase and mitochondrial iron-sulphur protein deficiency in Friedreich ataxia. *Nat Genet* 17: 215–7.
- Rouzaud, F, Costin, GE, Yamaguchi, Y, *et al.* (2006). Regulation of constitutive and UVR-induced skin pigmentation by melanocortin 1 receptor isoforms. *FASEB J* 20: 1927–9.
- Rubinsztein, DC, Mariño, G, Kroemer, G (2011). Autophagy and aging. *Cell* 146: 682–95.
- Ryan, BJ, Hoek, S, Fon, E a., *et al.* (2015). Mitochondrial dysfunction and mitophagy in Parkinson's: from familial to sporadic disease. *Trends Biochem Sci* 40: 200–10.
- Sanches Silveira, E, Pedroso, MM (2014). UV light and skin aging 29: 243–54.
- Sarasin, A (1997). [DNA lesions: mechanisms of recognition and repair]. *Bull Cancer* 84: 467–72.
- Schapira, A, Gu, M, Taanman, J, *et al.* (1998). Mitochondria in the etiology and pathogenesis of Parkinson's disease. *Ann Neurol* 44: 89–98.
- Schauer, E, Trautinger, F, Köck, a., *et al.* (1994). Proopiomelanocortin-derived peptides are synthesized and released by human keratinocytes. *J Clin Invest* 93: 2258–62.
- Schreck, R, Grassmann, R, Fleckenstein, B, *et al.* (1992). Antioxidants selectively suppress activation of NF-kappa B by human T-cell leukemia virus type I Tax protein. *J Virol* 66: 6288–93.
- Schwarz, A, Bhardwaj, R, Aragane, Y, *et al.* (1995). Ultraviolet-B-induced apoptosis of keratinocytes: evidence for partial involvement of tumor necrosis factor-alpha in the formation of sunburn cells. *J Invest Dermatol* 104: 922–7.
- Schwarz, T (2005). Mechanisms of UV-induced immunosuppression. *Keio J Med* 54: 165–71.
- Scott, MC, Suzuki, I, Abdel-Malek, Z a (2002). Regulation of the human melanocortin 1 receptor expression in epidermal melanocytes by paracrine and endocrine factors and by ultraviolet radiation. *Pigment Cell Res* 15: 433–9.
- Seité, S, Zucchi, H, Moyal, D, *et al.* (2003). Alterations in human epidermal Langerhans cells by ultraviolet radiation: quantitative and morphological study. *Br J Dermatol* 148: 291–9.
- Shinohara, A, Ogawa, T (1995). Homologous recombination and the roles of double-strand breaks. *Trends Biochem Sci* 20: 387–91.

- Shreedhar, V, Giese, T, Sung, VW, *et al.* (1998). A cytokine cascade including prostaglandin E2, IL-4, and IL-10 is responsible for UV-induced systemic immune suppression. *J Immunol* 160: 3783–9.
- Simon, J, Krutmann, J, Elmetts, C, *et al.* (1992). Ultraviolet B-irradiated antigen-presenting cells display altered accessory signaling for T-cell activation: relevance to immune responses initiated in skin. *J Invest Dermatol* 98: 66S – 69S.
- Simon, M, Aragane, Y, Schwarz, A, *et al.* (1994). UVB light induces nuclear factor kappa B (NF kappa B) activity independently from chromosomal DNA damage in cell-free cytosolic extracts. *J Invest Dermatol* 102: 422–7.
- Singh, A, Compe, E, Le May, N, *et al.* (2015). TFIIH Subunit Alterations Causing Xeroderma Pigmentosum and Trichothiodystrophy Specifically Disturb Several Steps during Transcription. *Am J Hum Genet* 96: 194–207.
- Van der Spek, PJ, Kobayashi, K, Bootsma, D, *et al.* (1996). Cloning, tissue expression, and mapping of a human photolyase homolog with similarity to plant blue-light receptors. *Genomics* 37: 177–82.
- Stock, D, Gibbons, C, Arechaga, I, *et al.* (2000). The rotary mechanism of ATP-synthase. *Curr Opin Struct Biol* 10: 672–9.
- Stojic, L, Brun, R, Jiricny, J (2004). Mismatch repair and DNA damage signalling. *DNA Repair (Amst)* 3: 1091–101.
- Strachan, T, Read, a P (2004). Chapter 9: Organization of the human genome. *Hum Mol Genet* 3.
- Streilein, JW, Taylor, JR, Vincek, V, *et al.* (1994). Immune surveillance and sunlight-induced skin cancer. *Immunol Today* 15: 174–9.
- Sutherland, B, Bennett, P, Schenk, H, *et al.* (2001). Clustered DNA damages induced by high and low LET radiation, including heavy ions. *Phys Med* 17: 202–4.
- Thoma, F (1999). NEW EMBO MEMBER ' S REVIEW Light and dark in chromatin repair : repair of UV- induced DNA lesions by photolyase and nucleotide. *EMBO J* 18: 6585–98.
- Thompson, LH, West, MG (2000). XRCC1 keeps DNA from getting stranded. *Mutat Res - DNA Repair* 459: 1–18.
- Todo, T, Tsuji, H, Otonari, E, *et al.* (1997). Characterization of a human homolog of (6-4) photolyase. *Mutat Res - DNA Repair* 384: 195–204.
- Tomkinson, AE, Mackey, ZB (1998). Structure and function of mammalian DNA ligases. *Mutat Res Repair* 407: 1–9.
- Tomlinson, IPM, Alam, NA, Rowan, AJ, *et al.* (2002). Germline mutations in FH predispose to dominantly inherited uterine fibroids, skin leiomyomata and papillary renal cell cancer. *Nat Genet* 30: 406–10.

- Tornaletti, S, Pfeifer, G (1996). UV damage and repair mechanisms in mammalian cells. *Bioessays* 18: 221–8.
- Trachootham, D, Lu, W, Ogasawara, M a, *et al.* (2008). Redox regulation of cell survival. *Antioxid Redox Signal* 10: 1343–74.
- Trifunovic, A, Wredenberg, A, Falkenberg, M, *et al.* (2014). Aging: A mitochondrial DNA perspective, critical analysis and an update. *World J Exp Med* 4: 46.
- Ullrich, S (1995). Modulation of immunity by ultraviolet radiation: key effects on antigen presentation. *J Invest Dermatol* 105: 30S – 36S.
- Valko, M, Leibfritz, D, Moncol, J, *et al.* (2007). Free radicals and antioxidants in normal physiological functions and human disease. *Int J Biochem Cell Biol* 39: 44–84.
- Valko, M, Rhodes, CJ, Moncol, J, *et al.* (2006). Free radicals, metals and antioxidants in oxidative stress-induced cancer. *Chem Biol Interact* 160: 1–40.
- Vaupel, P (2004). The role of hypoxia-induced factors in tumor progression. *Oncologist* 9 Suppl 5: 10–7.
- Vermeer, B, Hurks, M (1994). The clinical relevance of immunosuppression by UV irradiation. *J Photochem Photobiol B* 24: 149–54.
- Vermeulen, W, Scott, RJ, Rodgers, S, *et al.* (1994). Clinical heterogeneity within xeroderma pigmentosum associated with mutations in the DNA repair and transcription gene ERCC3. *Am J Hum Genet* 54: 191–200.
- Vink, a a, Strickland, FM, Bucana, C, *et al.* (1996). Localization of DNA damage and its role in altered antigen-presenting cell function in ultraviolet-irradiated mice. *J Exp Med* 183: 1491–500.
- Vyas, VK, Ghate, M (2011). Recent Developments in the Medicinal Chemistry and Therapeutic Potential of Dihydroorotate Dehydrogenase (DHODH) Inhibitors. *Mini Rev Med Chem* 11: 1039–55.
- Wallace, D (2001). A mitochondrial paradigm for degenerative diseases and ageing. *Novartis Found Symp* 235: 247–63.
- Wallace, DC (2005). A Mitochondrial Paradigm of Metabolic and Degenerative Diseases, Aging, and Cancer: A Dawn for Evolutionary Medicine. *Annu Rev Genet* 39: 359.
- Wang, K, Deubel, V (2011). Mice with different susceptibility to Japanese encephalitis virus infection show selective neutralizing antibody response and myeloid cell infectivity. *PLoS One* 6.
- Wang, Z-C, Wang, X-M, Jiao, B-H, *et al.* (2003). Detection of mitochondrial DNA deletion by a modified PCR method in a ⁶⁰Co radiation-exposed patient. *IUBMB Life* 55: 133–7.
- Warburg, O (1956). On the origin of cancer cells. *Science* 123: 309–14.

- Warburg, O, Wind, F, Negelein, E (1927). the Metabolism of Tumors in the Body. *J Gen Physiol* 8: 519–30.
- Ward, PS, Thompson, CB (2012). Metabolic Reprogramming: A Cancer Hallmark Even Warburg Did Not Anticipate. *Cancer Cell* 21: 297–308.
- Watmough, NJ, Frerman, FE (2010). The electron transfer flavoprotein: Ubiquinone oxidoreductases. *Biochim Biophys Acta - Bioenerg* 1797: 1910–6.
- Wei, Y-H, Wu, S-B, Ma, Y-S, *et al.* (2009). Respiratory function decline and DNA mutation in mitochondria, oxidative stress and altered gene expression during aging. *Chang Gung Med J* 32: 113–32.
- Wintzen, M, Gilchrest, B (1996). Proopiomelanocortin, its derived peptides, and the skin. *J Invest Dermatol* 106: 3–10.
- Wise, DR, Thompson, CB (2010). Glutamine Addiction: A New Therapeutic Target in Cancer. *Trends Biochem Sci* 35: 427–33.
- Wong, ASL, Cheung, ZH, Ip, NY (2011). Molecular machinery of macroautophagy and its deregulation in diseases. *Biochim Biophys Acta - Mol Basis Dis* 1812: 1490–7.
- Wood, RD (1999). DNA repair. Variants on a theme. *Nature* 399: 639–40.
- Yang, L, Munck, M, Swaminathan, K, *et al.* (2013). Mutations in LMNA Modulate the Lamin A - Nesprin-2 Interaction and Cause LINC Complex Alterations. *PLoS One* 8.
- Yang, NC, Hu, ML (2005). The limitations and validities of senescence associated-beta-galactosidase activity as an aging marker for human foreskin fibroblast Hs68 cells. *Exp Gerontol* 40: 813–9.
- Yoshikawa, T, Rae, V, Bruins-Slot, W, *et al.* (1990). Susceptibility to effects of UVB radiation on induction of contact hypersensitivity as a risk factor for skin cancer in humans. *J Invest Dermatol* 95: :530–6.
- Young, C (2009). Solar ultraviolet radiation and skin cancer. *Occup Med (Chic Ill)* 59: 82–8.
- Yu, S, Bordeaux, J, Baron, E (2014). The immune system and skin cancer. *Adv Exp Med Biol* 810: 182–91.
- Zamzami, N, Susin, S a, Marchetti, P, *et al.* (1996). Mitochondrial control of nuclear apoptosis. *J Exp Med* 183: 1533–44.
- Zheng, J (2012). Energy metabolism of cancer: Glycolysis versus oxidative phosphorylation (review). *Oncol Lett* 4: 1151–7.

ABSTRACT

Objective of the present research study was investigating the role of oxidative and energy metabolism in skin aging and UVB-induced skin cancer. In the first part, we aimed to find the link between genetic instability, ROS generation and metabolism alteration in the process of aging. The obtained results on XPC KO mice model demonstrated that excess of oxidative stress in addition to alterations in energy metabolism due to over activation of NOX1 play a causative role in premature skin aging. Topical application of novel NOX inhibitor prevented the premature aging in XPC KO mice through inhibition of ROS generation and alteration of energy metabolism. Our results suggest that the InhNOX can be considered as a promising target in prevention of premature aging and NOX-associated diseases.

Little information is available on the contribution of energy metabolism reprogramming in cancer initiation and promotion. To assess the role of metabolic reprogramming in different phases of carcinogenesis, in the second part of my thesis we employed a multistage model of ultraviolet B (UVB) radiation-induced skin cancer. We showed that chronic UVB irradiation results in decreased glycolysis, TCA cycle and fatty acid β -oxidation while at the same time mitochondrial ATP synthesis and a part of the electron transport chain (ETC) are up-regulated. Increased ETC was further found to be related to the over-activation of dihydroorotate dehydrogenase (DHODH). Decreased activity of DHODH or ETC (chemically or genetically) led to hypersensitivity to UVB irradiation. Our results indicated that DHODH pathway through induction of ETC and ATP synthesis represents the relation between DNA repair efficiency and metabolism reprogramming during UVB-induced carcinogenesis.

RÉSUMÉ

L'objectif de notre étude était de montrer le rôle du métabolisme oxydatif et énergétique au cours du vieillissement cutané et dans les cancers cutanés UVB-induits. Dans une première partie, nous avons cherché à établir un lien entre l'instabilité génétique, la production de ROS et l'altération métabolique dans le processus de vieillissement. Les résultats obtenus sur le modèle de souris XPC KO ont démontré qu'un excès de stress oxydatif dû à une sur activation du NOX1, couplé à des altérations métaboliques, jouaient un rôle prépondérant dans le vieillissement prématuré. L'application topique de notre nouvel inhibiteur de NOX, induisant l'inhibition de la production de ROS et ainsi l'apparition d'altération métabolique, a permis d'empêcher le vieillissement cutané prématuré chez les souris XPC KO. Nos résultats suggèrent que l'InhNOX peut être considéré comme une cible prometteuse dans la prévention du vieillissement prématuré et les maladies liées à NOX.

Très peu d'informations sont disponibles sur la contribution de la reprogrammation du métabolisme énergétique dans l'initiation et la progression du cancer. Dans la deuxième partie de ma thèse, nous avons utilisé un modèle multi-étapes de cancer de la peau UVB-induits, nous permettant ainsi d'évaluer le rôle de la reprogrammation métabolique dans les différentes étapes de la cancérogenèse. Nous avons ensuite démontré que l'irradiation chronique à UVB entraînait une diminution de l'activité de la glycolyse, du cycle TCA et de la β -oxydation des acides gras, tandis que la synthèse d'ATP mitochondriale et une partie de la chaîne de transport d'électrons (CTE) étaient up-régulés. Nous avons montré que l'augmentation accrue de CTE été liée à la sur-activation des dihydroorotate déshydrogénase (DHODH). Alors que la diminution de l'activité DHODH ou ETC (chimiquement ou génétiquement) a conduit à une hypersensibilité à l'irradiation UVB. Nos résultats indiquent que la voie DHODH par l'induction de la synthèse d'ATP et de CTE joue un rôle majeur entre l'efficacité de réparation d'ADN et la reprogrammation métabolique au cours de la cancérogenèse UVB-induits.

